CALIFORNIA INSTITUTE OF TECHNOLOGY

DYNAMICS LABORATORY

RESEARCH ON FAILURE OF EQUIPMENT WHEN SUBJECT TO VIBRATION

by

Charles E. Crede

First Annual Report under Contract No. NAS 8-2451
with Marshall Space Flight Center,
National Aeronautics and Space Administration.
July 10, 1961 to October 10, 1962

Pasadena, California

1962

First Annual Report

on

RESEARCH ON FAILURE OF EQUIPMENT WHEN SUBJECT TO VIBRATION

by

Charles E. Crede

for

Marshall Space Flight Center
National Aeronautics and Space Administration

under

Contract No. NAS8-2451

during the period

July 10, 1961 to October 10, 1962

California Institute of Technology
Pasadena, California
October 31, 1962

INTRODUCTORY NOTE

This report is in the nature of a progress report; it sets forth in some detail the status of the research on the several tasks as of the date of the report. In general, the research was incomplete on that date and no conclusions are presented. The report is written primarily to keep personnel of the sponsoring agency apprised of work that has been accomplished. It is not intended for outside distribution or publication.

ABSTRACT

This is the first annual report under a continuing research project whose objective is to gain a better understanding of the failure of equipment when subjected to vibration. This is essential to (1) the attainment of improved practices in design of equipment that is required to withstand vibration and (2) to the application of more rational procedures for conducting vibration tests in the laboratory. In principle, the laboratory test creates a vibration condition that causes such failure of the equipment as would occur during actual service use. However, a laboratory test cannot reproduce the service condition in all of its details; thus, a good knowledge of the mechanics of failure is necessary to relate laboratory and service conditions in a constructive manner.

The research program includes two general aspects that are being pursued concurrently, at least in the initial phase of the research program:

1. Actual electronic and mechanical components of equipment with known susceptibility to failure; e.g., a vacuum tube in the initial task, are subjected to vibration of various defined types. The components are connected in circuits designed to simulate a typical application and the effect of vibration on the operation of the circuits is monitored. An objective of the experiment is to infer from the circuit operation and response of the component an analog that may be used to describe the characteristics of the component that are significant with respect to vibration. Such analogs are then used in further analyses of the component.

2. Concurrent with the above experiments using actual components, a group of analogs having apparent application to known components is

selected initially. Additional analogs are added to this group as experimental evaluation of actual components proceeds. The response of each selected analog to various idealized forms of vibration is investigated. Then from the relation between the response of the analog to such vibration and observed performance of the component to which the analog is related, the response of the component and its operational capability under more general types of vibration can be predicted.

A representative vacuum tube has been mounted upon a vibration exciter and subjected to both sinusoidal and random vibration. Its performance was monitored by noting the voltage output (microphonic noise) that could be ascribed to vibration. This report includes records of output voltage as a function of vibration frequency, for further use in attempting to infer an appropriate mechanical analog.

Five idealized forms of excitation have been selected for initial investigation: (1) sinusoid, (2) combined sinusoids, (3) scanning or sweeping sinusoid, (4) broad band random with Gaussian distribution and (5) broad band random with magnitude limitation. For each type of excitation, the response of the most common mechanical analog, a damped, single degree of freedom system, has been analyzed. By relating the characteristics of the analog to an actual component and applying appropriate criteria of failure, these responses are of use in predicting the performance capability of the component. For example, consider a structure vulnerable to failure by fatigue; then the distribution of response cycles included in the analysis of the analog response when taken with hypotheses of cumulative damage is applicable to predict the fatigue life.

Some experiments on fatigue have been carried out, with the objective of determining whether existing hypotheses of cumulative damage are applicable to the problem being discussed here. A simplified structure having certain characteristics of a typical equipment has been subjected to fatigue tests. Because of certain unanticipated characteristics of the response of the structure, it has become evident that additional experiments are required to interpret the results obtained to date. This phase of the program is continuing.

Section 1 of the report includes a detailed discussion of research program, its hypotheses and objectives. A brief summary of the results also is included in Section 1, with references to other sections of the report and to the appendices when complete details are set forth.

Acknowledgment

It is a pleasure to acknowledge the contributions of a group of students at the California Institute of Technology to the results reported herein. In particular, Mr. S. F. Masri and Mr. P. Y. Hu, graduate students, were associated with the project part-time during the academic year and full time during the summer, and made significant contributions. The following graduate students were associated with the project less extensively: Messrs. N. M. Bhatia, D. L. Cronin, K. Kawamo, H. Kendrick and S. R. Varanasi. In addition, the following undergraduate students were employed during the summer: Messrs. D. L. Colton, L. M. Molho, D. R. Owen and Y. B. Woo. Frequent conversations with Professor D. E. Hudson were very helpful, as were discussions with Dr. A. J. Curtis of Hughes Aircraft Company and Mr. F. B. Safford and Mr. J. M. Brust of Nortronics Division, Northrop Corporation. The report was typed primarily by Mrs. Ruth Toy and Mrs. Madeline Fagergren, and most of the drawings were prepared by Mr. G. Parker.

Table of Contents

Appendices

1. INTRODUCTION

1.1. Statement of the Problem

An investigation of the failure of equipment as a consequence of vibration must be approached in the context of real equipments and vibration that is representative of that existing in real environments. In general, real equipments are complicated assemblies of structures and devices which have many modes of failure. To define the terms used in this report, the word "failure" is a generic term that covers both damage and malfunction. The former is considered to be a permanent degradation of the equipment of such nature as to impair proper operation even though the vibration ceases. The latter is an improper operation which occurs while the vibration is being applied but which permits reversion to proper operation when the vibration ceases.

The primary objective of the research reported here is to gain an understanding of the mechanisms of failure that can be ascribed to vibratory conditions. The term "mechanism of failure" is used here to denote the process (mechanical, electrical, chemical, etc.) of degradation that leads to improper operation of or damage to equipment. Ideally, it would be desireable to know enough about the failure mechanisms so that an examination and analysis of an equipment would permit a prediction of its capability to withstand certain specified vibration conditions. In the present state of the art, such a prediction is feasible for only the most simple structures and devices. For real equipments, there is not much hope in the forseeable future to gain this objective solely by analysis. According to the state of the art that exists at present and is forseeable for the immediate future, it would be possible only to determine certain relevant

characteristics of the equipment by observing its response to certain specified vibration conditions and to use the results of such tests to predict the response of the equipment to other types of vibration. Considerable research will be required to reach this stage of technological advance, and it is hoped that the present program contributes constructively towards this end.

The principal incentives motivating the present research are first a desire to achieve a greater capability to carry forth a rational design process and second to gain knowledge to make possible a more rational testing program. In the present state of the art, the usual design process consists of alternate design changes and laboratory vibration tests. Although this process is largely empirical in nature, it leads ultimately to the construction of equipment that has demonstrated capabilities of withstanding the type of vibration that is imposed by laboratory vibration tests. Such tests usually have been devised with the objective of revealing weaknesses in equipment before such equipment is placed in actual service. In general, it is not feasible to reproduce the vibration conditions that will be encountered in actual service because the vehicle has not yet been built or the equipment must be designed to be used alternatively in several vehicles. Furthermore, the required service life of an equipment may be as great as several years whereas the time allotted for laboratory qualification tests may be only a few days.

The usual practice in devising laboratory tests is to employ such field test data as may be available to determine the characteristics (frequencies, variation of magnitude with frequency, etc.) of the vibration measured in the field. Such characteristics are then embodied in the

laboratory test after having been simplified to adapt them to laboratory testing practices, and the general severity is increased somewhat in the hope that this will compensate for the necessarily short duration of the laboratory test. The resulting test is often referred to as a "simulated" test; i.e., it does not reproduce the vibration expected in actual service but rather is designed to cause the same failures during the period of the laboratory test as would occur during the actual service.

If the simulated tests are to be valid, it is necessary to know how the failures resulting from the simplified vibration used in the laboratory are related to those caused by the vibration experienced in actual service. Furthermore, it is necessary to know how the failure of the equipment is related to the increase of severity that is introduced to account for the relatively short time available for laboratory testing. In general, it is necessary to understand the mechanisms of failure of equipments so that failure can be related to the nature and severity of the vibration. Only in this manner will it be possible to predict whether the laboratory test of simplified form but increased severity is appropriate as means to qualify equipment for ultimate use in actual service.

The problem of correlating the failure caused by one form of vibration with that caused by another form of vibration has attracted considerable interest. For example, a number of papers have appeared in the technical literature on the question of the equivalence of sinusoidal and random vibration. This subject is usually considered on the basis of a sinusoidal vibration of constant frequency and constant amplitude, compared with a random vibration having a Gaussian distribution of magnitude values and a flat spectrum of mean square acceleration density over a band width

of interest. This is an interesting philosophical problem, and it supplies a good starting point for considering the more realistic aspects of the problem.

Random vibration as experienced in the field usually has been filtered by vehicle structure; thus the power spectral density exhibits pronounced peaks and valleys. This concentration of vibration energy at particular frequencies introduces some of the characteristics of sinusoidal vibration. Furthermore, laboratory testing procedures involving sinusoidal vibration usually require that the excitation frequency be scanned rather than remain constant. In studying the problem of damage to equipment, it is important to consider these degradations from classical mathematical formulations which are introduced by real field and laboratory conditions.

In evaluating the reasons for failure of equipment, it is often considerably more difficult to understand a malfunction than to understand damage. In the latter instance, the equipment ceases to operate permanently and the reasons for the inoperative condition usually are revealed upon disassembling and inspecting the equipment. If the damage results from vibration, the nature of the damage often is a fracture of structural elements as a consequence of fatigue, or some condition related to fatigue. On the other hand, failure involving a malfunction is often much more subtle. There often is no physical evidence of degradation of the equipment, and the malfunction can be noted only by monitoring the performance of the equipment while exposed to a vibratory condition. From an observation and measurement of the degraded performance, it may be possible to infer the nature of a physical mechanism that would lead to an equivalent degradation of performance. Then, a mechanical analog of the equipment is hypothesized in such a manner that some aspect of its

response to vibration can be interpreted in terms of the observed degradation of performance of the equipment. Thus, the research effort is directed toward the following aspects of the problem:

(a) Devising the mechanical analog so that its response correlates with the observed degradation of the equipment.

(b) Investigating the response of the analog to various forms of vibration.

(c) By combining the results of (a) and (b), predicting the performance of the equipment when subjected to various forms of vibration.

1.2. An Outline of the Research Program

The basic concept of the present program is to determine, by such means as may be appropriate, the most suitable mechanical analogs of actual equipment that are deemed useful in understanding the nature of the failure mechanism, and to study the relation between the response of such analogs and observed failure of the equipment. A fundamental problem, then, is the creation of the analog.

In principle, the program involves the examination of a large number of typical structures and components with the objective of determining the type of analog by which each can be represented. Such an examination has been started by choosing a few selected electronic and mechanical components. This report includes the results of preliminary tests on one of them; others will be tested as the program proceeds. To evaluate a single component may require extensive experimentation, and progress may be slow. To expedite the program, it has been assumed that certain simple, linear analogs are basic to many devices. An

investigation of the response of these analogs to various types of vibration has been started, in anticipation that concurrent or subsequent tests of actual devices will reveal that the chosen analogs are appropriate for representing the devices.

1.2.1. Selected Analogs

The analog structures adopted for analysis during the initial phases of the investigation are shown schematically in Fig. 1.1. Each of these structures is considered to be subjected to each of the several types of vibration outlined in Section 1.2.3. For each analog structure and each type of vibration, several criteria of failure have been selected to define the capabilities of the several structures to withstand various types of vibration. The criteria of failure are outlined in Section 1.2.2. The various analog structures illustrated in Fig. 1.1 are as follows:

a) The most generally useful type of analog structure for vibration analysis is the linear single degree of freedom system with viscous damping, illustrated in Fig. 1.1(a). Many component parts of actual equipments are either close approximations to single degree of freedom systems, or they respond predominantly in one mode and may be treated mathematically as a single degree of freedom system. In formulating the analog structure, it is necessary to idealize the real system in terms of the mass, stiffness and damping of the analog. Such an analog is useful only if the criterion can be expressed in terms of maximum values of displacement, velocity, or acceleration of the mass.

b) Where the analog requirements are met by a structure which responds as a single degree freedom system but wherein the

criteria of failure involve stress or strain, including fatigue, it becomes necessary to replace the hypothetical spring of the system at (a) by a structure in which stress and strain can be related to those of the real structure. One convenient analog structure which meets these requirements is the massless beam with concentrated load illustrated in Fig. 1.1(b). Then the results obtained with the analog structure of Fig. 1.1(a) apply, provided the displacement of the mass relative to the support is transformed to stress or strain in the beam. Beams with a large variety of end conditions and load positions may be used in the analysis, several of which are illustrated in Fig. 1.1(b).

c) In many instances the mass of the beam or the loads carried by the beam are distributed along the length of the beam in such a manner that the mass of the beam cannot be neglected, as assumed in the analog structures illustrated in Fig. 1.1(b). The most simple analog structure involving a distribution of mass is a beam of uniform section and uniform mass distribution. Such a structure is typical of many non-load carrying structural members and of structural members carrying a multiplicity of relatively small loads. Various end conditions can be assumed, corresponding to those used in Fig. 1.1(b), as illustrated at Fig. 1.1(c).

d) A more complicated type of analog structure which is required in some instances combines the essential features of the structures illustrated in Figs. 1.1(b) and 1.1(c). In Fig. 1.1(d), the mass

of the beam is distributed uniformly from end to end but the beam in addition carries a concentrated load similar to that illustrated in Fig. 1.1(b). This is an analog of a type of structure encountered frequently in mechanical devices, and may embody the various end conditions illustrated in Fig. 1.1(d).

1.2.2. Criteria of Failure

In postulating possible criteria of failure of equipment when subjected to vibration, it is hypothesized that each instance of failure can be related to some definable characteristic of the response of the applicable analog structure, selected from among those illustrated in Fig. 1.1. Thus, if the equipment under study is considered to have a vulnerable structure which can be represented properly by one of the analog structures illustrated in Fig. 1.1, the response of the analog to vibration is noted. Depending upon the type of equipment failure would be indicated by some characteristic of the response. Such characteristics may then be cataloged as criteria of failure. Several possible criteria have been formulated and are outlined in the following paragraphs:

a) Failure of equipment may occur because some part of the equipment experiences vibration whose displacement amplitude exceeds the maximum permissible displacement of that part. In general, the critical displacement is a displacement relative to the principal chassis or mounting points of the equipment. For example, a malfunction may occur because uninsulated electrical wiring of the equipment experience a sufficiently large displacement during vibration that a short-circuit results. As a further example, a fragile element such as an envelope of

a vacuum tube is subject to damage if its displacement during vibration becomes sufficiently great to permit impact or contact with an adjacent structure. Then the criterion of failure is an excessive displacement.

b) A malfunction may occur in certain types of mechanisms or structures not because the displacement becomes excessively great during a single cycle of vibration but rather because the displacement exceeds allowable values for an excessively large percentage of the time. For example, in an equipment using an incandescent lamp as a light source, vibration of the lamp filament with excessively large amplitude causes the light source to go out of focus in the optical system and the equipment becomes inoperative. As another example, the microphonic noise from a vacuum tube can be related to the relative motion of the conducting elements within the vacuum tube. When such elements vibrate with relatively large amplitudes during an excessively large percentage of the time, the vacuum tube then no longer performs its intended function because of excessive microphonic noise. Then improper operation of the equipment results. The criterion of failure is that the displacement exceeds a stated value during greater than a maximum permissible fraction of the time.

c) Damage to equipment may occur because the stress or strain exceeds the allowable value, and rupture or permanent deformation of a mechanical element may occur. This criterion is different from the maximum-displacement criterion mentioned in

paragraph (a) above, because a relatively compliant structure may experience a large displacement even though the stress is small. Then the criterion of failure is excessive stress.

d) Although the stress in a structure is not excessive for a single cycle of vibration or even for several cycles of vibration, damage may occur from fatigue if a significantly large stress is applied for many cycles of repetition. This is an important cause of damage to equipment during vibration, and is hypothesized here as a criterion of failure.

1.2.3. Types of Vibration

The vibration that has been found from measurements to exist in actual field service is relatively complex and often defies an orderly description of its characteristics. Ultimately, an investigation of the mechanism of failure in equipment subjected to vibration must take cognizance of the complexities of this vibration. For purposes of the initial phase of the investigation, however, the vibration is idealized by assuming several classical forms which are used to evaluate the response of the analog structures illustrated in Fig. 1, using the several criteria of failure set forth in the preceding paragraph. The idealized forms of vibration included in this initial phase of the investigation are illustrated in Fig. 2 and described in the following paragraphs:

1) The fundamental form of vibration is the sinusoid illustrated in Fig. 1.2(a). Although this classical form of vibration seldom exists in field conditions, it is sometimes used for laboratory testing and finds great use in defining the dynamic characteristics

of physical systems. Then such characteristics are applied later in evaluating the response of such systems to more complex forms of vibration.

2) The second idealized form of vibration is the combination of sinusoids illustrated in Fig. 1.2(b). If the frequencies of such sinusoids are nearly equal, the result is beats.

3) A form of vibration that is simple in concept but complicated in analysis is the sinusoid with continuous change in frequency, as illustrated in Fig. 1.2(c). Such a vibration pattern exists during starting or stopping of a rotating machine, and has been sugject to analysis with this interest in mind. More in the context of the present research, however, is the common practice of laboratory testing in which the vibration frequency is scanned or swept over a relatively wide band of frequencies.

4) The broad band random vibration with Gaussian distribution of magnitudes and flat spectrum of power density, illustrated in Fig. 1.2(d), is a classical type of vibration which provides a basis for understanding certain real problems even though it seldom exists in real circumstances.

5) The random vibration illustrated in Fig. 1.2(e) is similar to that illustrated in Fig. 1.2(d) except that the relatively large values which occur occasionally in vibration which conforms to the classical theory are clipped or eliminated. The magnitude--limited vibration is more consistent with many actual conditions because inherent limitations of many physical processes prevent the occurrences of extremely large magnitudes of vibration.

1.3. Status of the Research Program

Several phases of the research program have been pursued concurrently; some interim results have been obtained but many of the tasks are only partially complete at this time. This report is to be interpreted as an account of the work done during the first year of the project rather than a report on conclusions reached.

Some progress has been made toward determining an appropriate analog by which to represent a vacuum tube when the criterion of failure is based upon microphonic noise output from the tube. After many delays resulting from necessary modifications of the monitoring circuit, records of noise output have been obtained for a number of conditions of sinusoidal and random vibration. For sinusoidal excitation, the total microphonic noise in volts rms was measured and plotted as a function of the excitation frequency as shown, for example, in Fig. 2.8. For random excitation, the noise output from the tube was passed through a band bass filter with variable center frequency; the output from the filter was plotted in terms of volts rms as a function of the center frequency of the filter, as shown, for example, in Fig. 2.11. The curves of Figs. 2.8 and 2.11 exhibit two well-defined peaks at frequencies less than 800 cps with a very well-defined valley therebetween. Further effort will be directed toward hypothesizing a mechanical analog that would produce the observed results; the depth of the valley suggests coupling between two mechanical elements of the tube but this suggestion has not been explored in detail. A more detailed account of work accomplished to date on this task is set forth in Section 2.

To form a basis for later evaluation of more complicated systems, the response of a damped single degree of freedom system to various forms of vibration has been investigated. In general, the forms of vibration are those set forth in Section 1.2.3 and the results are presented in a form adapted for ready evaluation in terms of the criteria given in Section 1.2.2.

The response of a system to sinusoidal vibration is discussed in Section 4.1. This material is not original; rather it is taken from the established technical literature and set forth here in a form particularly adapted for use in the analysis of more complicated systems wherein each normal mode is treated as a single degree of freedom system.

The response of a system to an excitation consisting of combined sinusoids is considered in Section 4.2. In principle, the results of Section 4.1 can be superposed inasmuch as only linear systems are considered. However, in applying certain of the criteria of Section 1.2.2, the distribution curves given in Fig. 4.6 offer a convenient means of evaluation.

A number of investigators (see the references to Section 4) have studied the response of a simple system in which the excitation is quasi-sinusoidal in that the excitation frequency varies continuously in a prescribed manner. In general, most of the efforts have been concerned with the maximum value of the response. In the present study, additional information on the distribution of response cycles of different magnitudes is required to apply the several criteria of failure outlined in Section 1.2.2. This problem cannot be solved readily by theoretical analysis because of mathematical complexities; neither is it well adapted

to solution by digital computer because of the extensive computation time required to obtain the necessary range of results. Furthermore, the excitation cannot be described in general terms but rather a number of specific excitation forms must be investigated. One such form, in which the excitation frequency varies exponentially with time, has been studied using an analog computer. The results are in terms of maximum response, as shown in Figs. 4.9 to 4.11 for several values of the fraction of critical damping, and in terms of the distribution of the response cycles with respect to magnitude. The latter results are given in Fig. 4.12. The data given in Figs. 4.9 to 4.12 inclusive are adequate for application to the criteria of failure given in Section 1.2.2 for the specific excitation considered; work is continuing with the objective of investigating other forms of excitation and generalizing the results.

The material in Section 4.4 on the response of a system to broad band random vibration with flat spectrum of power density and Gaussian distribution of magnitude values is taken largely from the established literature. It is included here for ready reference, in a form suitable for application to the criteria of failure outlined in Section 1.2.2.

In many practical situations, the excitation has characteristics that are quasi-Gaussian in the sense that the higher values do not exist because of physical limitations; e.g., limited power, inability of structures to transmit very large forces, etc. The consequence of limiting the magnitude of the random excitation has been investigated by analog computer and the results are set forth in Section 4.5. These results are believed to be original. In general, they show that the response has nearly-Gaussian characteristics even though the excitation may have

strongly non-Gaussian properties. The rms value of the response increases relative to that of the excitation as the higher values in the excitation are eliminated; this result is summarized in Fig. 4.30.

A considerable effort was applied to the study of fatigue, with the objective of investigating the possibility of relating fatigue damage to the particular pattern of stress variation. One task, thought initially to be well defined, involves the stress pattern in a beam when the excitation is a variable frequency sinusoid whose frequency band includes the lowest natural frequency of the beam. All of the complexities of the problem were not foreseen at the time the task was initiated; as a consequence, a considerable quantity of experimental data has been accumulated and cannot be applied toward the intended end result without, at least, additional experimental work and analysis. It was not anticipated, for example, that a change in the direction of frequency variation would make the difference shown by a comparison of Figs. 3.12 and 3.13 (or Figs. 3.14 and 3.15) or that the rate of frequency variation would make the difference shown by a comparison of Figs. 3.13 and 3.15. A much better appreciation of the complexities of the problem has now been gained, and additional experimental work is planned to provide an interpretation of results obtained and to be obtained. In order that the report be complete, all of the test results on this task are set forth in Appendix C, even though their proper interpretation must remain in doubt at this time.

One of the primary hypotheses of the present research is that much can be predicted about the failure of equipment in service or

laboratory conditions if the response of a structure to various forms of vibration can be calculated. Such a calculation is greatly facilitated by the normal mode method of analysis. This involves finding the normal modes of a structure, determining the response of each mode to an excitation by considering it to be a single degree of freedom system, and then superposing the responses. It is to this end that the response of a simple system to various ideal forms of excitation has been investigated, as set forth in Section 4. It is also to this end that normal mode information on a variety of classical beam types is set forth in Section 5. The information includes expressions for displacement, acceleration and stress, together with frequency equations, normal mode expressions and numerical values for mode participation factors.

The following sections discuss in detail the work done to date and the results obtained. Section 2 discusses the experiments with the type 12AU7A vacuum tube, Section 3 gives an account of the experiments directed toward obtaining an understanding of the fatigue of a beam with variable frequency sinusoidal excitation, Section 4 discusses the response of a simple system to various forms of excitation, and Section 5 discusses beams from the normal mode approach. Three appendices are included: Appendix A describes the analog computer used for some of the work reported in Section 4, particularly Section 4.5; Appendix B is a detailed discussion of vibrating systems, in support of Section 5; Appendix C sets forth the results of endurance tests, the context for which is supplied by Section 3.

2. VIBRATION TESTS OF A VACUUM TUBE

This section of the report describes the results obtained to date in that phase of the program which attempts to relate malfunction of actual components to the characteristics of the applied vibration. An ultimate objective is to infer from the nature of the malfunction a mechanical analog of the component which can be used in subsequent analyses to predict malfunction as a consequence of various types of excitation.

Previous attempts, reported in references 2. 1 and 2. 2, to relate malfunction of equipment to the characteristics of vibration had been concerned with tests of complete equipments rather than tests of individual components (a vacuum tube or a relay). The correlation sought in the previous tests was difficult to achieve, in part because the equipments included many components and many modes of failure. It was pointed out by Crandall and Cohoon (ref. 2. 3) that some apparent correlation exists in the results reported in reference 2. 2 between sinusoidal and random vibration. However, it is not possible to determine whether this can be ascribed to a particular component or to the equipment as a whole. To minimize such uncertainties, the present program is concerned with tests of selected individual components.

For the initial experiment in the present program, a 12AU7A vacuum tube has been selected. The experiment consists of mounting the tube in several positions on an electrodynamic vibration exciter, and subjecting it first to sinusoidal vibration and then to random vibration, at several different magnitudes of excitation. Figure 2. 1 shows the tube mounted with the axis of symmetry of the glass envelope parallel to the direction of vibration; for the alternative test, as shown in Fig. 2. 2,

the axis of symmetry is perpendicular to the direction of the vibration.

The tube is connected in a circuit intended to energize the tube in a manner corresponding to one typical mode of operation and to monitor that part of the electrical output which can be ascribed to the effects of vibration. The details of the circuit used to energize the tube and to monitor its output, together with a description of the experimental method, are included in Section 2. 1. The results obtained to data are set forth in Section 2. 2.

2. 1 Monitoring Circuit and Method of Operation

The vacuum-tube vibration-test apparatus may be divided into three functional parts: (1) the vacuum-tube activation circuits, (2) the mechanical driver, and (3) the readout instrumentation. The details of the read-out instrumentation depend upon the type of excitation (sinusoidal or random) and are described with reference to the particular excitation.

2. 1. 1 Vacuum-Tube Activation Circuits. From the standpoint of supplying its needs, a 12AU7A tube is a five-terminal device. (The 12AU7A is actually a twin tube, but only one section is used in this experiment.) Two of the terminals are for filament power supply; they are directly and permanently connected to a 6-volt automobile storage battery. The remaining three terminals (cathode, grid, and plate) are brought away from the exciter to the instrumentation area. As indicated in Fig. 2. 3, the 12AU7A vacuum tube is operated as a grounded-grid amplifier. This circuit permits two of the three tube terminals to be at low impedance to ground, thus minimizing stray electrostatic pickup. Grid bias of six volts is provided by a battery of four dry cells, whose internal impedance is much less than the 20 ohm cathode resistor. (The

large bypass capacitor insures a similarly low ac impedance.) Plate potential is supplied by a Philbrick Type R100B high-stability, low-noise power supply fixed at 300 volts. This unit, of a type used with analog computer amplifiers, ensures that random noise from the power supply does not mask mechanically-produced random noise.

The "local oscillator" provides a 300 millivolt rms input to the tube at a frequence of approximately 14,000 cycles. The oscillator signal is amplified and balanced out in a differential amplifier by adjustment of the balance and phase controls in the comparison circuit. The oscillator signal is turned on only during equipment setup time and in calibration periods; observed on the monitor scope, it assures that the 12AU7A, its power supplies, and the differential amplifier are operating correctly. Damage to the tube or operation thereof in a nonlinear range would be immediately apparent.

Output is taken from the tube via a 1 μf capacitor and fed to the Alinco Type 516A differential amplifier, whose low-impedance output is fed to the readout instrumentation which is described in subsequent sections.

2.1.2 Excitation and Readout

2.1.2.1 Sinusoidal excitation. In the experiments involving sinusoidal vibration, the excitation is maintained with a constant acceleration amplitude of a predetermined value, scanned at a slow rate between the limits of 100 cps and 1500 cps. This frequency band was selected because significant output from the tube was observed at frequencies between 100 cps and 1500 cps; below 100 cps the output was not appreciable and above 1500 cps the tube mounting tended to vibrate in its natural modes and thereby prevent control of the vibration applied to the

tube. An audio oscillator provides the signal source for the exciter; it is used in conjunction with an accelerometer and includes a servomechanism adapted to maintain the acceleration amplitude at a predetermined value. The signal from the oscillator passes through a low pass filter having a cut-off frequency of 1500 cps en route to the amplifier from which it is fed directly to the exciter. The circuit is shown schematically in Fig. 2.4.

Output from the Alinco differential amplifier is monitored by a Hewlett Packard Type 122A oscolloscope and another Ballantine Type 320B true rms meter, after which it is fed through a Krohn-Hite Type 330MR bandpass filter with a pass band of 100 to 1500 cps. The filtered signal enters a Moseley Model 60B logarithmic converter, which supplies the logarithm of the rms voltage to the Y axis of a Moseley Model 135 X-Y plotter. The X (frequency) axis of the plotter is driven from a potentiometer on the frequency control knob of the audio oscillator. Before each graph is made, switch S is thrown , connecting an oscillator and counter into the readout instrumentation line. The point defined by X = 700 cps, Y = - 10 db is set to a predetermined position on each graph prior to writing a curve so that the curves can be compared directly.

2.1.2.2 Random excitation. When the tube is tested under random excitation, a General Radio Type 1390B random noise generator replaces the audio oscillator as the signal source. It is fed through a Krohn-Hite Type 330MR bandpass filter with pass band set at 100 to 1500 cps, amplified in a small variable-gain audio amplifier, and then sent to a 1500 cps low pass filter. Output from this filter drives the power amplifier and exciter. Acceleration is monitored in the same manner as with sinusoidal excitation, except that the servomechanism is

inoperative, but each component of vibration throughout the frequency band is controlled by filters to maintain a constant value of mean square acceleration density.

Output from the Alinco differential amplifier is monitored by the scope and rms meter as before. Now, however, the signal enters a Radiometer-Copenhagen Type FRA2T (spec.) wave analyzer. This instrument incorporates a nearly square filter with a bandwidth of 25 cps. It has two amplitude readouts, a meter, and a modulated 1500 cps signal. The latter is sent to the logarithmic converter and on to the X-Y plotter. Calibration is achieved as before, except that the wave analyzer is first calibrated to read -10 db before the plotter is calibrated. The circuit is shown schematically in Fig. 2.5.

The remaining problem is to sweep the X-axis of the plotter in synchronism with the harmonic analyzer. This is not as simple as in the sinusoidal case, since there is no direct frequency sweep voltage source in the harmonic analyzer as there is in the audio oscillator. To further complicate matters, the harmonic analyzer dial is neither linear nor logarithmic, but a combination of the two.

This problem is resolved by use of the frequency-tracker circuit shown in Fig. 2.5. An output at (60kc - F_1) is available from the wave analyzer, where F_1 is the frequency from the audio oscillator which is used in this instance only to drive the X-Y recorder on the X-axis. The resultant signal is applied to a diode shunting the terminals of a second wave analyzer tuned to 60 kc. The diode is nonlinear; given inputs at (60 kc - F_1 + F_2) and F_2, it will yield additional outputs at (60 kc - F_1+F_2) and (60 kc - F_1-F_2). If and only if $F_1 = F_2$ will there be output

at 60 kc. Thus an operator can manually "follow" the sweeping audio oscillator frequency with the Radiometer wave analyzer by turning it so that output is seen at 60 kc on the second analyzer.

2. 2 Discussion of Results

The results obtained to date are in terms of the rms voltage output of the type 12AU7A vacuum tube ascribable to the effects of vibration, monitored as explained in Section 2. 1. Two sets of results are given; one for the tube in the position shown in Fig. 2. 1 (hereinafter designated " vertical position"), and one for the tube in the position shown in Fig. 2. 2 (hereinafter designated "horizontal position"). For each mounting position, results are given for both sinusoidal and random excitation, several magnitudes of each. For sinusoidal vibration, the excitation is defined in terms of frequency and acceleration amplitude; the output of the tube is total voltage in rms volts. For random vibration, the excitation is defined in terms of mean square acceleration density over a nominal bandwidth of 100 to 1500 cps. The output with random excitation is plotted in terms of voltage as a function of frequency, where the frequency is the center frequency of a band pass filter having a bandwidth of 25 cps.

2. 2. 1 Tube in Vertical Position. With the tube in the vertical position, excitation magnitudes in sinusoidal vibration were 1. 9, 2, 2. 5, 3, 4, 5, 6, 8, and 10 g acceleration amplitude. Corresponding excitation magnitudes for random vibration were 0. 0004, 0. 0008, 0. 0016, 0. 0025, 0. 0066, 0. 0105, and 0. 0150 g^2/cps mean square acceleration density. Representative records of output voltage versus excitation magnitude are reproduced here, Figs. 2. 6 to 2. 9 for sinusoidal vibration

and Figs. 2. 10 to 2. 13 for random vibration.

As indicated in Figs. 2. 6 to 2. 13, the output voltage shows two well-defined peaks and a well-defined valley within the frequency band of 100 cps to approximately 800 cps. Above 800 cps, the output voltage shows less orderly characteristics, particularly for the case of sinusoidal vibration. The ragged appearance of the trace in Figs. 2. 10 to 2. 13 is substantially normal for the output of a narrow band filter when the input is random vibration.

A concerted effort has not yet been made to interpret the data in Figs. 2. 6 to 2. 13 in terms of a physical structure. A somewhat superficial inspection suggests (1) a structure with at least two resonance frequencies, and (2) possibly some coupling between the modes to which such resonance frequencies correspond. The possible existence of coupling is inferred from the fact that the voltage output at the bottom of the valley is at a minimum for the entire record. To assist in future interpretation of the results, some of the characteristics of Figs. 2. 6 to 2. 13 are summarized in Figs. 2. 14 to 2. 16. It is noted that the frequencies of the peaks and valleys tend to decrease somewhat as the magnitude of the excitation increases. The variation of these frequencies is shown graphically in Fig. 2. 14 as a function of output voltage, the dotted lines indicating random vibration and the solid lines sinusoidal vibration. The magnitudes of the output voltage at the two peaks and the valley, as a function of the excitation magnitude, is shown in Fig. 2. 15 for the sinusoidal vibration and in Fig. 2. 16 for random vibration. No attempt has yet been made to draw inferences from the trends of these curves.

2.2.2 Tube in Horizontal Position. With the tube in the horizontal position, excitation magnitudes in sinusoidal vibration were 1, 2, 3, 4, 6, and 8 g acceleration amplitude. Corresponding excitation magnitudes for random vibration were 0.0016, 0.0066, 0.015, 0.027, 0.041, 0.092, and 0.160 g^2/cps mean square acceleration density. Representative records of output voltage are reproduced here, Figs. 2.17 to 2.20 for sinusoidal vibration and Figs. 2.21 to 2.24 for random vibration. In general, these records show two peaks and a valley in the frequency band of 100 to 600 cps; the frequencies at which the peaks and valley occur tend to be lower than those indicated by Figs. 2.6 to 2.13 for the vertical position. Moreover, the peaks and valleys tend to merge as the excitation magnitude increases and are hardly discernible at the most severe excitation.

References

2.1 "An Investigation of Functional Failure Due to Random and Sinusoidal Vibration," by A. J. Curtis and H. T. Abstein, WADD Tech. Note 61-24, September 1961.

2.2 "Random-Sinusoidal Vibration Correlation Study," by J. E. Foster, WADD Tech. Note 61-43, July 1961.

2.3 Informal communication by S. H. Crandall and J. Cohoon, Massachusetts Institute of Technology.

2.4 "The Reduction of Microphonics in Triodes," by A. H. Waynick, J. Appl. Phys., Vol. 18, Feb. 1947.

2.5 "Microphonism in a Subminiature Triode," by V. W. Cohen and A. Bloom, Proc. I.R.E., August 1948.

2.6 "Microphonism in the Dynamically Operated Planar Triode," by J. A. Wenzel and A. H. Waynick, Proc. I.R.E., May 1950.

2.7 "A Practical Design Theory for Minimization of Vibration Noise in Grid-Controlled Vacuum Tubes," by G. H. Gross, preprint for I.R.E. National Convention, March 18-21, 1957.

2.8 "The 7625-A Small Rugged Ceramic Tube for Low Level Amplifier Use," by J. M. Connelly, preprint for Winter Meeting, A. I. E. E., Feb. 2, 1960.

2.9 "An Impulse Test for Evaluating the Vibrational Characteristics of Receiving Tubes Over a Wide Frequency Range," by S. A. Jolly and W. U. Shipley, 1958 I. R. E. National Convention Record.

2.10 Military Specification MIL-E-1/246D on Electron Tube, Receiving, 7 August 1961.

3. FATIGUE

This section sets forth in the initial subsections the supporting information in the theory of fatigue that is necessary to evaluate criteria of failure involving fatigue. This includes, particularly, the theory of cumulative damage when the stress amplitude varies from cycle to cycle throughout the life of the structure. In later subsections, a description is given of the experimental work that has been carried out with the objective of evaluating failure by fatigue of a beam excited by sinusoidal vibration in which the excitation frequency varies continuously.

3.1 Unbonding During Reversed Slip -- An Hypothesis

One important criterion of failure involves damage to a structure as a consequence of fatigue; i.e., repeated reversal of stress until actual rupture occurs. The theory of fatigue is not well understood in a fundamental sense. It is, therefore, difficult to relate the effect of variations of the physical conditions to failures that occur in service. For example, it has been a conventional practice for many years to evaluate the fatigue properties of materials by subjecting carefully manufactured specimens of the material to tests in which the stress is varied in a sinusoidal manner until failure occurs. The stress amplitude is maintained constant throughout the test, and the results are recorded simply by plotting the stress amplitude versus the number of cycles to failure. The test parameters vary over a wide range of numerical values, e.g., the number of cycles to failure may vary in one group of specimens from a few tens or hundreds of cycles to tens of millions of cycles.. Test results of this type find wide usefulness in comparing the endurance properties of different materials.

It is difficult to extend the results of laboratory fatigue tests to actual service conditions. These difficulties are the result of several important factors:

(a) The stress distribution and surface finish of an actual structure may be significantly different from that of the specimen used to evaluate in the laboratory the fatigue properties of the material. Failure by fatigue involves growth of a crack, and therefore is greatly influenced by local stress conditions.

(b) The stress amplitude is seldom a constant throughout the service life of an actual structure; this is a significant difference from the usual laboratory test.

(c) Failure of structures in actual service often occurs because the structure responds in a resonant manner to a vibratory excitation. The stress is a function of the damping and elastic linearity of the structure itself, properties which are not of first order importance in the conventional laboratory thest wherein the stress results from an imposed load.

A great deal of attention has been directed in recent years to attempts at the formulation of theories of fatigue damage for evaluating the cumulative effect of cycles of stress in which the stress amplitude varies from cycle to cycle. One of the simplest theories of cumulative damage, and one quite well adapted to the purposes of the present research, was proposed in various forms by Palmgren, Langer, and Miner (refs. 3.1 and 3.3). It is based upon the observation that when the results of conventional fatigue tests are plotted with stress amplitude on the ordinate and number of cycles to failure on the abscissa, a continuous

curve can be drawn through the experimental points, as suggested in Fig. 3.1. When the number of cycles to failure is small, the stress in a ductile material is greater than the yield stress and the curve deviates from a straight line, as suggested by the horizontal dotted line at the left of Fig. 3.1. By interpreting stress as the product of strain and modulus of elasticity, the curve obtained at lower values of stress may be extended to higher values, as indicated by the dotted line. For a very large number of cycles to failure, the results seem to depend upon the type of material. For some materials, such as steel, there is considerable evidence that an endurance limit stress exists, below which failure does not occur after an infinitely large number of cycles of stress reversal. For other materials, such as aluminum, failure seems to occur for relatively small values of stress amplitude, even though this may involve a very large number of cycles of stress reversal. These alternatives are indicated by the dotted lines at the right of Fig. 3.1.

It has been shown by Shanley (ref. 3.4)* that the curve of stress amplitude versus number of cycles to failure illustrated in Fig. 3.1 can be explained by assuming that failure in fatigue occurs by growth of a crack propagating through the material in accordance with the following mathematically expressed physical law:

$$h = Ae^{\beta n} \tag{3.1}$$

where h = crack depth,

A = a constant,

β = a factor depending on the stress amplitude,

---

* Much of the material in Sections 3.1 and 3.2, including Figs. 3.1 through 3.5, inclusive, is taken from reference 3.4.

n = number of cycles of stress reversal.*

A hypothetical curve of crack depth versus cycles of stress reversal is shown in Fig. 3.2.

The expression given by Eq. (3.1) may be related to fatigue life by the following interpretations:

a) Let $h = h_o$ be the crack depth at which failure occurs.

b) Let $n = N$ be the number of cycles to failure.

c) In accordance with the Ramberg-Osgood hypothesis (ref. 3.2) on inelastic strain, let the crack growth parameter β be replaced by the following expression:

$$\beta = C\sigma^{\alpha} \tag{3.2}$$

where σ = nominal stress, e.g., $\sigma = P/A$ in direct tension,

α = an exponent determined by curve fitting, and

C = a constant.

Substituting from Eq. (3.2) into Eq. (3.1), letting $h = h_o$, and letting $n = N$, the following expression is obtained

$$h_o = A\, e^{C\sigma^{\alpha}N} . \tag{3.3}$$

Taking the natural logarithm of both sides:

$$\log_e h_o = \log_e A + C\sigma^{\alpha}N . \tag{3.4}$$

Equation (3.4) may be solved for $\sigma^{\alpha}N$ as follows:

$$\sigma^{\alpha}N = (\log_e h_o - \log_e A)/C . \tag{3.5}$$

The right hand side of Eq. (3.5) may be replaced by a constant:

$$\sigma^{\alpha}N = B \tag{3.6}$$

---

* Strictly speaking, n is the number of cycles of stress reversal after the first, and should be written n-1 in Eq. (3.1) and subsequent equations. However, in fatigue, n is usually a large number, and $n \cong n-1$.

where α defines the slope of the σ-N curve when plotted to double logarithmic coordinates, as indicated in Fig. 3.1. Experimental data usually justify the straight line required by Eq. (3.6).

3.2 Effect of Stresses of Varying Amplitude

An hypothesis for evaluating the cumulative effect of stress cycles of different amplitudes may be developed with reference to Fig. 3.3, which indicates several cycles at each of the stress amplitudes, $\sigma_1, \sigma_2, \ldots$. The objective is to find the constant stress amplitude σ_r indicated in Fig. 3.4 for which failure occurs after a number of cycles equal to the summation $\Delta n_1 + \Delta n_2 + \Delta n_3$, where Δn_1, Δn_2, and Δn_3 are the numbers of cycles at σ_1, σ_2, and σ_3, respectively. A diagram of crack size versus number of cycles, similar to Fig. 3.2, is shown in Fig. 3.5, wherein a curve is included for two of the stresses σ_1, σ_2. It is assumed that Δn_1 and Δn_2 are small relative to the fatigue life N, and that failure occurs as a consequence of a few cycles of stress reversal on the σ_1 curve, then a few on the σ_2 curve, followed by a few on the σ_1 curve, etc. Then the curves of h versus n may be considered straight lines for short increments of their lengths, and the incremental growth patterns for the cracks are as indicated. A single crack must have a growth pattern without discontinuities, as indicated by curve σ_r in Fig. 3.5. Since the rate of crack growth is assumed to be a function of crack depth, the effective rate of growth at any value of n will be determined by the weighted average of the rates for σ_1 and σ_2, at the same crack depth:

$$\left(\frac{dh}{dn}\right)_r = \frac{\Delta n_1 \left(\frac{dh}{dn}\right)_1 + \Delta n_2 \left(\frac{dh}{dn}\right)_2}{\Delta n_1 + \Delta n_2} \quad . \tag{3.7}$$

If more than two stress amplitudes are involved in the sequence of stress cycles, the above expression may be generalized as follows:

$$\left(\frac{dh}{dn}\right)_r = \frac{\sum_i \Delta n_i \left(\frac{dh}{dn}\right)_i}{\sum_i \Delta n_i} \quad . \tag{3.8}$$

An expression for crack depth at any given stress amplitude σ_i, for use in Eq. (3.8), can be obtained by combining Eqs. (3.1) and (3.2):

$$h_i = A\, e^{C\sigma_i^{\alpha} n} \quad . \tag{3.9}$$

Differentiating with respect to n:

$$\left(\frac{dh}{dn}\right)_i = AC\sigma_i^{\alpha}\, e^{C\sigma_i^{\alpha} n} \quad . \tag{3.10}$$

The resultant rate of growth then is obtained from the weighted average of the rates at the several stress amplitudes, as indicated by Eq. (3.8),

$$\left(\frac{dh}{dn}\right)_r = AC \left(\frac{\sum_i \Delta n_i \sigma_i^{\alpha}}{\sum_i \Delta n_i} \right) e^{C\sigma_r^{\alpha} n} \tag{3.11}$$

where σ_r is used in the exponent because, by definition, σ_r would produce the same depth of crack as the sequence of stress amplitudes σ_i. The corresponding expression for a constant stress amplitude σ_r is, from Eq. (3.10):

$$\left(\frac{dh}{dn}\right)_r = AC\sigma_r^{\alpha}\, e^{C\sigma_r^{\alpha} n} \quad . \tag{3.12}$$

Combining Eqs. (3.11) and (3.12), the following expression is obtained for σ_r^{α}:

$$\sigma_r^{\alpha} = \frac{\sum_i \Delta n_i \, \sigma_i^{\alpha}}{\sum_i \Delta n_i} \quad . \tag{3.13}$$

Solving Eq. (3.13) for σ_r :

$$\sigma_r = \left[\frac{\sum_i \Delta n_i \, \sigma_i^{\alpha}}{\sum_i \Delta n_i} \right]^{1/\alpha} \quad . \tag{3.14}$$

A comparison of the results predicted by the above expression with those obtained experimentally (ref. 3.5) indicated that a greater weight should be given in the theory to stress cycles of greater stress amplitude. This suggested a re-examination of Eq. (3.1), which indicates, when $n = 1$, that A is the depth of crack produced on the first stress cycle. On the hypothesis that the depth of this crack would be a function of stress, Eq. (3.9) is modified to the following form:

$$h = A' \sigma^{\varepsilon\alpha} \, e^{C\sigma^{\alpha} n} \quad . \tag{3.15}$$

Differentiating Eq. (3.15) with respect to n to obtain an expression corresponding to Eq. (3.12):

$$\left(\frac{dh}{dn}\right)_r = A' C \sigma^{(1+\epsilon)\alpha} \, e^{C\sigma^{\alpha} n} \quad . \tag{3.16}$$

Proceeding now in the manner used to obtain Eq. (3.14) and substituting $\lambda = (1+\epsilon)$, the following expression is now obtained for the equivalent stress σ_r :

$$\sigma_r = \left[\frac{\sum_i \Delta n_i \, \sigma_i^{\lambda\alpha}}{\sum_i \Delta n_i} \right]^{1/\lambda\alpha} \quad . \tag{3.17}$$

The reduced stress σ_r may be defined dimensionlessly with reference to the rms stress $\bar{\sigma}$ of the sequence of varying stress cycles:

$$\frac{\sigma_r}{\bar{\sigma}} = \left[\frac{\sum_i \Delta n_i \left(\frac{\sigma_i}{\bar{\sigma}}\right)^{\lambda\alpha}}{\sum_i \Delta n_i} \right]^{1/\lambda\alpha} . \qquad (3.18)$$

3.3 Random Vibration

A commonly encountered situation involving failure by fatigue is indicated in Fig. 3.6 which shows a mathematical model of a mechanical structure. Excitation consists of vibration x of the base, and fatigue would occur as a consequence of repeated cyclic stress in the structure represented by the spring k. Denoting relative motion by $z = y-x$, the stress in the structure can be represented by $\sigma = az$. When the excitation x is broad-band random vibration defined in terms of mean square acceleration density, the sequence of stress cycles is expressed in terms of probabilities defined by the Rayleigh distribution expressed mathematically by Eq. (4.23). This is written in terms of stress as follows:

$$p\left(\frac{\sigma}{\bar{\sigma}}\right) = \frac{\sigma}{\bar{\sigma}} e^{-\frac{1}{2}\left(\frac{\sigma}{\bar{\sigma}}\right)^2} d\left(\frac{\sigma}{\bar{\sigma}}\right) . \qquad (3.19)$$

The integral of the expression for probability density given by Eq. (3.19) is the total number of cycles of stress reversal occurring between the stress values defined by the limits of integration. By integrating from zero to infinity, the integral becomes equal to the total number of stress reversals, indicated by $\sum \Delta n_i$. Making this substituting for $\sum \Delta n_i$ in Eq. (3.18), the following expression is obtained for the equivalent stress expressed with reference to the rms stress:

$$\frac{\sigma_r}{\bar{\sigma}} = \left[\frac{\int_0^\infty \left(\frac{\sigma}{\bar{\sigma}}\right)^{\lambda\alpha+1} e^{-\frac{1}{2}\left(\frac{\sigma}{\bar{\sigma}}\right)^2} d\left(\frac{\sigma}{\bar{\sigma}}\right)}{\int_0^\infty \left(\frac{\sigma}{\bar{\sigma}}\right) e^{-\frac{1}{2}\left(\frac{\sigma}{\bar{\sigma}}\right)^2} d\left(\frac{\sigma}{\bar{\sigma}}\right)} \right]^{1/\lambda\alpha} \tag{3.20}$$

To evaluate the preceding expression, it is convenient to change the variable by substituting $(\sigma/\bar{\sigma}) = \sqrt{u}$. Equation (3.20) then takes the following form:

$$\frac{\sigma_r}{\bar{\sigma}} = \left[\frac{\int_0^\infty (\sqrt{u})^{\lambda\alpha+1} e^{-u/2} \frac{du}{2\sqrt{u}}}{\int_0^\infty \sqrt{u}\, e^{-u/2} \frac{du}{2\sqrt{u}}} \right]^{\frac{1}{\lambda\alpha}} = \left[\frac{\int_0^\infty u^{\frac{\lambda\alpha}{2}} e^{-u/2} du}{\int_0^\infty e^{-u/2} du} \right]^{\frac{1}{\lambda\alpha}} \tag{3.21}$$

The denominator of Eq. (3.21) can be integrated directly to give the following result:

$$\int_0^\infty e^{-u/2} du = -2e^{-u/2} \Big|_0^\infty = 2 \quad . \tag{3.22}$$

Integration of the numerator of Eq. (3.21) is accomplished by the use of gamma functions and may be expressed as a factorial as follows:

$$\int_0^\infty u^{\lambda\alpha/2} e^{-u/2} du = \frac{(\lambda\alpha/2)!}{\left(\frac{1}{2}\right)^{\lambda\alpha/2+1}} \quad . \tag{3.23}$$

The factorial term in the preceding expression is evaluated approximately by applying Stirling's formula:

$$n! \cong \sqrt{2\pi}\, n^{(n+\frac{1}{2})} e^{-n} \quad . \tag{3.24}$$

The factorial expression on the right hand side of Eq. (3.23) is evaluated using Eq. (3.24). Substituting this result together with the result of Eq. (3.22) into Eq. (3.21), the following expression is obtained for the equivalent stress:

$$\frac{\sigma_r}{\bar{\sigma}} = \left[\frac{\sqrt{2\pi} \left(\frac{\lambda\alpha}{2}\right)^{\lambda\alpha/2 + \frac{1}{2}} e^{-\lambda\alpha/2}}{2 \left(\frac{1}{2}\right)^{\lambda\alpha/2 + 1}} \right]^{1/\lambda\alpha} . \qquad (3.25)$$

The preceding expression may be reduced to the following form:

$$\frac{\sigma_r}{\bar{\sigma}} = \left[\frac{\frac{1}{(2\pi)^{2\lambda\alpha}} \left(\frac{\lambda\alpha}{2}\right)^{\frac{1}{2}(1 + 1/\lambda\alpha)} e^{-\frac{1}{2}}}{\frac{1}{2^{\lambda\alpha}} \left(\frac{1}{2}\right)^{(\frac{1}{2} + 1/\lambda\alpha)}} \right] \qquad (3.26)$$

Considering the physical aspect of this problem, it is known that the product $\lambda\alpha$ is great relative to unity and the reciprocal $1/\lambda\alpha$ consequently is small. Introducing these approximations, the expression given by Eq. (3.26) reduces to the following expression for the equivalent stress:

$$\frac{\sigma_r}{\bar{\sigma}} = \left[\sqrt{2\pi}/2\right]^{1/\lambda\alpha} \sqrt{\frac{\lambda\alpha}{e}} . \qquad (3.27)$$

The relation of Eq. (3.27) is shown in Fig. 3.7.

3.4 Variable Frequency Sinusoidal Vibration

Another commonly encountered situation involving failure by fatigue, of particular importance in laboratory testing, is one in which the excitation is sinusoidal with continuously varying frequency. The response of a linear system to this type of excitation, as determined by analog

computer, is discussed in Section 4.3 of this report. The particular type of excitation discussed there is one in which the excitation frequency is varied monotonically between limits in such a manner that the rate of change of frequency is always proportional to the frequency. This so-called "logarithmic sweep" is characteristic of much laboratory vibration testing.

With the objective of evaluating the effect of the excitation outlined in the preceding paragraph, a physical testing program was planned to include the following tasks:

1. A conventional fatigue testing program intended to describe the endurance properties of a typical material in terms of the conventional curve of stress versus number of cycles to failure.

2. A test to determine the endurance properties of the material when experiencing random vibration. This test uses specimens similar to those used in the conventional fatigue testing program; however, in this instance the specimens respond as beams attached to a support which experiences random vibration.

3. A test to determine the endurance properties of similar specimens when the excitation is sinusoidal vibration with continuously variable frequency.

The specimens, as shown in Figs. 3.8 and 3.9, were made from 2024-T4 aluminum alloy. The contour of the specimen was chosen to ensure failure at approximately the same section each time, such section being remote from areas of unknown stress concentration. The conventional fatigue tests mentioned in sub-paragraph 1 immediately above were conducted on a Baldwin Universal Fatigue Testing Machine; a

description of the machine, the method of testing, and the test results are set forth in Part 1 of Appendix C. Because of the unavailability at Contractor's facility, during much of the period covered by this report, of adequate vibration testing facilities, the initial tests performed in accordance with sub-paragraphs 2 and 3 immediately above were performed at Hughes Aircraft Company under sub-contract. Results from those tests are set forth in Part 2 of Appendix C.

The test set-up at Contractor's laboratory, used to conduct fatigue tests using either random vibration or sinusoidal vibration with variable excitation frequency, is shown in Figs. 3.10 and 3.11. The former figure shows a view of the Ling Model 175 vibration exciter with Model CP 5/6 R amplifier and console, together with the Optron Model 701 displacement follower. Figure 3.11 shows a close-up view of the beam shown in Figs. 3.8 and 3.9 mounted upon the vibration exciter, with the sensing head of the displacement follower in position to sense the displacement of the beam. As discussed subsequently in this section, the strain in the beam was measured with resistance wire strain gages; the application of the strain gages is shown in Fig. 3.9.

The response of a linear single degree of freedom system with viscous damping had previously been investigated using an analog computer, as shown in Fig. 4.7 and discussed in Section 4.3 of this report. Because of the fairly orderly nature of these results, the significantly different results obtained from the physical system were not anticipated and were not fully appreciated until considerable experimentation had been carried out. Only then was it learned, in retrospect, that the initial plans should have included provision for evaluating certain variables which had not been thought initially to be of first order importance. The

principal difficulties encountered may be outlined as follows:

1. The sign of the frequency variation, i.e., increasing or decreasing excitation frequency, proved to be of much greater significance physically than suggested by the analog computer experiments. Figure 4.7 shows a typical time-history of the response of the analog for both increasing and decreasing frequency. Corresponding results for the physical system are shown in Figs. 3.12 to 3.15, with the oscillograph operating at a slower speed so that all cycles of vibration are shown in a short record. Figures 3.12 and 3.13 show time-histories of displacement for increasing and decreasing frequency, respectively, of the beam shown in Fig. 3.8, for a scanning rate of 0.14 octave per minute. Figures 3.14 and 3.15 are similar to Figs. 3.12 and 3.12, for a scanning rate of 0.46 octave per minute.

2. The rate of frequency variation, or scanning rate, proved to be very significant. Its significance is apparent from a comparison of Figs. 3.12 and 3.14, and a comparison of Figs. 3.13 and 3.15. An effect of this magnitude was not anticipated in view of the results obtained from the analog computer.

3. Some difficulties of measurement are inherent in the experiment. To evaluate the endurance properties of the beam in the context of Section 3.2 of this report, it is necessary to know the time-history of stress or strain throughout the test. The use of a resistance wire strain gage cemented to the beam is not feasible to accomplish this function for two principal reasons: (a) the endurance properties of the gage are not as great as those of the beam; thus, the gage becomes inoperative before completion of the test; and (b) the gage adds damping to the beam, in a manner that tends to vary as the fatigue test continues.

To illustrate the effect of damping on the response of the beam, Fig. 3.16 is included. This should be compared with Fig. 3.14 which shows the response to the same excitation of a beam without a strain gage. It seems fundamental that the fatigue tests should be made on beams without strain gages; thus, the following procedure has been devised which promises to give the desired results with sufficiently good approximation:

(a) Using an Optron Model 701 Displacement Follower (shown in Figs. 3.10 and 3.11), the time-history of the displacement of a point on the beam is monitored during the fatigue test. This can be done continuously or at intervals, as necessary to document the continuing response of the beam. The Optron Displacement Follower uses a beam of light as the sensing element and thus does not influence the vibration of the beam.

(b) With the strain gage mounted upon the beam, strain and displacement are recorded simultaneously at various excitation levels and frequencies. A typical record of this nature is shown in Fig. 3.17. As indicated in Fig. 3.17, the ratio of strain to displacement varies with frequency as the mode shape changes. It is unlikely, however, that the mode shape will be influenced significantly by the presence or absence of the strain gage. Therefore, the relation shown in Fig. 3.17 can be used in conjunction with displacement readings taken during the fatigue test to infer the values of strain for the fatigue test.

Considerable time and effort have been expended in gaining an appreciation of the several problems involved in evaluating the fatigue properties of a structure when subjected to the sweeping sinusoidal type of excitation. Plans are being made to overcome these difficulties. An important objective will be to devise a structure which more nearly

corresponds in its response characteristics to the analog circuit. The present discrepancy between the two may be the result of nonlinearity of elasticity and/or damping. It is planned to explore this and the other problems in detail, and to continue the investigation toward an understanding of the mechanism of failure of a structure when the excitation is a scanning sinusoid.

References

3.1 "Cumulative Damage in Fatigue," by M. A. Miner, J. App. Mech., Vol. 12, No. 3, 1945, p. A-159.

3.2 "Description of Stress-Strain Curves by Three Parameters," by W. Ramberg and W. R. Osgood, NACA Tech. Note No. 902, July 1943.

3.3 "Fatigue Failure from Stress Cycles of Varying Amplitudes," by B. F. Langer, J. App. Mech., Vol. 4, No. 4, December 1937, p. A-160.

3.4 "A Theory of Fatigue Based on Unbonding During Reversed Slip," by F. R. Shanley, The Rand Corp., Report P-350, November 1952.

3.5 "An Experimental Investigation of the Behavior of 245-T4 Aluminum Alloy Subjected to Repeated Stresses of Constant and Varying Amplitudes," by H. F. Hardrath and E. C. Utley, NACA Tech. Note 2798, October 1952.

4. RESPONSE OF SIMPLE SYSTEM TO VARIOUS EXCITATIONS

This section discusses the response in forced vibration of a damped, single degree of freedom system. The significance of the simple system is two-fold: (a) Many systems can be analyzed for practical purposes as single degree of freedom systems and (b) complicated systems can be considered as an array of uncoupled single degree of freedom systems by using the normal mode concept discussed in Appendix B. Five types of excitation are considered explicitly: (1) Classical steady-state sinusoidal vibration; (2) combined sinusoids, forming beats in combination; (3) variable frequency sinusoid in which the excitation frequency is "swepth" or "scanned"; (4) broad band random vibration with classical Gaussian distribution of magnitudes; and (5) broad band random vibration in which the magnitudes are limited at various values. The excitations are discussed in this order in the following sub-sections.

4.1 Sinusoidal Vibration

The differential equation of motion of the mass m of the single degree-of-freedom system with viscous damping shown in Fig. 4.1 is

$$m\ddot{y} = k(s - y) + c(\dot{s} - \dot{y}) \tag{4.1}$$

The preceding equation is written in terms of the relative displacement between the mass and the support by substituting $z = s - y$; then $\dot{z} = \dot{s} - \dot{y}$, $\ddot{y} = \ddot{s} - \ddot{z}$ and Eq. (4.1) becomes

$$m\ddot{z} + c\dot{z} + kz = m\ddot{s} \tag{4.2}$$

Neglecting the transient terms and assuming the excitation and response to be respectively of the form $s = \mathrm{Re}\,(s_o e^{j\omega t})$, $z = \mathrm{Re}\,(z_o e^{j\omega t + \Psi})$, where Re indicates "real part of", Eq. (4.2) takes the following form:

$$(-m\omega^2 + k + j\omega c)\, z_o e^{j(\omega t + \Psi)} = -m s_o \omega^2 e^{j\omega t}$$

For purposes of the present analysis, the phase relation of z to s is not important. Then taking the maximum value of $e^{j\Psi}$ as unity, the relative displacement amplitude z_o may be written in terms of the excitation amplitude as follows:

$$z_o = \left| \frac{-ms_o\omega^2}{(k-m\omega^2) + j\omega c} \right|$$

The magnitude of z_o is the square root of the sum of the squares of the real and imaginary parts. The result may be expressed in dimensionless terms by dividing numerator and denominator by $m\omega^2$ and substituting $k/m = p^2$, $k = c_c^2/4m$, $\zeta = c/c_c$ where c_c is the value of the viscous damping coefficient in a critically damped system:

$$\frac{z_o}{s_o} = \frac{\omega^2/p^2}{\sqrt{\left(1 - \frac{\omega^2}{p^2}\right)^2 + \left(2\zeta \frac{w}{p}\right)^2}} \qquad (4.3)$$

where ω is the excitation frequency, p is the undamped natural frequency and ζ is the fraction of critical damping. The parameter $\frac{z_o}{s_o}$ given by Eq. (4.3) is shown graphically in Fig. 4.2 as a function of ζ and ω/p.

If the excitation is defined in terms of an acceleration amplitude $\ddot{s}_o = s_o\omega^2$, Eq. (4.3) takes the following form:

$$\frac{z_o p^2}{\ddot{s}_o} = \frac{1}{\sqrt{\left(1 - \frac{\omega^2}{p^2}\right)^2 + \left(2\zeta \frac{\omega}{p}\right)^2}} \qquad (4.4)$$

The parameter $\frac{z_o p^2}{\ddot{s}_o}$ is shown graphically in Fig. 4.3 as a function of ζ and ω/p.

The results shown graphically in Figs. 4.2 and 4.3 are generally useful in determining the response of a mechanical system to vibration. For the classical case of the mass-spring-damper system mounted upon a support which experiences sinusoidal vibration, the maximum displacement of the mass relative to the support may be determined from Fig. 4.2 if the vibration of the support is described in terms of its displacement amplitude or from Fig. 4.3 if described in terms of its acceleration amplitude. If the excitation is not classical sinusoidal vibration of fixed frequency; e.g., sinusoidal vibration with a continuously changing frequency (see Section 4.3) or random vibration (see Section 4.4), the response of the system can be expressed conveniently in terms of its response to sinusoidal vibration. Then if the mechanical system under investigation cannot be represented as a single degree-of-freedom system, its total response can be expressed as a summation of its responses in its several normal modes. For a particular system with several degrees-of-freedom, each normal mode is coupled to the excitation in a characteristic manner defined by a "mode participation factor" as described for beams, for example, in Section 5 and Appendix B. Finally, the response of a system with several degrees-of-freedom to non-sinusoidal vibration may be determined by combining the response of a single degree-of-freedom system with the normal mode concept.

One of the more troublesome practical problems in predicting the response of a mechanical structure to vibration is determination of an applicable damping relation. In the preceding discussion, viscous damping is assumed in order to facilitate the analysis. Although a device

having approximately the characteristics of a classical viscous damper can be constructed physically, in most mechanical structures the predominant inherent damping results from either hysteresis losses in the material or friction at connections. However, this discrepancy is not of first order importance because the overall response of a mechanical system is quite insensitive to the particular type of damping mechanism but rather depends upon the quantity of energy dissipated. Thus it becomes convenient to more or less ignore the details of the damping mechanism and to express the damping as viscous damping having equivalent energy dissipation. The problem of defining the damping thus becomes phenomenological; the response of a structure to a known condition of vibration is noted and the damping for that particular structure is expressed as the equivalent of a specified fraction of critical damping.

4.2 Combined Sinusoids

This section considers the characteristics of the response of a single degree-of-freedom system shown in Fig. 4.1 to an excitation consisting of the sum of two sinusoidal functions of small frequency difference. This produces the well-known modulated or beat pattern shown in Fig. 4.4 where the beat frequency is the difference of the component frequencies, the maximum amplitude is the sum of the amplitudes of the component sinusoids and the minimum amplitude is the difference of the amplitudes of the component sinusoids.

The response of the system to the excitation shown in Fig. 4.4(a) has the same characteristic form; this is shown in Fig. 4.4(b) where the frequencies are identical to those of Fig. 4.4(a) but the amplitudes are

modified by the response properties of the system. Inasmuch as the system is linear, the principle of superposition is applicable. Then the response to each sinusoidal component of the excitation may be determined by noting the amplitude of relative displacement from Fig. 4.2 or 4.3, and adding the components of the response to obtain the resultant response shown in Fig. 4.4(b). This response is described by the following expression:

$$z_r = z_1 \sin \omega_1 t + z_2 \sin \omega_2 t \tag{4.5}$$

Writing the frequency ω_2 in terms of ω_1 and the frequency difference, $\omega_2 = \omega_1 + \Delta\omega$, Eq. (4.5) becomes

$$z_r = z_1 \sin \omega_1 t + z_2(\sin \omega_1 t \cos \Delta\omega t + \cos \omega_1 t \sin \Delta\omega t) \tag{4.6}$$

The preceding expression may be written in terms of sine and cosine of the frequency term $\omega_1 t$:

$$z_r = (z_1 + z_2 \cos \Delta\omega t) \sin \omega_1 t + z_2 \sin \Delta\omega t \cos \omega_1 t \tag{4.7}$$

This is a sinusoidally varying quantity whose amplitude is the square root of the sum of the squares of the coefficients of the sine and cosine terms:

$$z_r = \sqrt{z_1^2 + z_2^2 + 2z_1 z_2 \cos \Delta\omega t} \quad \sin (\omega_1 t + \Psi) \tag{4.8}$$

where the phase angle Ψ is of no particular importance in the present context. It is evident from Eq. (4.8) that z_r varies between $z_1 + z_2$ and $z_1 - z_2$ at the beat frequency $\Delta\omega$. If the criterion of failure is maximum response, $z_{r(max)} = z_1 + z_2$ is the significant parameter.

To evaluate other criteria of failure, it is necessary to know the distribution of peak values z_r. This distribution is determined by the envelope of the time-history of Fig. 4.4(b), as defined by the coefficient of $\sin (\omega_1 t + \Psi)$ in Eq. (4.8):

$$z_e = \sqrt{z_1^2 + z_2^2 + 2z_1 z_2 \cos \Delta\omega t} \tag{4.9}$$

Squaring both sides of the preceding equation, dividing by z_1^2 to obtain a dimensionless form, and solving for t:

$$t = \frac{1}{\Delta\omega} \cos^{-1} \left[\frac{\left(\frac{z_e}{z_1}\right)^2 - \left(\frac{z_2}{z_1}\right)^2 - 1}{2\frac{z_2}{z_1}} \right] \tag{4.10}$$

As indicated in Fig. 4.5, the fraction of time that the envelope (z_e/z_1) is above any particular value is equal to the time t at that value divided by $\pi/\Delta\omega$, for $t \leq \pi/\Delta\omega$. This may be expressed as a probability P as follows:

$$P\left(\frac{z_o}{z_1} \geq\right) = \frac{t}{\pi/\Delta\omega} \tag{4.11}$$

Substituting t from Eq. (4.10):

$$P\left(\frac{z_e}{z_1} \geq\right) = \frac{1}{\pi} \cos^{-1} \left[\frac{\left(\frac{z_e}{z_1}\right)^2 - \left(\frac{z_2}{z_1}\right)^2 - 1}{2\frac{z_2}{z_1}} \right] \tag{4.12}$$

The relation given by Eq. (4.12) is shown graphically in Fig. 4.6 for several values of z_2/z_1 ; this may be used to evaluate the several criteria of failure set forth in Section 1 by first determining the relative displacement amplitudes z , z_2 from the excitation data and then finding the effect of superposing them by referring to Fig. 4.6.

4.3 Variable Frequency Sinusoid

A vibration condition of considerable practical importance, particularly in laboratory tests, involves a sinusoidal excitation in which the frequency of the excitation is continuously varied, in a predetermined

manner, between limits. This general problem first received attention in connection with vibration which occurred during starting or stopping a machine wherein the normal operating speed was greater than important resonant frequencies of the machine. In recent years the problem has received considerably greater attention because of its significance in laboratory testing procedures. In the present state of the art, several attempts have been made to define the response of a linear single degree of freedom system with viscous damping when the excitation frequency is continuously varied according to some selected pattern. It is evident that there are an infinitely great number of patterns from which to choose. It has proved very difficult to obtain an analytical solution in closed form for any one of the selected patterns. It would be much more difficult to describe the pattern of frequency variation in general terms and to obtain a solution describing the response in equally general terms. Past efforts at solving this problem have been limited to the selection of several possible patterns of frequency variation and to the determination of the response of the system for each of the selected patterns. This approach has been followed in the present investigation with the hope of ultimately combining the solutions and finding empirical relations which describe the response in terms of parameters that can be related to any given pattern of frequency variation.

If the single-degree-of-freedom system is adopted as the analog of the actual structure being investigated and the criteria of failure set forth in Section 1 are used, it becomes necessary to know the following characteristics of the response to an excitation involving a continuously varying excitation frequency:

(1) The maximum relative displacement of the system or, in other words, the maximum deflection or strain in the analog system.

(2) The maximum stress in the structure: This can be deduced from the maximum relative displacement when the analog system is related to the real structure.

(3) The distribution of cycles involving various values of maximum relative displacement, for ultimate use in applying the criterion of failure due to fatigue.

The response characteristics set forth in the above sub-paragraphs are defined in terms of the natural frequency and fraction of critical damping for the responding system, in addition to parameters which characteristically define the nature of the excitation. Such parameters would be expressed in different forms for the various possible types of excitation.

The response of a system with relatively small damping to an excitation of the type described in the preceding paragraphs is an interesting phenomenon. It is similar in some respects to driving a system at its resonant frequency but starting with the system at rest. Then the amplitude of the response tends to increase linearly with time; if the damping is small, a relatively long time is required to reach the maximum amplitude. When the excitation is sinusoidal with continuously varying frequency, the frequency of the excitation approaches the resonant frequency and the amplitude of response increases in a monotonic manner. However, before the amplitude of response reaches that value which would

apply to steady-state vibration, the forces which tend to cause the amplitude increase have ceased to exist. The maximum amplitude is thus smaller than that which would occur during steady-state vibration, and the effect is accentuated by a faster rate of variation of the excitation frequency. Thus the maximum response attained by the system tends to vary inversely with the sweep rate in a manner that depends upon the characteristics of the sweep or excitation frequency variation.

The results of the analysis show that the maximum response of the system occurs at a later moment than that in which the excitation frequency coincides with the natural frequency of the responding system. The magnitude of this lag depends upon the sweep rate and the sweep characteristics. A short time interval after the excitation frequency coincides with the natural frequency, the response amplitude is a maximum. If the excitation were to cease suddenly at this moment or maximum response amplitude, the subsequent vibration of the responding system would be free vibration with a continuously decreasing amplitude as controlled by the damping of the system. However, the excitation continues with a gradually increasing frequency and the forced vibration of the system thus has the same frequency as the excitation. The response of the system thus embodies two frequencies of nearly equal value, the free vibration continuing from the maximum response and the forced vibration at the excitation frequency. The addition of these two components of vibration at slightly different frequencies produces the beat pattern of the response amplitude shown in Fig. 4.7(a) for an increasing excitation frequency and in Fig. 4.7(b) for a decreasing excitation frequency. It may be noted that the beat period decreases continuously with time as the difference between the natural frequency and the excitation frequency increases during the sweep pattern. For values of damping that are

characteristic of mechanical structures, the decay of the free vibration is sufficiently rapid that the amplitudes involved in the beat pattern are small relative to the amplitude at maximum response. Thus the later fluctuations of vibration amplitude characterized by the beat pattern contribute little or nothing to fatigue of the structure.

An analytical solution of the phenomenon illustrated in Fig. 4.7 is not feasible except for a few special cases. This has been done for the case of the linearly varying excitation frequency (ref. 4.1) but evaluation of the results is laborious. The most feasible method of obtaining a solution to the problem is through the use of an analog or a digital computer but each has its limitations. In principle, the analog computer is well adapted to the solution of a problem of this type. The response can be recorded photographically and the record analyzed to obtain the value of the maximum response and the distribution of cycles of response having amplitudes smaller than the maximum. However, to use the analog computer it is necessary to generate a voltage proportional to the excitation. An audio oscillator adapted to continuously vary the frequency of the output signal would appear appropriate for this application but most commercially available oscillators tend to generate unwanted transients during the interim in which the frequency is being varied.

One commercially available oscillator includes means to vary the excitation frequency in a logarithmic manner; i.e., the time to vary the frequency over an octave band of frequencies remains constant throughout the frequency spectrum. Such an oscillator has been found useful for one particular sweep pattern. The spectrum analyzer described in detail in reference 4.10 is useful for a wide variety of sweep patterns but has certain limitations which restrict its usefulness for this application. In

the first place, it can accommodate only a limited number of cycles of excitation because the excitation must be transcribed around the periphery of a disk of limited size. In the second place, a template must first be made and subsequently converted by photoelectric means to a voltage which is the input to the analog computer; inaccuracies in tracing the template lead to resultant inaccuracies in the results.

A digital computer has been used in an exploratory manner to compute the response for certain special types of excitation; this is not efficient because it is necessary that the computer calculate the complete time history of the response for a relatively long time and that this be plotted in a form for subsequent analysis. The result when plotted out is then analyzed for the maximum response and for the distribution of response cycles having peak values smaller than the maximum.

The results reported herein are limited to the sweep pattern in which the excitation frequency is varied logarithmically, i.e, the time required to effect an octave change in the frequency is constant independent of the position of the octave in the frequency spectrum. The numerical values have been obtained using the analog computer described in Appendix A with excitation being provided by Bruel and Kjaer audio oscillator Model 1018 equipped with means to sweep the excitation frequency at selected sweep rates. The frequency control dial of the oscillator is marked in degrees of dial position and in excitation frequency with units of cycles per second. The relation between dial setting and frequency is

$$\log_{10} f = \frac{\theta}{72} + \log_{10} f_o \qquad (4.13)$$

where f = frequency at any setting, cps

θ = dial position, degrees

f_o = frequency at $\theta = 0$, 4.6 cps

The relation given by Eq. (4.13) is shown graphically in Fig. 4.8.

The excitation frequency at any time t is then defined by the following expression:

$$f = f_i \, e^{\frac{11.3t}{s}} \qquad (4.14)$$

where f = instantaneous frequency, cps

t = time, sec

f_i = initial frequency, at $t = 0$, cps

s = sweep rate, octaves/min.

If a single degree of freedom system undergoes forced vibration by excitation of the support (see Section 4.1), the maximum response of the system is defined by the transmissibility T where T is the ratio of the response amplitude to the excitation amplitude. In this context, the amplitudes may be of acceleration, velocity or displacement, provided the same dimensions are used for excitation and response. The transmissibility at resonance is a function only of the damping in the system:

$$T = \frac{1}{2\zeta} \qquad (4.15)$$

where ζ = fraction of critical damping.

When the excitation frequency is changing continuously, the transmissibility may be designated T_s where $T_s < T$. From an examination of a large quantity of data obtained from the analog computer described

above, an empirical expression has been derived relating T and T_s as follows:

$$\frac{T_s}{T} = 1 - 0.186 \log_{10} \left[1 + \left(\frac{A}{8.0 \times 10^{-5} \times \sqrt{10^{\frac{\zeta - 0.005}{0.017}} - 1}} \right)^2 \right] \quad (4.16)$$

where ζ = fraction of critical damping

$$A = \frac{s}{11.3 f_n}$$

s = sweep rate of oscillator, octave/min.

f_n = natural frequency of responding system, cps

The above expression for T_s/T has been compared with results obtained from the analog computer for several values of ζ, f_n and s. The degree of correspondence between calculated and experimentally obtained values of T/T_s is illustrated in Figs. 4.9 to 4.11 for values of ζ = 0.01, 0.02 and 0.05, respectively. The results were verified by use of several natural frequencies at each of the sweep rates. In each of Figs. 4.9 to 4.11, the experimental points are coded to indicate the applicable value of natural frequency and the direction (increasing or decreasing) of frequency change.

When the criterion of failure involves fatigue, discussed in Section 3, it is important to know the distribution of cycles at the various response amplitudes. With this end in view, the response of a system to a sweeping sinusoid was examined to determine not only the maximum response but also the distribution of response cycles having amplitudes smaller than the maximum amplitude. It has been found possible to plot the data for all values of ζ, f_n and s on a single graph, using as a reference the number of cycles at 0.707 times the amplitude of the

cycle having the greatest response. The data are shown in Fig. 4.12 where the maximum amplitude is found from Figs. 4.9 to 4.11. The curve of Fig. 4.12 seems to be quite reliable in predicting the number of cycles at amplitudes greater than 0.5 times the maximum; for lower amplitudes, the beats illustrated in Fig. 4.7 tend to become significant. The characteristics of such beats have not yet been fully documented, and data which include the effect of the beats may be unreliable. This limitation does not interfere seriously with use of the data for fatigue purposes, however, because the stress values are taken to a large power and even moderately large values become negligible in an appraisal of damage.

4.4 Broad Band Random Vibration

The response of a single degree of freedom system to broad band random vibration is discussed extensively in the technical literature. In the criteria for failure of equipment, the most significant parameter by which to define the response is the relative displacement $z = y - x$. It is most convenient to define the excitation in terms of the mean square acceleration density. The mean square acceleration density of the excitation is related to the mean square displacement density of the response for the system of Fig. 4.1 by a transfer function as follows (see ref. 4.9):

$$W_z(\omega) = W_{\ddot{x}}(\omega) \left[H(j\omega) \right]^2 \qquad (4.17)$$

where $W_{\ddot{x}}(\omega)$ is the mean square acceleration density of the support, $W_z(\omega)$ is the mean square relative displacement density of mass m, and $H(j\omega)$ is a transfer function (generally a complex number). The transfer function $H(j\omega)$ is defined in terms of the response of the system to sinusoidal excitation.

The transfer function $H(j\omega)$ is determined by the ratio of relative displacement amplitude to acceleration amplitude in steady state sinusoidal vibration:

$$\left|H(j\omega)\right| = \frac{1}{\omega_n^2 \sqrt{\left[1 - \left(\frac{\omega}{\omega_n}\right)^2\right]^2 + \left(2\zeta \frac{\omega}{\omega_n}\right)^2}} \tag{4.18}$$

The mean square value of a random motion is related to its mean square density by the following relation:

$$\overline{z^2} = \int_{\omega_1}^{\omega_2} W_z(\omega)\, d\omega \tag{4.19}$$

where ω_1, ω_2 are the bounds of the frequency interval over which the mean square density $W_z(\omega)$ has a value significantly greater than zero. The notation $\overline{z^2}$ denotes mean square relative displacement and $W_z(\omega)$ is the mean square relative displacement density. The mean square relative displacement $\overline{z^2}$ is related to the excitation by substituting from Eqs. (4.17) and (4.18) into Eq. (4.19):

$$\overline{z^2} = \int_{\omega_1}^{\omega_2} \frac{W_{\ddot{x}}(\omega)\, d\omega}{\omega_n^4 \left\{\left[1 - \left(\frac{\omega}{\omega_n}\right)^2\right]^2 + \left(2\zeta \frac{\omega}{\omega_n}\right)^2} \tag{4.20}$$

The integral of Eq. (4.20 is readily evaluated for small values of ζ, for $W_{\ddot{x}}(\omega)$ which is a constant independent of frequency, and for limits 0 and ∞ on the integral. These restrictions are not severe because the integral applies with acceptable accuracy if the mean square density is substantially constant in the region of the natural frequency of the responding system and does not embody significantly higher values in other regions.

Then the mean square relative displacement obtained by integrating Eq. (4.20) is

$$\overline{z^2} = \frac{\pi W_{\ddot{x}}(\omega)}{4\zeta\,\omega_n^3} \tag{4.21}$$

where z has units of inches, $W_{\ddot{x}}(\omega)$ has units of $(\text{in/sec}^2)^2$ / (rad/sec) and ω_n has units of rad/sec. It is more common to express acceleration as a dimensionless multiple of the gravitational acceleration and to express frequencies in units of cycles/sec (cps). Substituting $\omega_n = 2\pi f_n$, $W_{\ddot{x}}(f)\ \frac{(\text{in/sec}^2)^2}{\text{cps}} = 2\pi W_{\ddot{x}}(\omega)\ \frac{(\text{in/sec}^2)^2}{\text{rad/sec}}$ and $W_{\ddot{x}}(f)\ \frac{(\text{in/sec}^2)2}{\text{cps}} = g^2 W_{\ddot{x}/g}(f)\ \frac{g^2}{\text{cps}}$, Eq. (4.21) becomes

$$\overline{z^2} = \frac{g^2 W_{\ddot{x}/g}(f)}{64\pi^3\zeta\, f_n^3} \tag{4.22}$$

For relatively small values of ζ, the time-history of z exhibits the characteristics of a narrow band random process, as illustrated in Fig. 4.13. The probability density of the peak values for the narrow band random trace of Fig. 4.13 is given by

$$p\left(\frac{z}{\bar{z}}\right) = \frac{z}{\bar{z}}\ e^{-\frac{1}{2}\left(\frac{z}{\bar{z}}\right)^2}\ d\left(\frac{z}{\bar{z}}\right) \tag{4.23}$$

The relation of Eq. (4.23) is shown graphically in Fig. 4.14 where the rms value $\bar{z}$ is obtained from Eq. (4.22).

The probability distribution indicates the number of peaks on the average which exceed the respective values and is found by integrating Eq. (4.23):

$$P\left(\frac{z}{\bar{z}}\right) = \int_0^\infty p\left(\frac{z}{\bar{z}}\right)\ d\left(\frac{z}{\bar{z}}\right) = e^{-\frac{1}{2}\left(\frac{z}{\bar{z}}\right)^2} \tag{4.24}$$

This relation is shown graphically in Fig. 4.15. Peak values greater

than approximately three times the rms value occur only infrequently; thus, numerical values are difficult to obtain from a linear scale. The dotted line in Fig. 4.15 is an extension of the solid line but wherein the values on the ordinate are reduced by a factor of 100.

4.5 Magnitude-Limited Broad Band Random Vibration

In many real situations, encountered both in the laboratory and in the field, the vibration has many of the characteristics of broad band random vibration with Gaussian distribution of instantaneous values except that the higher values predicted by the classical theory do not appear. Inasmuch as information on the change in the response of a responding system resulting from deleting large values in the excitation does not appear to be available from other sources, this problem has been investigated using an analog computer. The results are set forth in this section. The results obtained are believed to be original, and are set forth here simply as observations obtained from analog computer experiments. A theoretical study of the problem is continuing with the objective of ultimately presenting a more complete solution.

Figure 4.1 is a mathematical model of the system that was studied; it represents in ideal form a mechanical structure in which the excitation is a motion s of the support. Then the response characteristic of primary interest is the relative displacement $z = s - y$ where z is directly proportional to the strain in the structure. The differential equation of motion for the mass m in Fig. 4.1 is given by Eq. (4.1). Substituting $z = s - y$, Eq. (4.1) becomes

$$\ddot{z} + \frac{c}{m}\dot{z} + \frac{k}{m} z = \ddot{s} \qquad (4.25)$$

The analog computer (See Appendix A for details of analog computer circuit.) provides a solution to Eq. (4.25) where the input voltage (v_i corresponds to $\ddot{s}$ and the output voltage v_o corresponds to z. The voltages are related to the physical characteristics of the system by

$$\frac{v_o}{v_i} = \frac{p^2 z}{\ddot{s}} \qquad (4.26)$$

where p is the natural frequency of the responding system. For any given ststem, p is a constant and $z/\ddot{s}$ is proportional to v_o/v_i.

The source of excitation for the analog computer is a General Radio Type 1390 B Random Noise Generator. The nominal bandwidth of the signal from this instrument is 20 to 20,000 cps, and the natural frequency of the analog circuit is approximately 90 cps. Inasmuch as the response of a system is negligible when the excitation frequency is much greater than the natural frequency, no significant change is introduced by limiting the bandwidth to 2 to 2000 cps. Not only does this restriction of bandwidth make the excitation easier to record oscillographically but it eliminates the frequency components which are responsible for the non-symmetry in the output of the noise generator when the full bandwidth is used. With respect to the latter consideration, the filtered random signal tends to become more Gaussian, as predicted by theory.

By use of the magnitude-limiting circuit described in Appendix A, the maximum voltage in the excitation v_i is limited successively to predetermined voltage levels. These limit voltages are defined for

convenience with reference to the rms voltage of the non-limited output from the noise generator. The limit levels used are 2.5, 2.0, 1.5 and 1.0 times the rms value of the unlimited signal. Time-histories of the input voltage v_i for each of these limit levels are illustrated in Fig. 4.16.

The relation between the rms value of a classical broad-band random vibration with Gaussian distribution of instantaneous values (Fig. 4.16a) and the same vibration pattern in which the maximum values are limited (Fig. 4.16b to e) is determined in the following manner. The mean square value of a vibration trace v(t) is

$$\overline{(v^2)} = 2\int_0^\infty v^2\, p(v)\, dv \qquad (4.27)$$

where p(v) is the probability density of instantaneous values of v. The applicable expression for probability density of a Gaussian distribution, expressed non-dimensionally with reference to its rms value or standard deviation σ, is

$$p\left(\frac{v}{\sigma}\right) = \frac{1}{\sqrt{2\pi}}\, e^{-\frac{1}{2}\left(\frac{v}{\sigma}\right)^2} \qquad (4.28)$$

Substituting from Eq. (4.28) into Eq. (4.27), the mean square value for the classical Gaussian distribution is

$$\left(\frac{\overline{v}}{\sigma}\right)^2 = \sqrt{\frac{2}{\pi}}\int_0^\infty \left(\frac{v}{\sigma}\right)^2 e^{-\frac{1}{2}\left(\frac{v}{\sigma}\right)^2} d\left(\frac{v}{\sigma}\right) \qquad (4.29)$$

With the type of limiting circuit used in this investigation, all values of v less than v_c remain substantially unaffected whereas all those

greater than v_c are reduced to v_c, a constant value. Then Eq. (4.29) is modified as follows:

$$\overline{\left(\frac{v}{\sigma}\right)^2} = \sqrt{\frac{2}{\pi}}\left[\int_0^{\frac{v_c}{\sigma}} \left(\frac{v}{\sigma}\right)^2 e^{-\frac{1}{2}\left(\frac{v}{\sigma}\right)^2} d\left(\frac{v}{\sigma}\right) + \left(\frac{v_c}{\sigma}\right)^2 \int_{\frac{v_c}{\sigma}}^{\infty} e^{-\frac{1}{2}\left(\frac{v}{\sigma}\right)^2} d\left(\frac{v}{\sigma}\right)\right] \qquad (4.30)$$

The integrand of the first integral is shown in Fig. 4.17 and the integrated value is shown by the shaded area. The integrand of the second integral is shown in Fig. 4.18; the integrated value is shown shaded and is multiplied by $\left(\frac{v_c}{\sigma}\right)^2$ to form the second term in Eq. (4.30). The mean square value $\overline{\left(\frac{v}{\sigma}\right)^2}$ has been evaluated numerically for several values of (v_c/σ), and the rms value $\sqrt{\overline{\left(\frac{v}{\sigma}\right)^2}}$ is shown by the curve in Fig. 4.19 with reference to the rms value of the unclipped signal, as defined by Eq. (4.29). Corresponding values as obtained by analog computer are shown as experimental points in Fig. 4.19(a) for comparison with the theoretical values. The probability distribution of instantaneous values as determined experimentally is shown in Fig. 4.19(b).

The response of a lightly damped system to the nonlimited broad band random excitation shown in Fig. 4.16(a) is characteristically a narrow band random vibration in which the natural frequency of the system is predominant. Systems having fractions of critical damping ζ = 0.01, 0.02 and 0.05 were each excited by each of the excitations illustrated in Fig. 4.16. Samples of the time-histories of the output voltage v_o are shown in Figs. 4.20 to 4.24, inclusive, for each combination of parameters investigated.

The statistical properties of the response v_o shown in Figs. 4.20 to 4.24 are of interest; in particular, the distribution of peak values of v_o is significant in predicting the likelihood of damage to a structure as a consequence of excessive strain or fatigue. The number of peaks of voltage v_o exceeding various levels was counted by a Quan-Tech Model 317 Amplitude Distribution Analyzer. For convenience of experimental procedure, the heights of the voltage peaks v_o were measured in dimensions of volts while holding the rms value of the excitation voltage v_i constant at 0.4 volts before limiting. The results are plotted in Figs. 4.25 to 4.27 where the vertical scale indicates the value of the voltage peak v_o* and the upper horizontal scale indicates the fraction of peaks found to be above the corresponding voltage level. In statistical terms, the upper horizontal scale is the probability of a peak exceeding the corresponding voltage and the lower horizontal scale is the probability that the peak is lower than the corresponding voltage.

The coordinate scales in Figs. 4.25 to 4.27 are chosen so that a Rayleigh distribution plots as a straight line. By taking the counting interval to be relatively long (as long as five minutes for a system with a natural frequency of 90 cps), it has been possible to extend the curve to probabilities considerably less than 0.1 percent. The curves appear to be straight lines to approximately five times the rms value, considering the relatively low confidence level of the data at low probabilities.

In a vibration pattern having a Rayleigh distribution of peak values, the rms value is the level below which 39.4 percent of the peak

---

*The voltages v_o plotted in Figs. 4.20 to 4.24 are those actually measured on the analog computer. They reflect the multiplying effect of the time-constant of the integrators and would be much smaller if reduced to the scale of the input voltage.

values lie. This is indicated by the σ index mark on the abscissae of Figs. 4.25 to 4.27 and can be used to determine the rms value of the output voltage v_o. For convenience in carrying out the experimental program, the rms value of the input voltage was maintained constant at 0.4 volts for all experimental conditions. Then the output voltage v_o, representing response of the physical system, had the rms values of voltage shown in Fig. 4.28 for several values of the fraction of critical damping.

The reference used in plotting Fig. 4.28, a constant value of rms voltage before passing through the limiting circuit, tends to lack real significance even though convenient for experimental purposes. In a real sense, if the excitation exhibits the characteristics of magnitude-limited random vibration, it is possible to determine the properties of only the magnitude-limited signal. The decrease of response shown in Fig. 4.28 for severe limitation in magnitude is related to the decrease of excitation due to magnitude limitation, as defined in Fig. 4.19(a). Thus, a more real description of the effect of magnitude limiting is the dimensionless response determined by dividing the rms value of the response in Fig. 4.28 by the rms value of the actual excitation. This is a real transmissibility, relating actual response to actual excitation. It is shown in Fig. 4.29, for several values of the fraction of critical damping, as a function of the magnitude limit. The effect of the limitation in magnitude of the excitation may be shown in dimensionless terms by normalizing the curves of Fig. 4.29 so that the transmissibility is unity for a non-limited excitation. The normalized curves are shown in Fig. 4.30.

The results obtained from the experiment with the magnitude-limited excitation may be summarized as follows:

1. The probability of occurrence of the peak values of the response is in accordance with the Rayleigh distribution, to the lowest probability (less than 0.1 percent) that could be evaluated within reasonable limits of counting time. The analog computer as used in this experiment does not indicate a limit to the maximum response that can be expected, although with small probability, even though the larger values in the excitation have been eliminated.

2. Inasmuch as the distribution of peak values in the response follows a Rayleigh distribution to at least small values of probability, there is a fixed relation between the various peak values and the rms value. Therefore, the values of the peaks in the response to a magnitude-limited random excitation may be determined by multiplying the peak values in the response to a classical Gaussian excitation by the dimensionless transmissibility shown in Fig. 4.30.

References

4.1 "Vibration During Acceleration Through a Critical Speed" by F. M. Lewis, Trans. ASME, Vol. 54, 1932.

4.2 "Response of Linear Resonant Systems to Excitation of a Frequency Varying Linearly with Time", by G. Hok, J. App. Phys., Vol. 19, March 1948, p. 242.

4.3 "On Running a Machine Through its Resonant Frequency", by J. P. Ellington and H. McCallion, J. Royal Aero. Soc., Vol. 60, Sept. 1956, p. 620.

4.4 "The Acceleration of a Single Degree of Freedom System Through its Resonant Frequency", by S. Hother-Lushington and D. C. Johnson, J. Royal Aero. Soc., Vol. 62, Oct. 1958, p. 752.

4.5 "The Mechanics of Vibration", by R. E. D. Bishop and D. C. Johnson, Cambridge University Press, 1960, pp

4.6 "The Response of a Vibrating System to Several Time Dependent Frequency Excitations" by A. V. Parker, M.S. Thesis, Iowa State University, 1962.

4.7 "Statistical Aspects of Random Loads" by Y. C. Fung, Preprint 376 of Inst. Aero. Sciences, 1952.

4.8 "On Structural Fatigue Under Random Loading", by J. W. Miles, J. Aero. Sciences, Nov. 1954.

4.9 "Statistical Concepts in Vibration" by J. W. Miles and W. T. Thomson, Vol. 1, Chap. 11 of Shock and Vibration Handbook, Ed. C. M. Harris and C. E. Crede, McGraw-Hill Book Co., Inc., New York, 1961, Eq. (11.37), p. 11-10

4.10 "A Response Spectrum Analyzer for Transient Loading Studies", by T. K. Caughey and D. E. Hudson, Proc. Soc. Exper. Stress Anal., Vol. 13, No. 1, p. 199, 1956.

4.11 Eq. (11.36), p. 11-9 of reference 4.9.

5. RESPONSE OF BEAMS TO VIBRATION

The curves of Figs. 4.2 and 4.3 may be used to determine the relative displacement amplitude in steady-state sinusoidal vibration of any linear system which may be approximated as a single degree-of-freedom system. When it is necessary to consider the stress in a member, however, the mathematical model shown in Fig. 4.1 must be replaced by a model in which the stress can be related to the relative displacement z. For example, consider the three typical beam types shown in Fig. 5.1: the simple (pinned-pinned) beam at (a), the built-in (fixed-fixed) beam at (b), and the cantilever (fixed-free) beam at (c). If the mass of the load W is large relative to that of the supporting beam, the beams behave approximately as single degree-of-freedom systems and it is possible to relate the stress in the beam directly to the displacement of the load W relative to the beam support. The applicable relations are outlined in Table 5-1 for the several beams illustrated in Fig. 5.1, assuming the beams to be of uniform section from end to end.

In Table 5-1, the first line gives the deflection of the beam measured at the position of load W and the second line gives the maximum stress in the beam as a function of the load W. Eliminating W between the first and second lines gives the maximum stress as a function of the deflection, as set forth in the third line. From the relations of the third line, values of the displacement amplitude Z_o determined from Figs. 4.2 and 4.3 can be transformed to values of maximum stress in the beam when the damping is known. For a discussion of damping, see the next paragraph and section B-3.3 of Appendix B. The natural frequencies of the several beams are given in the fourth and fifth lines.

When the mass of the beam is not negligible relative to the mass of the load, the preceding analysis becomes inapplicable and the mass of the beam must be considered in determining the response of the beam to an applied vibration. The type of beam most amenable to analysis is one in which the total mass is distributed uniformly throughout the length of the beam; i.e., a discrete load W as illustrated in Fig. 5.1 does not exist. Each type of beam has characteristic mode shapes which are determined most readily for a beam without damping; for the small damping which is characteristic of most structures, the mode shapes are nearly similar to those for an undamped beam. However, when the excitation frequency is approximately equal to a natural frequency of the beam, a near-resonant condition exists and the response of the beam depends greatly upon the damping. It is convenient in engineering analysis to neglect the damping terms in determining analytical expressions for natural frequencies and mode shapes; then each mode is considered to have a characteristic value of damping. By this means the response in any mode can be related to the excitation.

Figure 5.2 illustrates ten beams of uniform section and uniform mass distribution from end to end, three of the beams having the same end conditions as the massless beams illustrated in Fig. 5.1. Each of the beams has an infinitely large number of natural frequencies; there are characteristic mode shapes which describe the shape of the beam when it vibrates in the mode corresponding to the respective frequency. Taking the x axis along the length of the beam and using the y coordinate to designate deflection of the beam relative to the x axis, y is defined as follows:

$$y(x,t) = \sum_{k=1}^{\infty} \varphi_k(x)\, e^{jp_k t} \tag{5.1}$$

where p_k are the natural or normal mode frequencies of the beam and φ_k are the characteristic shapes of the beam in its normal modes. The normal modes are orthogonal, as discussed in Section 3-1 of Appendix B.

Each type of beam has characteristic conditions of constraint at its ends; using these conditions, the differential equation of motion [Eq. (B-32) of Appendix B] can be solved to obtain (1) an equation whose roots yield the natural frequencies p_k and (2) an expression for the characteristic mode shapes φ_k. Examples of the method for obtaining p_k and φ_k are given in Section B-3.2 of Appendix B for the fixed-free (cantilever) beam and the hinged-hinged (simple) beam. The applicable frequency equations for the ten beam types shown in Fig. 5.2 are set forth in Table 5-2. The roots of these equations are a sequence of numerical values $\beta_k \ell = \alpha_k$ which are related to the natural frequencies as follows [see Section B-3.2 of Appendix B]:

$$p_k = \frac{\alpha_k^2}{\ell^2}\sqrt{\frac{EI}{\mu}} \text{ rad/sec} \tag{5.2}$$

where ℓ = length of beam, in.

E = Young's modulus, lb/in.^{2}

I = area moment of inertia of beam cross section, in.^{2}

μ = mass per unit length of beam, lb sec^2/in.^{2}

Numerical values of α_k are set forth in Table 5-3 for the ten types of beams illustrated in Fig. 5.2.

Expressions for the characteristic mode shapes for the beams illustrated in Fig. 5.2 are set forth in Table 5-4.

The response of each of the beams of Fig. 5.2 in a normal mode is determined from a differential equation that is analogous to Eq. (4.2); it is expedient, however, to delete the damping term from the differential equation and to introduce damping into the solution by assuming an effective damping value for each mode. Then the applicable differential equation, Eq. (B-30) of Appendix B, is as follows:

$$\ddot{\xi} + p_k^2 \xi_k + \eta_k \ddot{s}(t) = 0 \tag{5.3}$$

where ξ_k is the normal mode coordinate for the k^{th} mode and η_k is defined as follows [See Eq. (B-36) of Appendix B]:

$$\eta_k = \frac{\int_0^{\ell} \mu \varphi_k(x)\, dx}{\int_0^{\ell} \mu \varphi_k^2(x)\, dx} \tag{5.4}$$

The parameter η_k is designated the mode participation factor for the k^{th} mode and $\varphi_k(x)$ is described with reference to Eq. (5.1). Numerical values of η_k are given in Table 5-5 for the first five modes of each of the ten beams illustrated in Fig. 5.2.

When the excitation is steady-state, sinusoidal motion of the support defined in terms of frequency and acceleration amplitude, $\ddot{s} = \ddot{s}_o \sin \omega t$, the solution to Eq. (5.3) is, in accordance with Eq. (B-61) of Appendix B:

$$\xi_k(t) = \frac{-\eta_k (\ddot{s}_o / p_k^2) \sin \omega t}{1 - \omega^2 / p_k^2} \tag{5.5}$$

If the response of the beam when vibrating at resonance is to be predicted, it is necessary to include a damping term in Eq. (5.3), as discussed above.

Then the solution, corresponding to Eq. (5.5) for the undamped beam, is written as follows [See Eq. (B-62) of Appendix B]:

$$\xi_k = \frac{-\eta_k (\ddot{s}_o / p_k^2) \sin \omega t}{\sqrt{\left(1 - \omega^2/p_k^2\right) + \left(2 \zeta_k \omega/p_k\right)^2}} \tag{5.6}$$

where ζ_k is the effective fraction of critical damping for the k^{th} mode.

The deflection $y_k(x, t)$ of the beam may be defined in terms of the normal mode shape $\varphi_k(x)$ and the normal coordinate $\xi_k(t)$ as follows [See Eq. (B-65) of Appendix B]:

$$y_k(x, t) = \xi_k(t)\, \varphi_k(x) \tag{5.7}$$

It is assumed, as indicated by Eq. (5.5), that the beam vibrates at the forcing frequency ω. Then an expression for acceleration may be written directly from Eq. (5.6) using the relation $\ddot{y} = \omega^2 y$:

$$\ddot{y}(x, t) = \omega^2\, \xi_k(t)\, \varphi_k(x) \tag{5.8}$$

The stress in the beam, from Eq. (B-66) of Appendix B, is

$$\sigma_k(x, t) = c\, E\, \xi_k(t)\, \frac{\partial^2 \varphi_k(x)}{\partial x^2} \tag{5.9}$$

Table 5-1

Characteristics of Massless Beams with Concentrated Loads Shown in Fig. 5.1

Type of Beam	(a) Hinged - hinged	(b) Fixed - fixed	(c) Fixed - free
1. Deflection of load W relative to base	$z = \frac{W\ell^3}{48\,EI}$	$z = \frac{W\ell^3}{192\,EI}$	$z = \frac{W\ell^3}{3\,EI}$
2. Maximum Stress	$\sigma_{max} = \frac{W\ell b}{8I}$	$\sigma_{max} = \frac{W\ell b}{16I}$	$\sigma_{max} = \frac{W\ell b}{2I}$
3. Ratio: $\frac{\text{stress}}{\text{deflection}}$	$\frac{\sigma_{max}}{z} = \frac{6Eb}{\ell^2}$	$\frac{\sigma_{max}}{z} = \frac{12Eb}{\ell^2}$	$\frac{\sigma_{max}}{z} = \frac{3Eb}{2\ell^2}$
4. Natural frequency, rad/sec	$p = 4\sqrt{\frac{3EIg}{W\ell^3}}$	$p = 8\sqrt{\frac{3EIg}{W\ell^3}}$	$p = \sqrt{\frac{3EIg}{W\ell^3}}$
5. Natural frequency, cycles/sec	$\frac{p}{2\pi} = \frac{2}{\pi}\sqrt{\frac{3EIg}{W\ell^3}}$	$\frac{p}{2\pi} = \frac{4}{\pi}\sqrt{\frac{3EIg}{W\ell^3}}$	$\frac{p}{2\pi} = \frac{1}{2\pi}\sqrt{\frac{3EIg}{W\ell^3}}$

Notation:

ℓ = length of beam (See Fig. 5.1), in.

W = load carried by beam, lb.

E = Young's modulus for beam, lb/in^2

I = moment of inertia of cross section, in^4

g = acceleration of gravity, in/sec^2

b = depth of beam section, in.

Table 5-2

Frequency Equations for Beams in Fig. 5.2

1. Fixed-free: $\cos \alpha_k \cosh \alpha_k + 1 = 0$
2. Hinged-hinged: $\sin \alpha_k = 0$
3. Fixed-fixed: $\cos \alpha_k \cosh \alpha_k - 1 = 0$
4. Free-free: $\cos \alpha_k \cosh \alpha_k - 1 = 0$
5. Fixed-hinged: $\tan \alpha_k - \tanh \alpha_k = 0$
6. Hinged-free: $\tan \alpha_k - \tanh \alpha_k = 0$
7. Sliding-pinned: $\cos \alpha_k = 0$
8. Sliding-sliding: $\sin \alpha_k = 0$
9. Fixed-sliding: $\tan \alpha_k + \tanh \alpha_k = 0$
10. Sliding-free: $\tan \alpha_k + \tanh \alpha_k = 0$

Table 5-3

Values of a_k in Eq. (5.2) for Beams Illustrated in Fig. 5.3

	Beam Type	a_1	a_2	a_3	a_4	a_5
1.	Fixed-free	1.8751	4.6941	7.8548	10.9955	14.1372
2.	Hinged-hinged	3.1416	6.2832	9.4248	12.5664	15.7080
3.	Fixed-fixed	4.7300	7.8532	10.9956	14.1372	17.2788
4.	Free-free	4.7300	7.8532	10.9956	14.1372	17.2788
5.	Fixed-hinged	3.9266	7.0686	10.2102	13.3518	16.4934
6.	Hinged-free	3.9266	7.0686	10.2102	13.3518	16.4934
7.	Sliding-pinned	1.5708	4.7124	7.8540	10.9956	14.1372
8.	Sliding-sliding	3.1416	6.2832	9.4248	12.5664	15.7080
9.	Fixed-sliding	2.3650	5.4978	8.6394	11.7810	14.9226
10.	Sliding-free	2.3650	5.4978	8.6394	11.7810	14.9226

Table 5-4

Characteristic Mode Shapes for Beams Illustrated in Fig. 5.2

1. Fixed-free: $\phi_k(x) = \cosh \beta_k x - \cos \beta_k x - \psi_k(\sinh \beta_k x - \sin \beta_k x)$

$$\text{where } \psi_k = \frac{\sinh \beta_k \ell - \sin \beta_k \ell}{\cosh \beta_k \ell + \cos \beta_k \ell}$$

2. Hinged-hinged: $\phi_k(x) = \sin \beta_k x$

3. Fixed-fixed: $\phi_k(x) = \cosh \beta_k x - \cos \beta_k x - \psi_k(\sinh \beta_k x - \sin \beta_k x)$

$$\text{where } \psi_k = \frac{\cosh \beta_k \ell - \cos \beta_k \ell}{\sinh \beta_k \ell - \sin \beta_k \ell}$$

4. Free-free: $\phi_k(x) = \cosh \beta_k x - \cos \beta_k x - \psi_k(\sinh \beta_k x - \sin \beta_k x)$

$$\text{where } \psi_k = \frac{\cosh \beta_k \ell - \cos \beta_k \ell}{\sinh \beta_k \ell - \sin \beta_k \ell}$$

5. Fixed-hinged: $\phi_k(x) = \cosh \beta_k x - \cos \beta_k x - \psi_k(\sinh \beta_k x - \sin \beta_k x)$

$$\text{where } \psi_k = \cot \beta_k \ell \quad \coth \beta_k \ell$$

6. Hinged-free: $\phi_k(x) = \cosh \beta_k x + \cos \beta_k x - \psi_k(\sinh \beta_k x + \sin \beta_k x)$

$$\text{where } \psi_k = \cot \beta_k \ell \quad \coth \beta_k \ell$$

7. Sliding-pinned: $\phi_k(x) = \cos \beta_k x$

8. Sliding-sliding: $\phi_k(x) = \cos \beta_k x$

9. Fixed-sliding: $\phi_k(x) = \cosh \beta_k x - \cos \beta_k x - \psi_k(\sinh \beta_k x - \sin \beta_k x)$

$$\text{where } \psi_k = \tanh \beta_k \ell$$

10. Sliding-free: $\phi_k(x) = \cosh \beta_k x + \cos \beta_k x - \psi_k(\sinh \beta_k x + \sin \beta_k x)$

$$\text{where } \psi_k = \tanh \beta_k \ell$$

Table 5-5

Mode Participation Factors η_k Defined by Eq. (5.4) for Beams Illustrated in Fig. 5.2

Beam Type	η_1	η_2	η_3	η_4	η_5
1. Fixed-free	0.7830	0.4339	0.2544	0.1819	0.1415
2. Hinged-hinged	1.2732	0.0000	0.4233	0.0000	0.2546
3. Fixed-fixed	0.8386	0.0000	0.3638	0.0000	0.1158
4. Free-free	0.0000	0.0000	0.0000	0.0000	0.0000
5. Fixed-hinged	0.8600	0.0826	0.3344	0.0439	0.2070
6. Hinged-free	-0.3703	0.1998	-0.1385	0.1059	-0.0857
7. Sliding-pinned	1.2732	-0.4233	0.2546	-0.1819	0.1415
8. Sliding-sliding	0.0000	0.0000	0.0000	0.0000	0.0000
9. Fixed-sliding	0.8309	0.3638	0.2315	0.1698	0.1340
10. Sliding-free	0.0000	0.0000	0.0000	0.0000	0.0000

APPENDIX A

Analog Computer Circuits

This appendix describes the fundamentals of the operational analog computer used to study certain aspects of random vibration, and sets forth the design of several special circuits that have been devised.

A. 1 Analog Computing Units

A. 1. 1 Summing Amplifier. A very large gain dc amplifier with with input resistances $R_1, R_2, R_3, \ldots$ and feedback resistance R, as illustrated in Fig. A-1, are the components used for the summing functions in accordance with the following equations. Assuming that the amplifier draws no grid current, the current flow in the circuit is defined as follows:

$$\frac{e_{i1} - e_g}{R_1} + \frac{e_{i2} - e_g}{R_2} + \frac{e_{i3} - e_g}{R_3} + \ldots = \frac{e_g - e_o}{R} \quad . \tag{A-1}$$

The voltage relation for the amplifier is

$$e_o = - A e_g \tag{A-2}$$

where A is the gain of the amplifier.

Combining Eqs. (A-1) and (A-2) and using the fact that A is very large, $e_g \cong 0$ and e_o is defined as follows:

$$e_o = - \left(\frac{R}{R_1} e_{i1} + \frac{R}{R_2} e_{i2} + \frac{R}{R_3} e_{i3} + \ldots \right) . \tag{A-3}$$

Any number of inputs can be summed when appropriate scales are determined by the ratios of the feedback resistances to the input resistance.

A. 1. 2 Integrating Amplifier. When the feedback resistor in the summing amplifier is replaced by a capacitor, as shown in Fig. A-2, the operation performed by the circuit is integration. Then the current flow

in the circuit is defined as follows:

$$\frac{e_{i1} - e_g}{R_1} + \frac{e_{i2} - e_g}{R_2} + \frac{e_{i3} - e_g}{R_3} + \ldots = C \frac{d(e_g - e_o)}{dt} \quad . \tag{A-4}$$

Assuming no grid current:

$$e_g \cong 0 \quad . \tag{A-5}$$

Combining equations (A-4) and (A-5):

$$e_o = -\frac{1}{R_1 C} \int (e_{i1} + e_{i2} + e_{i3}) dt \quad . \tag{A-6}$$

Thus, the output e_o is the integral of the sum of the respective inputs. For a single input e_i :

$$e_o = -\frac{1}{R_i C} \int e_i \, dt \quad . \tag{A-7}$$

A. 1. 3 Inverting Amplifier. The inverting amplifier is used to change or invert the input voltage from positive to negative, or vice versa. The arrangement of this amplifier, as shown in Fig. A-3, resembles that of the summing amplifier. It includes an input resistance R_i and a feedback resistance R . Kirchhoff's law for current flow in the circuit gives the following equation:

$$\frac{e_{i1} - e_g}{R_i} + \frac{e_o - e_g}{R} = 0 \quad . \tag{A-8}$$

Assuming again no grid current, i.e., $e_g \cong 0$:

$$e_o = -\frac{R}{R_i} e_{i1} \quad . \tag{A-9}$$

The ratio of the feedback resistance R to the input resistance R_i can be adjusted to obtain the desired gain.

A. 1. 4 Potentiometer. A potentiometer is used in computer applications to perform multiplication by a constant coefficient less than

unity. Frequently it is used to adjust the input to an operational amplifier to attain the required parameters of the system. Appropriate total resistances should be chosen so as to avoid loading effects. The circuit diagram for the potentiometer is shown in Fig. A-4. The relation between the input and output voltages is

$$e_o = a\, e_i \qquad [0 \leq a \leq 1] \,. \tag{A-10}$$

A. 2 Analog Simulation of the Single Degree of Freedom Vibration System

From the schematic diagram of the single degree of freedom system shown in Fig. A-5, the differential equation describing the motion of the system is written as follows:

$$m\ddot{x} + c(\dot{x} - \dot{y}) + k(x - y) = 0 \,. \tag{A-11}$$

Substituting $z = x - y$, $\ddot{z} = \ddot{x} - \ddot{y}$:

$$m\ddot{z} + c\dot{z}' + kz = -m\ddot{y} \,. \tag{A-12}$$

Dividing through by m and letting $k/m = p^2$, $c/m = 2\rho p$:

$$\ddot{z} + 2\rho p\dot{z} + p^2 z = -\ddot{y} \,. \tag{A-13}$$

The analog simulation of Eq. (A-13) is accomplished by the configuration of analog computing elements shown in Fig. A-6. The relationship among the several voltages is:

$$e_2 = -\frac{1}{R_1 C_1} \int e_1 \, dt \tag{A-14}$$

$$e_3 = -\frac{1}{R_2 C_2} \int e_2 \, dt \tag{A-15}$$

where $R_1 C_1$ are the values of resistance and capacitance associated with integrator (1) [see Fig. A-2] and $R_2 C_2$ are corresponding values for integrator (2). Combining Eqs. (A-14) and (A-15):

$$e_3 = -\frac{1}{R_2C_2}\int\left[-\frac{1}{R_1C_1}\int e_1\,dt\right]dt = \frac{1}{R_1R_2C_1C_2}\int\int e_1(dt)^2 . \quad (A-16)$$

The output of the summing amplifier is

$$e_1 = -\left[e_o - ae_2 + be_3\right] = -\left[e_o + \frac{a}{R_1C_1}\int e_1 dt + \frac{1}{R_1R_2C_1C_2}\int\int e_1(dt)^2\right] . \quad (A-17)$$

Rearranging the preceding equation:

$$e_1 + \frac{a}{R_1C_1}\int e_1 dt + \frac{b}{R_1R_2C_1C_2}\int\int e_1(dt)^2 = -e_o .$$

Values of resistance and capacitance used in the experimental work discussed in this report are as follows: $R_1 = 1.0001$ MΩ ; $R_2 = 1.0060$ MΩ ; $C_1 = 0.004030$ μf ; and $C_2 = 0.00039765$ μf. The relations between corresponding quantities of the mechanical and electrical systems are given in Table A-1.

The analog voltages representing displacement, velocity, and acceleration of the mechanical system can be obtained easily from the measurable quantities e_1 , e_2 , and e_3 . It is known from Eq. (A-15) that

$$e_3 = \frac{1}{R_1R_2C_1C_2}\int\int e_1(dt)^2 .$$

From Table A-1:

$$z = \int\int e_1(dt)^2 .$$

Combining the preceding relations:

$$z = (R_1R_2C_1C_2)e_3 . \quad (A-18)$$

From Eq. (A-14) :

$$e_2 = -\frac{1}{R_1C_1}\int e_1 dt .$$

From Table A-1:

$$z = \int e_1 \, dt .$$

Combining the preceding relations:

$$\dot{z} = (-R_1 C_1) e_2 . \tag{A-19}$$

From Table A-1:

$$\ddot{z} = e_1 . \tag{A-20}$$

The effect of the time constants of the integrators should be noted in interpreting the voltages read on the analog computer. For example, Eq. (4.21) gives the relation between the mean square value of the displacement response and the mean square acceleration density (power spectral density) of the excitation. If the voltage e_o in Fig. A-6 represents the acceleration $\ddot{y}$ in Fig. A-5, the relation between the power spectral densities of the physical and analog systems is

$$W_{\ddot{y}}(\omega) = W_{e_o}(\omega) . \tag{A-21}$$

Then the relation between the voltage e_3 and the power spectral density $W_{e_o}(\omega)$ is, using the relation of Eq. (A-18):

$$e_3^2 = \frac{1}{R_1 R_2 C_1 C_2} \frac{\pi W_{e_o}(\omega)}{4\zeta \omega_n^3} . \tag{A-22}$$

A.3 Complete Analog System

In the current phase of the investigation, the analog computer has been used primarily to investigate the response of a mechanical system to a particular type of non-Gaussian excitation, a broad band random vibration in which the maximum values are limited at certain predetermined levels. As indicated in Fig. A-5, the excitation is defined by acceleration of the support $\ddot{y}$ and the response is the relative displace-

ment $x-y$, a parameter whose physical significance is explained in Section 4. 4 of this report.

A block diagram of the analog system is shown in Fig. A-7, built around the analog of the single degree of freedom system shown in Fig. A-6. A General Radio Type 1390B Random Noise Generator is used as the excitation. The bandwidth of the excitation is reduced to a value more readily recorded oscillographically by a Krohn-Hite Model 330-M Band Pass Filter, adjusted in general to have a pass band of 2 to 2000 cps. The amplitude limiting circuit is described in Section A. 3. 1 below. The output z is a narrow band random vibration (see Fig. 4. 20) for which both the rms value and the distribution of peak values are measured by the circuit shown. A Quan-Tech Model 317 Amplitude Distribution Analyzer provides a direct reading of the percentage of time that the signal exceeds a designated value. It also has a digital output that can be used with an electronic counter to determine the total number of peaks exceeding a designated value, over any desired averaging time. For the particular experiments discussed herein, the squaring circuit in the Ballantine Model 320 True rms Voltmeter is used to square the instantaneous voltage that represents z. For a narrow band vibration, the mean square value fluctuates rapidly between relatively wide limits; a significant reading can be obtained only by using an instrument with a long time constant. The long time constant is obtained, in effect, by using the low pass filter described in Section A. 3. 2 and a dc voltmeter. A photograph of the analog computer described by the block diagram of Fig. A-7 is included as Fig. A-8.

A. 3. 1 Amplitude Limiting Circuit. The important components of the limiting circuit shown in Fig. A-9 are an operational amplifier A,

two diodes D , a decade resistance box or potentiometer R_4 , and a battery E_o . Fixed resistances shown are the input resistance R_1 , feedback resistance R_f , and the resistances R_2 , R_3 in series with the diodes. The variable resistance R_4 allows the limiting voltage level to be set to any convenient magnitude, above which the signal is limited. This is illustrated by the plot of output voltage e_o as a function of input voltage e_i shown in Fig. A-10. The limiting level is indicated by e_c . The resistances R_2 and R_3 are matched to be approximately equal so as to obtain symmetrical upper and lower limiting values e_c . The input resistance and feedback resistance are set equal to achieve unity gain within the voltage range from $-e_c$ to e_c .

A. 3. 2 Low Pass Filter. The low pass filter discussed in Section A. 3 and indicated in Fig. A-7 serves the function of an averaging device. It consists of an operational amplifier, a resistance R and a capacitance C in shunt across the amplifier, and an input resistance R_i . The circuit diagram is shown in Fig. A-11.

The time constant RC is adjusted to a value where a steady reading is made possible on the dc voltmeter. As damping in the system is reduced, the bandwidth becomes smaller and the time constant required to obtain an accurate reading of the rms value is increased. The resistances R, R_i and the capacitance C have the following values: $R = 5\ M\Omega$; $R_i = 1\ M\Omega$; and $C = 1\ \mu f$.

TABLE A-1

Relation Between Corresponding Quantities of the Mechanical System and Electrical System

Item	Mechanical System	Electrical System
Relative Acceleration	$\ddot{z}$	e_1
Relative Velocity	$\dot{z}$	$\int e_1 \, dt$
Relative Displacement	z	$\int\int e_1 \, (dt)^2$
Support Acceleration	$\ddot{y}$	e_o
Natural Frequency	$p = \frac{k}{m}$	$\sqrt{\frac{b}{R_1 R_2 C_1 C_2}}$
Damping Parameter	$\frac{c}{m} = 2\zeta p$	$\frac{a}{R_1 C_1}$
Fraction of Critical Damping	$\frac{c}{c_c} = \zeta$	$\frac{a}{2}\sqrt{\frac{R_2 C_2}{b R_1 C_1}}$

Appendix B

FREE AND FORCED VIBRATION OF A MULTIPLE DEGREE OF FREEDOM SYSTEM

B-1 Free Vibration of a Discrete System

This appendix develops the equations for the free and forced vibration of a multiple degree of freedom system, starting with Lagrange's equation. Then the results are extended to the vibration of a beam by choosing as the generalized coordinates the normal mode coordinates of the beam. Lagrange's equation for the free vibration of an undamped system is

$$\frac{d}{dt}\left(\frac{\partial T}{\partial \dot{q}_i}\right) - \frac{\partial T}{\partial q_i} + \frac{\partial V}{\partial q_i} = 0 \qquad \text{(B-1)}$$

where T is the kinetic energy of the system, V is the potential energy and q_i are the generalized coordinates used to define the motion of the system.

Applicable expressions for kinetic and potential energy for use in Eq. (B-1) are as follows:

$$T = \frac{1}{2}\sum_{i=1}^{n}\sum_{j=1}^{n} a_{ij}\,\dot{q}_i\,\dot{q}_j \qquad i,j=1,2,\ldots n \qquad \text{(B-2)}$$

where

$$a_{ij} = \sum_{r=1}^{s} m_r\left(\frac{\partial x_r}{\partial q_i}\,\frac{\partial x_r}{\partial q_j} + \frac{\partial y_r}{\partial q_i}\,\frac{\partial y_r}{\partial q_j} + \frac{\partial z_r}{\partial q_i}\,\frac{\partial z_r}{\partial q_j}\right) \qquad \text{(B-3)}$$

In the above expression, x_r, y_r, z_r are the Cartesian coordinates which define the positions of the discrete masses m_r where r=1, 2, --s.

$$V = \frac{1}{2} \sum_{i=1}^{n} \sum_{j=1}^{n} c_{ij} \; q_i \; q_j \qquad i,j=1,2,\ldots\ldots,n \qquad \text{(B-4)}$$

where $c_{ij} = \left(\frac{\partial^2 V}{\partial q_i \; \partial q_j} \right)_o$ (B-5)

It should be noted that $c_{ij} = c_{ji}$ since the order of differentiation is unimportant.

The expressions for T and V given by Eqs. (B-2) and (B-4), respectively, are now substituted in Eq. (B-1) by carrying out the indicated differentiation successively with respect to i = 1, 2, . . . , n. This results in n differential equations each of the following form

$$\sum_{j=1}^{n} a_{ij} \; \ddot{q}_j + \sum_{j=1}^{n} c_{ij} \; q_j = 0 \qquad i=1, 2, \ldots, n \qquad \text{(B-6)}$$

where the coefficients a_{ij}, c_{ij} may be found by the partial differentiation indicated by Eqs. (B- 3) and (B-5), respectively. Often it is more expedient to write a_{ij} and c_{ij} by inspection, by comparing the expressions for potential and kinetic energy with Eqs. (B-2) and (B-4). It should be kept in mind that $c_{ij} \; q_i \; q_j = c_{ji} \; q_j \; q_i$ and $a_{ij} \; \dot{q}_i \; \dot{q}_j = a_{ji} \; \dot{q}_j \; \dot{q}_i$ to avoid introducing a factor of 2 in determining c_{ij} and a_{ij}.

The solution of Eq. (B-6) is of the following form:

$$q_j = A_j \sin (pt + \Phi)$$

Differentiating this expression twice to obtain $\ddot{q}_j$, and substituting q_j, $\ddot{q}_j$ in Eq. (B-6):

$$\sum_{j=1}^{n} (c_{ij} - p^2 \; a_{ij}) \; A_j = 0 \qquad i=1,2,\ldots,n \qquad \text{(B-7)}$$

There is a non-trivial solution to Eq. (B-7) only if the determinant of the coefficient of A_j vanishes. Expanding the summation and writing the equation for i = 1, 2,..., n, the determinant is as follows:

$$\begin{vmatrix} c_{11} - p^2 a_{11} & c_{12} - p^2 a_{12} \ldots\ldots & c_{1n} - p^2 a_{1n} \\ c_{21} - p^2 a_{21} & c_{22} - p^2 a_{22} \ldots\ldots & c_{2n} - p^2 a_{2n} \\ \ldots\ldots & \ldots\ldots\ldots\ldots & \ldots\ldots \\ c_{n1} - p^2 a_{n1} & c_{n2} - p^2 a_{n2} & c_{nn} - p^2 a_{nn} \end{vmatrix} = 0 \quad \text{(B-8)}$$

This determinant when expanded gives an algebraic equation of the nth degree with p^2 as the variable. Solution of this equation gives n values of p^2 and hence n positive values of p. These positive values of p are the natural or normal frequencies of the system; the numerically equal negative values are discarded as lacking physical significance.

The normal mode frequencies p_k are designated by the subscript k = 1, 2, ..., n where k refers to a particular root of the polynomial obtained from the determinant, Eq. (B-8). For each normal frequency there is a set of amplitudes A_j for the generalized coordinates q_j. The complete array of amplitudes is designated A_{jk} where the first subscript indicates the coordinate and the second subscript indicates the mode corresponding to the frequency p_k. Values for the normal mode amplitudes A_{jk} are found from Eq. (B-7) by substituting successively the values of p_k found from Eq. (B-8), together with appropriate values for i and j, and solving for A_{jk}. From the information available from Eq. (B-7), absolute values of A_{jk} are not obtainable but rather only values relative to one A_{jk} in the set can be found. For example,

the calculation would yield the ratios A_{21}/A_{11} , A_{31}/A_{11}, ... A_{n1}/A_{11}. Then the value of A_{11} must be determined from other information relevant to the problem, as discussed in subsequent sections.

The generalized coordinates that describe the system may be expressed as summations of normal mode amplitudes as follows:

$$q_j = \sum_{k=1}^{n} \xi_k \, A_{jk} \qquad j = 1, 2, \ldots, n \qquad \text{(B-9)}$$

where $\xi_k = B_k \cos p_k t$ is a time-varying parameter for each normal mode and B_k is a dimensionless constant whose value is determined by the initial conditions of the system in free vibration or by the forcing function in forced vibration. Inasmuch as the values of A_{jk} cannot be determined absolutely but only relative one to the other from the information available from Eq. (B-9), expressions for q_j can be written from Eq. (B-9) by eliminating B_k and writing ratios of A_{jk} as follows:

$$\left.\begin{aligned}
q_1 &= \xi_1 + \xi_2 + \ldots + \xi_n \\
q_2 &= \frac{A_{21}}{A_{11}} \xi_1 + \frac{A_{22}}{A_{12}} \xi_2 + \ldots + \frac{A_{2n}}{A_{1n}} \xi_n \\
q_3 &= \frac{A_{31}}{A_{11}} \xi_1 + \frac{A_{32}}{A_{12}} \xi_2 + \ldots + \frac{A_{3n}}{A_{1n}} \xi_n \\
&\ldots\ldots\ldots\ldots\ldots\ldots\ldots \\
q_n &= \frac{A_{n1}}{A_{11}} \xi_1 + \frac{A_{n2}}{A_{12}} \xi_2 \ldots + \frac{A_{nn}}{A_{1n}} \xi_n
\end{aligned}\right\} \qquad \text{(B-10)}$$

Now if the generalized coordinates q_j are given the displacements indicated by Eq. (B-10) at time t = 0 so that each ξ_k has a value of unity, the system will vibrate in free but steady-state vibration.

This vibration is characterized by simultaneous vibration in each of the natural frequencies p_k; the mode shapes associated with these natural frequencies exist concurrently and independently, and the resultant motion is obtained by uperposition of normal modes. This concept is of great usefulness in the analysis of a multiple degree of freedom system undergoing forced vibration, whether periodic or non-periodic.

If the generalized coordinates q_j as defined by Eq. (B-10) are substituted into the expressions for potential and kinetic energy, Eqs. (B-2) and (B-4), the coefficients c_{ij} and a_{ij} are equal to zero when $i \neq j$. Then the variables in the Eqs. (B-6) are not q_j but rather ξ_k where the values of the normal mode amplitudes A_{jk} are reflected in the coefficients. Then, inasmuch as $c_{ij} = a_{ij} = 0$ when $i \neq j$, the set of equations becomes k uncoupled second order equations which may be solved independently for the normal mode frequencies p_k.

A convenient property of the normal mode amplitudes is based upon the orthogonality of the normal mode amplitudes, defined mathematically as follows:

$$\sum_{i=1}^{n} \sum_{j=1}^{n} a_{ij} A_{jk} A_{i\ell} = 0 \qquad [k \neq \ell] \qquad \text{(B-11)}$$

This is the orthogonality relation of the normal modes. For this relation to be of optimum simplicity and thus of maximum usefulness, it is desirable that the coordinates be chosen so that there is no

dynamic coupling; i.e., $a_{ij} = 0$ when $i \neq j$. With this limitation, the double summation in Eq. (B-11) becomes unnecessary and the orthogonality relation can be written in the following somewhat more concise form:

$$\sum_{j=1}^{n} a_{ij} \; A_{jk} \; A_{j\ell} = 0 \qquad [k \neq \ell] \qquad \text{(B-12)}$$

The orthogonality relation can be extended to define a further condition of the system and thereby eliminate the need for the coefficient B_k introduced in connection with Eq. (B-9) to recognize that one parameter of the system had remained undefined. This further condition is normalization, the adoption of some arbitrary relation among the normal mode amplitudes when $k = \ell$. A convenient condition which makes possible a consistent notation with the orthogonality relation is the following:

$$\sum_{j=i}^{n} a_{jj} \; A_{jk} \; A_{j\ell} = 1 \qquad [k = \ell] \qquad \text{(B-13)}$$

B-2 Forced Vibration of a Discrete System

B-21 Force Excitation.

To write the expression for forced vibration of an undamped, multiple degree of freedom system. A generalized force Q_i is added on the right side of Eq. (B-1) and evaluated in terms of the work done on the system. It should be noted that Q_i is derived from the virtual work; therefore, Q_i is not generally a force but rather has such dimensions that its product with the generalized coordinate q_i has the dimensions of work.

The following analysis of forced vibration contemplates that the system will have first been analyzed in free vibration to determine the normal mode frequencies and the normal mode amplitudes associated with these frequencies. The equations of motion in generalized coordinates q_j, Eq. (B-6), are first written as an array of equations as follows:

$$a_{11}\ddot{q}_1 + a_{12}\ddot{q}_2 + \ldots a_{1n}\ddot{q}_n + c_{11}q_1 + c_{12}q_2 + \ldots c_{1n}q_n = Q_1$$

$$a_{21}\ddot{q}_1 + a_{22}\ddot{q}_2 + \ldots a_{2n}\ddot{q}_n + c_{21}q_1 + c_{22}q_2 + \ldots c_{2n}q_n = Q_2$$

$$\ldots\ldots\ldots\ldots\ldots\ldots\ldots\ldots$$

$$a_{n1}\ddot{q}_1 + a_{n2}\ddot{q}_2 + \ldots a_{nn}\ddot{q}_n + c_{n1}q_1 + c_{n2}q_2 + \ldots c_{nn}q_n = Q_n$$

As pointed out in connection with Eq. (B-12), it is convenient to choose the coordinates so that there is no dynamic coupling; i.e., $a_{ij} = 0$ when $i \neq j$. Applying this qualification to the preceding array of equations, the differential equations for forced vibration may be written as follows:

$$a_{ii}\ddot{q}_i + \sum_{j=1}^{n} c_{ij}\, q_j = Q_i \qquad i = 1, 2, \ldots, n \qquad \text{(B-14)}$$

The generalized coordinates q_j are defined by Eq. (B-9) in terms of the normal coordinates ξ_k and the normal mode applitudes A_{jk}. Substituting from Eq. (B-9) into Eq. (B-14), the following differential equations are obtained in terms of the normal coordinates:

$$a_{ii} \sum_{k=1}^{n} \ddot{\xi}_k A_{ik} + \sum_{j=1}^{n} c_{ij} \sum_{k=1}^{n} \xi_k A_{jk} = Q_i \quad i=1, 2, \ldots, n \tag{B-15}$$

It is now convenient to introduce a new parameter γ_k which relates Q_i, a_{ii} and A_{ik} as follows:

$$\frac{Q_i}{a_{ii}} = \sum_{k=1}^{n} \gamma_k A_{ik} \tag{B-16}$$

Substituting from Eq. (B-16) into Eq. (B-15) to eliminate Q_i from the latter:

$$a_{ii} \sum_{k=1}^{n} \ddot{\xi}_k A_{ik} + \sum_{j=1}^{n} c_{ij} \sum_{k=1}^{n} \xi_k A_{jk} - a_{ii} \sum_{k=1}^{n} \gamma_k A_{ik} = 0 \quad i=1, 2, \ldots, n \tag{B-17}$$

The second term on the left side of the preceding equation is evaluated from Eq. (B-7) by taking one of the frequencies p_k and noting that $a_{ii} = 0$ when $i \neq j$;

$$\sum_{j=1}^{n} c_{ij} A_{jk} = p_k^2 a_{ii} A_{ik} \qquad i=1, 2, \ldots, n$$

Substituting this relation in Eq. (B-17):

$$a_{ii} \sum_{k=1}^{n} \ddot{\xi}_k A_{ik} + a_{ii} \sum_{k=1}^{n} p_k^2 \xi_k A_{ik} - a_{ii} \sum_{k=1}^{n} \gamma_k A_{ik} = 0$$

Collecting terms, the preceding equation becomes

$$\sum_{k=1}^{n} (\ddot{\xi}_k + p_k^2 \xi_k - \gamma_k) a_{ii} A_{ik}) = 0$$

Multiplying the preceding equation by $A_{i\ell}$ and summing over i:

$$\sum_{k=1}^{n} (\ddot{\xi}_k + p_k^2 \xi_k - \gamma_k) \sum_{i=1}^{n} a_{ii} A_{ik} A_{i\ell} = 0 \tag{B-18}$$

In the preceding expression, $\sum_{i=1}^{n} a_{ii} A_{ik} A_{i\ell} = 0$ when $k \neq \ell$, in accordance with the orthogonality relation of Eq. (B-12). When $\ell = k$, the summation $\sum_{i=1}^{n} a_{ii} A_{ik}^2 \neq 0$ and the summation over k reduces to a single term. Then Eq. (B-18) may be written as follows:

$$(\ddot{\xi}_k + p_k^2 \xi_k - \gamma_k) \sum_{i=1}^{n} a_{ii} A_{ik}^2 = 0$$

Since the summation over i is not zero, in accordance with the orthogonality relation, it follows that the expression within parentheses must be zero:

$$\ddot{\xi}_k + p_k^2 \xi_k - \gamma_k = 0 \qquad \text{(B-19)}$$

where γ_k is to be evaluated at the condition $\ell = k$.

The parameter γ_k is evaluated by first multiplying Eq. (B-16) by $a_{ii} A_{i\ell}$:

$$Q_i A_{i\ell} = \sum_{k=1}^{n} \gamma_k a_{ii} A_{ik} A_{i\ell}$$

Taking a summation over *i*:

$$\sum_{i=1}^{n} Q_i A_{i\ell} = \sum_{k=1}^{n} \gamma_k \sum_{i=1}^{n} a_{ii} A_{ik} A_{i\ell}$$

From the orthogonality relation, Eq. (B-12), the summation over i on the right side of the preceding equation is zero except when $\ell = k$. Thus the summation over k reduces to a single term, and each occurrence of ℓ may be changed to k. Then the equation becomes

$$\sum_{i=1}^{n} Q_i A_{ik} = \gamma_k \sum_{i=1}^{n} a_{ii} A_{ik}^2$$

Solving for γ_k:

$$\gamma_k = \frac{\sum_{i=1}^{n} Q_i \, A_{ik}}{\sum_{i=1}^{n} a_{ii} \, A_{ik}^2} \qquad \text{(B-20)}$$

where γ_k is sometimes called the "mode participation factor". Substituting from Eq. (B-20) into Eq. (B-19), the differential equation for forced vibration of the system is

$$\ddot{\xi}_k + p_k^2 \, \xi_k = \frac{\sum_{i=1}^{n} Q_i \, A_{ik}}{\sum_{i=1}^{n} a_{ii} \, A_{ik}^2} \qquad k = 1, 2, \ldots, n \qquad \text{(B-21)}$$

where this equation applies independently to the respective normal modes using the normal mode frequencies p_k and the normal mode amplitudes A_{ik}.

Sometimes the numerator and denominator of the right side of Eq. (B-21) are designated as follows:

$$\sum_{i=1}^{n} Q_i \, A_{ik} = \text{generalized force } \mathcal{F}_k \text{ in k mode}$$

$$\sum_{i=1}^{n} a_{ii} \, A_{ik}^2 = \text{generalized mass } \mathcal{M}_k \text{ in k mode} \qquad \text{(B-22)}$$

The former should not be confused with the generalized force Q_i which appears on the right side of the Lagrange equation.

The response of the system in forced vibration as determined from Eq. (B-21) is expressed in terms of the normal mode coordinates ξ_k. The resultant expressions for ξ_k are then substituted in Eq. (B-9) to obtain the response in terms of the generalized coordinates q_j.

B-2.2 Motion Excitation.

Suppose now that the support for the system experiences

a motion whose displacement is defined by a set of parameters $s_1, s_2, \ldots s_n$ where each parameter s_j is related to each generalized coordinate q_j in such a manner that q_j is now considered to be motion relative to the support and $\dot{s}_j + \dot{q}_j$ is the velocity in the j coordinate. Then the total kinetic energy is

$$T = \frac{1}{2} \sum_{j=1}^{n} a_{jj} (\dot{s}_j + \dot{q}_j)^2 \qquad \text{(B-23)}$$

where the coordinates are chosen so that there is no dynamic coupling; i.e., $a_{ij} = 0$ when $i \neq j$. The potential energy expression is identical to Eq. (B-4).

$$V = \frac{1}{2} \sum_{i=1}^{n} \sum_{j=1}^{n} c_{ij} q_i q_j \qquad \text{(B-4 repeated)}$$

The kinetic energy expression is written in terms of the normal mode coordinates by substituting q_j from Eq. (B-9) in Eq. (B-23).

$$T = \frac{1}{2} \sum_{j=1}^{n} a_{jj} \left[\sum_{k=1}^{n} \xi_k A_{jk} + \dot{s}_j \right]^2 \qquad \text{(B-24)}$$

In expanding the term in brackets, use is made of the expression given by Eq. (B-22) for generalized mass $\mathcal{M}_k$ and the orthogonality relation given by Eq. (B-12):

$$T = \frac{1}{2} \sum_{k=1}^{n} \mathcal{M}_k \dot{\xi}_k^2 + \sum_{j=1}^{n} a_{jj} \dot{s}_j \sum_{k=1}^{n} \dot{\xi}_k A_{jk} + \sum_{j=1}^{n} a_{jj} \dot{s}_j^2 \qquad \text{(B-25)}$$

Similarly, substituting from Eq. (B-9) in Eq. (B-4), the expression for potential energy is

$$V = \frac{1}{2} \sum_{i=1}^{n} \sum_{j=1}^{n} \sum_{k=1}^{n} c_{ij} A_{jk} A_{ik} \xi_k^2 \qquad \text{(B-26)}$$

The portion of the preceding equation involving the summations over i and j combine into the single summation $\sum_{j=1}^{n} a_{jj} A_{jk}^2$ when i=j. From Eq. (B-22), this is equal to the generalized mass $\mathcal{M}_k$ and the expression for potential energy may be written:

$$V = \frac{1}{2} \sum_{k=1}^{n} \mathcal{M}_k p_k^2 \xi_k^2 \qquad \text{(B-27)}$$

The differential equation of motion is now written by taking appropriate partial derivatives of Eqs. (B-25) and (B-27), and substituting in Eq. (B-1), noting that the derivative of the last term of Eq. (B-25) is zero:

$$\mathcal{M}_k \ddot{\xi}_k + \sum_{j=1}^{n} a_{jj} A_{jk} \ddot{s}_j + \mathcal{M}_k p_k^2 \xi_k = 0 \quad k= 1, 2, \ldots, n \qquad \text{(B-28)}$$

Placing the second term on the right side of the equation and dividing all terms by $\mathcal{M}_k$:

$$\ddot{\xi}_k + p_k^2 \xi_k = -\frac{1}{\mathcal{M}_k} \sum_{j=1}^{n} a_{jj} A_{jk} \ddot{s}_j \qquad \text{(B-29)}$$

where $\ddot{s}_j = \ddot{s}_j(t)$, the acceleration of the support expressed as a function of time. Equation (B-29) is similar to Eq. (B-21) if the excitation force Q_i in the former is replaced (the subscripts i and j are interchangeable since each varies from 1 to n) by $- a_{jj} \ddot{s}_j$. This means that the system responds as if a force acts on each element of mass equal to the product of the respective mass and the acceleration of the support. It should be kept in mind here that the generalized coordinate q_j in this instance is taken relative to the support.

Equation (B-29) may be placed in the form of Eq. (B-19) by introducing a form of the mode participation factor η_k that applies to

vibration excited by motion of the support:

$$\ddot{\xi}_k + p_k^2 \xi_k + \eta_k \ddot{s}(t) = 0 \qquad \text{(B-30)}$$

$$\text{where } \eta_k = \frac{\sum_{j=1}^{n} a_{jj} A_{ik}}{\sum_{j=1}^{n} a_{jj} A_{ik}^2} \qquad \text{(B-31)}$$

It should be noted that the mode participation factor γ_k defined by Eq. (B-20) includes the generalized force Q_i and must be evaluated for each particular excitation. On the other hand, the factor η_k defined by Eq. (B-31) is independent of the excitation and need be defined only once for a given system.

B-3 Vibration of Continuous Systems

B-3.1 Free and Forced Vibration

The essential concepts in the forced vibration of a multiple degree of freedom linear system considered in terms of a superposition of normal mode responses can be adapted by analogy to the forced vibration of a continuous system. The analogy is taken so that the discrete masses of the multiple degree of freedom system correspond to infinitesimal elements of mass in the continuous system. For example, consider a beam of uniform section in free vibration; the differential equation of motion is

$$\frac{\partial^4 y}{\partial x^4} + \frac{\mu}{EI} \cdot \frac{\partial^2 y}{\partial t^2} = 0 \qquad \text{(B-32)}$$

where μ = mass per unit length of beam

E = Young's modulus for the beam

I = area moment of inertia of beam cross section

The solution of Eq. (B-32) for free vibration of the beam is analogous to Eq. (B-9) for the discrete system considered previously, and may be written as follows:

$$y(x) = \sum_{k=1}^{\infty} \xi_k \varphi_k(x) \qquad \text{(B-33)}$$

where $\varphi_k(x)$ is the characteristic shape of the beam in the k^{th} mode of vibration and $\xi_k = B_k \cos p_k t$ is a time-varying parameter applicable to each normal mode. The coefficient B_k is a dimensionless constant whose value is determined by the intial conditions of the system.

Equation (B-19) applies to forced periodic and non-periodic vibration of beams when the mode participation factor γ_k is appropriately determined. The analogy between the beam and the system consisting of discrete masses is found by considering the beam to be comprised of an infinitely large number of infinitesimal lengths dx; then $a_{ii} = \mu\, dx$ and $A_{ik} = \varphi_k(x)$. Thus the generalized mass for the beam, by analogy with Eq. (B-22), is

$$\mathcal{M}_k = \int_0^{\ell} \mu \varphi_k^{\,2}(x)\, dx \qquad \text{(B-34)}$$

When the excitation is a force applied to the beam, the numerator of γ_k (the generalized force) is found by interpreting A_{jk} as the value of the characteristic shape φ_k evaluated at the value or values of φ_k at which the forces Q_j are applied. Then the generalized force is written as follows:

$$\mathcal{F}_k = \sum_{h=1}^{m} Q_h\, \varphi_k(x_h) \qquad \text{(B-35)}$$

where the forces $Q_1, Q_2, \ldots Q_m$ are applied at locations along the beam indicated by $x_1, x_2, \ldots x_m$.

Where the forced vibration occurs as a result of motion of the support for the beam, Eq. (B-30) is applicable upon appropriate interpretation of the mode participation factor η_k. The generalized mass defined by Eq. (B-34) is applicable. As discussed previously, excitation by motion of the support is analogous to excitation by applied forces which are equal to the acceleration of the support multiplied by the masses of the respective elements. In a beam,

there are an infinitely large number of masses and the summations in Eq. (B-31) are written as integrals:

$$\eta_k = \frac{\int_o^{\ell} \mu \, \varphi_k(x) \, dx}{\int_o^{\ell} \mu \, \varphi_k^2(x) \, dx} \qquad \text{(B-36)}$$

where $\varphi_k(x)$ is taken to describe the normal mode shapes of the beam relative to its support.

B-3.2 Natural Frequencies and Mode Shapes

The natural frequencies and mode shapes are determined by solving Eq. (B-32) for the condition of free vibration with boundary conditions that are applicable to particular types of beams. The solution to the differential equation, Eq. (B-33), may be written in the following form:

$$y(x,t) = \sum_{k=1}^{\infty} \varphi_k(x) \, e^{jp_k t} \qquad \text{(B-37)}$$

where p_k is the natural frequency of the beam in the k^{th} mode and the characteristic shapes $\varphi_k(x)$ are governed by orthogonality relations written by analogy with Eqs. (B-12) and (B-13) for the discrete system:

$$\int_o^{\ell} \varphi_k(x) \, \varphi_{\ell}(x) \, dx = 0 \qquad k \neq \ell \qquad \text{(B-38)}$$

$$\int_o^{\ell} \varphi_k(x) \, \varphi_{\ell}(x) \, dx = 1 \qquad k = \ell \qquad \text{(B-39)}$$

Substituting Eq. (B-37) into Eq. (B-32):

$$\frac{d^4 \varphi_k(x)}{dx^4} - p_k^2 \frac{\mu}{EI} \varphi_k(x) = 0 \qquad \text{(B-40)}$$

The solution to Eq. (B-40) is of the form

$$\varphi_k(x) = A'\sin\beta_k x + B'\cos\beta_k x + C'\sinh\beta_k x + D'\cosh\beta_k x \quad \text{(B-41)}$$

where β_k is defined as follows:

$$\beta_k = \sqrt[4]{\frac{p_k^2 \mu}{EI}} \quad \text{(B-42)}$$

The natural frequencies are found by solving Eq. (B-42) for p_k:

$$p_k = \beta_k^2 \sqrt{\frac{EI}{\mu}} \quad \text{(B-43)}$$

where the substitution of the boundary conditions into Eq. (B-41) yields a sequence of values for $\beta_k \ell$, the characteristic length of the beam being designated by ℓ. Equation (B-41) applies to beams in general; it can be made to apply to a particular beam by evaluating the coefficients A, B, C, D using the boundary conditions for the beam. For free vibration of a beam, the vibration amplitude is arbitrary; therefore, the coefficients cannot be evaluated in absolute terms but rather three of them can be evaluated in terms of the fourth which remains undetermined until the conditions of excitation are introduced.

B-3.2.1 Example: Cantilever Beam

The boundary conditions used to evaluate the coefficients in Eq. (B-41) are that the deflection and slope at the fixed end are zero, and

the bending moment and shear force at the free end are zero. These are expressed as follows, referring to Fig. B-1:

$$\text{(a) } y(o,t) = 0 \text{ ;(b) } \frac{\partial y}{\partial x}(o,t) = 0 \text{ ; } \frac{\partial^2 y}{\partial x^2}(\ell,t) = 0\text{; (d) } \frac{\partial^3 y}{\partial x^3}(\ell,t) = 0 \quad \text{(B-44)}$$

Frequently it is more expedient to evaluate the boundary conditions if Eq. (B-41) is written in the following form:

$$\varphi_k(x) = A(\cos \beta_k x + \cosh \beta_k x) + B(\cos \beta_k x - \cosh \beta_k x) + C(\sin \beta_k x + \sinh \beta_k x) + D(\sin \beta_k x - \sinh \beta_k x) \quad \text{(B-45)}$$

Applying condition (a) of Eq. (B-44), it is evident that A = 0. Then differentiating Eq. (B-44) once with respect to x:

$$\frac{d\varphi_k}{dx} = B\beta_k(-\sin \beta_k x - \sinh \beta_k x) + C\beta_k(\cos \beta_k x + \cosh \beta_k x) + D\beta_k(\cos \beta_k x - \cosh \beta_k x) \quad \text{(B-46)}$$

Applying condition (b) of Eq. (B-44), it is evident that C = 0. Now differentiating Eq (B-46) twice with respect to x and applying conditions (c) and (d) of Eq. (B-44):

$$\frac{\partial^2 \varphi_k(\ell)}{\partial x^2} = B\beta_k^2(-\cos \beta_k \ell - \cosh \beta_k \ell) + D\beta_k^2(-\sin \beta_k \ell - \sinh \beta_k \ell) = 0 \quad \text{(B-47)}$$

$$\frac{\partial^3 \varphi_k(\ell)}{\partial x^3} = B\beta_k^3(\sin \beta_k \ell - \sinh \beta_k \ell) + D\beta_k^3(-\cos \beta_k \ell - \cosh \beta_k \ell) = 0 \quad \text{(B-48)}$$

Solving each of the preceding equations for B/D and equating the results:

$$\frac{B}{D} = -\frac{(\sin \beta_k \ell + \sinh \beta_k \ell)}{\cos \beta_k \ell + \cosh \beta_k \ell} = \frac{\cos \beta_k \ell + \cosh \beta_k \ell}{\sin \beta_k \ell - \sinh \beta_k \ell}$$

The preceding expression simplifies to the following form:

$$1 + \cos \beta_k \ell \cosh \beta_k \ell = 0 \qquad \text{(B-49)}$$

This is the frequency equation for the fixed-free or cantilever beam. When Eq. (B-49) is solved numerically, it yields an infinitely large number of roots $\beta_k \ell = a_k$ which are significant in determining the natural frequencies and characteristic mode shapes of the beam. Substituting the root a_k in Eq. (B-43):

$$p_k = \frac{a_k^2}{\ell^2}\sqrt{\frac{EI}{\mu}} \qquad \text{rad/sec.} \qquad \text{(B-50)}$$

With the values of β_k determined from Eq. (B-49) and expressions for the coefficients A, B, C, D as determined above, Eq. (B-41) for the mode shape $\varphi_k(x)$ becomes

$$\varphi_k(x) = B_k\left[\cos \beta_k x - \cosh \beta_k x - \Psi_k (\sin \beta_k x - \sinh \beta_k x)\right] \qquad \text{(B-51)}$$

where Ψ_k is defined as follows:

$$\Psi_k = \frac{\sinh \beta_k \ell - \sin \beta_k \ell}{\cosh \beta_k \ell + \cos \beta_k \ell} \qquad \text{(B-52)}$$

The coefficient B_k is arbitrary for free vibration of the beam since the characteristic modes are orthogonal and there is no requirement on their relative amplitudes. In forced steady-state or transient vibration, the values of B_k are determined by the conditions of the excitation, as described in the examples below:

B-3.2.2 Example: Simply-Supported Beam

The boundary conditions used to evaluate the coefficients in Eq. (B-45) are that the deflection and bending moment are zero at both ends of the beam. Referring to Fig. B-2

$$(a)\ y(o,t) = 0 \quad (b)\ y(\ell,t) = 0 \quad (c)\frac{\partial^2 y}{\partial x^2}(o,t)=0 \quad (d)\frac{\partial^2 y}{\partial x^2}(\ell,t)=0 \qquad \text{(B-53)}$$

First applying condition (a) of Eq. (B-53) to Eq. (B-45), it is evident that A = 0. Then differentiating Eq. (B-45) twice with respect to x:

$$\frac{d^2\varphi_k}{dx^2} = B\beta_k^2(-\cos\beta_k x - \cosh\beta_k x) + C\beta_k^2(-\sin\beta_k x + \sinh\beta_k x) + D\beta_k^2(\sin\beta_k x - \sinh\beta_k x) \qquad \text{(B-54)}$$

According to condition (b) of Eq. (B-53), $\frac{d^2\varphi_k}{dx^2} = 0$ when x = 0.

Thus it is evident that B = 0.

Equations (B-45) and (B-54) when evaluated at the condition $x = \ell$ are each zero, in accordance with conditions (c) and (d) of Eq. (B-53):

$$\varphi_k(\ell) = C(\sin\beta_k\ell + \sinh\beta_k\ell) + D(\sin\beta_k\ell - \sinh\beta_k\ell) = 0 \qquad \text{(B-55)}$$

$$\frac{d^2\varphi_k(\ell)}{dx^2} = C\beta_k^2(-\sin\beta_k\ell + \sinh\beta_k\ell) + D\beta_k^2(\sin\beta_k\ell - \sinh\beta_k\ell) = 0 \qquad \text{(B-56)}$$

Subtracting Eq. (B-56) from Eq. (B-55), the following result is obtained:

$$\sin\beta_k\ell = 0 \qquad \text{(B-57)}$$

This is the frequency equation for the hinged-hinged or simple beam; its roots are $\beta_k \ell = \alpha_k = \pi, 2\pi \ldots\ldots$

The coefficient D is evaluated by noting in Eq. (B-56) that D = C. Substituting then in Eq. (B-45), the following expression is obtained for the mode shape $\varphi_k(x)$:

$$\varphi_k(x) = 2 C_k \sin \beta_k x \qquad \text{(B-58)}$$

where the coefficient C_k is arbitrary for free vibration of the beam but is determined by the conditions of forced vibration.

B-3.3 Forced Vibration of a Beam

The differential equation of motion for the vibration of a beam in response to steady-state vibration of the support is written directly from Eq. (B-30) by substituting $\ddot{s}(t) = \ddot{s}_o \sin \omega t$ and using η_k from Eq. (B-36) where $\varphi_k(x)$ is the normal mode function defined with reference to Eq. (B-33):

$$\ddot{\xi}_k + p_k^2 \xi_k = -\eta_k \ddot{s}_o \sin \omega t \qquad \text{(B-59)}$$

Neglecting the free vibration terms by assuming that the transient vibration is ultimately damped out, the form of the solution is

$$\xi_k = A \sin \omega t \qquad \text{(B-60)}$$

Substituting from Eq. (B-60) into Eq. (B-59) to evaluate the coefficient A, Eq. (B-60) becomes

$$\xi_k = \frac{-\eta_k \left(\ddot{s}_o / p_k^2 \right) \sin \omega t}{1 - \omega^2 / p_k^2} \qquad \text{(B-61)}$$

Equation (B-61) defines the response in each normal mode of a beam with zero damping. Damping has been omitted from the theory to avoid the complexities in defining the normal modes of a damped structure. Damping is conveniently introduced at this stage by considering Eq. (B-59) to include a damping term analagous to that in Eq. (4.2) but applicable particularly to the k^{th} mode. Then Eq. (B-61) is modified by analogy with Eq. (4.4) as follows:

$$\xi_k = \frac{-\eta_k \left(\ddot{s}_o / p_k^2 \right) \sin \omega t}{\sqrt{\left(1 - \omega^2 / p_k^2\right)^2 + \left(2 \zeta_k \omega / p_k\right)^2}} \qquad \text{(B-62)}$$

where ζ_k is the fraction of critical damping of the beam in the k^{th} mode. In general, the damping of a particular beam varies from mode to mode. In the present state of the art, it is not possible to derive applicable numerical values from theoretical considerations but rather from the observed motion of particular beams in free and forced vibration.

The stress in the beam may be expressed in terms of the deflection in a particular mode by combining the following expressions which involve the bending moment:

$$\sigma = \frac{Mc}{I} \qquad \text{(B-63)}$$

$$\frac{M}{EI} = \frac{\partial^2 y}{\partial x^2} \qquad \text{(B-64)}$$

where σ = stress, lb/in^2

c = distance from neutral plane to point at which σ is measured, in.

M = bending moment, lb-in.

x = coordinate along length of beam, in.

y = deflection of beam relative to X axis, in.

The deflection of the beam may be defined in terms of the normal mode shape $\varphi_k(x)$ and the normal coordinate $\xi_k(t)$ follows:

$$y_k(x,t) = \xi_k(t)\ \varphi_k(x) \qquad \text{(B-65)}$$

Combining Eqs. (B-63), (B-64) and (B-65):

$$\sigma_k(x,t) = cE\ \xi_k(t)\ \frac{\partial^2 \varphi_k(x)}{\partial x^2} \qquad \text{(B-66)}$$

where ξ_k is given by Eq. (B-62) and $\varphi_k(x)$ is defined with reference to Eq. (B-33). Values of $\varphi_k(x)$ and $\frac{\partial^2 \varphi_k(x)}{\partial x^2}$ for the ten types of beams illustrated in Fig. 5.2 are tabulated in ref. B-1.

References

B-1 "Tables of Characteristic Functions Representing Normal Modes of Vibration of a Beam", by D. Young and R. P. Felgar, Univ. of Texas Bur. Eng. Research Bulletin 44, July 1, 1949.

B-2 "The Mechanics of Vibration" by R. E. D. Bishop and D. C. Johnson, Cambridge University Press, 1960, pp. 374-402.

Appendix C

Results of Endurance Tests

As discussed in Sections 1 and 3, one of the tasks proposed as a part of the investigation described in this report was the determination of the fatigue life of a typical structure when subjected to various excitations. To accomplish this objective, it is necessary to know the properties of the structure when subjected to repeated reversal of stress with constant stress amplitude. Such results are conventionally plotted as a stress versus cycles-to-failure curve. This appendix sets forth the results of the conventional endurance tests and the test data for fatigue tests in which the excitation was a variable frequency sinusoid. As discussed in Section 3, numerous complications arose in attempting to interpret the results of the latter, and little use has been made to date of the data in this Appendix. However, the data are presented in the interests of complete reporting.

C-1. Results of Conventional Endurance Tests

This section of appendix C describes the means used to obtain quantitatively the curve of stress amplitude versus number of cycles to failure discussed in Section 3 and shown hypothetically in Fig. 3.1. The test is one in which the stress in a specimen varies sinusoidally with time in a steady-state manner, until failure of the specimen occurs. The test is conducted by first selecting a stress amplitude representing the most highly stressed region of the specimen; the machine applies the stress sinusoidally with time, uninterruptedly until failure occurs. Then a different number of cycles of stress reversal is required to cause failure.

For a given stress amplitude, there is usually some scatter of number of cycles to failure; hence it is normal practice to test several specimens at each of several stress amplitudes and to take the average number of cycles to failure.

The specimens were made of 2024-T4 aluminum alloy, machined to the dimensions shown in Fig. 3.8. A photograph of the specimens is included as Fig. 3.9. The tests were conducted on a Universal Fatigue Testing Machine, Model SF-1-U, manufactured by the Sonntag Scientific Corporation of Greenwich, Conn. A photograph of the machine is included as Fig. C-1, and a schematic drawing illustrating the principle of operation as Fig. C-2. A close-up view of the specimen in the machine is shown in Fig. C-3.

In the schematic drawing of Fig. C-2, the specimen (a) is clamped to the specimen support members (b) which in turn are supported by the pins (c). The support (d) for the right-hand pin (c) has horizontal compliance in the direction of the beam length so that the beam is free at all times of axial tension. The load is applied to the specimen equally through the pins (e); it is produced by the rotation about a horizontal axis of an eccentric member supported in a cage (f) which is attached by the linkage (g) to the pins (e). The eccentric member is comprised of a threaded rod (h) extending in a radial direction from a shaft (2) and carrying a weight (j) whose eccentricity relative to the shaft is adjustable. The cage (f) is constrained by the flexural members (k) to move in only the vertical direction. Coil springs (ℓ) are adapted to support all or a portion of the weight of the cage (f) so that the test can be conducted with a mean stress as selected. In the test reported herein, the springs (ℓ) were adjusted to

support the entire weight of cage and associated mechanism; consequently, the mean stress was zero.

The synchronous motor which drives the eccentric member operates at a speed of 1800 rpm. The bending moment in the specimen, and thus the maximum stress at the necked down portion, are directly proportional to the force applied by the links (g). The machine was calibrated by attaching resistance wire strain gages to a specimen placed in normal position in the machine, and noting the relation between the strain in the beam and the position of the weight (j) with the machine operating at normal speed. The calibration curve is shown in Fig. C-4. Readings at the higher stress values could not be readily obtained because the strain gage tends to fail in fatigue during the repeated stress reversal which is necessary for one reading.

The number of specimens tested was 117, of which all except one failed ultimately, after repeated reversals of stress. Data on each specimen is set forth in Table C-1. The data from the table are plotted in Fig. C-5 where the circles indicate the average number of cycles to failure at each stress amplitude and the horizontal lines through the circles indicate the spread of the data. In the context of Fig. 3.1, the slope of the curve in Fig. C-5 is such that $\alpha = 6$.

A-2. Results of Fatigue Tests— Variable Frequency Sinusoid

This section of Appendix C sets forth the test data obtained from tests of a beam mounted as shown in Fig. 3.11 and subjected to vibration in which the excitation frequency is continuously varied, as described in Section 4.3. Most of the tests were conducted at Hughes Aircraft Co.; the remainder were conducted at the California Institute of Technology. A few

tests were made using random vibration as the excitation in an attempt to correlate the effects of various types of excitation. For most tests, the time to the first noticeable crack and the time to separation of the specimen were both recorded.

Tests at Hughes Aircraft Company

Group No. 1 - Material Lot A

Sinusoidal sweep from 50 to 200 cps at a rate of six octaves per minute with an acceleration amplitude of 5g.

Specimen No.	Time to Fatigue Cracks	Time to Separation
1	*	1 hr. 56 min. 35 sec.
2	*	1 hr. 57 min. 30 sec.
3	*	3 hr. 35 min. 20 sec.
4	*	2 hr. 57 min. 25 sec.
5	*	1 hr. 19 min. 12 sec.
6	*	1 hr. 13 min. 35 sec.
7	*	2 hr. 9 min. 43 sec.
8	*	1 hr. 11 min. 20 sec.
9	*	1 hr. 11 min. 55 sec.
10	*	1 hr. 22 min.

* This time was not recorded for the Group 1 test

Group No. 2 - Material Lot A

Sinusoidal sweep from 50 to 200 cps at a rate of six octaves per minute with an acceleration amplitude of 10g.

Specimen No.	Time to Fatigue Cracks	Time to Separation
1	29 mins. 10 sec.	29 min. 15 sec.
2	19 mins.	20 min. 15 sec.
3	25 min. 10 sec.	29 min. 20 sec.
4	26 min. 25 sec.	26 min. 35 sec.
*5	12 min. 25 sec.	12 min. 25 sec.
6	28 min.	28 min.
7	21 min.	21 min. 30 sec.
8	24 min. 25 sec.	24 min. 25 sec.
9	25 min. 45 sec.	25 min. 45 sec.
10	21 min. 30 sec.	21 min. 30 sec.

* A slight scratch was noted prior to start of test on this specimen.

Group No. 3 - Material Lot A

Sinusoidal sweep from 50 to 200 cps at a rate of one octave per minute with an acceleration amplitude of 5g.

Specimen No.	Time to Fatigue Cracks	Time to Separation
1	2 hrs. 11 min. 30 sec.	2 hrs. 28 min. 40 sec.
2	1 hr. 42 min. 45 sec.	1 hr. 48 min. 35 sec.
3	1 hr. 35 min. 20 sec.	*
4	2 hrs. 13 min. 5 sec.	2 hrs. 19 min. 45 sec.
5	1 hr. 55 min. 55 sec.	2 hrs. 5 min. 19 sec.
6	1 hr. 47 min. 20 sec.	2 hrs. 10 min.
7	1 hr. 39 min.	1 hr. 39 min. 45 sec.
8	1 hr. 39 min. 15 sec.	2 hrs. 1 min. 10 sec.
9	1 hr. 35 min.	2 hrs. 41 min. 20 sec.
10	1 hr. 47 min. 10 sec.	1 hr. 47 min. 55 sec.

* Failed to separate after 3 hours 20 minutes.

Group No. 4 - Material Lot A

Sinusoidal sweep from 50 to 200 cps at a rate of one octave per minute with an acceleration amplitude of 10g.

Specimen No.	Time to Fatigue Cracks	Time to Separation
1	33 min.	34 min.
2	33 min.	34 min. 15 sec.
3	29 min. 25 sec.	29 min. 35 sec.
4	33 min. 50 sec.	34 min. 25 sec.
5	33 min. 50 sec.	34 min. 10 sec.
6	33 min. 50 sec.	33 min. 55 sec.
7	33 min. 50 sec.	34 min. 20 sec.
8	33 min. 50 sec.	34 min. 15 sec.
9	33 min. 50 sec.	38 min. 30 sec.
10	33 min. 50 sec.	33 min. 45 sec.

Group No. 5 - Material Lot A

Random noise, band limited within 50 to 200 cps, with a mean square acceleration density of 0.05 g^2/cps

Specimen No.	Time to Fatigue Cracks	Time to Separation
1	12 min. 40 sec.	12 min. 55 sec.
2	23 min.	23 min. 40 sec.
3	10 min. 30 sec.	11 min. 10 sec.
4	13 min. 45 sec.	16 min. 30 sec.
5	24 min. 40 sec.	*
6	22 min. 20 sec.	25 min. 5 sec.
7	12 min.	13 min. 30 sec.
8	12 min. 20 sec.	29 min. 20 sec.
9	28 min. 50 sec.	
10	20 min. 25 sec.	20 min. 45 sec.

* Failed to separate after 1 hour 28 minutes.

Group No. 6 - Material Lot A

Random noise, band limited within 50 to 200 cps, with a mean square acceleration density of 0.01 g^2/cps.

No cracks or separation after 11 hours of vibration with the exception of one specimen which separated after 8-1/2 hours.

Group No. 7 - Material Lot A

Random noise, band limited within 50 to 200 cps, with mean square acceleration density of 0.02 g^2/cps.

No evidence of fatigue failure after 8 hours and 27 minutes.

Group No. 8 - Material Lot A

Random noise, band limited within 50 to 200 cps, with mean square acceleration density of 0.035 g^2/cps

No evidence of fatigue failure after 2 hours and 45 minutes.

Group No. 9 - Material Lot A

Sinusoidal sweep from 50 to 200 cps at a rate of six octaves per minute with an acceleration amplitude of 7.5g.

Specimen No.	Time to Fatigue Cracks	Time to Separation
1	34 min.	34 min. 5 sec.
2	29 min.	29 min.
3	35 min.	35 min. 5 sec.
4	33 min.	33 min. 55 sec.
5	30 min.	30 min. 10 sec.
6	30 min.	30 min. 20 sec.
7	30 min.	30 min. 15 sec.
8	31 min.	31 min. 15 sec.
9	32 min.	35 min.
10	33 min.	33 min. 50 sec.

Group No. 10 - Material Lot A

Sinusoidal sweep from 50 to 200 cps at a rate of one octave per minute with an acceleration amplitude of 7.5g.

Specimen No.	Time to Fatigue Cracks	Time to Separation
1	38 min.	42 min. 35 sec.
2	38 min.	38 min. 35 sec.
3	38 min.	43 min.
4	35 min.	36 min. 5 sec.
5	32 min.	32 min. 40 sec.
6	35 min.	35 min. 45 sec.
7	35 min.	36 min. 6 sec.
8	35 min.	35 min. 35 sec.
9	35 min.	35 min. 36 sec.
10	39 min.	39 min. 15 sec.

Group No. 11 - Material Lot A

Sinusoidal sweep from 50 to 200 cps at a rate of 10 octaves per minute with an acceleration amplitude of 7.5g.

Specimen No.	Time to Fatigue Cracks	Time to Separation
1	27 min.	27 min. 40 sec.
2	32 min.	48 min. 50 sec.
3	29 min.	31 min. 10 sec.
4	25 min.	25 min. 20 sec.
5	27 min.	27 min. 5 sec.
6	30 min.	31 min. 15 sec.
7	28 min.	28 min. 40 sec.
8	33 min.	33 min. 15 sec.
9	28 min.	28 min. 10 sec.
10	26 min.	27 min. 35 sec.

Group No. 12 - Material Lot B

Sinusoidal sweep from 50 to 200 cps at a rate of 1 octave per minute with an acceleration amplitude of 10g.

Specimen No.	Time to Fatigue Cracks	Time to Separation
1	18 min.	18 min. 25 sec.
2	16 min.	18 min.
3	12 min.	12 min. 10 sec.
4	16 min.	24 min. 5 sec.
5	12 min.	12 min. 3 sec.
6	12 min.	12 min. 30 sec.
7	10 min.	10 min. 5 sec.
8	16 min.	18 min.
9	20 min.	27 min.
10	11 min.	11 min. 10 sec.

Tests at California Institute of Technology

Group No. 13 - Material Lot B

Sinusoidal sweep from 50 to 110 cps at a rate of one octave per minute with an acceleration amplitude of 10g.

Specimen No.	Time to Fatigue Cracks	Time to Separation
1	17 min. 50 sec.	17 min. 55 sec.
2	9 min. 45 sec.	11 min. 10 sec.
3	10 min. 30 sec.	11 min.
4	17 min. 55 sec.	18 min. 30 sec.
5	12 min.	14 min. 15 sec.
6	12 min. 15 sec.	12 min. 15 sec.
7	11 min. 45 sec.	12 min. 18 sec.
8	13 min. 25 sec.	14 min. 10 sec.

Group No. 14 - Material Lot B

Sinusoidal sweep from 50 to 110 cps at a rate of one octave per minute with an acceleration amplitude of 10g.

Specimen No.	Time to Fatigue Cracks	Time to Separation
1	12 min. 24 sec.	18 min. 25 sec.
2	10 min. 25 sec.	11 min.
3	10 min.	11 min. 1 sec.
4	18 min. 10 sec.	19 min. 5 sec.
5	12 min. 50 sec.	13 min. 15 sec.
6	12 min. 40 sec.	16 min. 15 sec.
7	12 min. 55 sec.	13 min. 30 sec.
8	15 min. 30 sec.	16 min. 15 sec.

Table C-1

Data from Fatigue Tests Conducted on Machine Shown in Fig. C-1

Dial Setting	Stress Amplitude lb/in^2	Thousands of Cycles to Failure
48	34,500	8
		8
		5
		6
		6
		6
		7
		7
		7
		4
	Ave. =	6.40
44	31,400	7
		9
		7
		9
		10
		8
		10
		11
		9
		8
		10
		11
	Ave. =	9.08
40	28,400	23
		17
		29
		23
		14
		19
		15
		22
		21
		21
		16
	Ave. =	20.0
36	25,200	31
		26
		21
		22
		32
		35
		28
		26
		36
		30
		38
	Ave. =	29.5
32	22,200	79
		79
		65
		58
		42
		52
		63
		70
		65
		75
		68
	Ave. =	65.1
28	19,200	188
		132
		155
		104
		147
		154
		157
		156
		160
		128
	Ave. =	148

Table C-1 (Continued)

Dial Setting	Stress Amplitude lb/in^2	Thousands of Cycles to Failure
24	16,000	411
		396
		414
		538
		375
		523
		421
		532
		480
		415
	Ave. =	45.1
20	12,900	836
		1229
		(16,100)
22	14,400	729
		1364
		1039
		894
		713
	Ave. =	948
21	13,600	5178
		1170
		698
		1121
		1482
		1223
		962
		841
		2264
	Ave. =	1649
26	17,500	245
		193
		201
		241
26	17,500	271
		288
		255
		235
		484
		443
		374
		411
	Ave. =	303
30	20,700	80
		65
		84
		93
		103
		103
		109
		101
		42
		122
	Ave. =	88.2
34	23,700	47
		48
		50
		64
	Ave. =	52.2

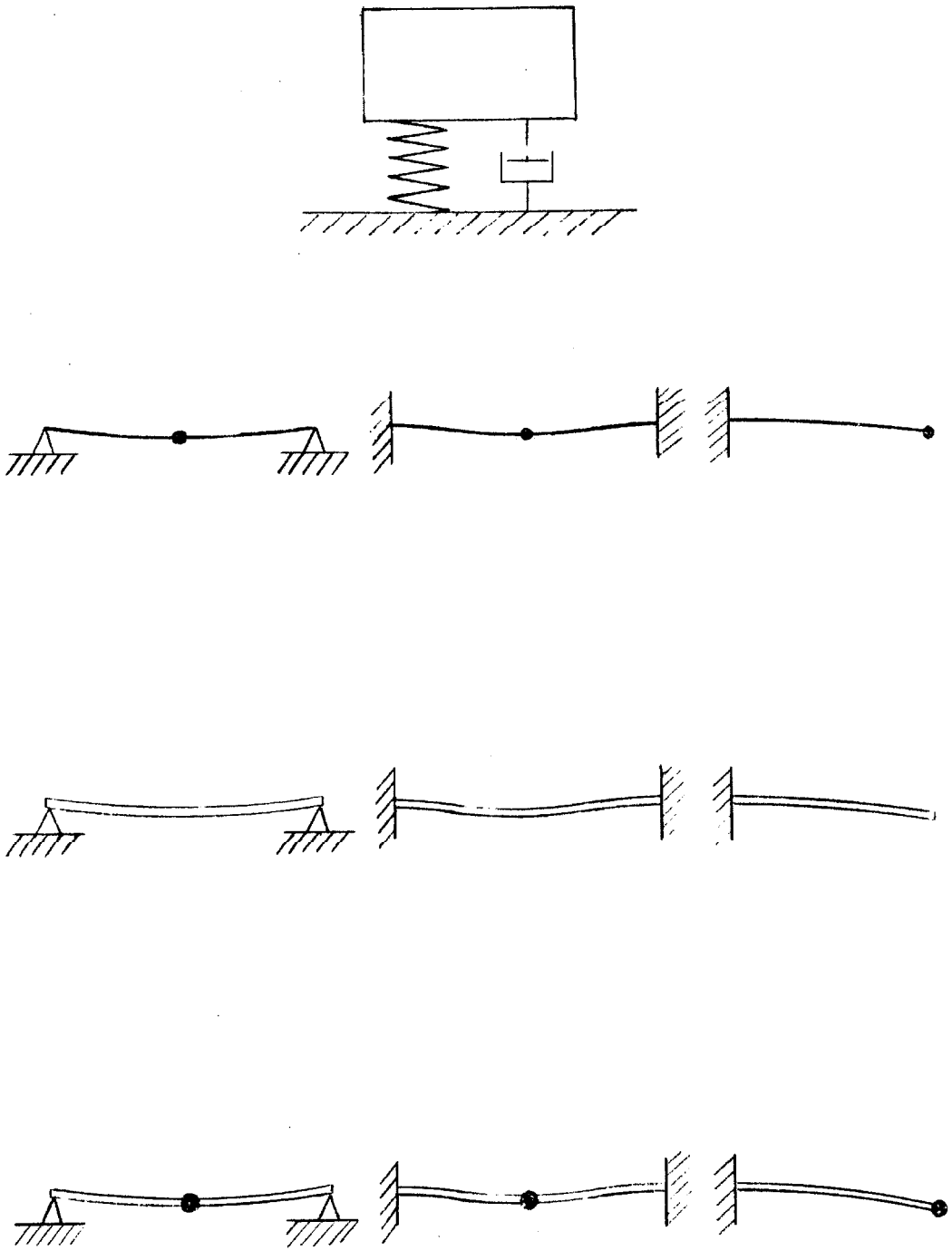

Fig. 1.1 Analog structures discussed in Section 1.2.1.

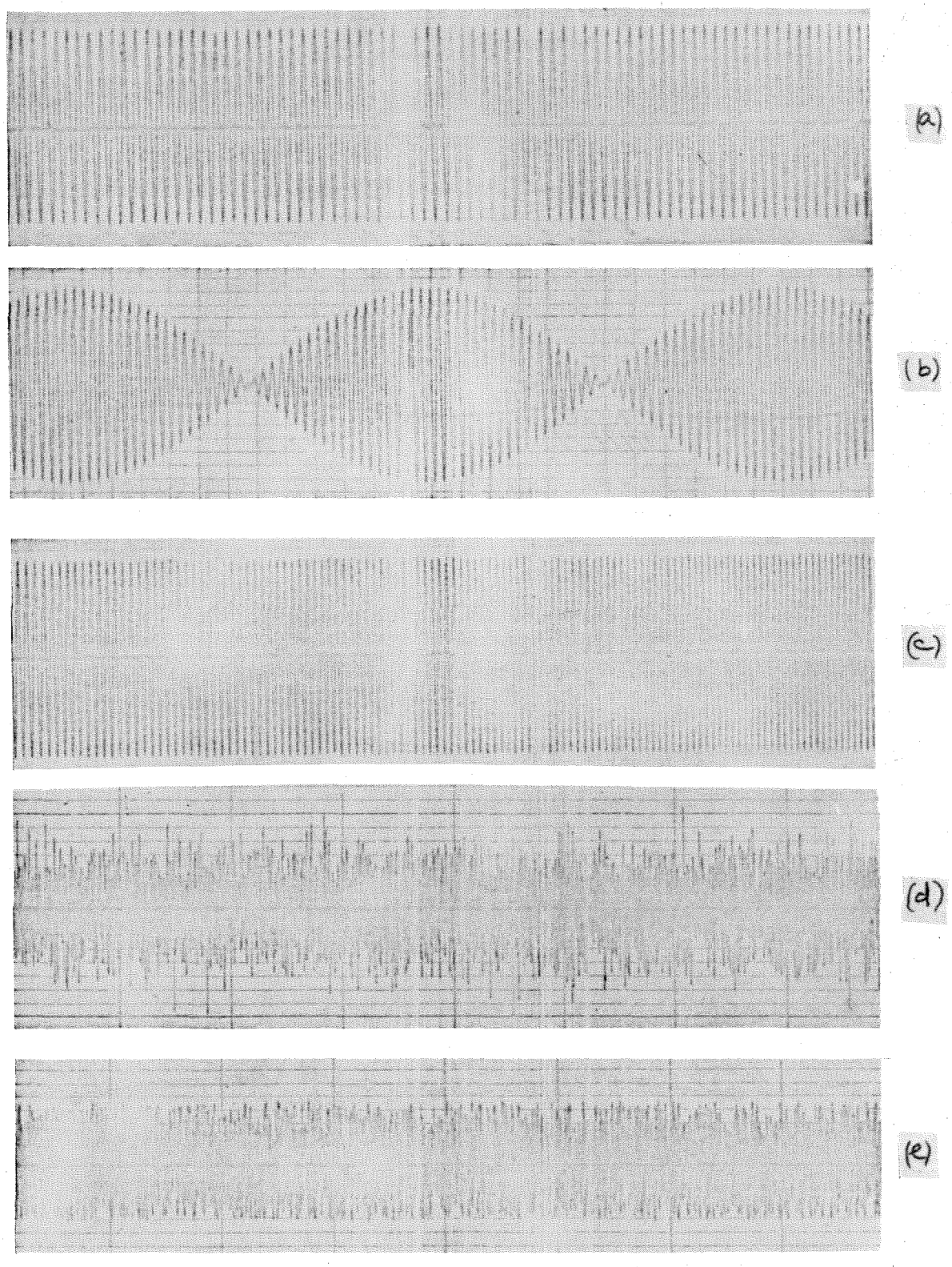

Fig. 1.2 Idealized vibration patterns: (a) sinusoid; (b) combined sinusoids; (c) variable frequency sinusoid; (d) broad band random (Gaussian) vibration; (3) broad band, magnitude-limited random vibration.

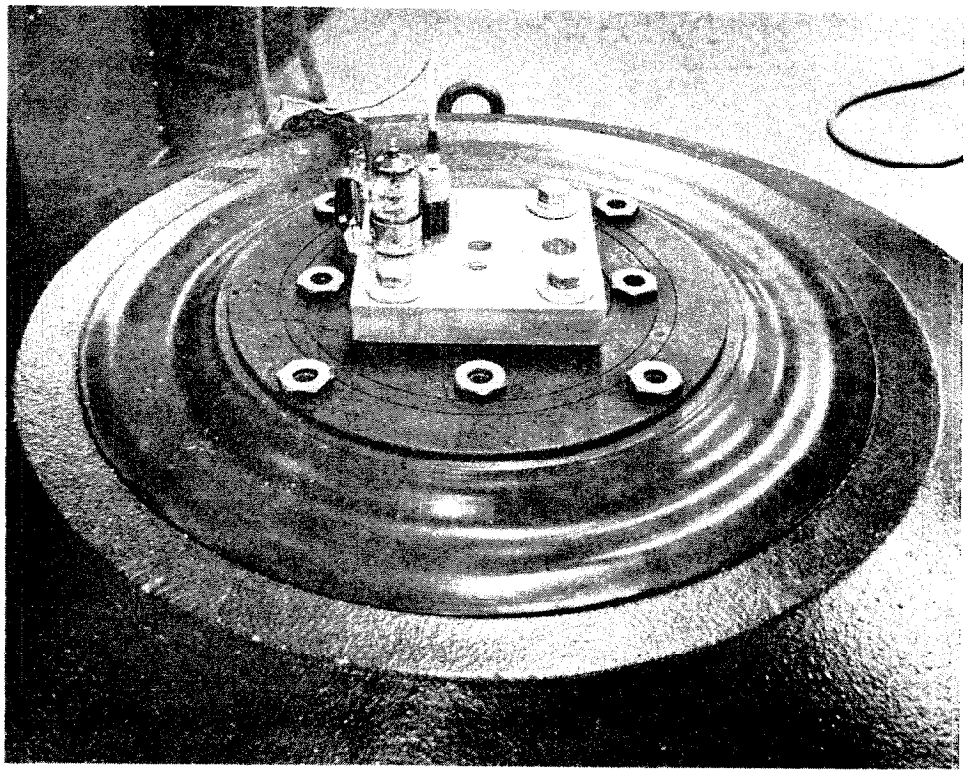

Fig. 2.1 Type 12AU7A vacuum tube mounted on vibration exciter in vertical position.

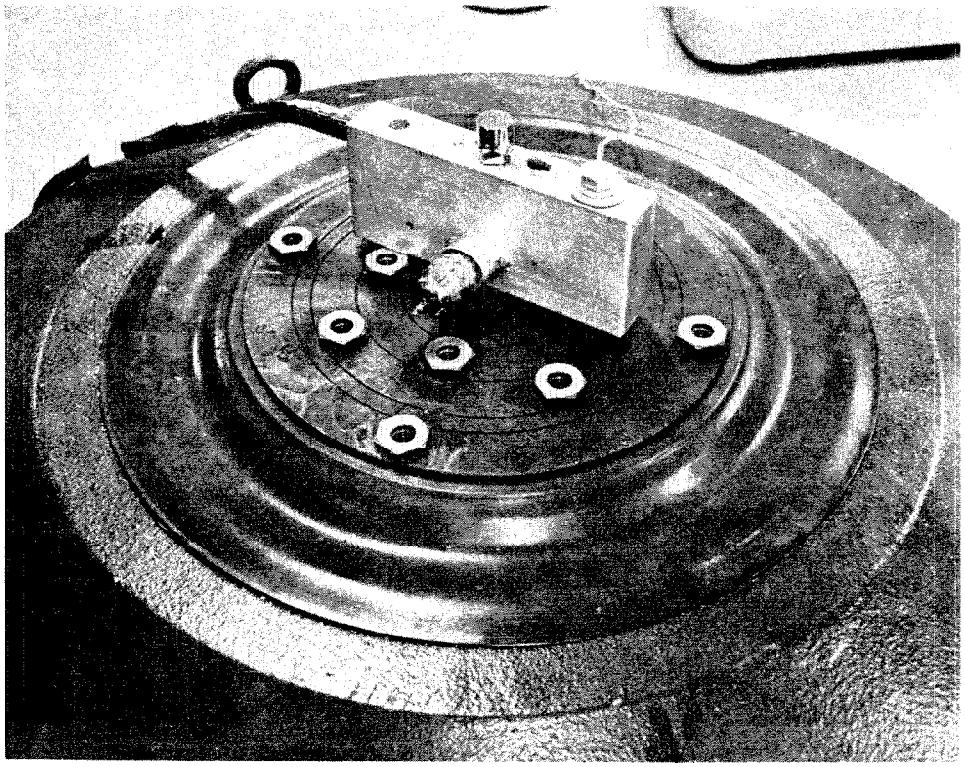

Fig. 2.2 Type 12AU7A vacuum tube mounted on vibration exciter in horizontal position.

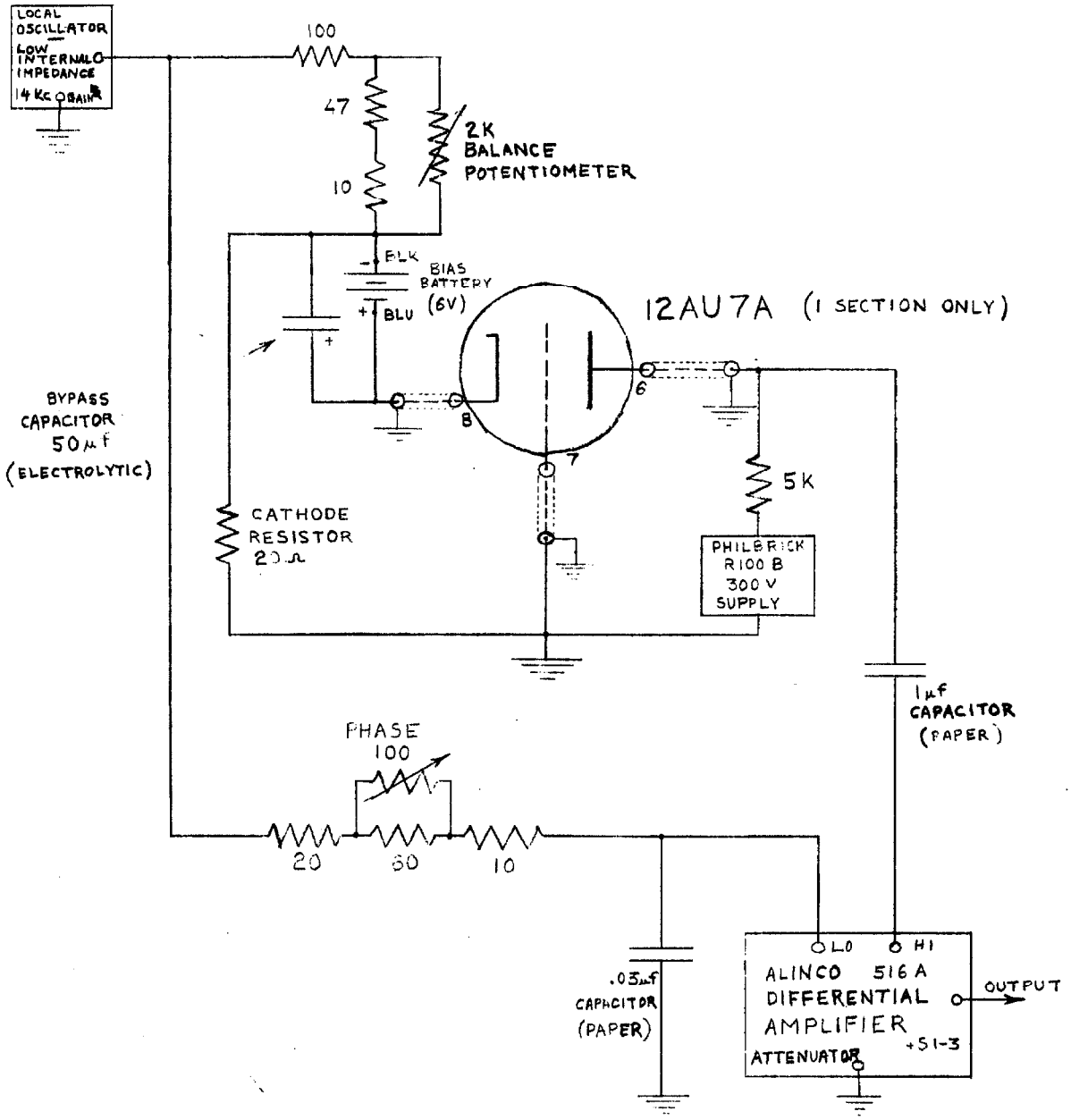

Fig. 2.3 Vacuum-tube activation circuit.

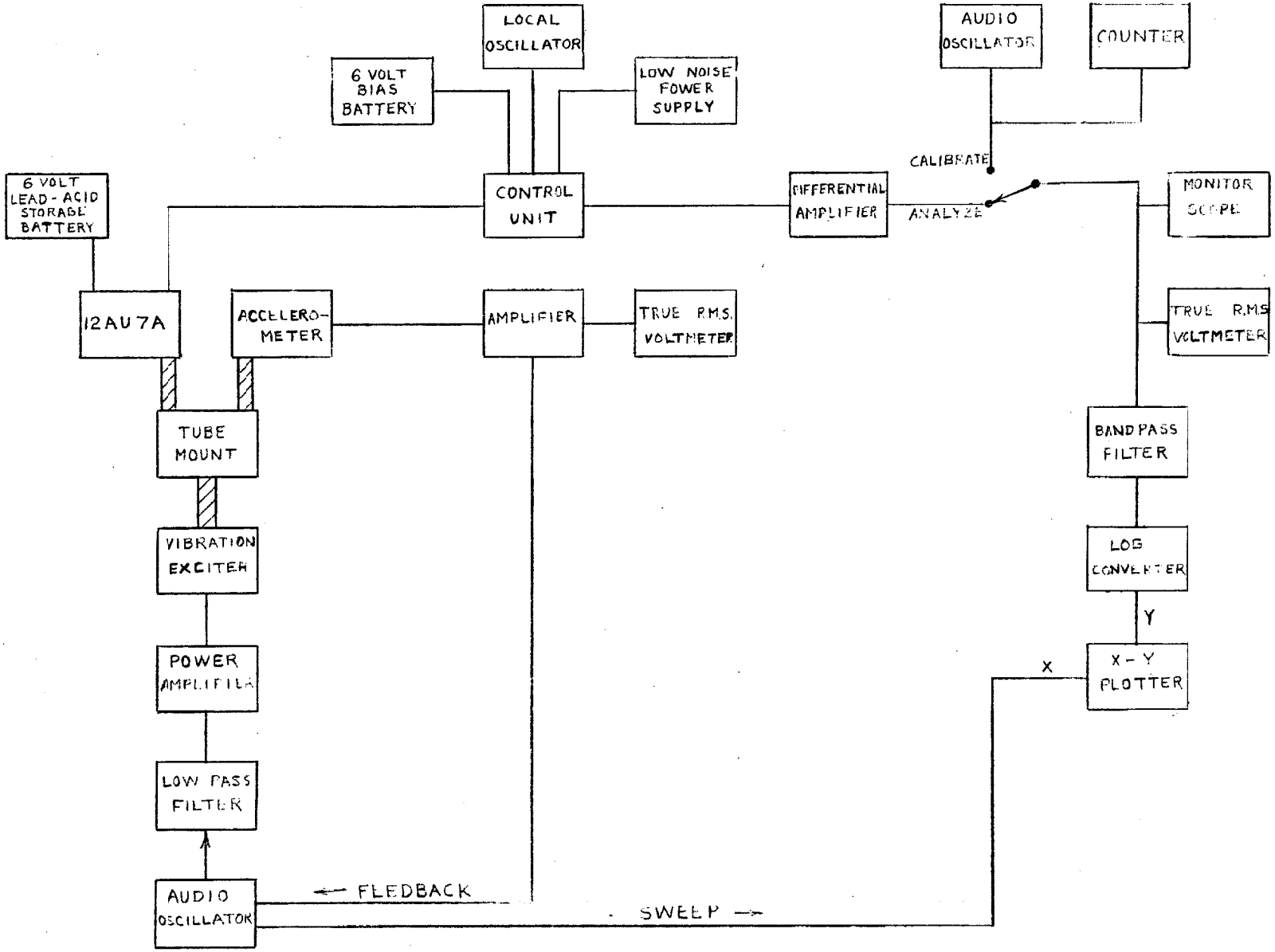

Fig. 2.4 Block diagram for sinusoidal vibration test.

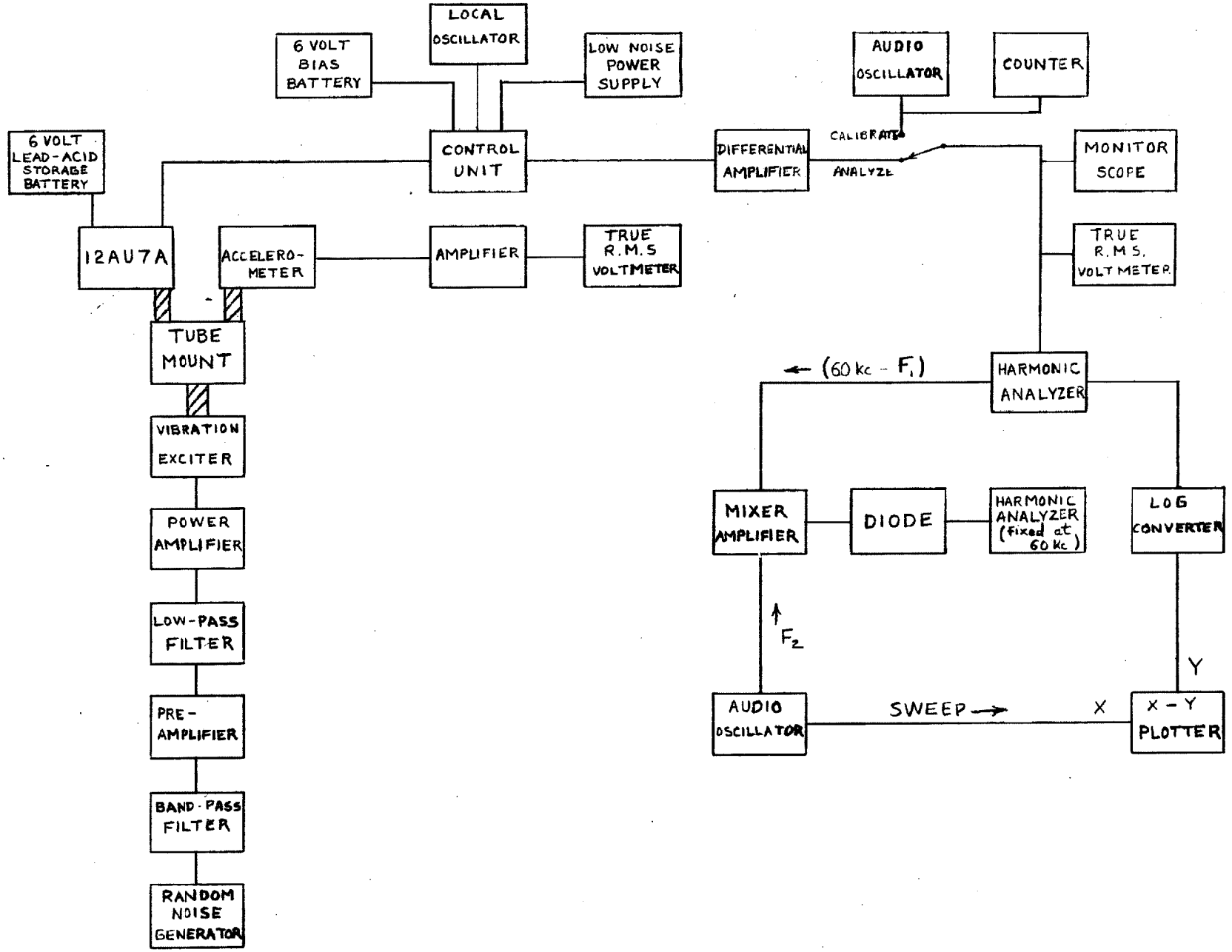

Fig. 2.5 Block diagram for random vibration test.

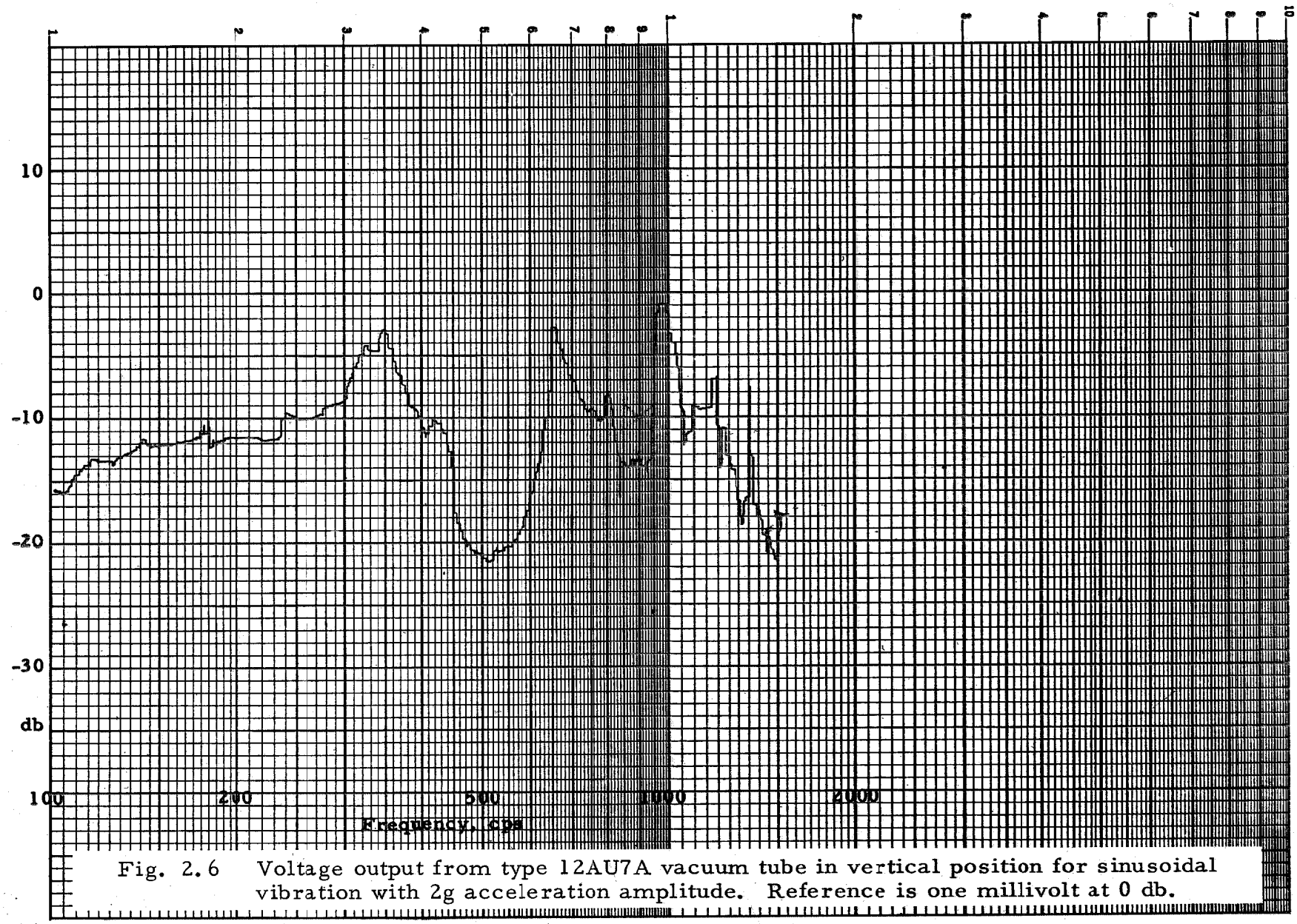

Fig. 2.6 Voltage output from type 12AU7A vacuum tube in vertical position for sinusoidal vibration with 2g acceleration amplitude. Reference is one millivolt at 0 db.

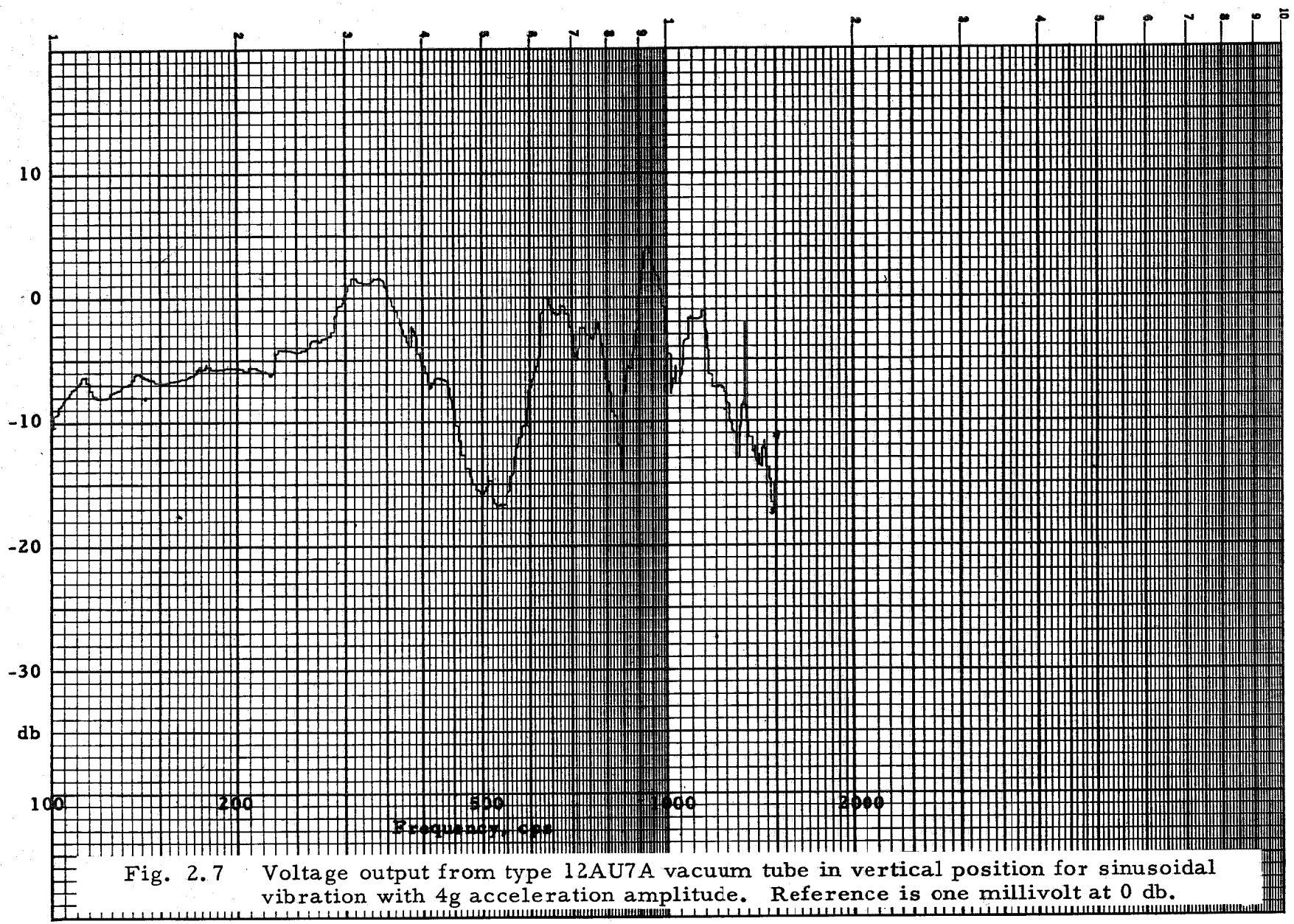

Fig. 2.7 Voltage output from type 12AU7A vacuum tube in vertical position for sinusoidal vibration with 4g acceleration amplitude. Reference is one millivolt at 0 db.

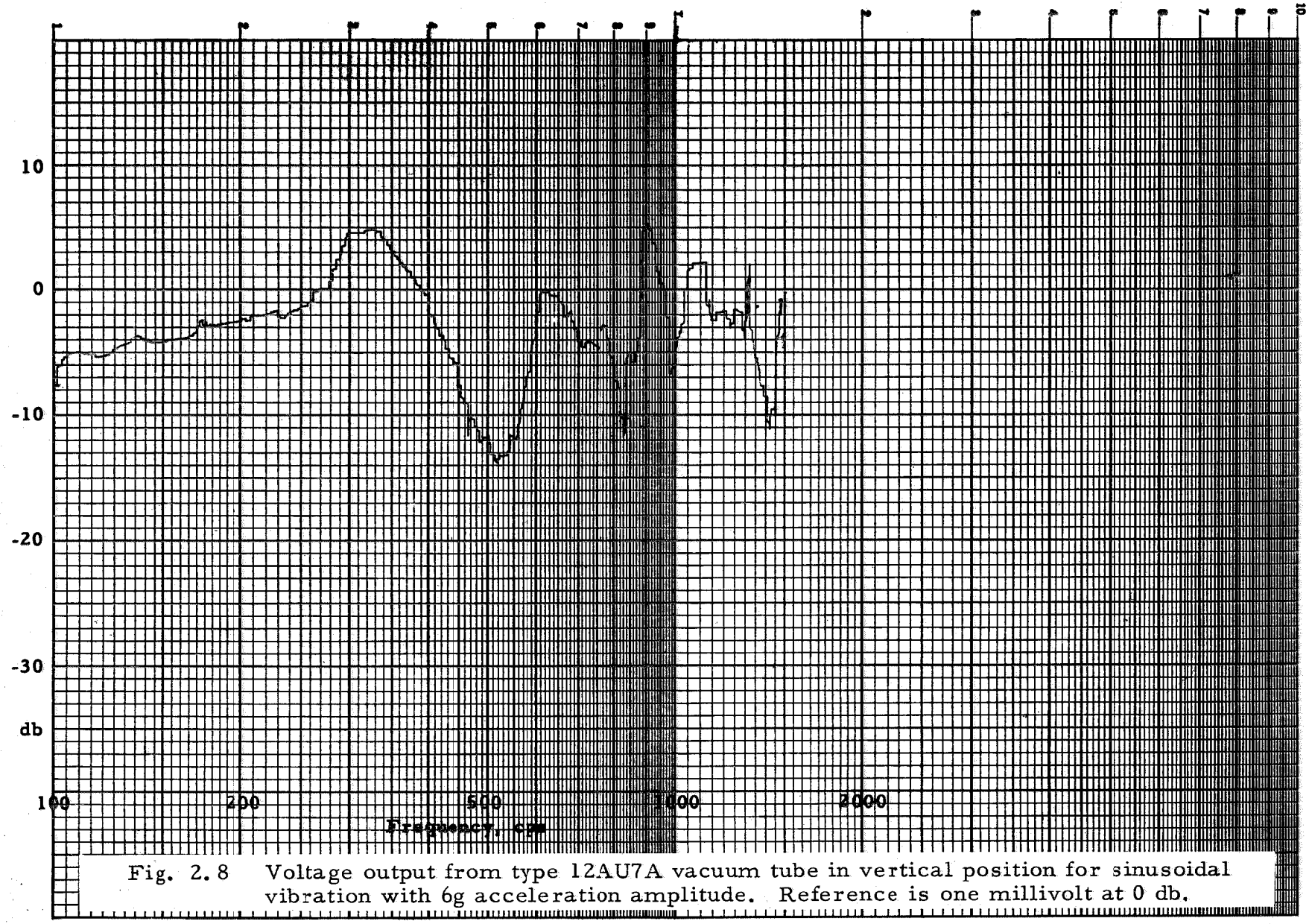

Fig. 2.8 Voltage output from type 12AU7A vacuum tube in vertical position for sinusoidal vibration with 6g acceleration amplitude. Reference is one millivolt at 0 db.

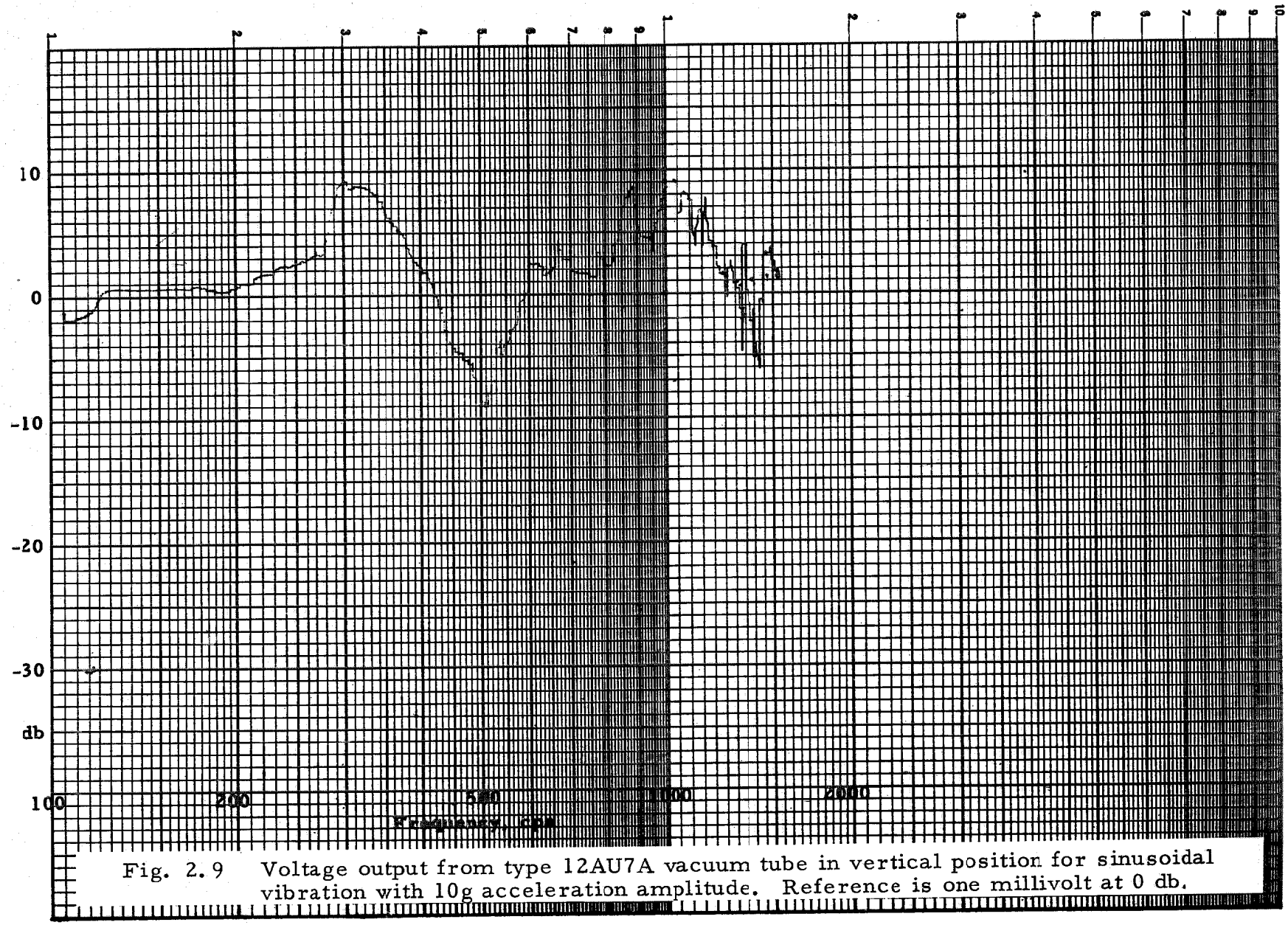

Fig. 2.9 Voltage output from type 12AU7A vacuum tube in vertical position for sinusoidal vibration with 10g acceleration amplitude. Reference is one millivolt at 0 db.

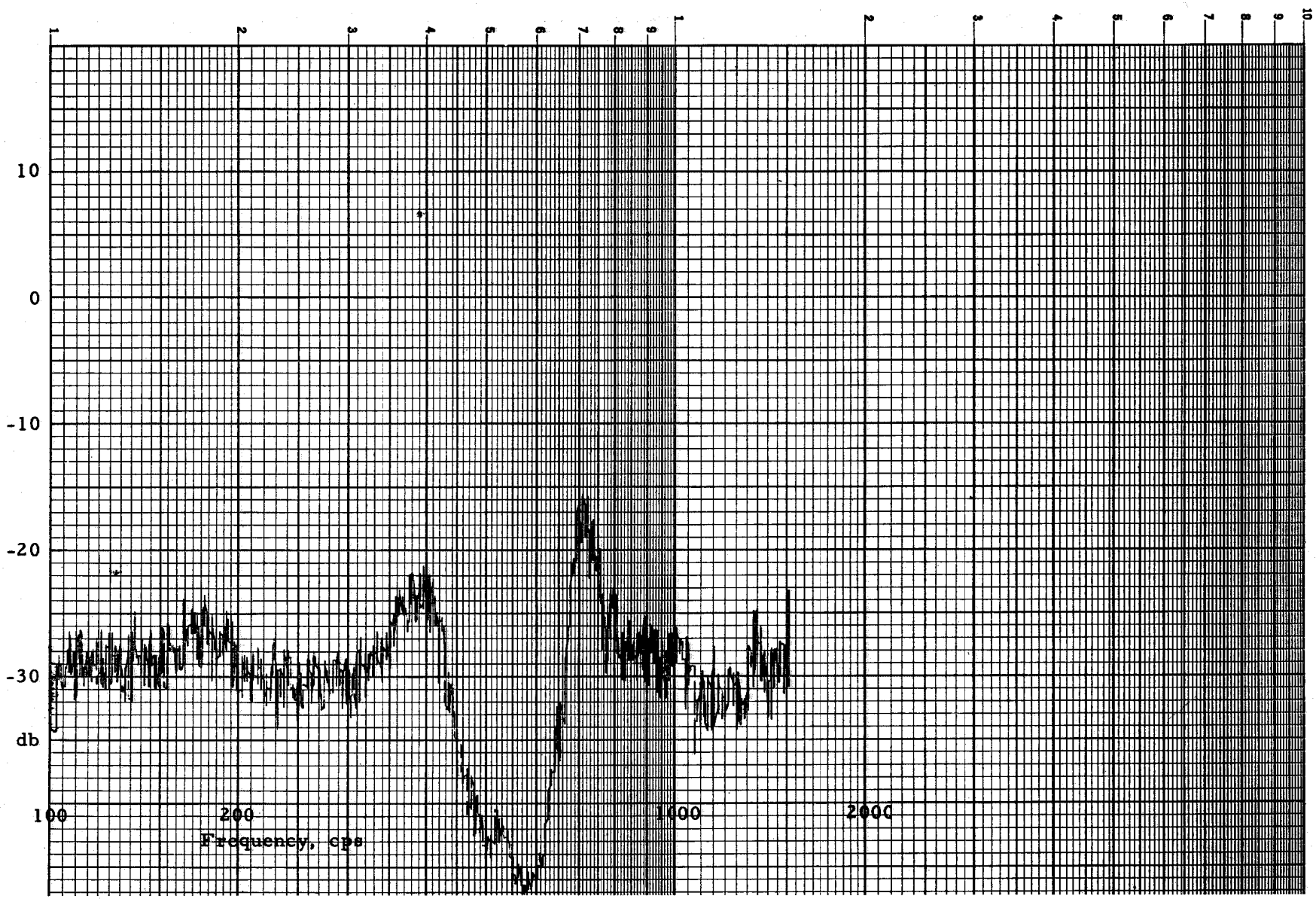

Fig. 2.10 Voltage output from type 12AU7A vacuum tube in vertical position for random vibration with 0.0004 g^2/cps mean square acceleration density. Reference is one millivolt at 0 db.

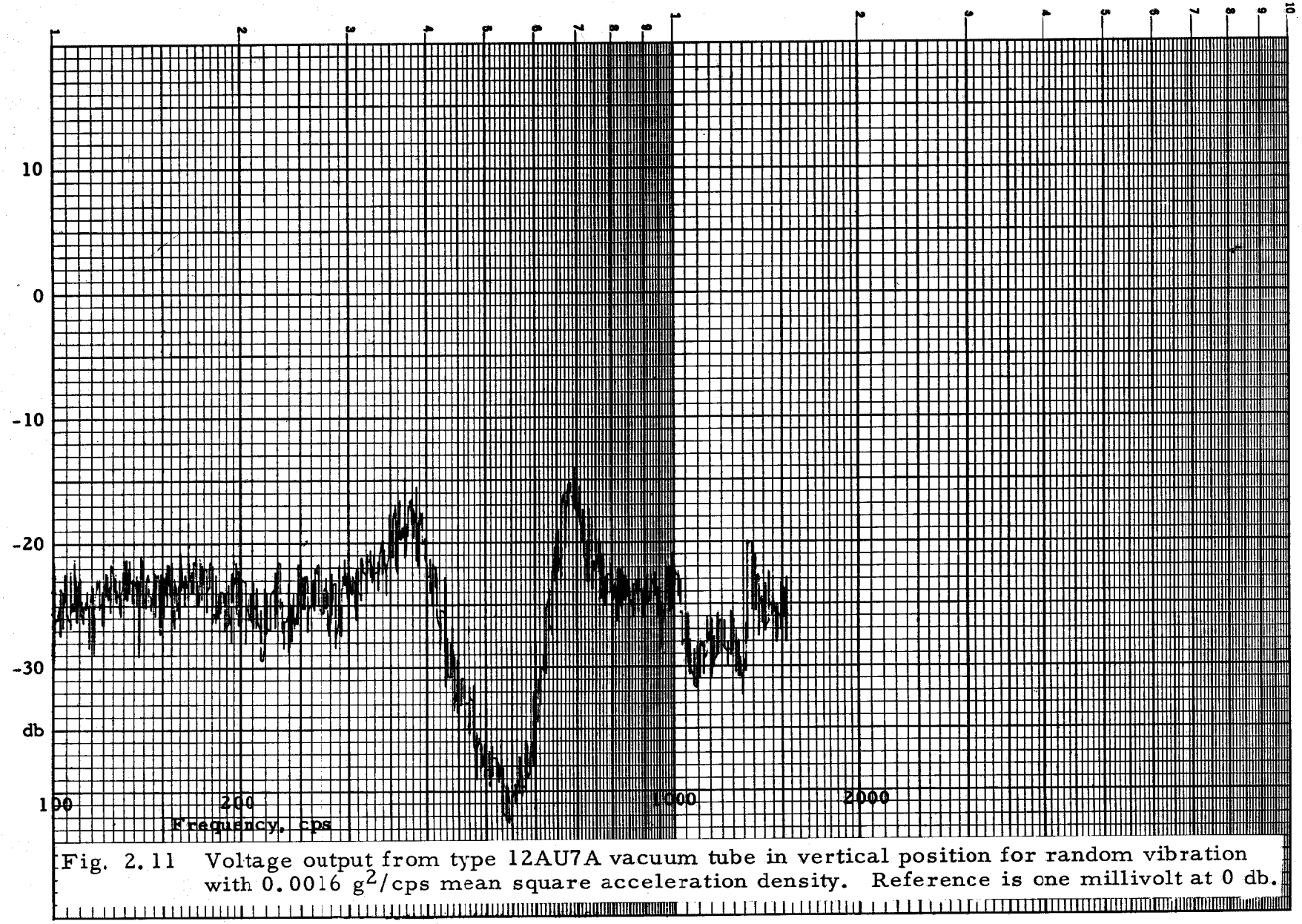

Fig. 2.11 Voltage output from type 12AU7A vacuum tube in vertical position for random vibration with 0.0016 g^2/cps mean square acceleration density. Reference is one millivolt at 0 db.

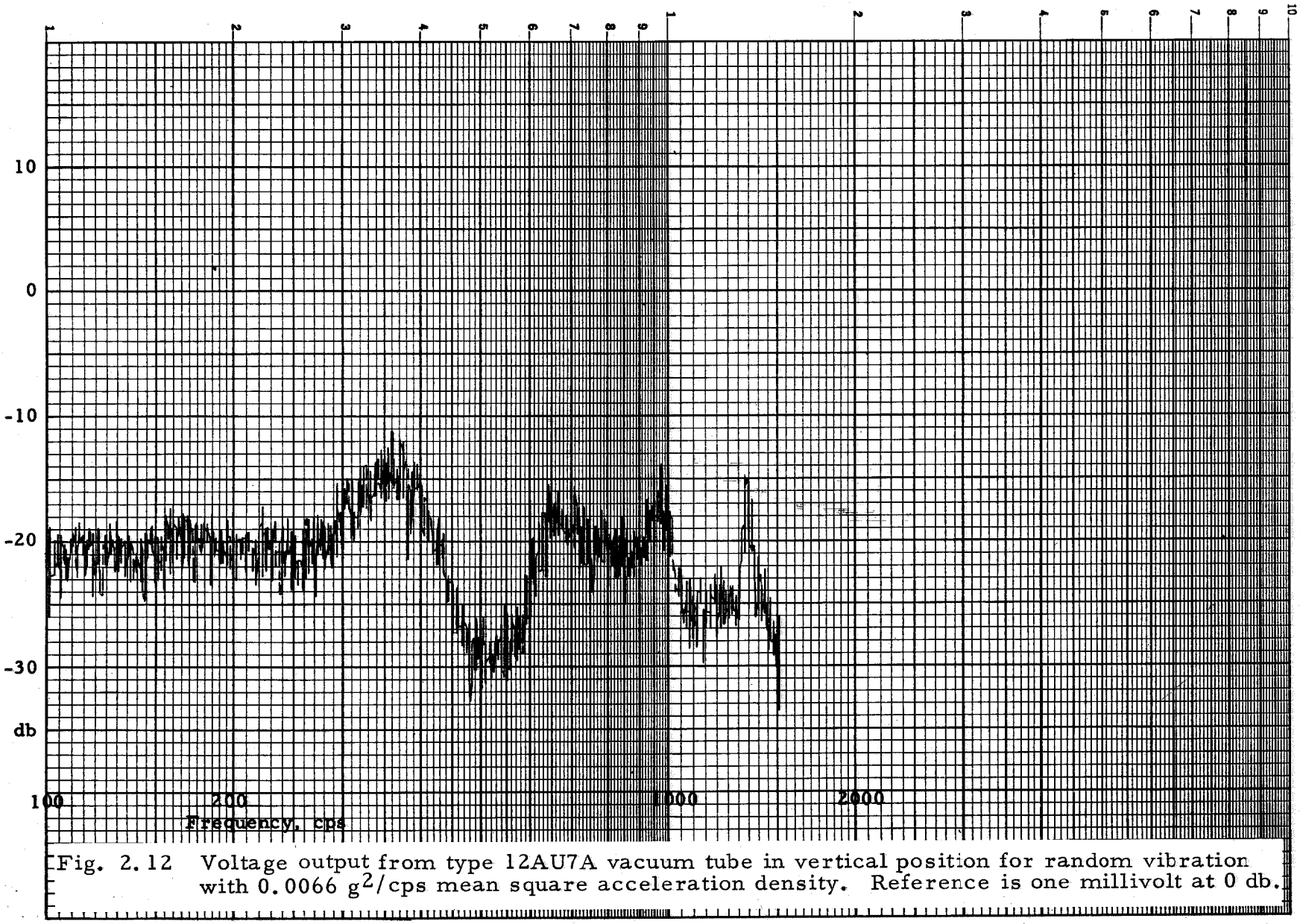

Fig. 2.12 Voltage output from type 12AU7A vacuum tube in vertical position for random vibration with 0.0066 g^2/cps mean square acceleration density. Reference is one millivolt at 0 db.

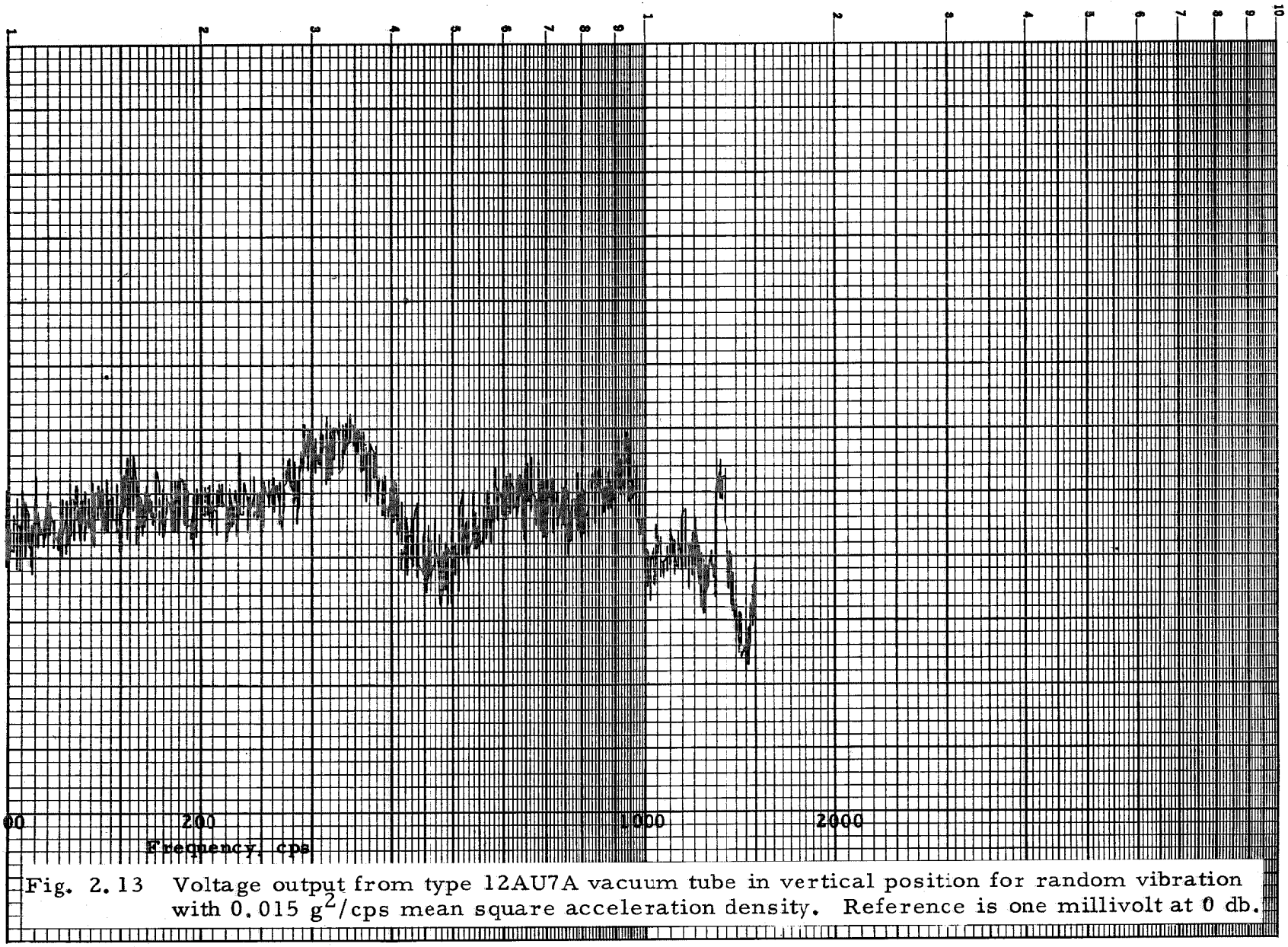

Fig. 2.13 Voltage output from type 12AU7A vacuum tube in vertical position for random vibration with 0.015 g^2/cps mean square acceleration density. Reference is one millivolt at 0 db.

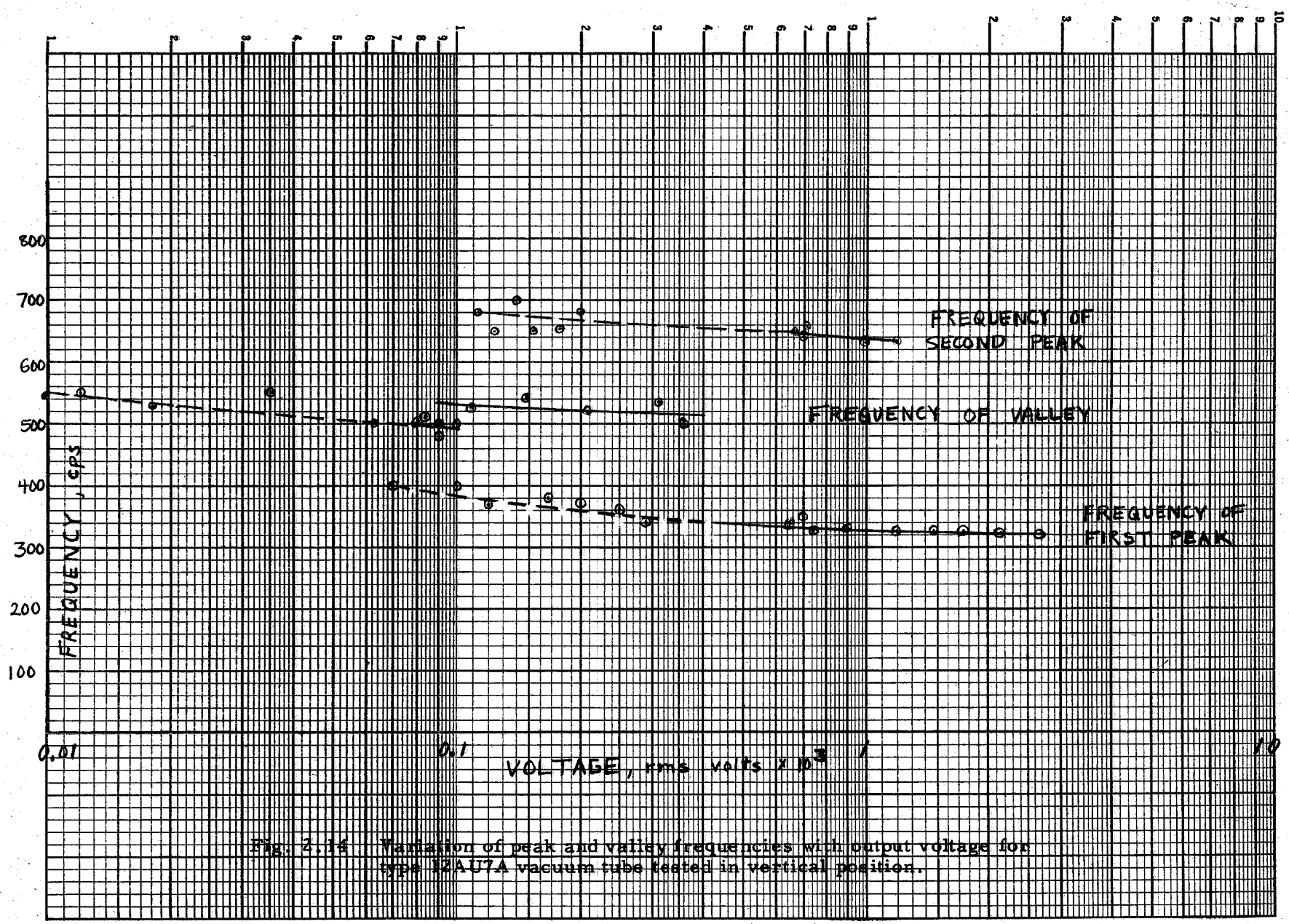

Fig. 2.14 Variation of peak and valley frequencies with output voltage for type 12AU7A vacuum tube tested in vertical position.

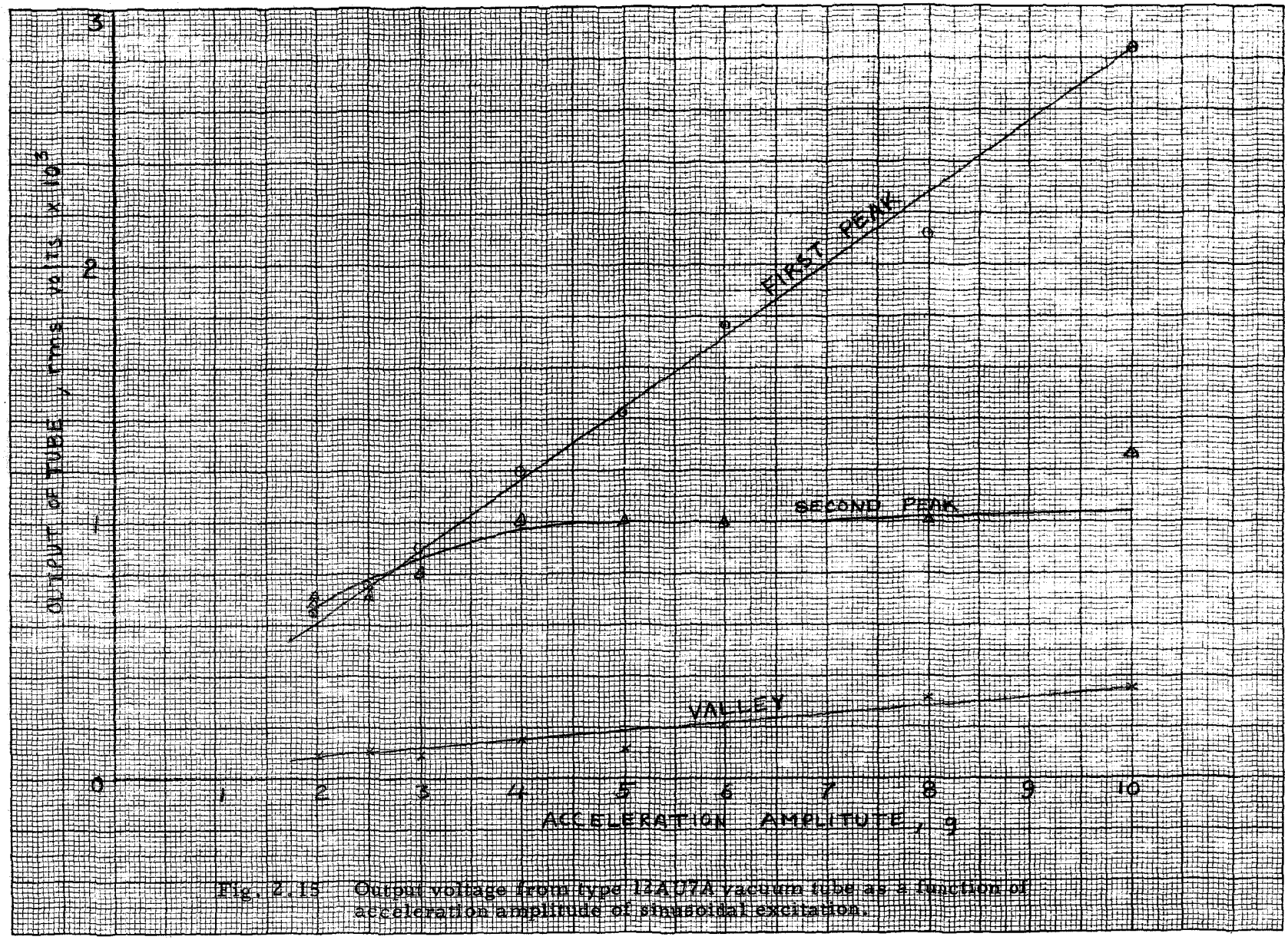

Fig. 2.15 Output voltage from type 12AQ7A vacuum tube as a function of acceleration amplitude of sinusoidal excitation.

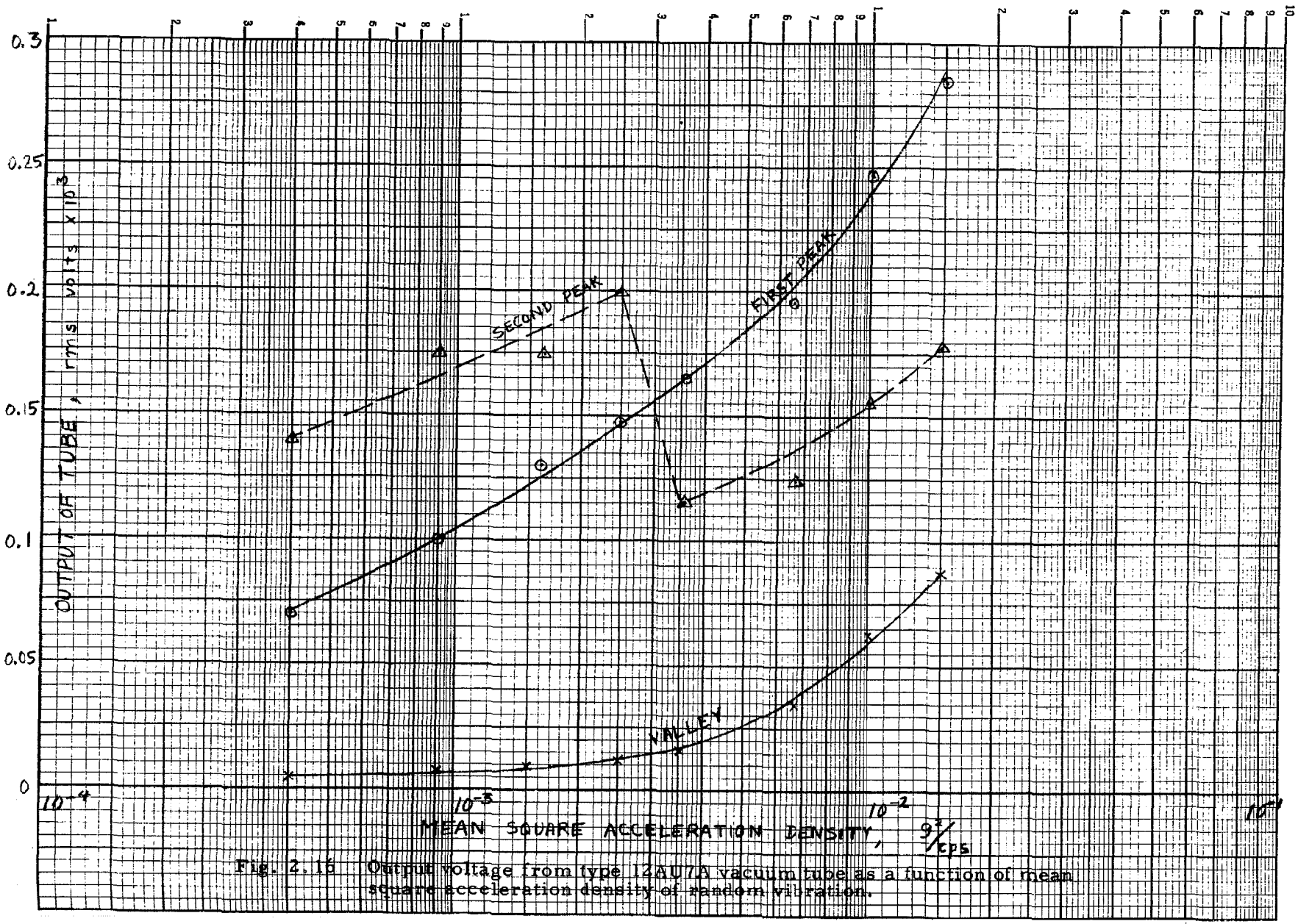

Fig. 2.16 Output voltage from type 12AU7A vacuum tube as a function of mean square acceleration density of random vibration.

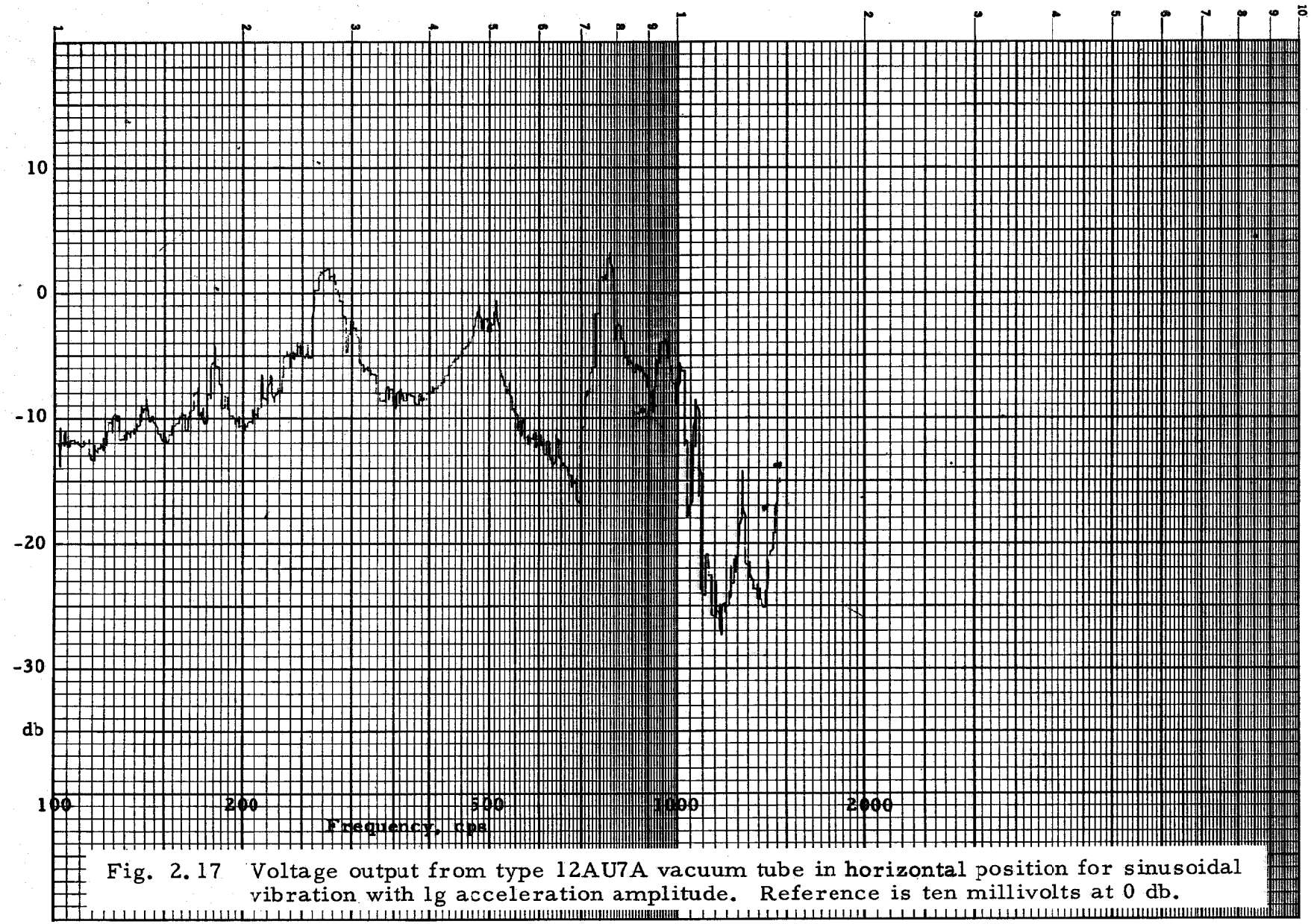

Fig. 2.17 Voltage output from type 12AU7A vacuum tube in horizontal position for sinusoidal vibration with 1g acceleration amplitude. Reference is ten millivolts at 0 db.

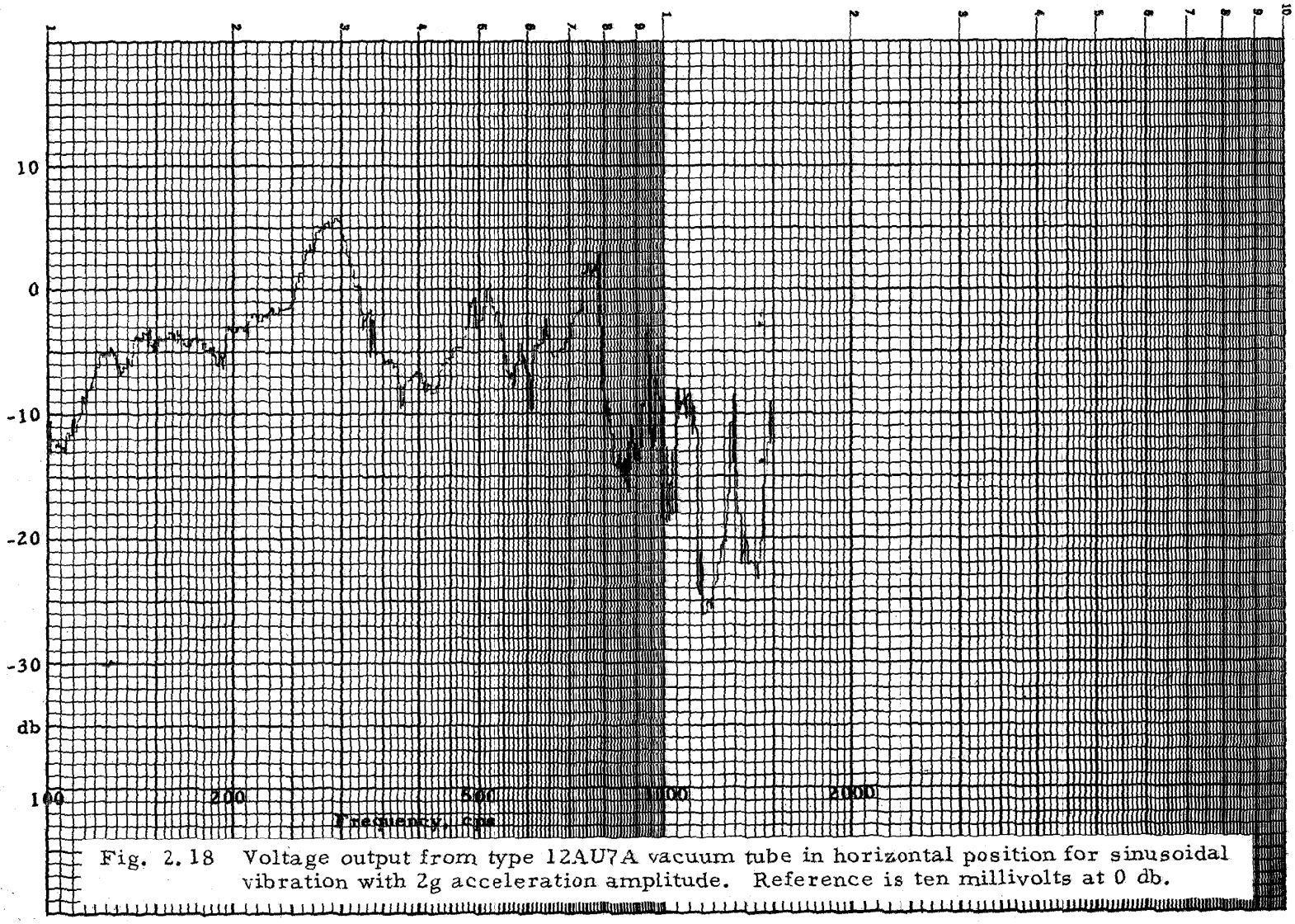

Fig. 2.18 Voltage output from type 12AU7A vacuum tube in horizontal position for sinusoidal vibration with 2g acceleration amplitude. Reference is ten millivolts at 0 db.

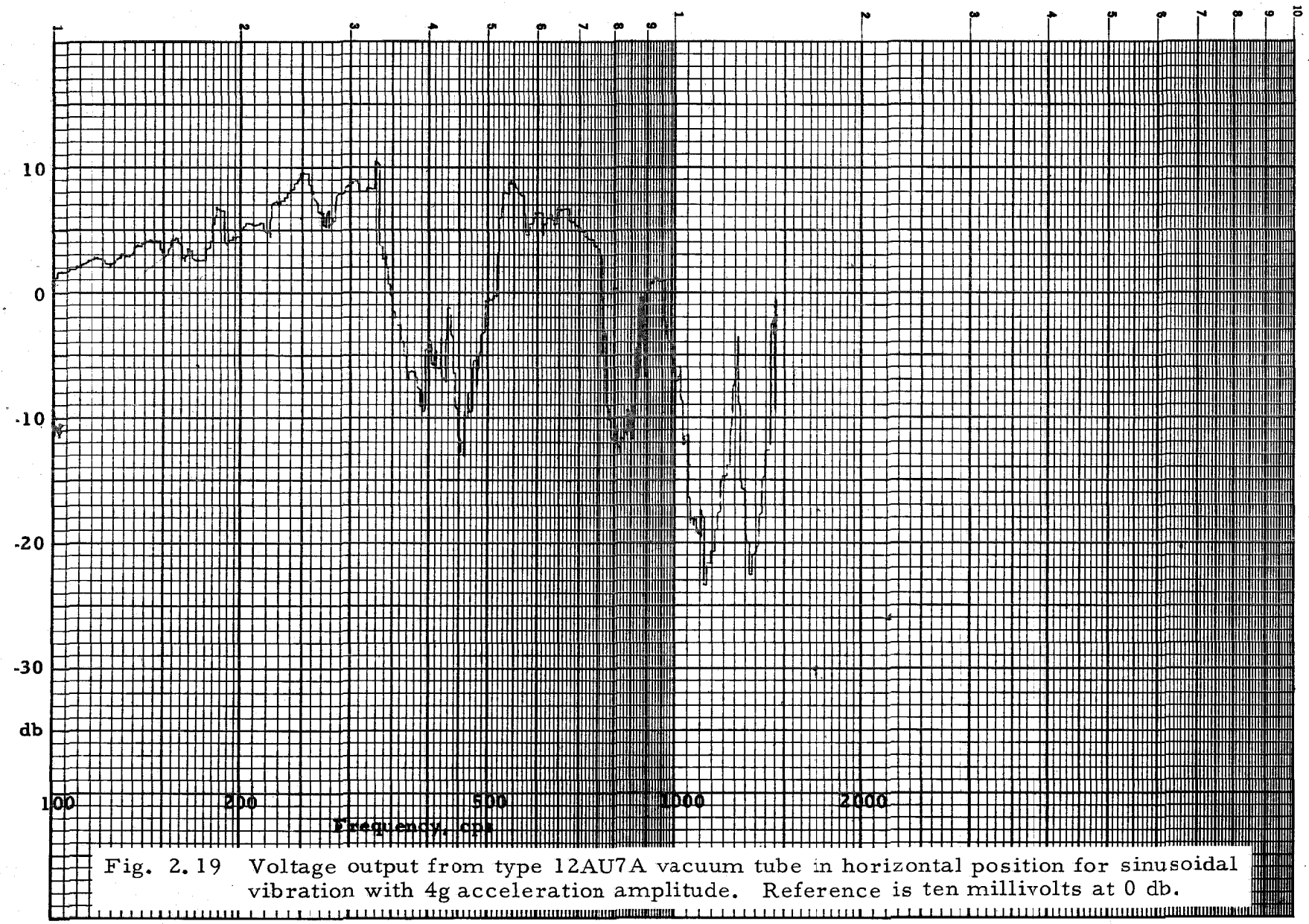

Fig. 2.19 Voltage output from type 12AU7A vacuum tube in horizontal position for sinusoidal vibration with 4g acceleration amplitude. Reference is ten millivolts at 0 db.

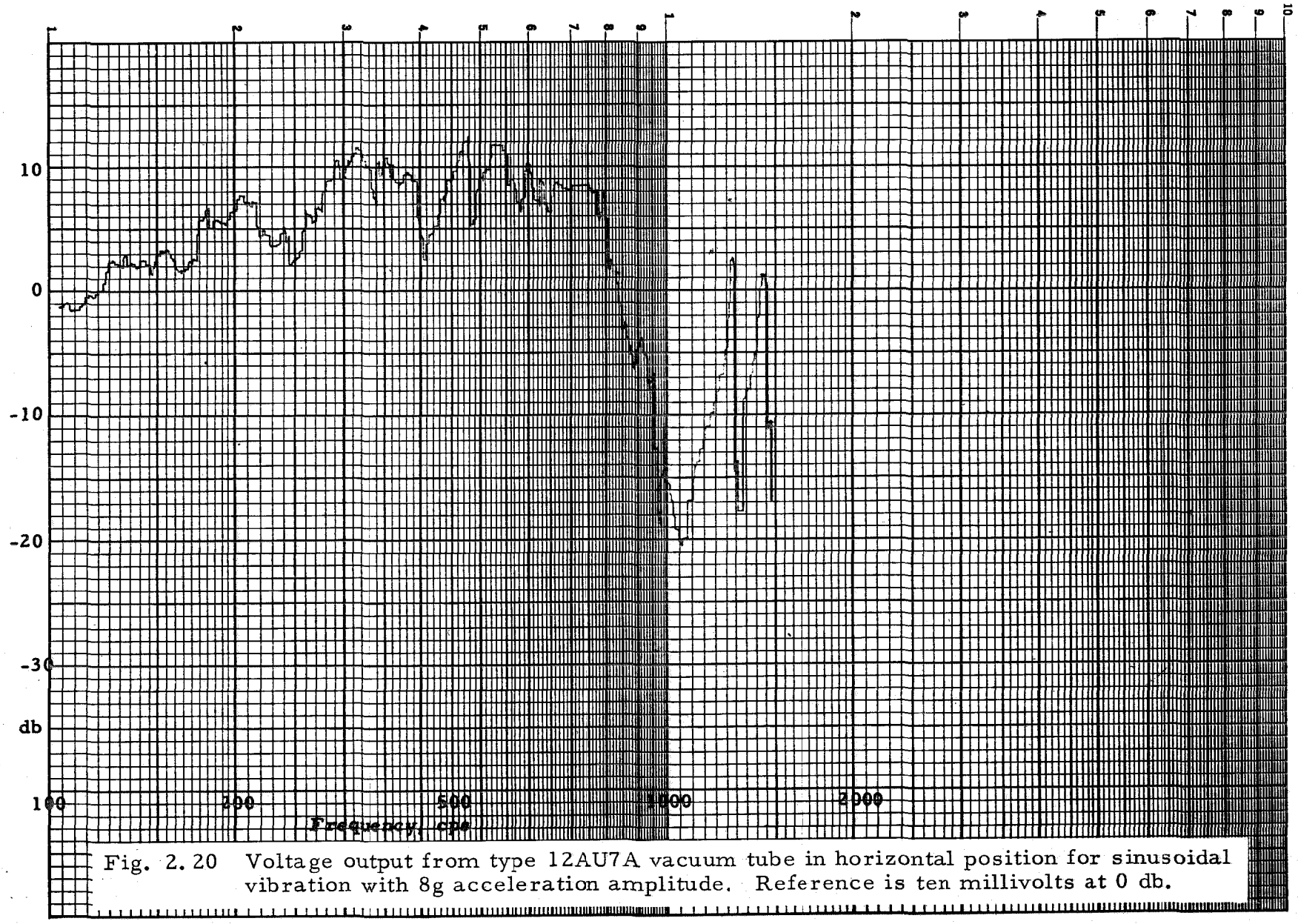

Fig. 2.20 Voltage output from type 12AU7A vacuum tube in horizontal position for sinusoidal vibration with 8g acceleration amplitude. Reference is ten millivolts at 0 db.

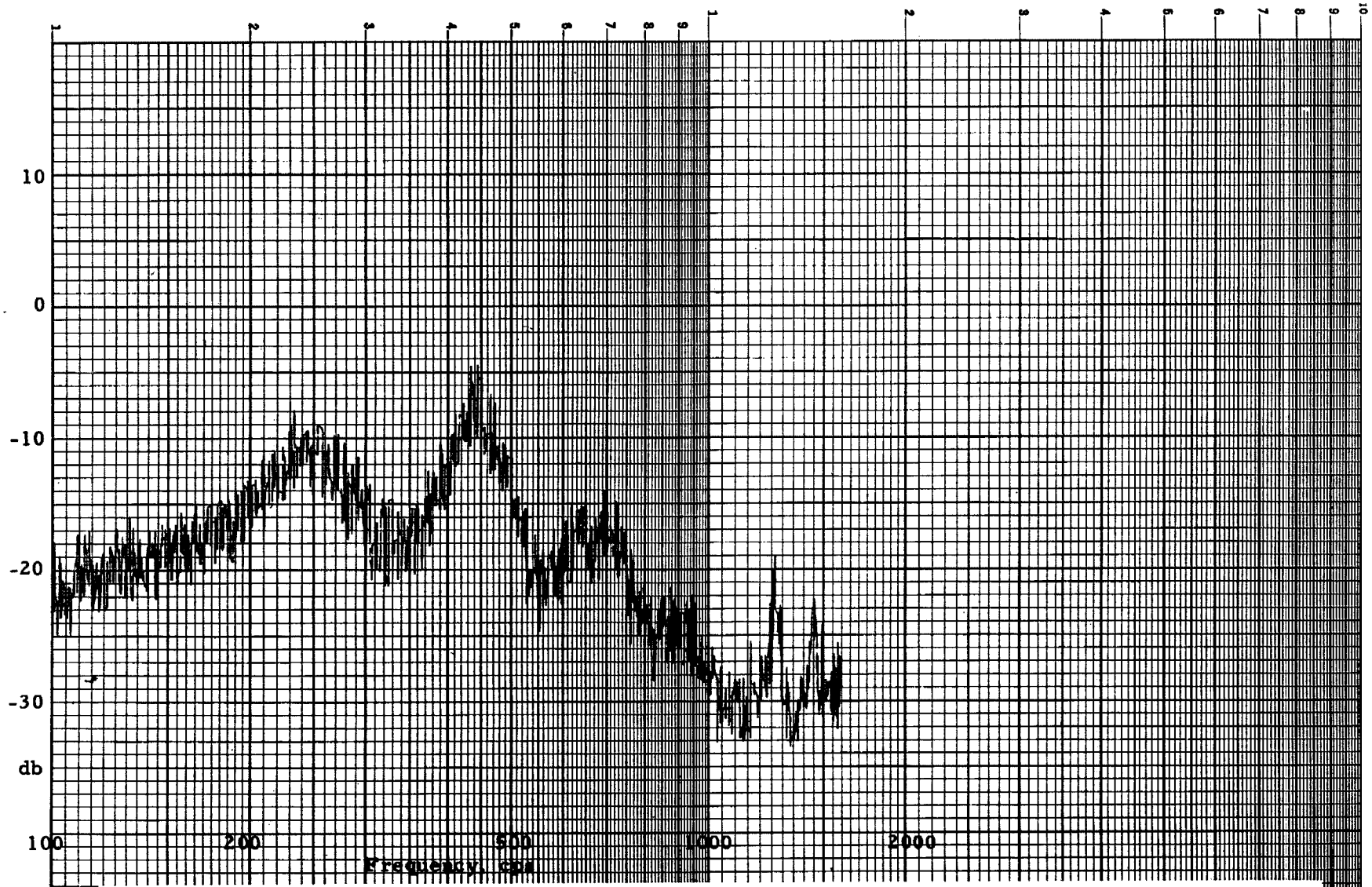

Fig. 2.21 Voltage output from type 12AU7A vacuum tube in horizontal position for random vibration with 0.0016 g^2/cps mean square acceleration density. Reference is ten millivolts at 0 db.

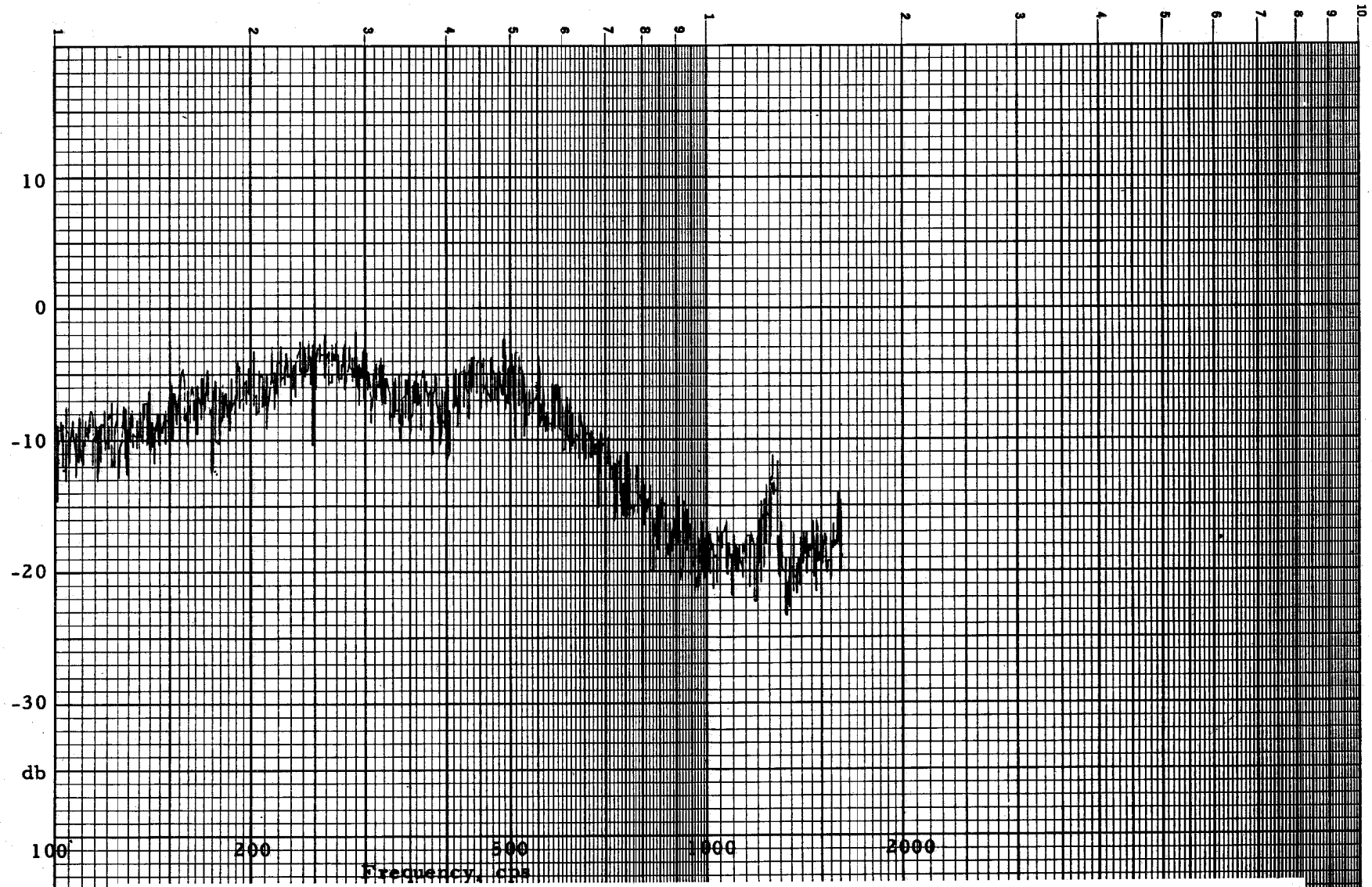

Fig. 2.22 Voltage output from type 12AU7A vacuum tube in horizontal position for random vibration with 0.015 g^2/cps mean square acceleration density. Reference is ten millivolts at 0 db.

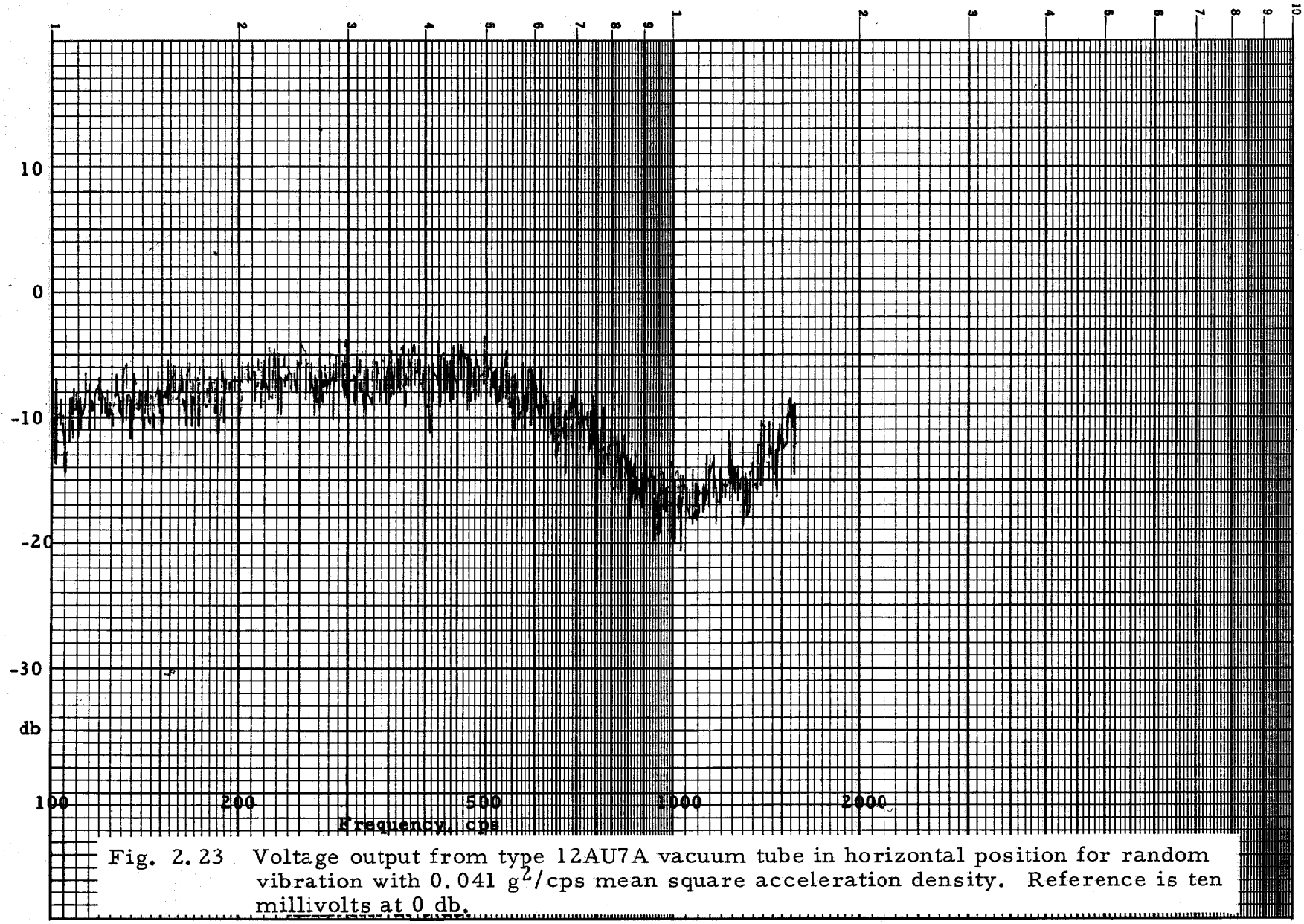

Fig. 2.23 Voltage output from type 12AU7A vacuum tube in horizontal position for random vibration with 0.041 g^2/cps mean square acceleration density. Reference is ten millivolts at 0 db.

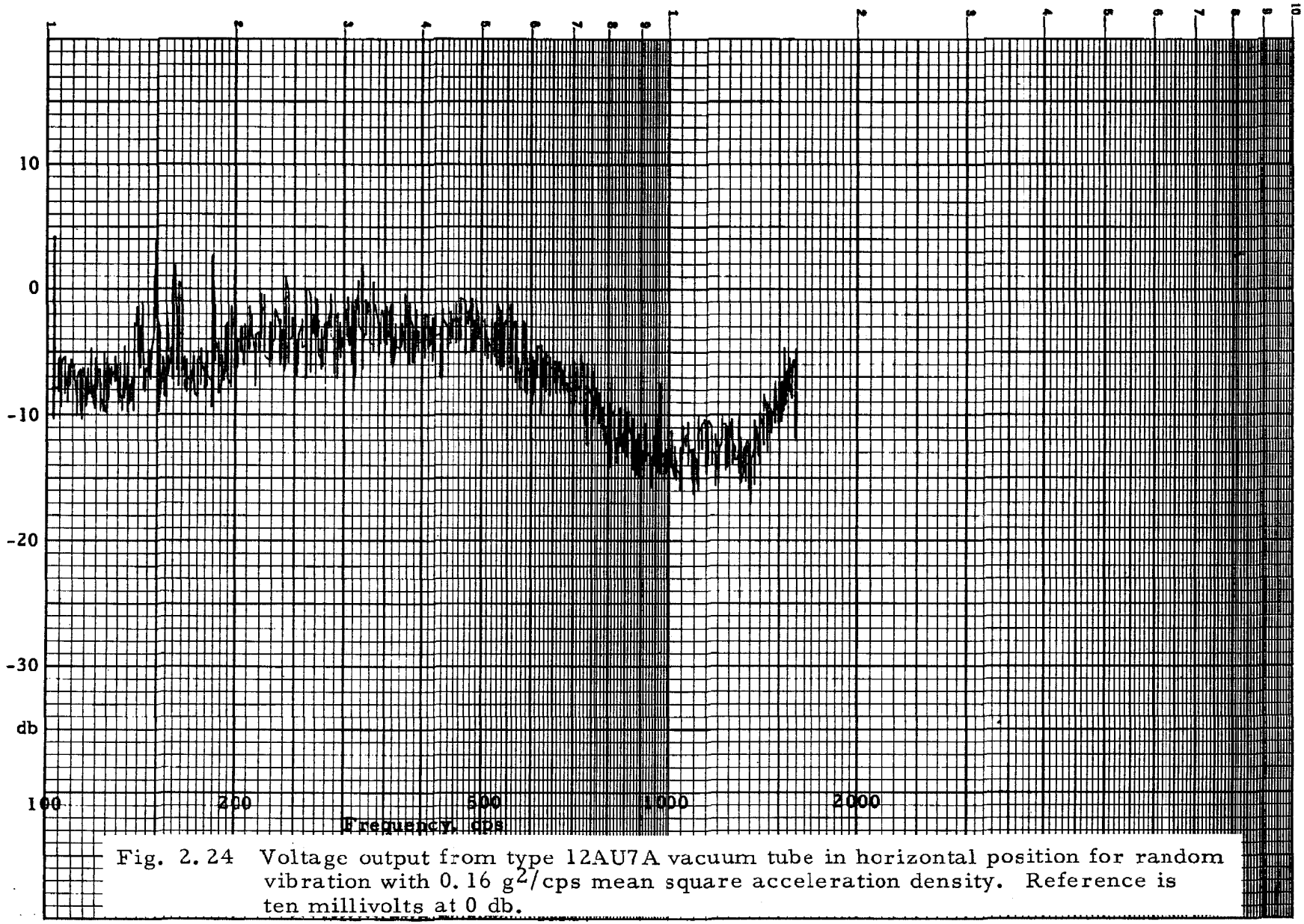

Fig. 2.24 Voltage output from type 12AU7A vacuum tube in horizontal position for random vibration with 0.16 g^2/cps mean square acceleration density. Reference is ten millivolts at 0 db.

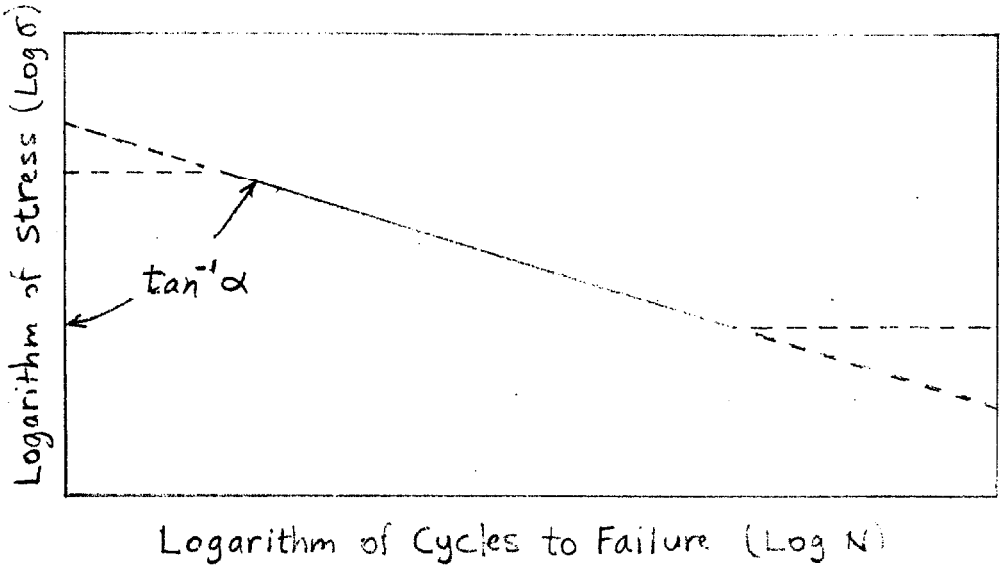

Fig. 3.1 Schematic curve of stress amplitude vs. number of cycles to failure.

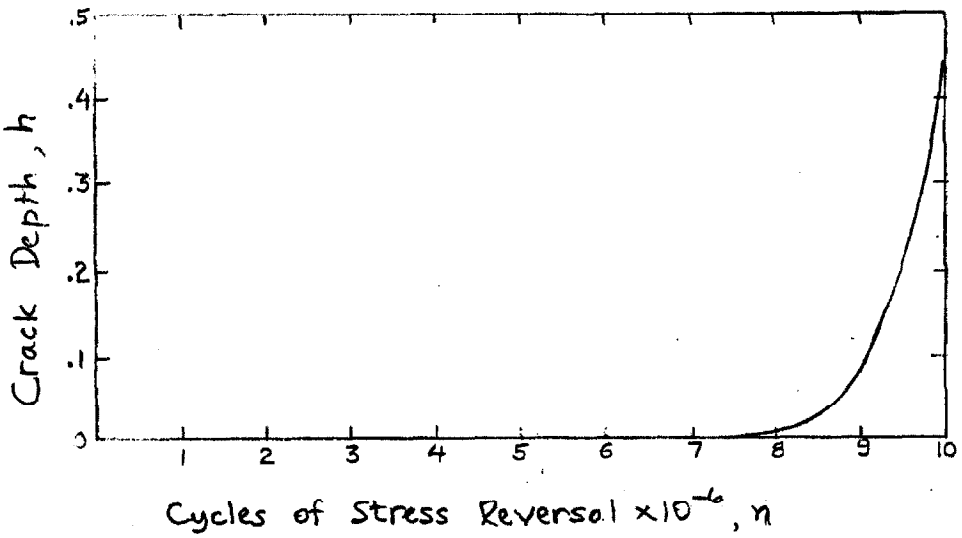

Fig. 3.2 Hypothetical curve of crack depth as a function of number of cycles of stress reversal.

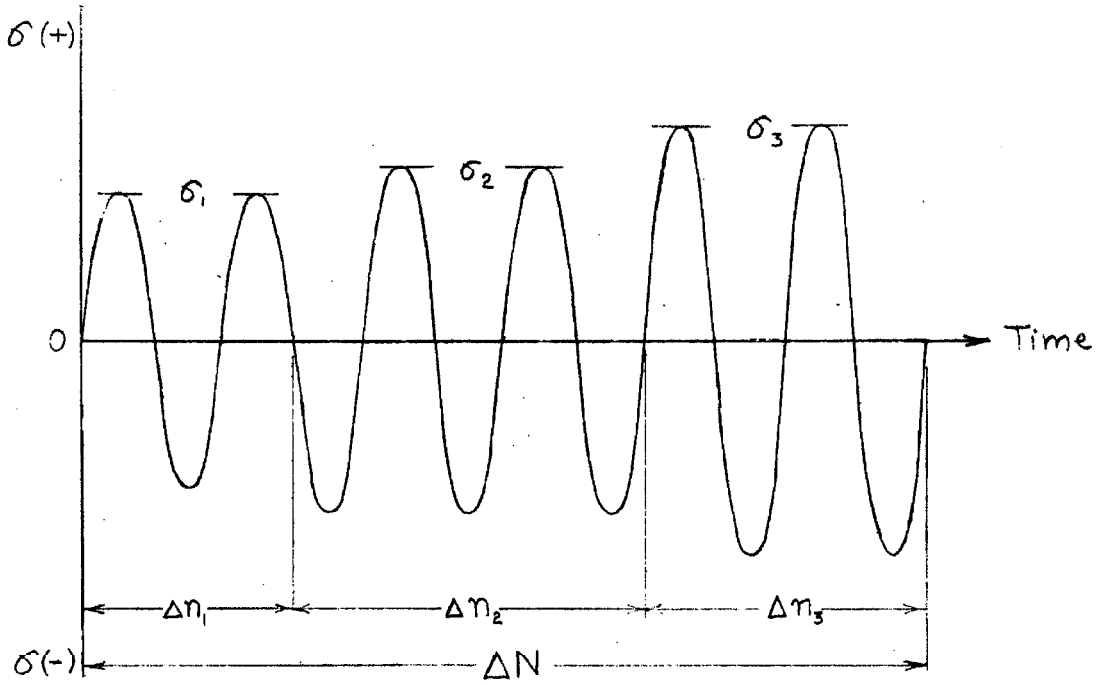

Fig. 3.3 Stress time-history for variable stress amplitude.

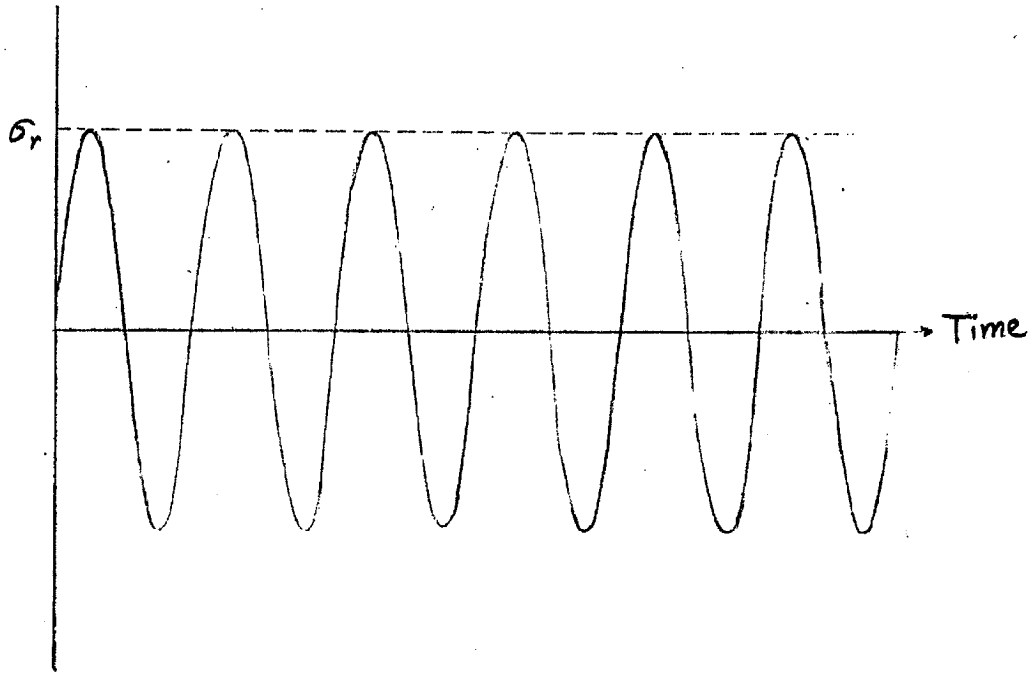

Fig. 3.4 Stress time-history with constant stress amplitude wherein crack growth is equivalent to condition of Fig. 3.3

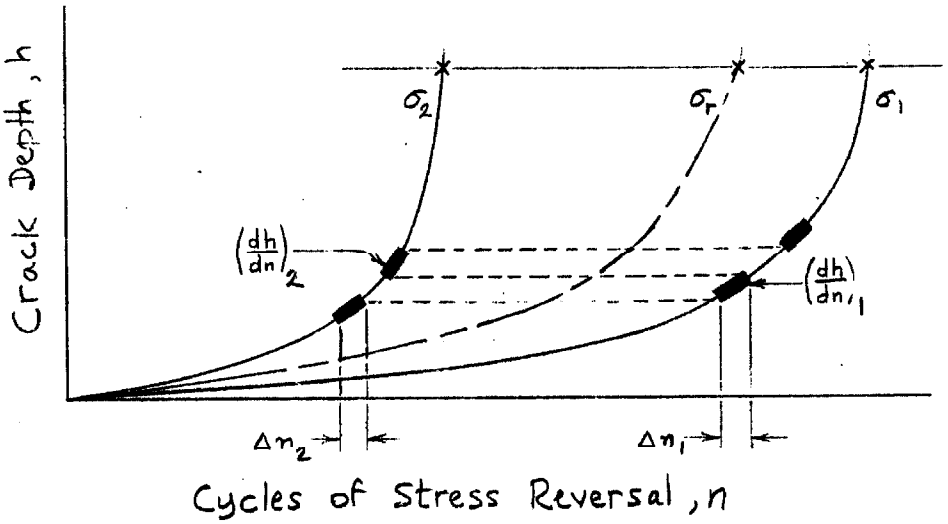

Fig. 3.5 Rate of crack growth for conditions shown in Figs. 3.3 and 3.4.

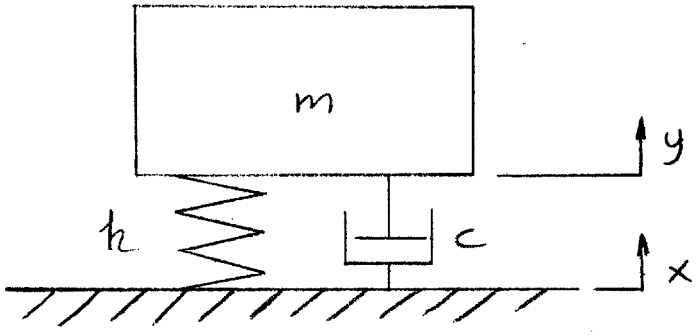

Fig. 3.6 Mathematical Model of mechanical structure

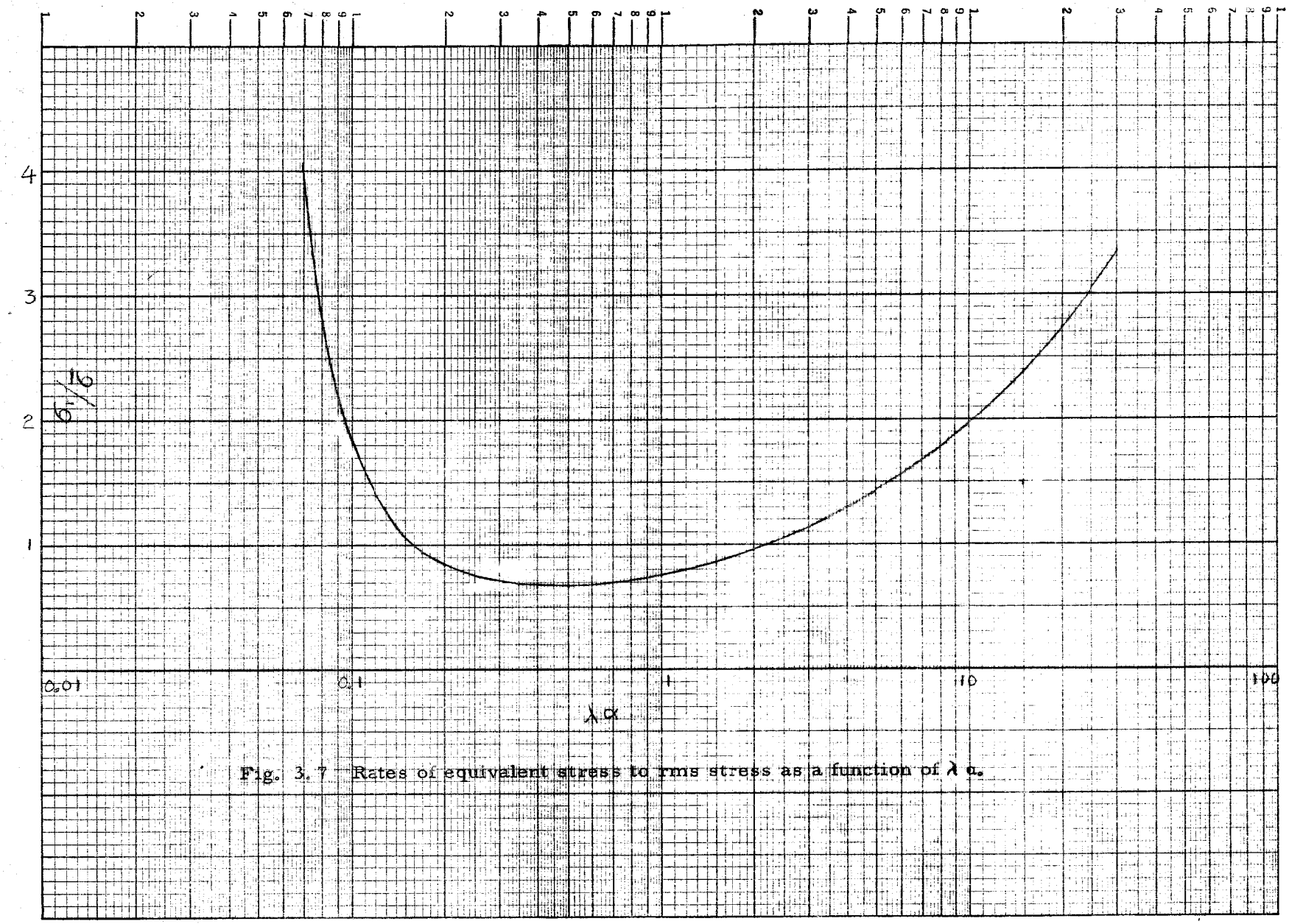

Fig. 3.7 Rates of equivalent stress to rms stress as a function of $\lambda\alpha$.

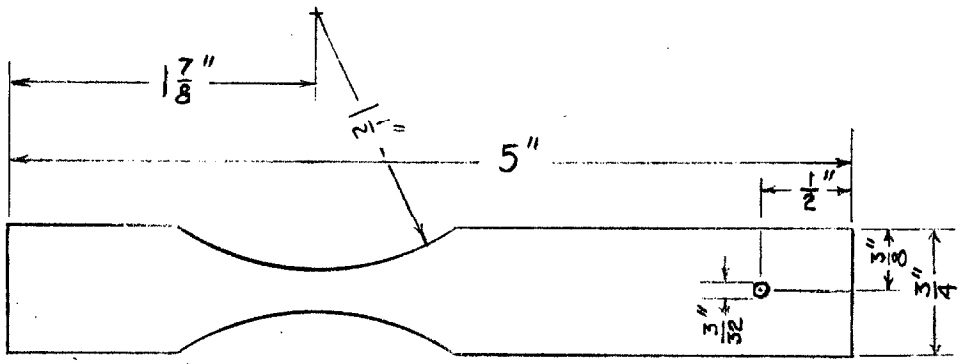

Fig. 3.8 Specimen for fatigue tests

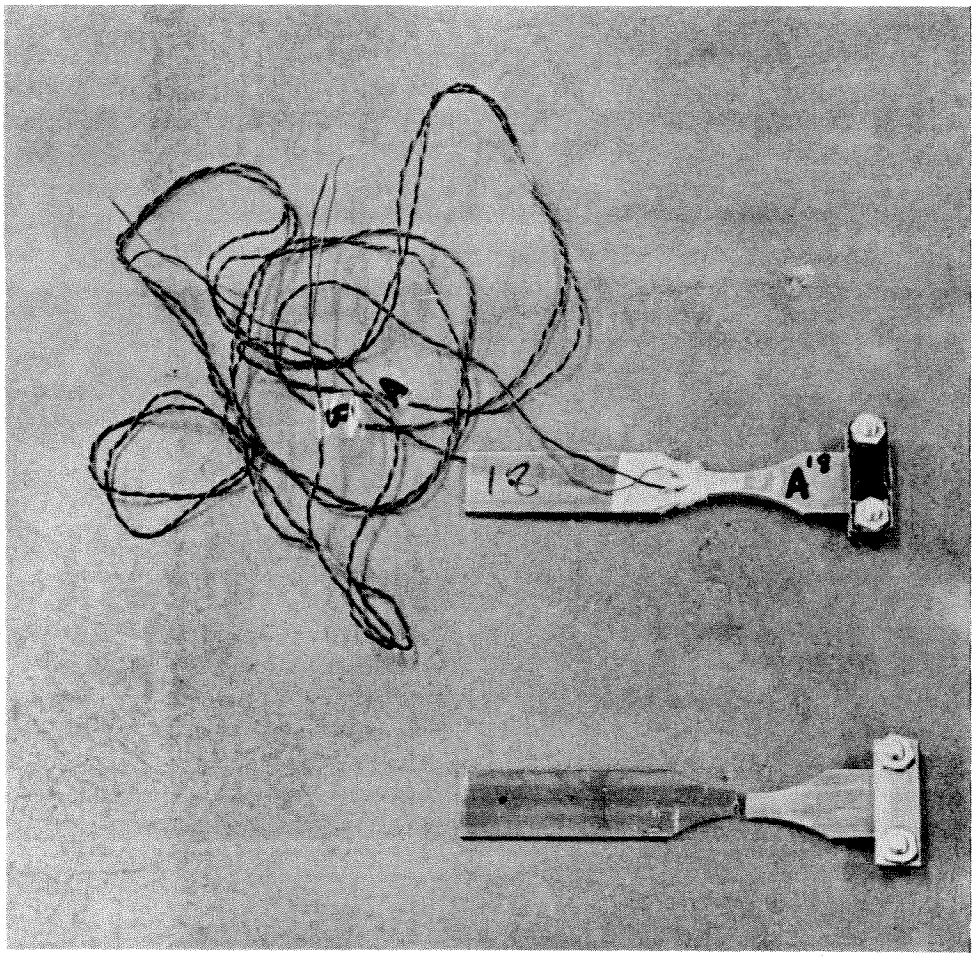

Fig. 3.9 Photograph of specimens used in fatigue tests.

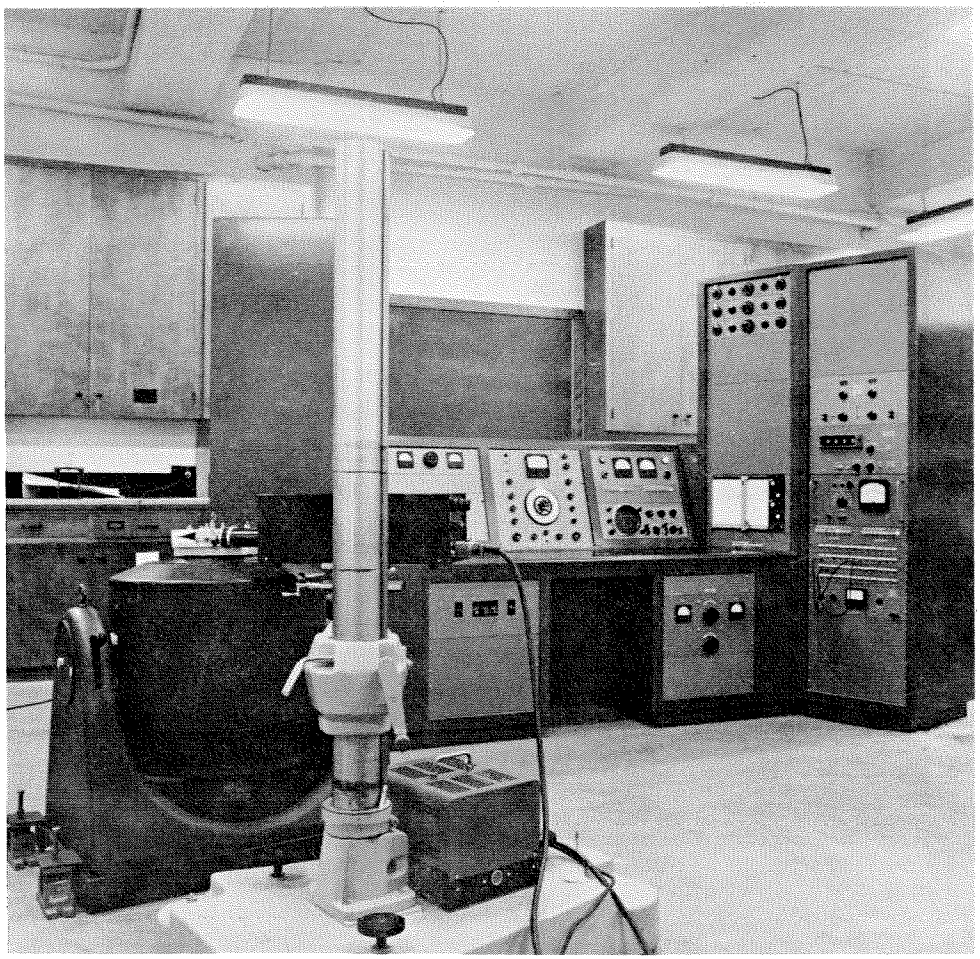

Fig. 3.10 Vibration exciter, console and displacement follower used in fatigue tests.

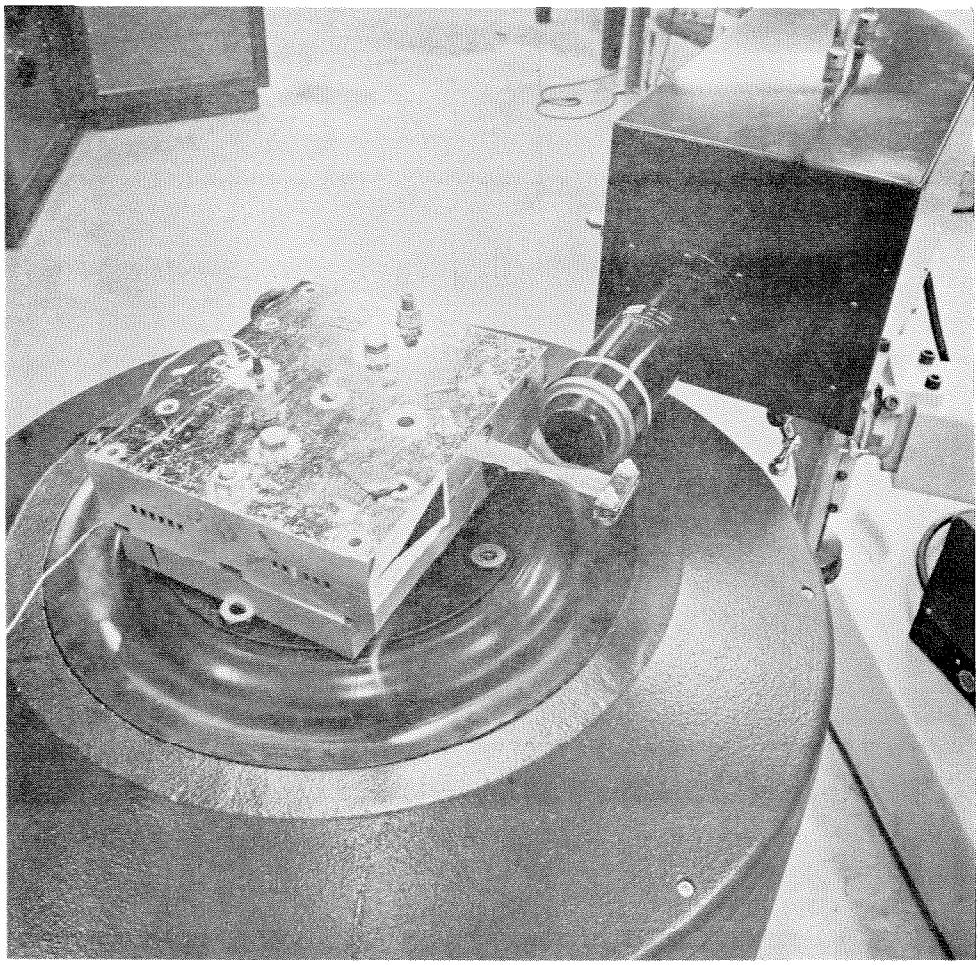

Fig. 3.11 Specimen in vibration exciter with displacement follower arranged to monitor fatigue test.

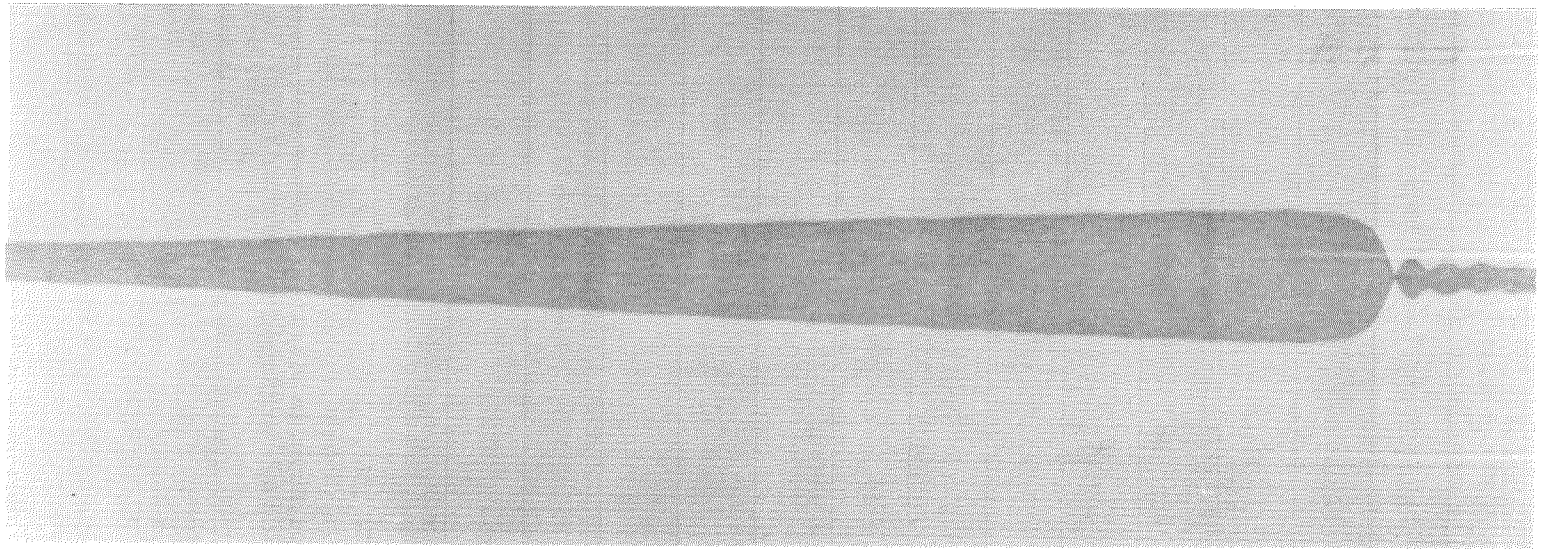

Fig. 3.12 Time-history on compressed time scale of beam displacement during fatigue test. Frequency increasing at rate of 0.14 octave per minute. Strain gage not fixed to beam.

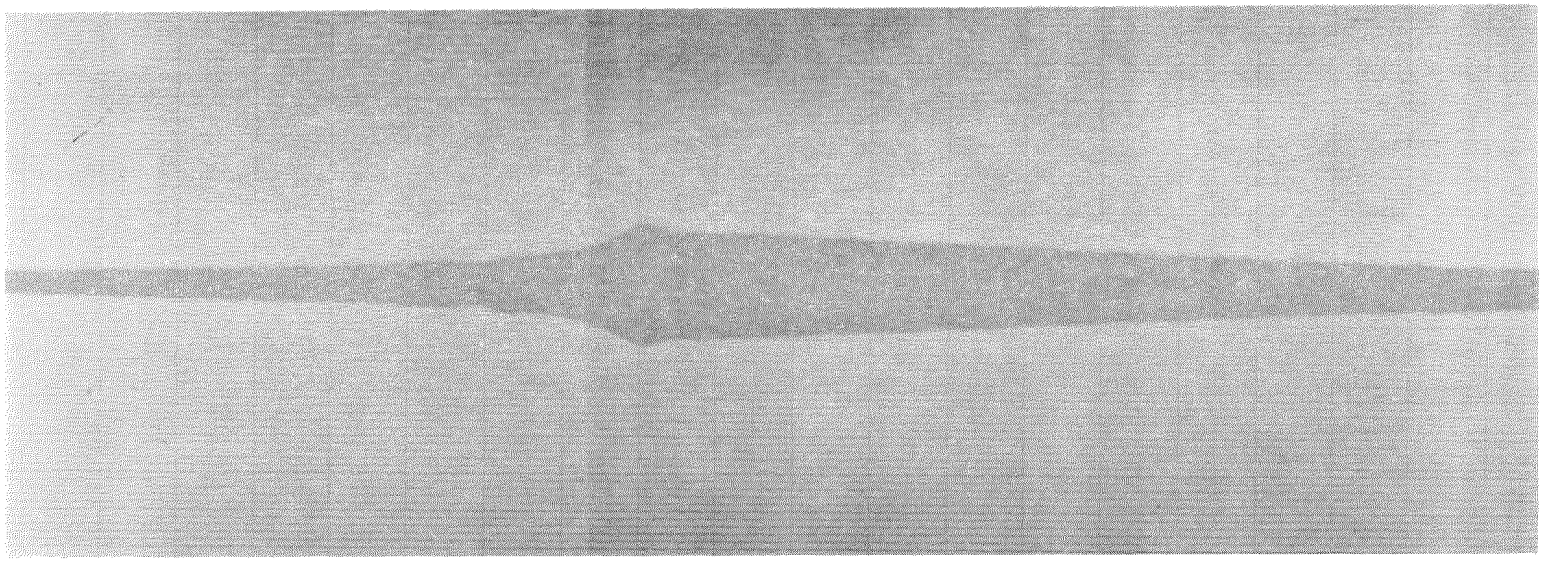

Fig. 3.13 Time-history on compressed time scale of beam displacement during fatigue test. Frequency decreasing at rate of 0.14 octave per minute. Strain gage not fixed to beam.

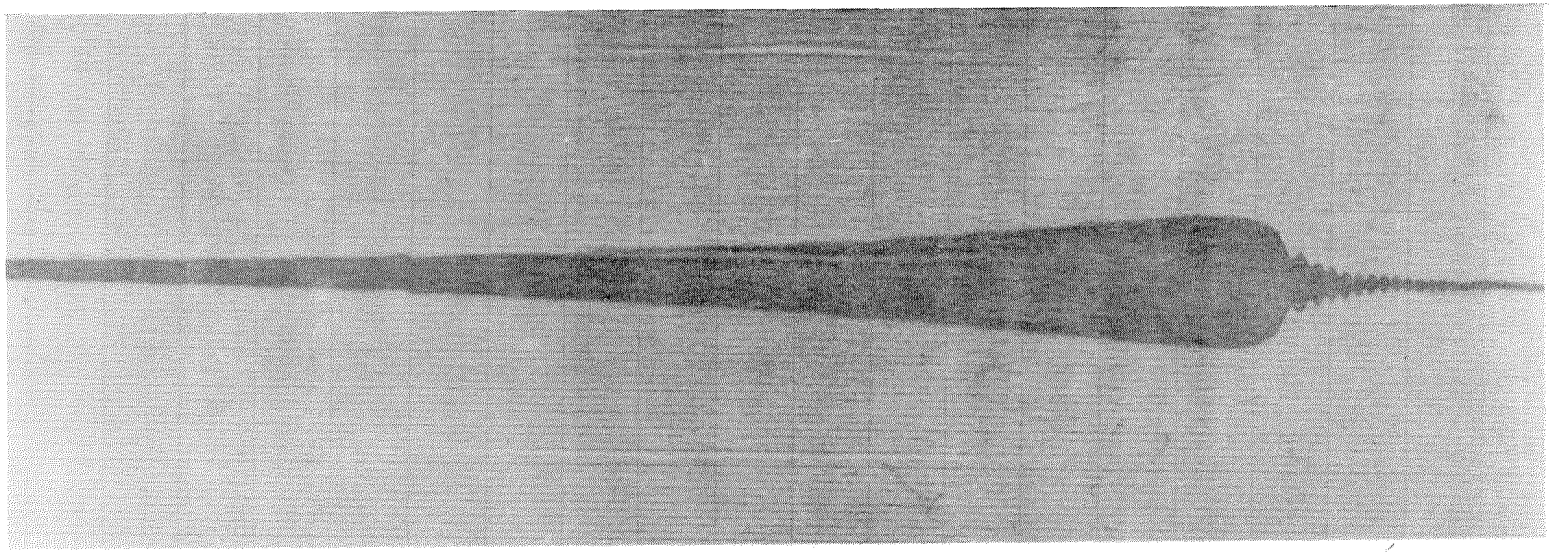

Fig. 3.14 Time-history on compressed time scale of beam displacement during fatique test. Frequency increasing at rate of 0.46 octave per minute. Strain gage not fixed to beam.

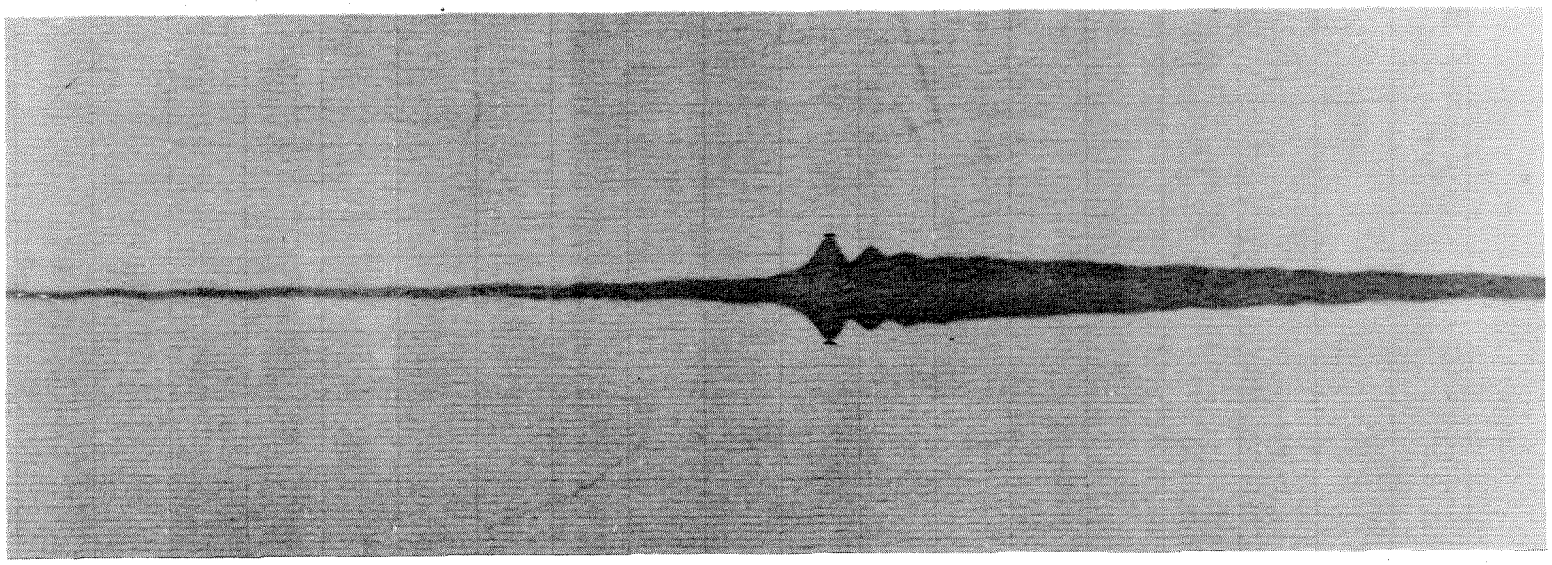

Fig. 3.15 Time-history on compressed time scale of beam displacement during fatigue test. Frequency decreasing at rate of 0.46 octave per minute. Strain gage not fixed to beam.

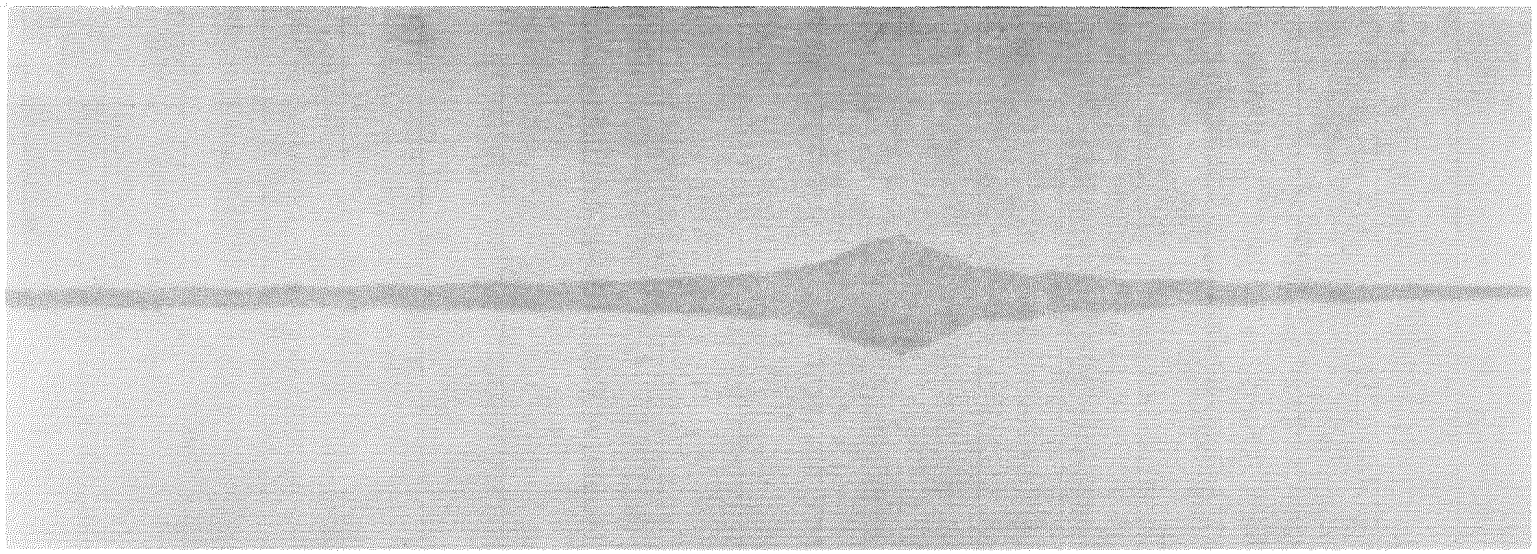

Fig. 3.16 Time-history on compressed time scale of beam displacement during fatigue test. Frequency increasing at rate of 0.46 octave per minute. Strain gage fixed to beam.

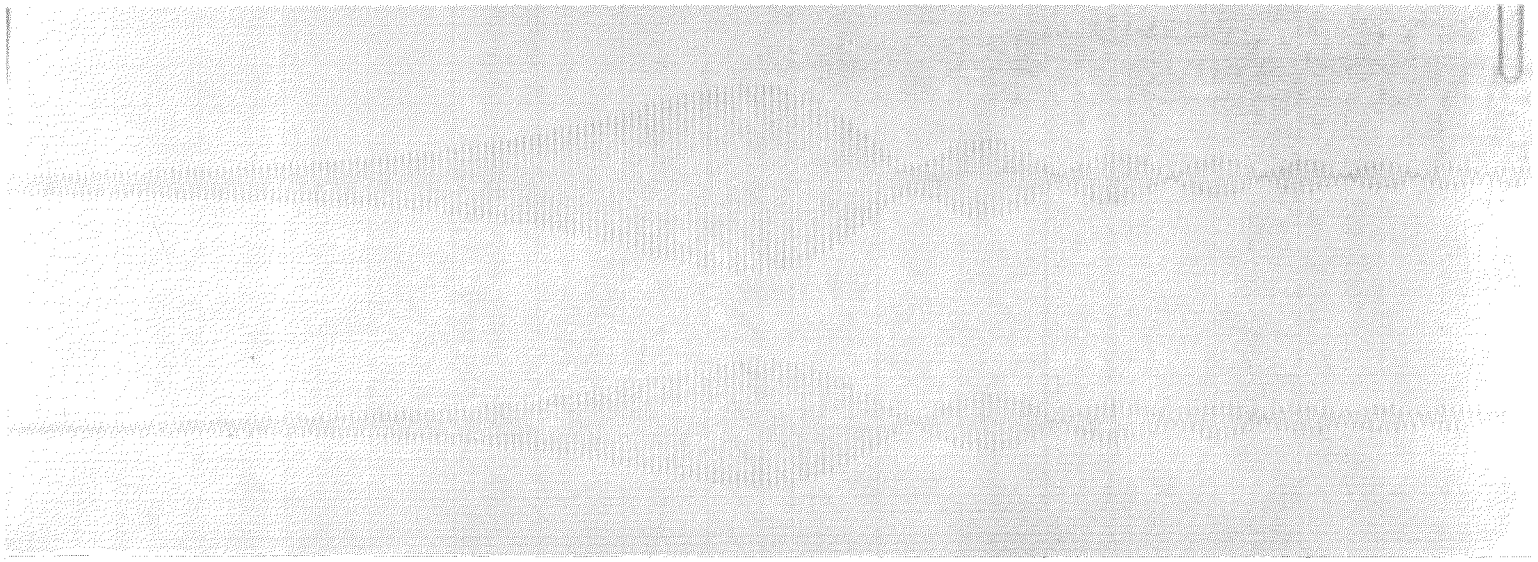

Fig. 3.17 Time-history of strain and displacement in a beam with frequency decreasing; upper trace is strain and lower trace is displacement.

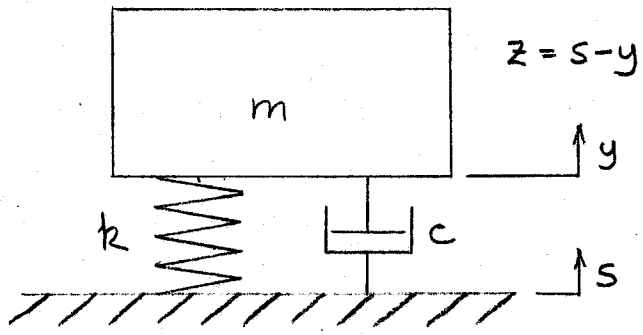

Fig. 4.1 Damped single degree of freedom system

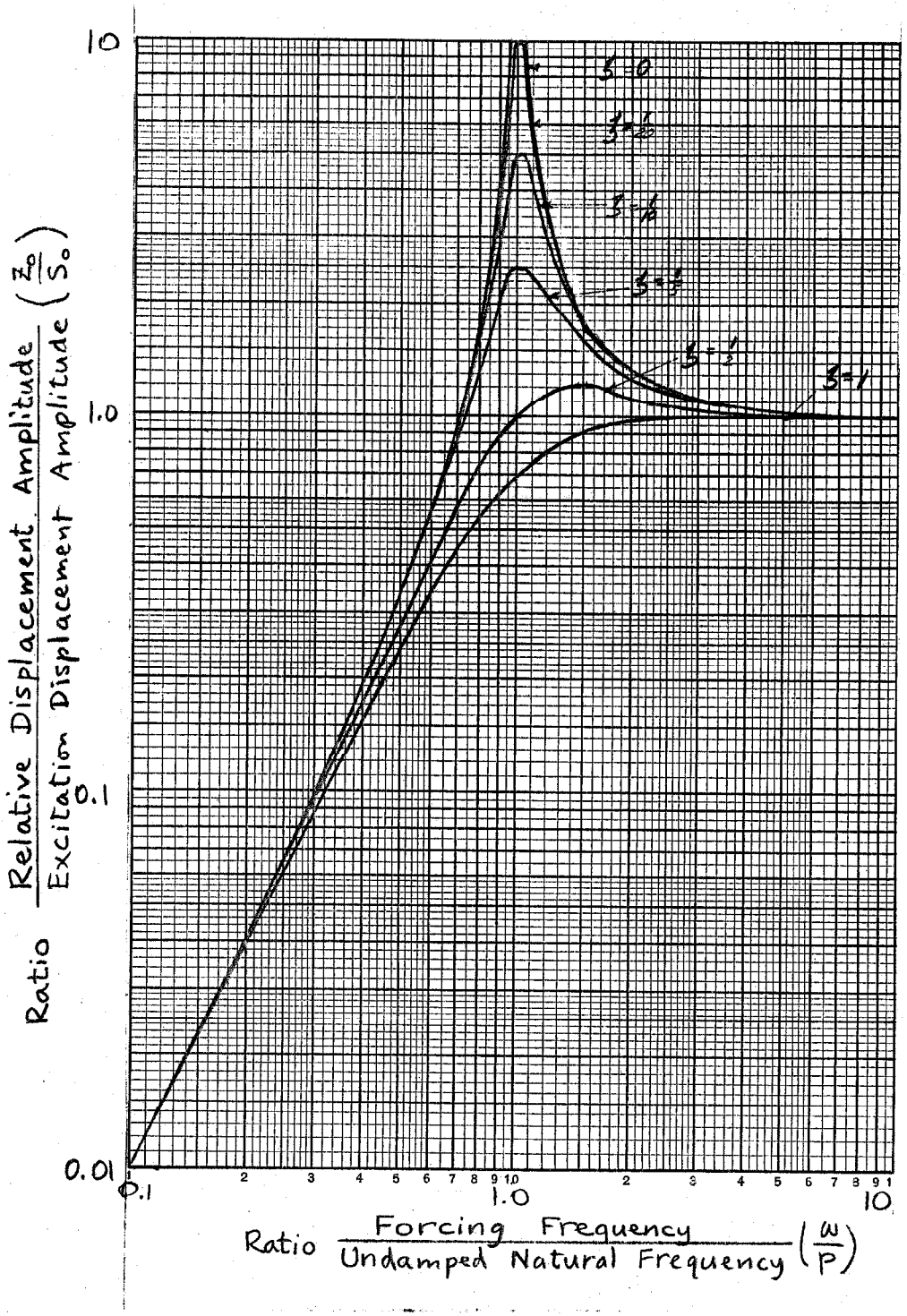

Fig. 4.2 Relative displacement amplitude with reference to excitation displacement amplitude.

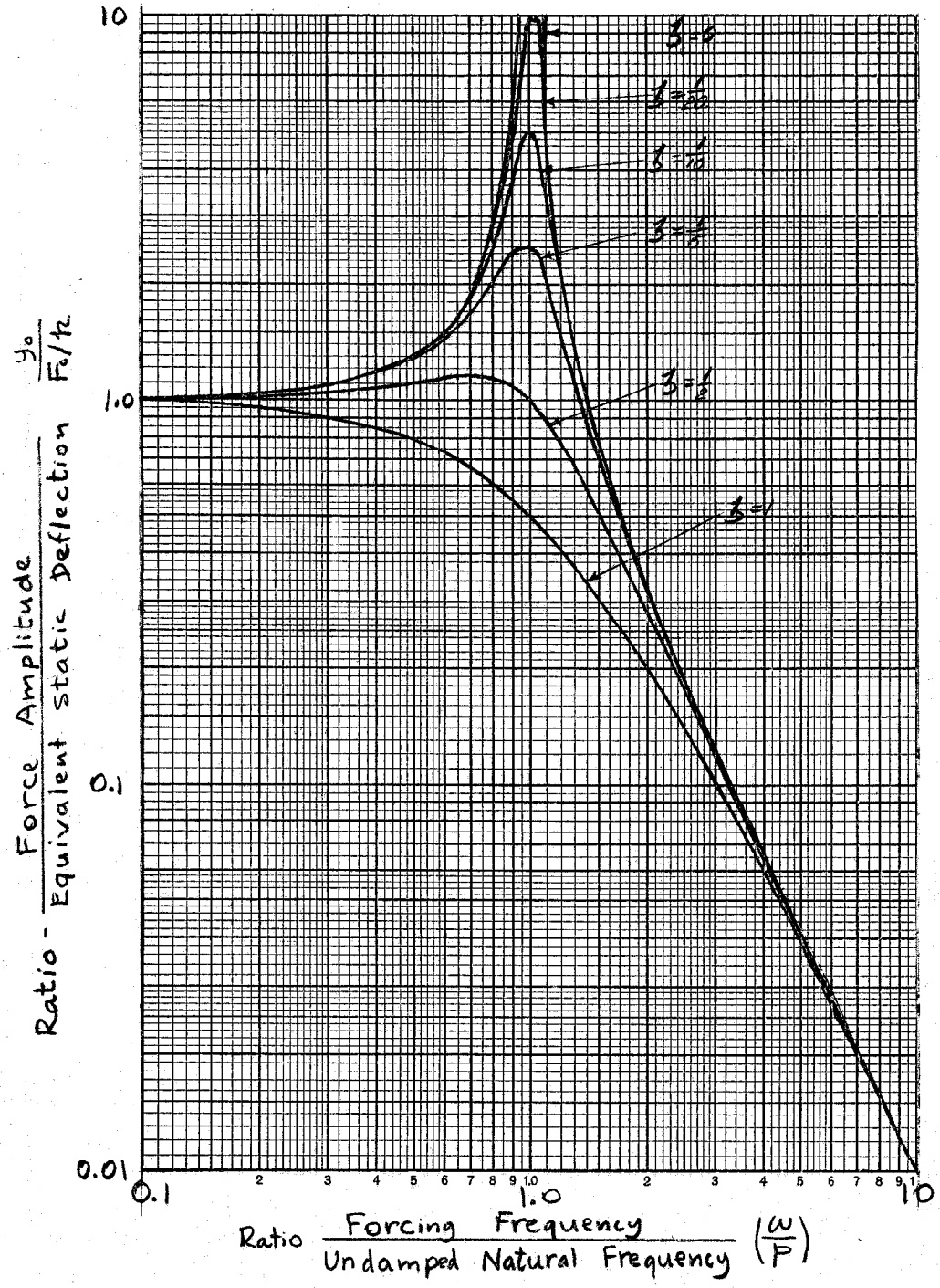

Fig. 4.3 Relative displacement amplitude with reference to excitation acceleration amplitude.

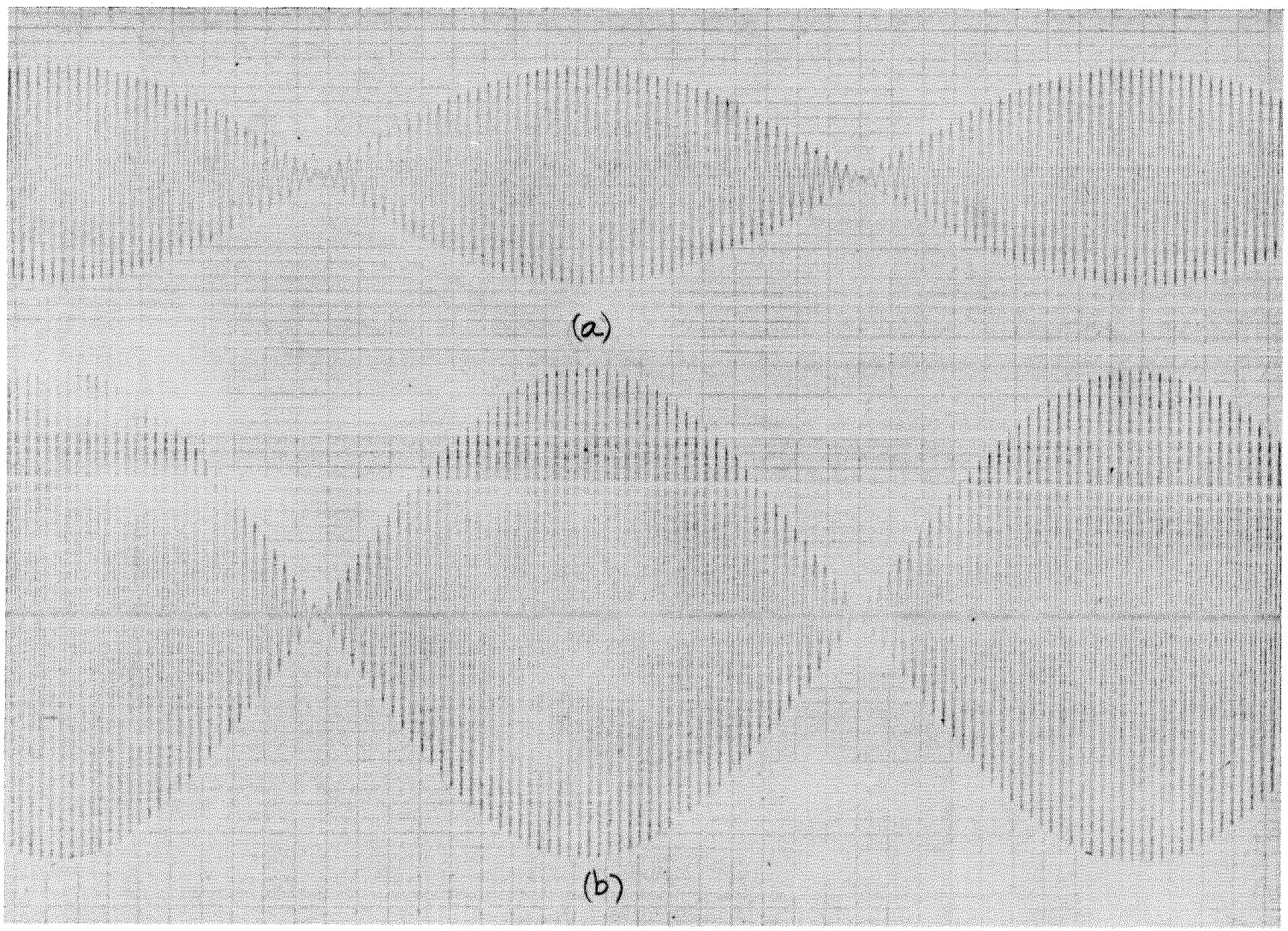

Fig. 4.4 Beats produced by combined sinusoids of nearly equal frequencies. Excitation is at (a) and response of simple system at (b).

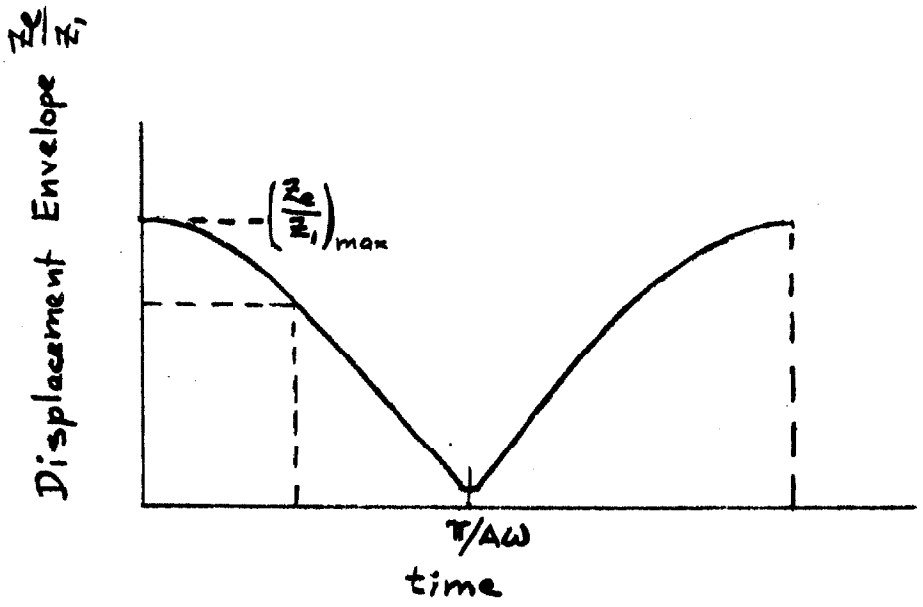

Fig. 4.5 Fraction of time that envelope is above z_e/z_1 for beat pattern.

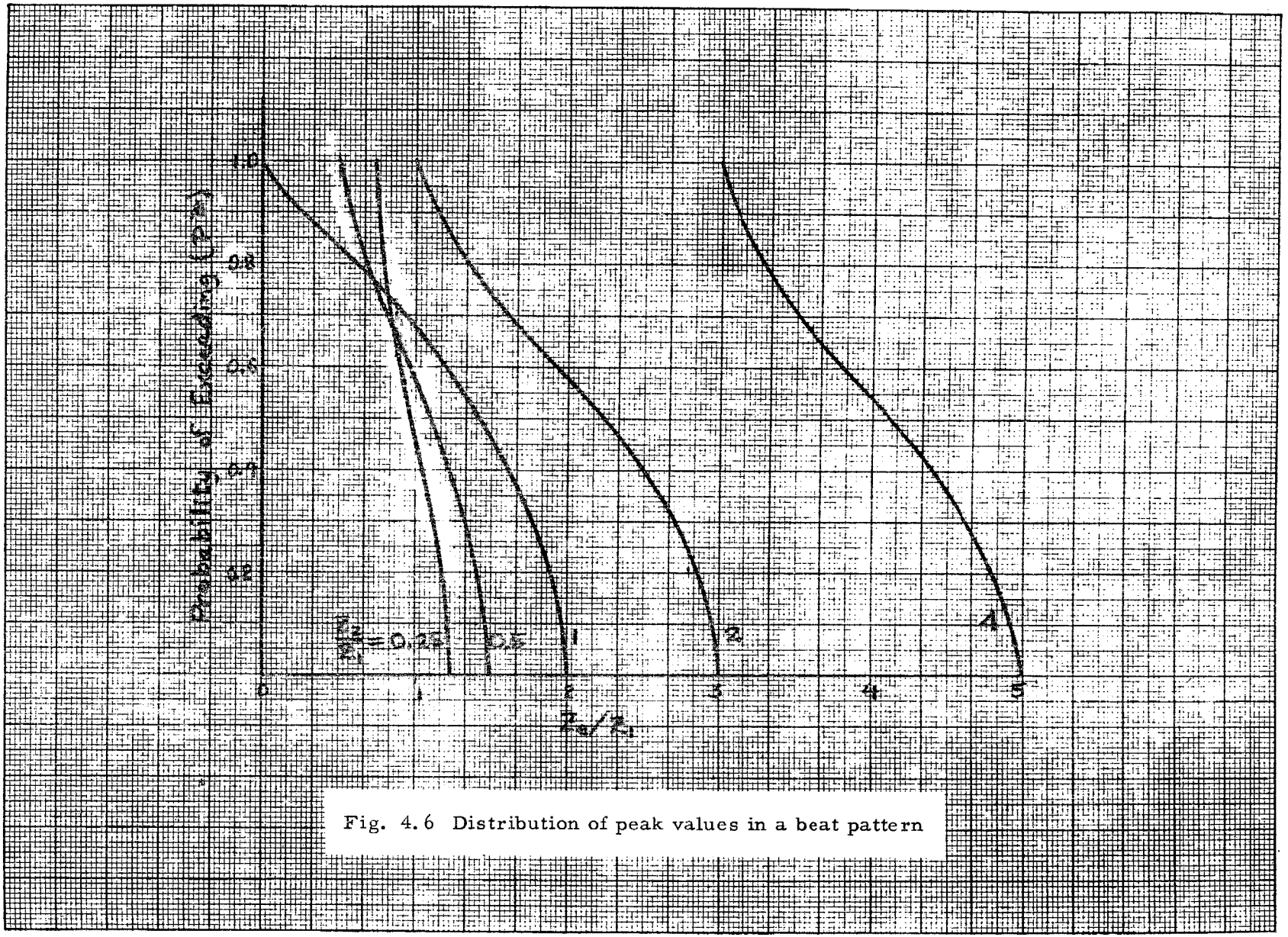

Fig. 4.6 Distribution of peak values in a beat pattern

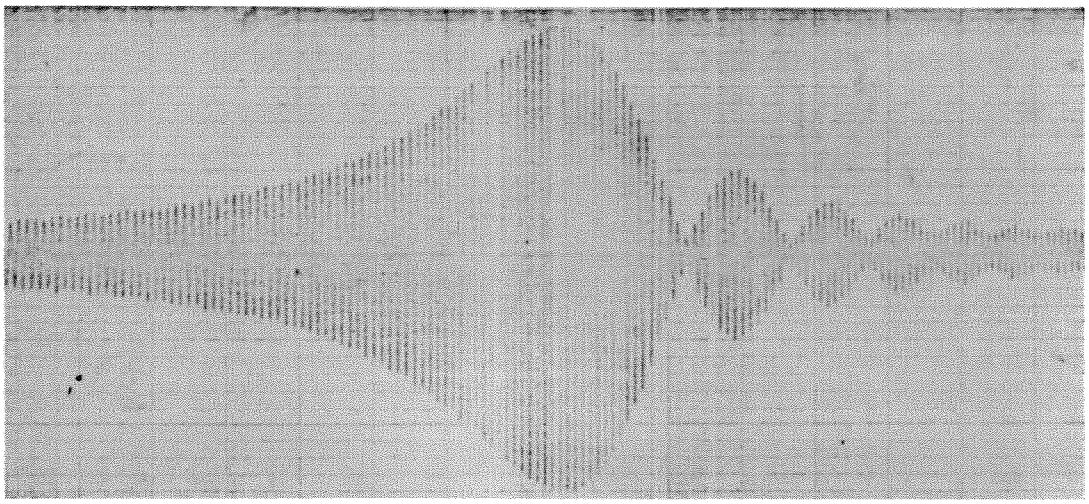

(a)

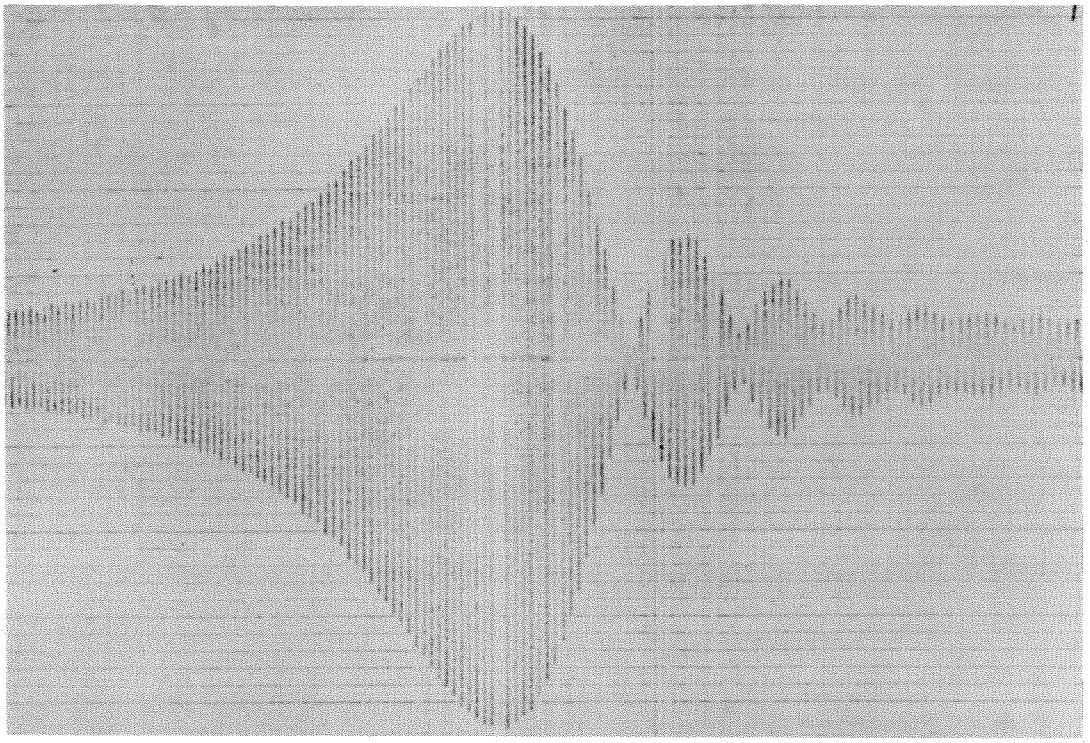

(b)

Fig. 4.7 Response of a simple system to variable frequency sinusoidal excitation. Increasing frequency is at (a); decreasing frequency is at (b). There is no significance to the different vertical scales.

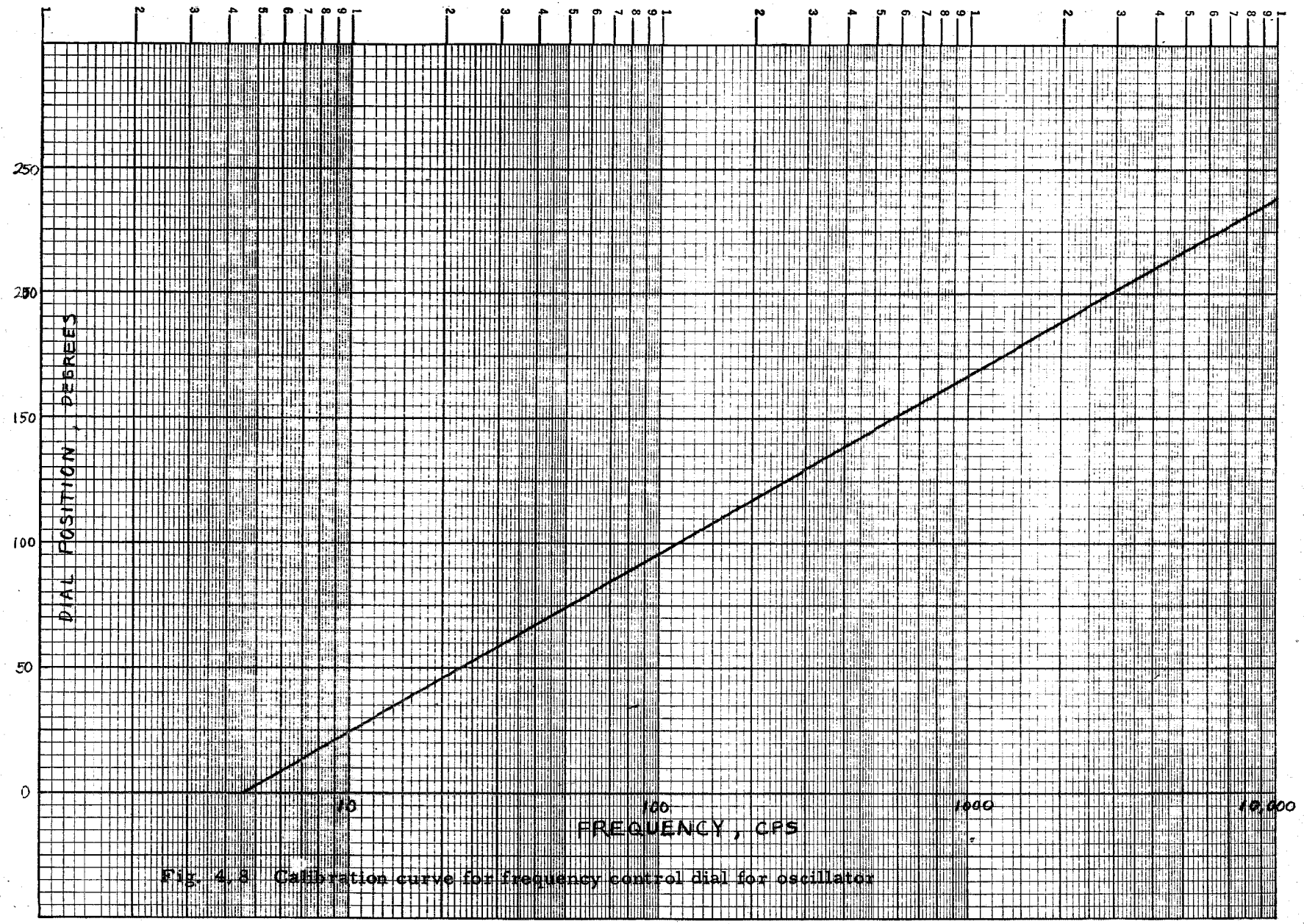

Fig. 4.3 Calibration curve for frequency control dial for oscillator

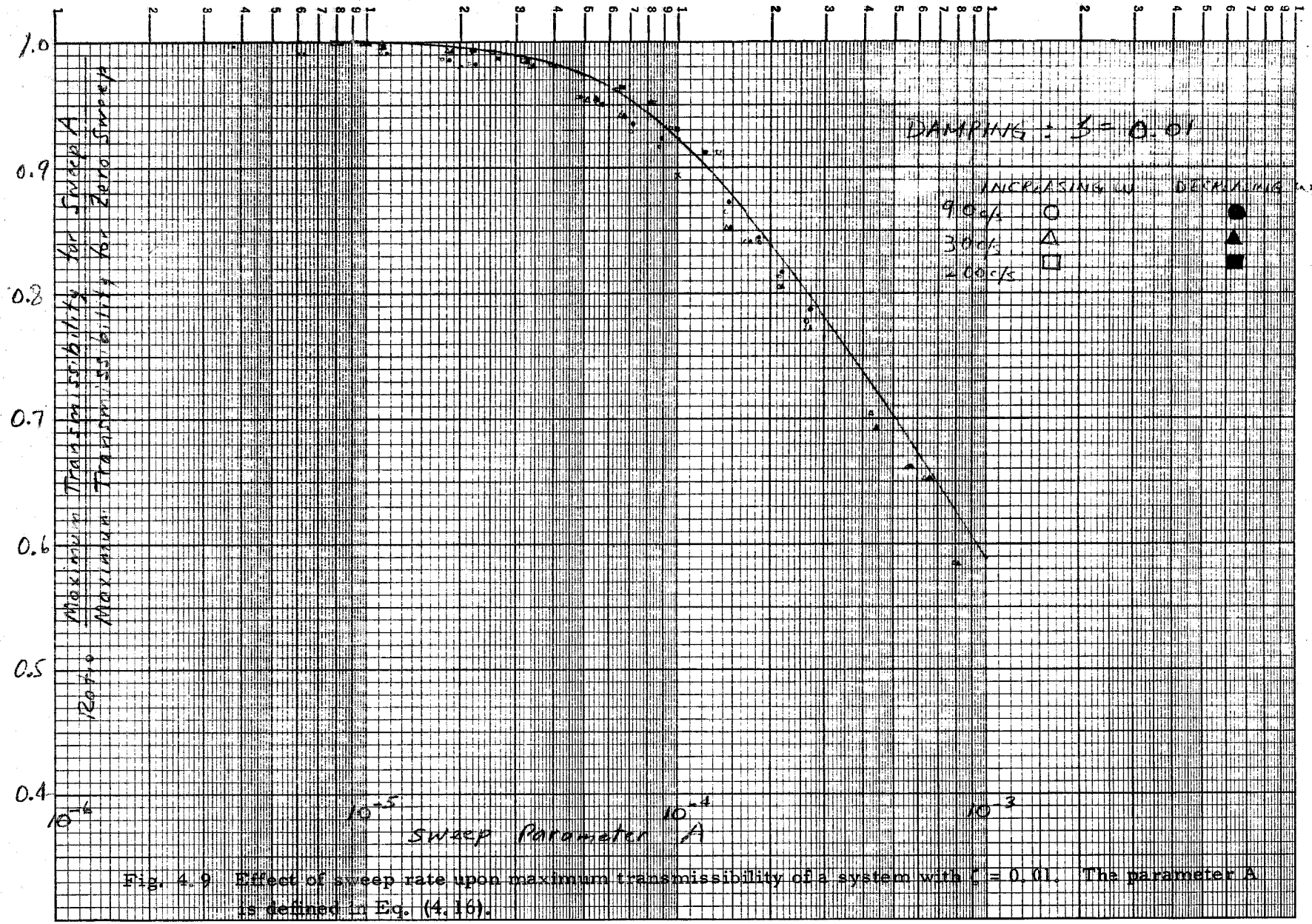

Fig. 4.9 Effect of sweep rate upon maximum transmissibility of a system with $\zeta = 0.01$. The parameter A is defined in Eq. (4.16).

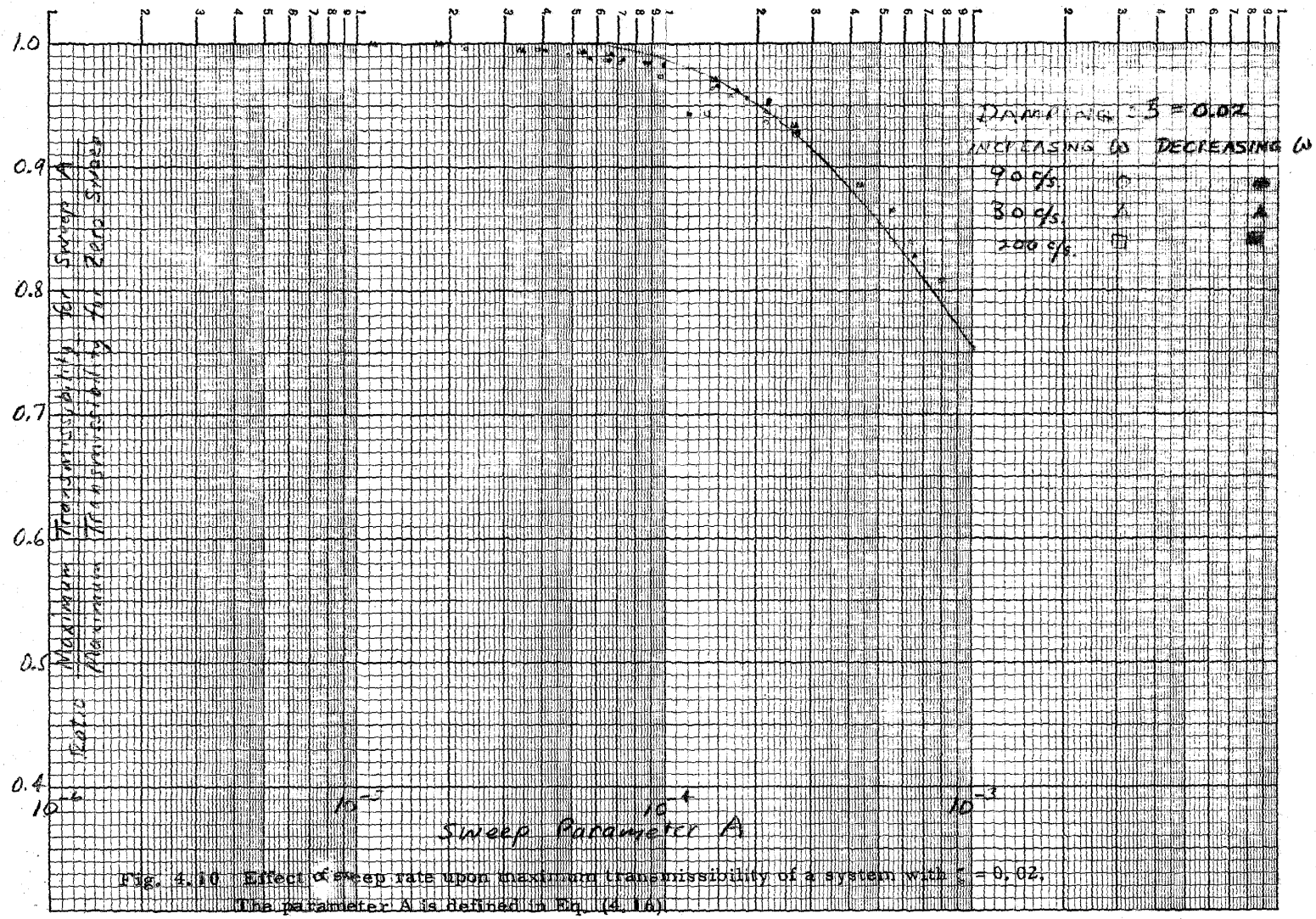

Fig. 4.10 Effect of sweep rate upon maximum transmissibility of a system with $\zeta = 0.02$. The parameter A is defined in Eq. (4.16)

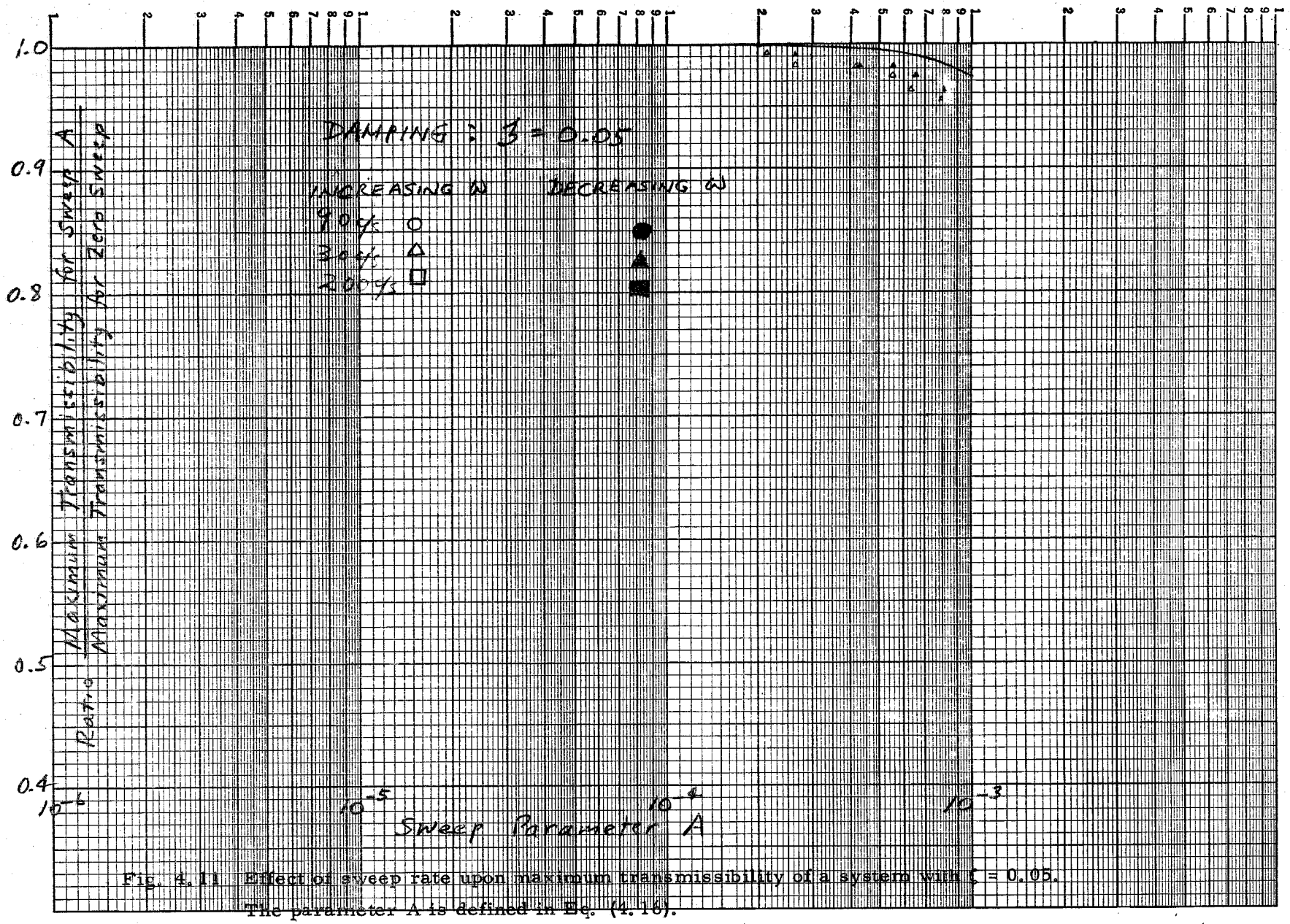

Fig. 4.11 Effect of sweep rate upon maximum transmissibility of a system with $\zeta = 0.05$. The parameter A is defined in Eq. (4.16).

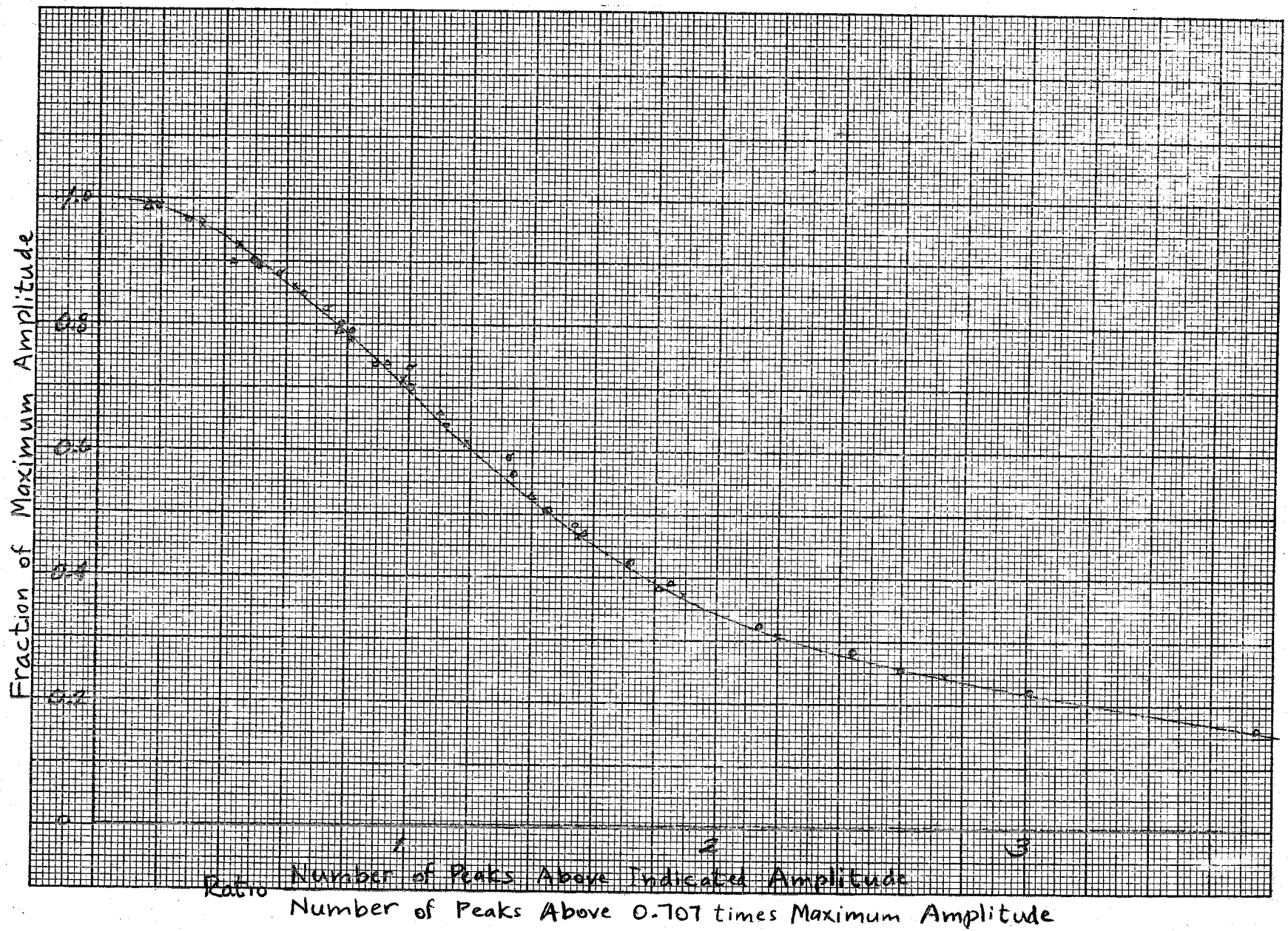

Fig. 4.12 Distribution of amplitudes in the response of a simple system to a variable frequency sinusoidal excitation. Maximum amplitude is given in Figs. 4.9 to 4.11

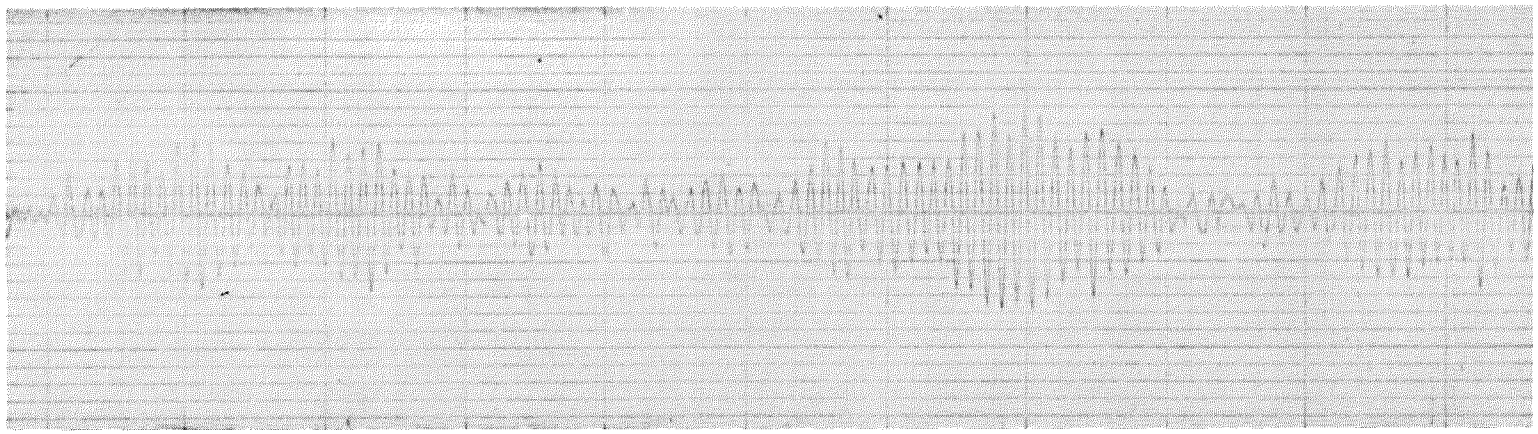

Fig. 4.13 Narrow band random vibration.

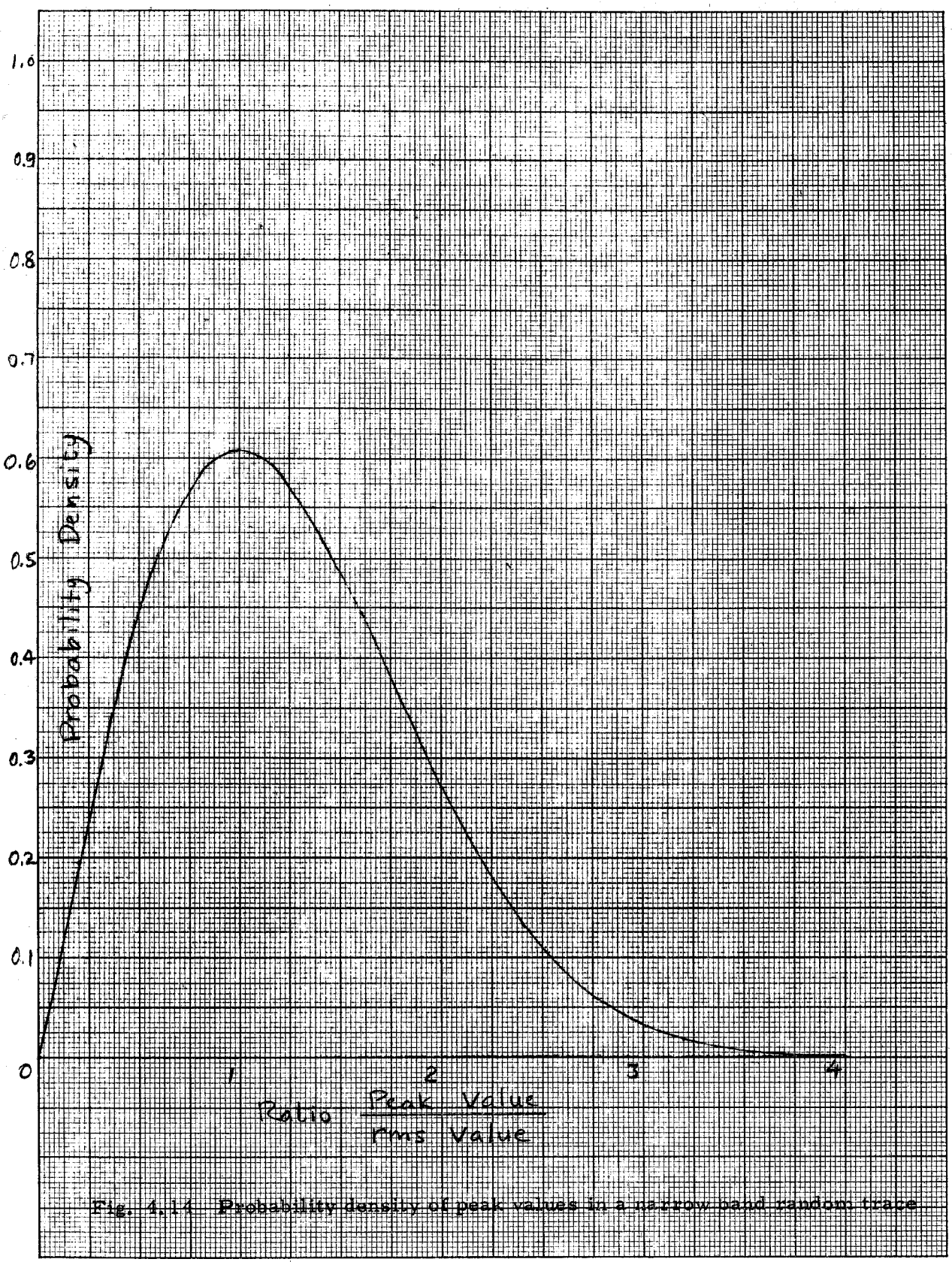

Fig. 4.14 Probability density of peak values in a narrow band random trace

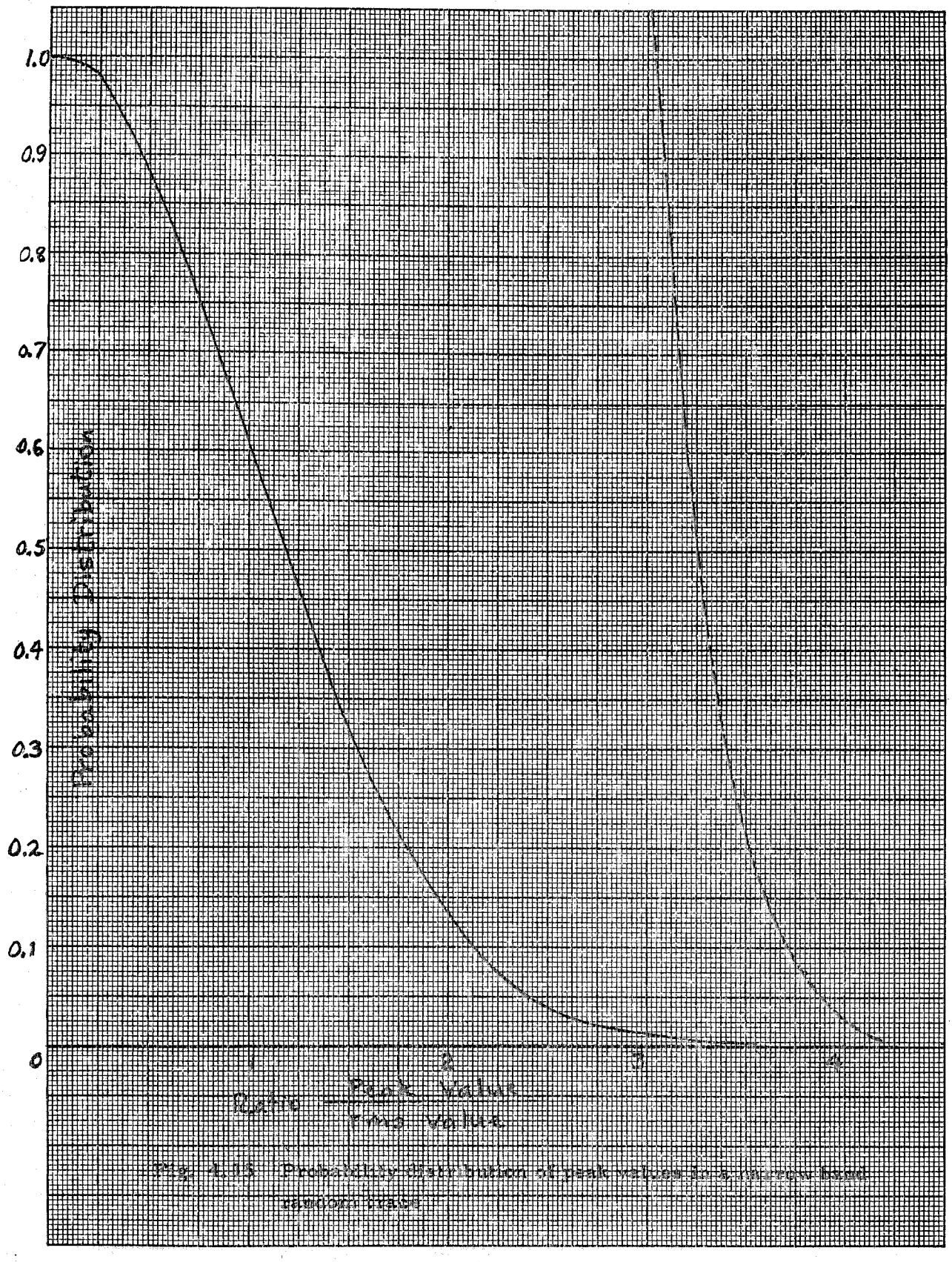

Fig. 4.13 Probability distribution of peak values in a narrow band random trace

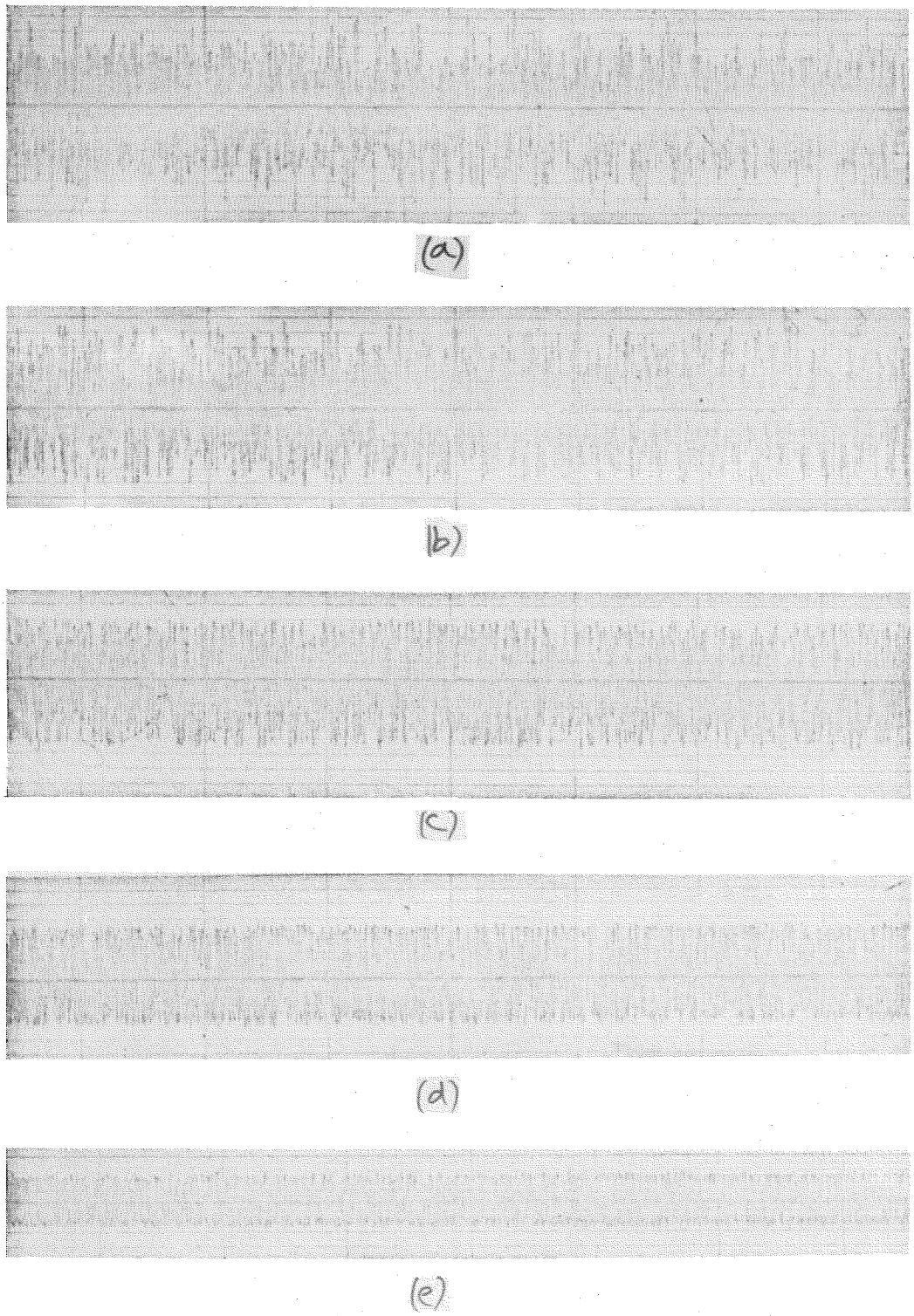

Fig. 4.16 Broad band random vibration with magnitude limited at different multiples of rms value: (a) unlimited; (b) 2.5 x rms value; (c) 2.0 x rms value; (d) 1.5 x rms value; (3) 1.0 x rms value.

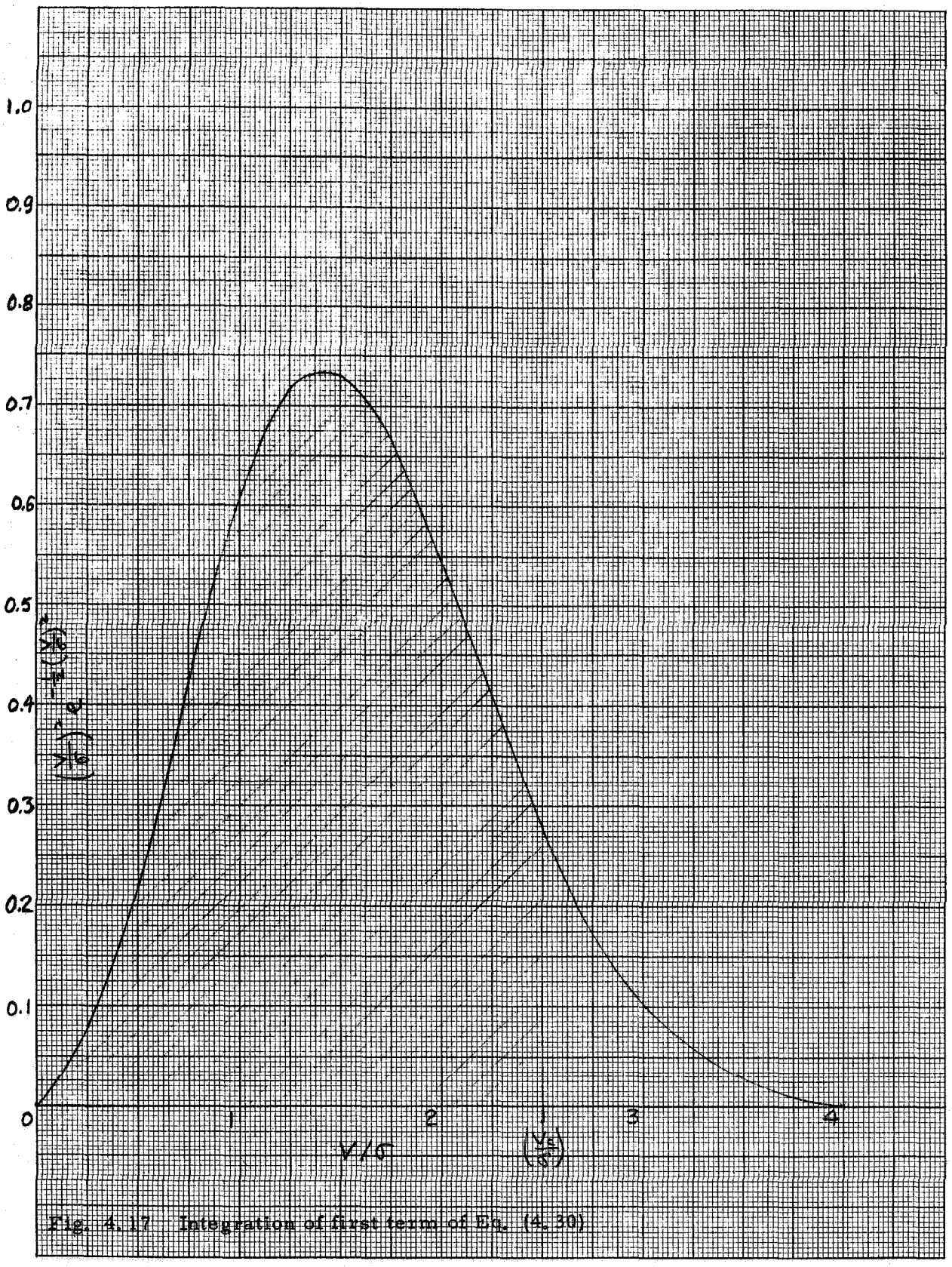

Fig. 4.17 Integration of first term of Eq. (4.30)

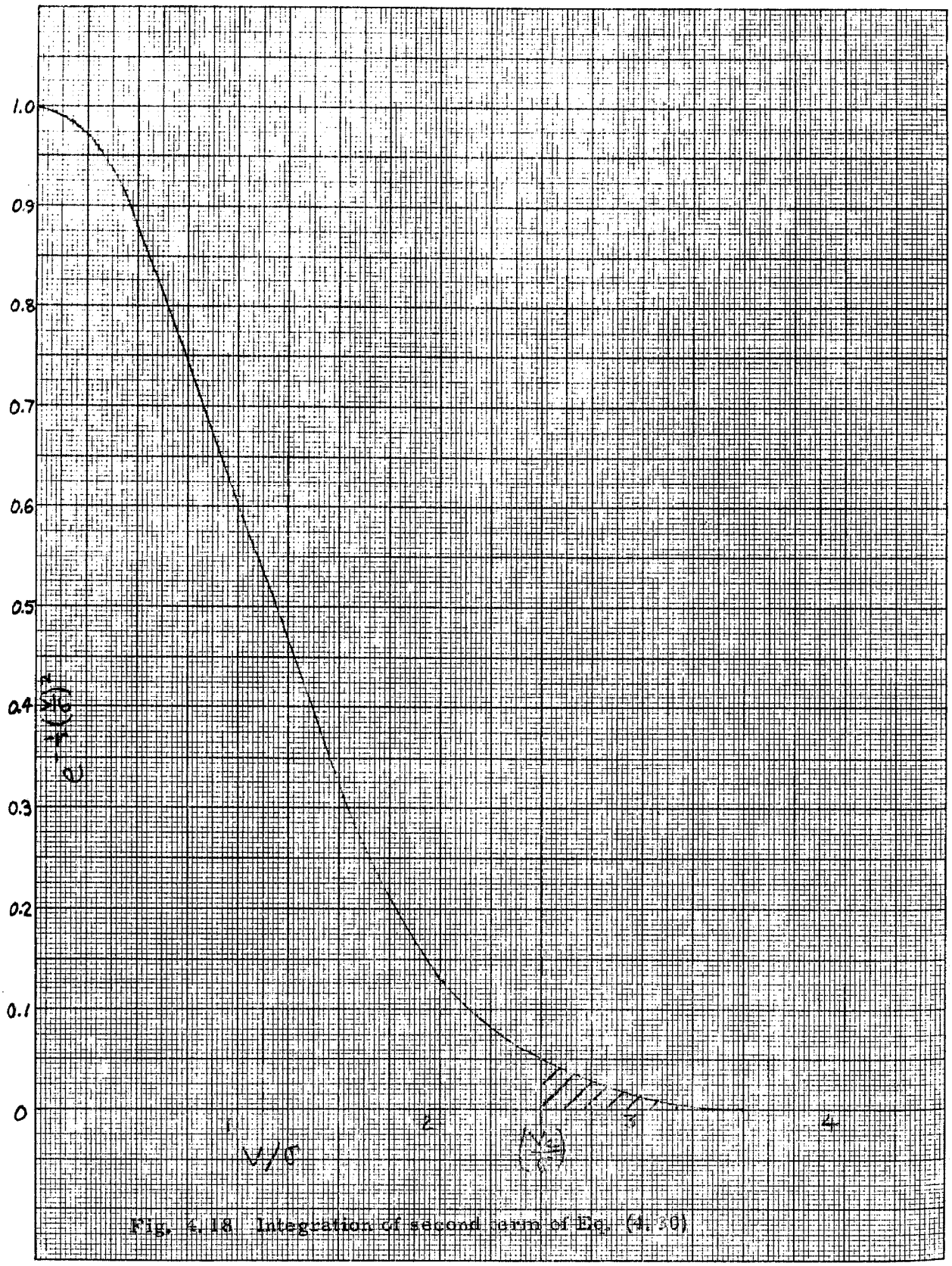

Fig. 4.18 Integration of second term of Eq. (4.30)

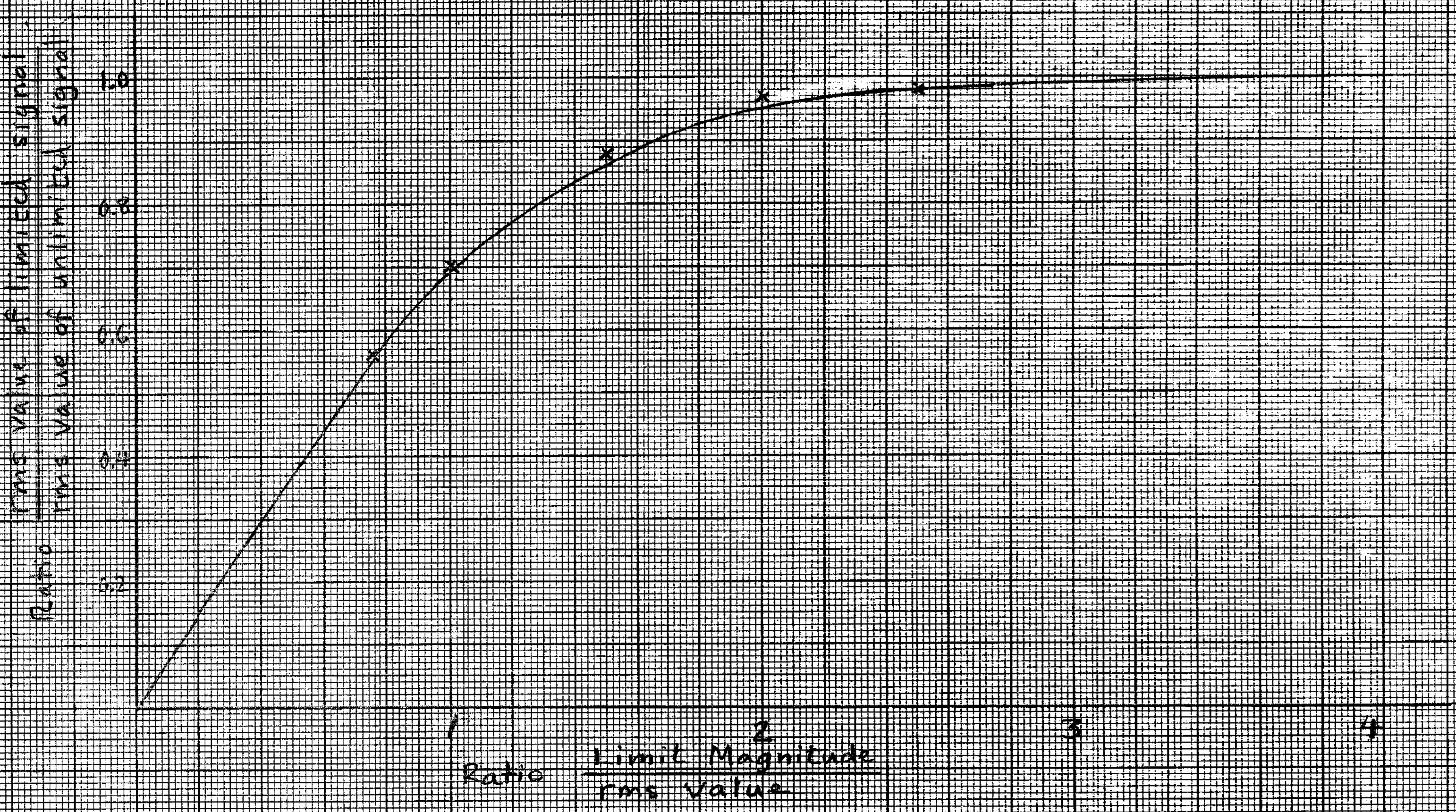

Fig. 4.19 (a) The rms level of magnitude-limited broad band random vibration, calculated from Eq. (4.30). Plotted points are analog computer results.

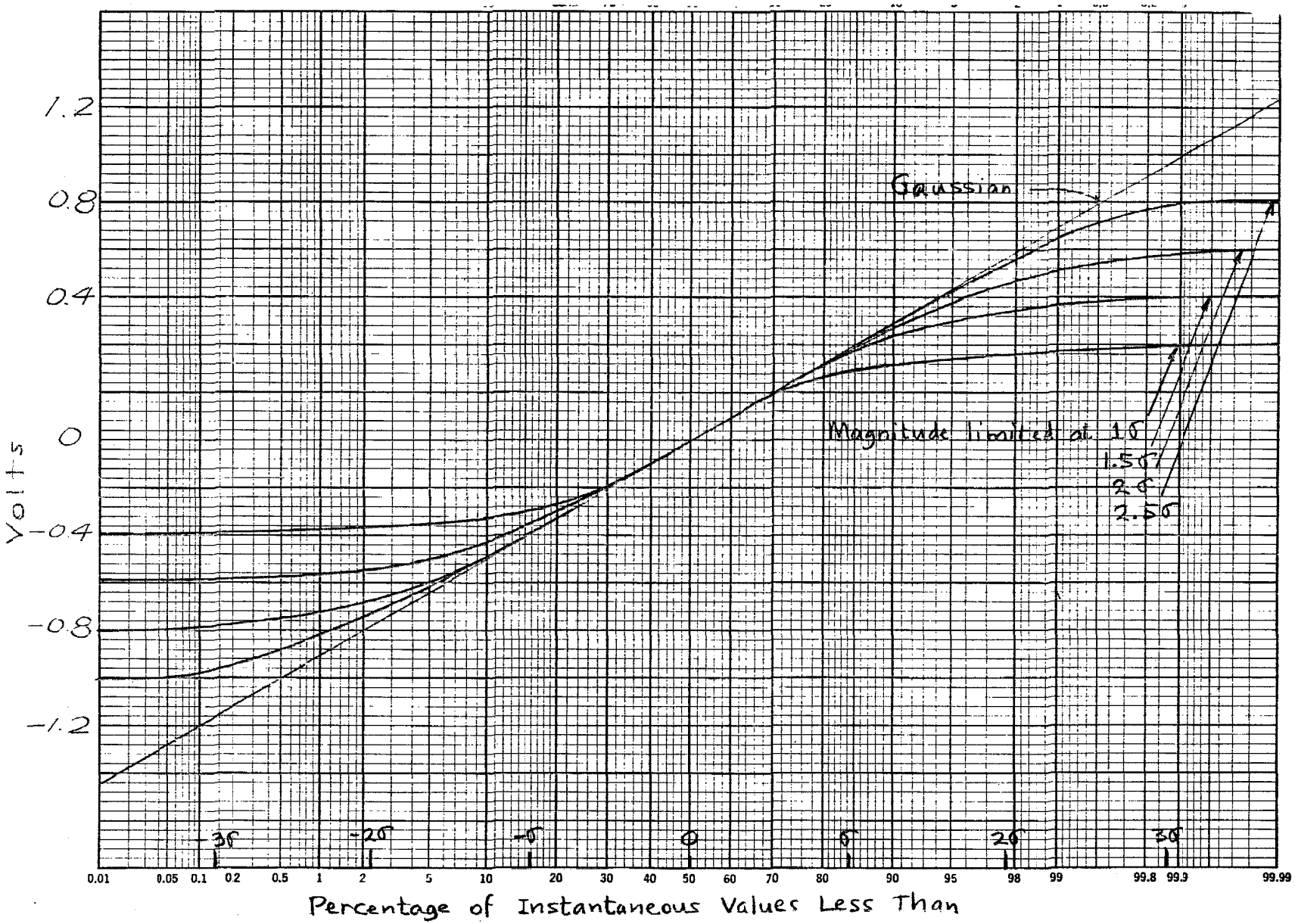

Fig. 4.19 (b) Probability distribution of magnitude-limited broad band random vibration. Reference is 0.4 volts rms for the unlimited signal.

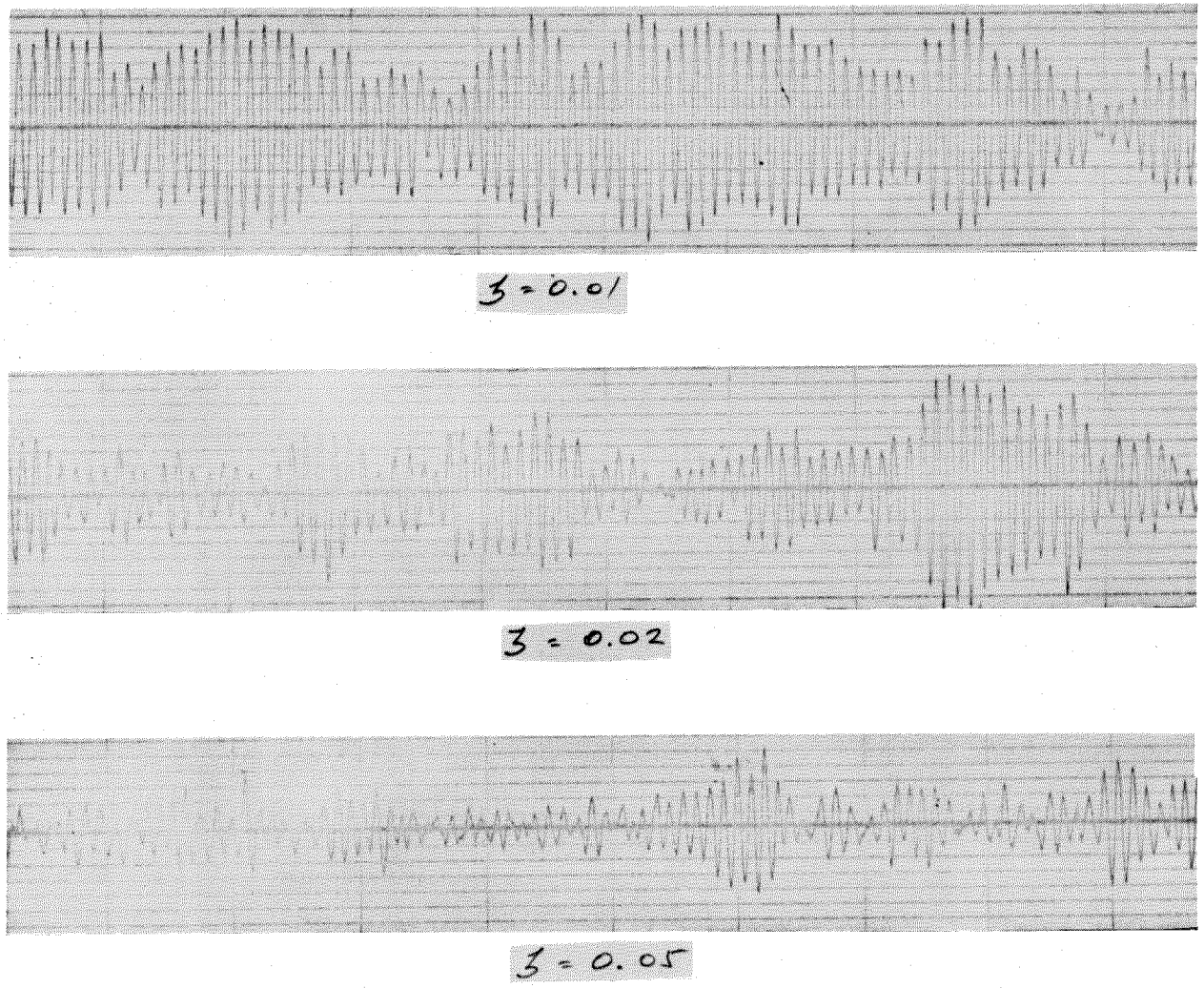

Fig. 4.20 Time-history of response of simple systems to Gaussian random vibration. Fraction of critical damping is indicated by ζ.

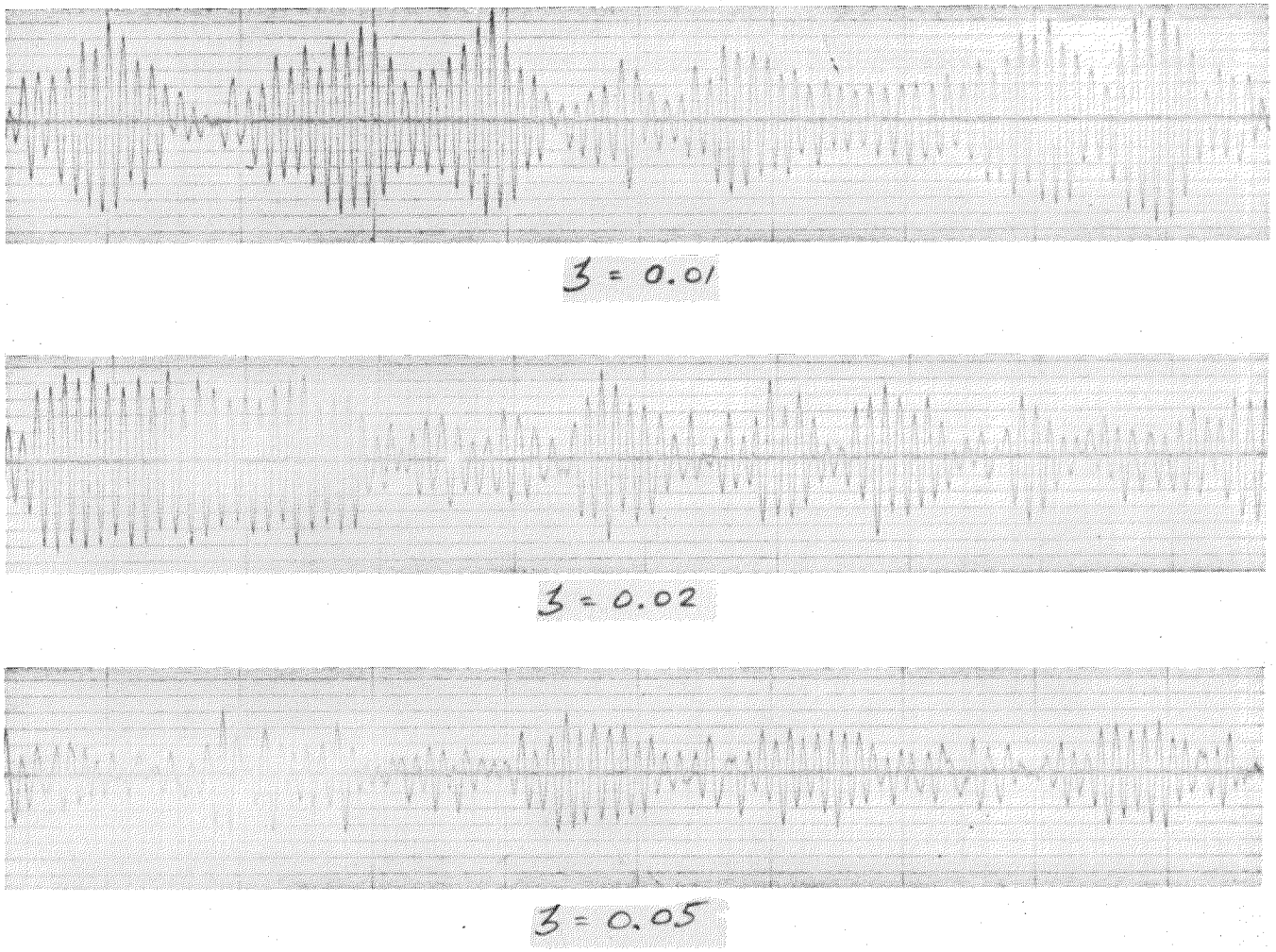

Fig. 4.21 Time-history of response of simple systems to broad band random excitation with magnitude of excitation limited at 2.5 times rms value. Fraction of critical damping is indicated by ζ.

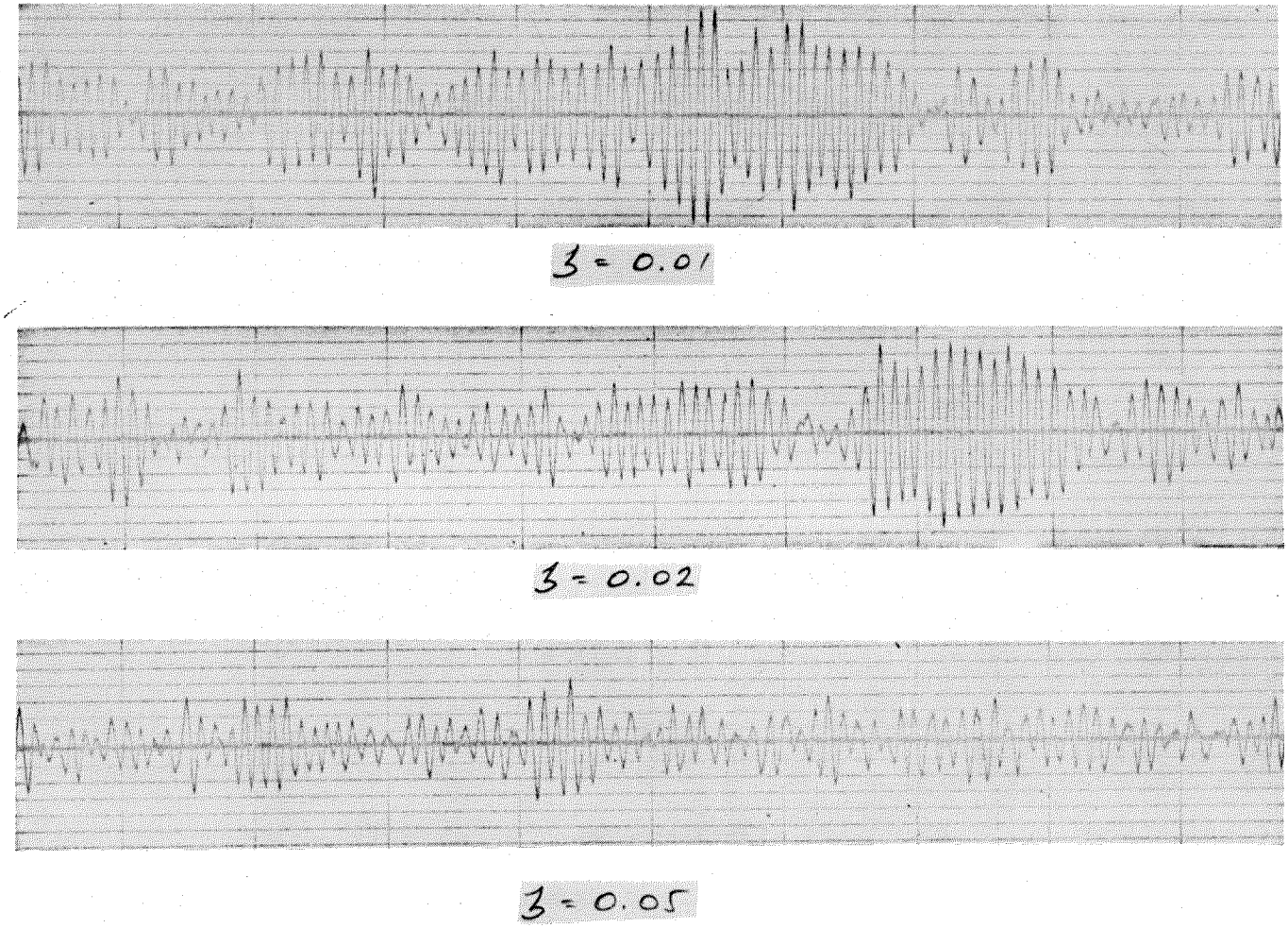

Fig. 4.22 Time-history of response of simple systems to broad band random excitation with magnitude of excitation limited at 2.0 times the rms value. Fraction of critical damping is indicated by ζ.

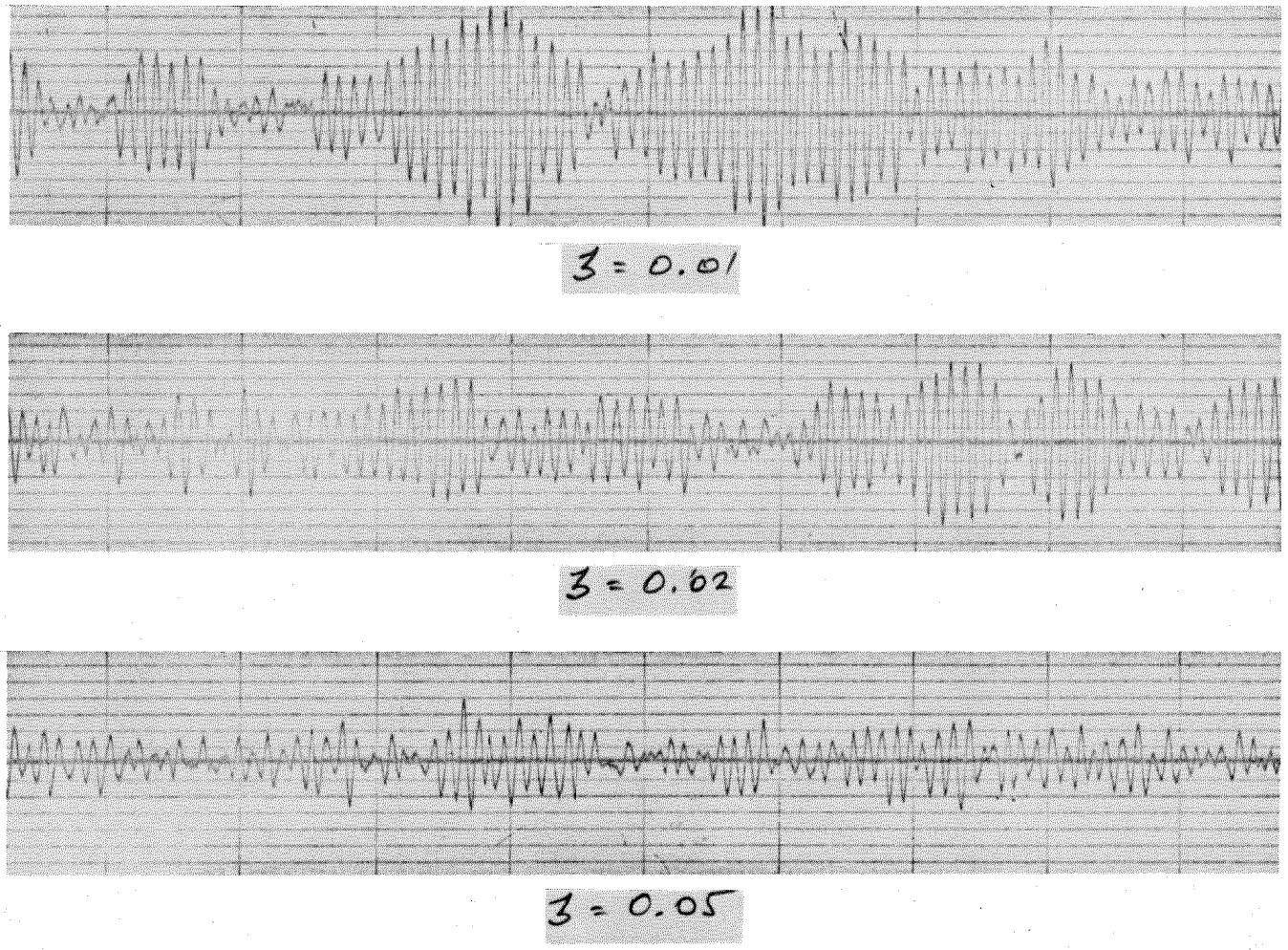

Fig. 4.23 Time-history of response of simple systems to broad band random excitation with magnitude of excitation limited at 1.5 times the rms value. Fraction of critical damping is indicated by ζ.

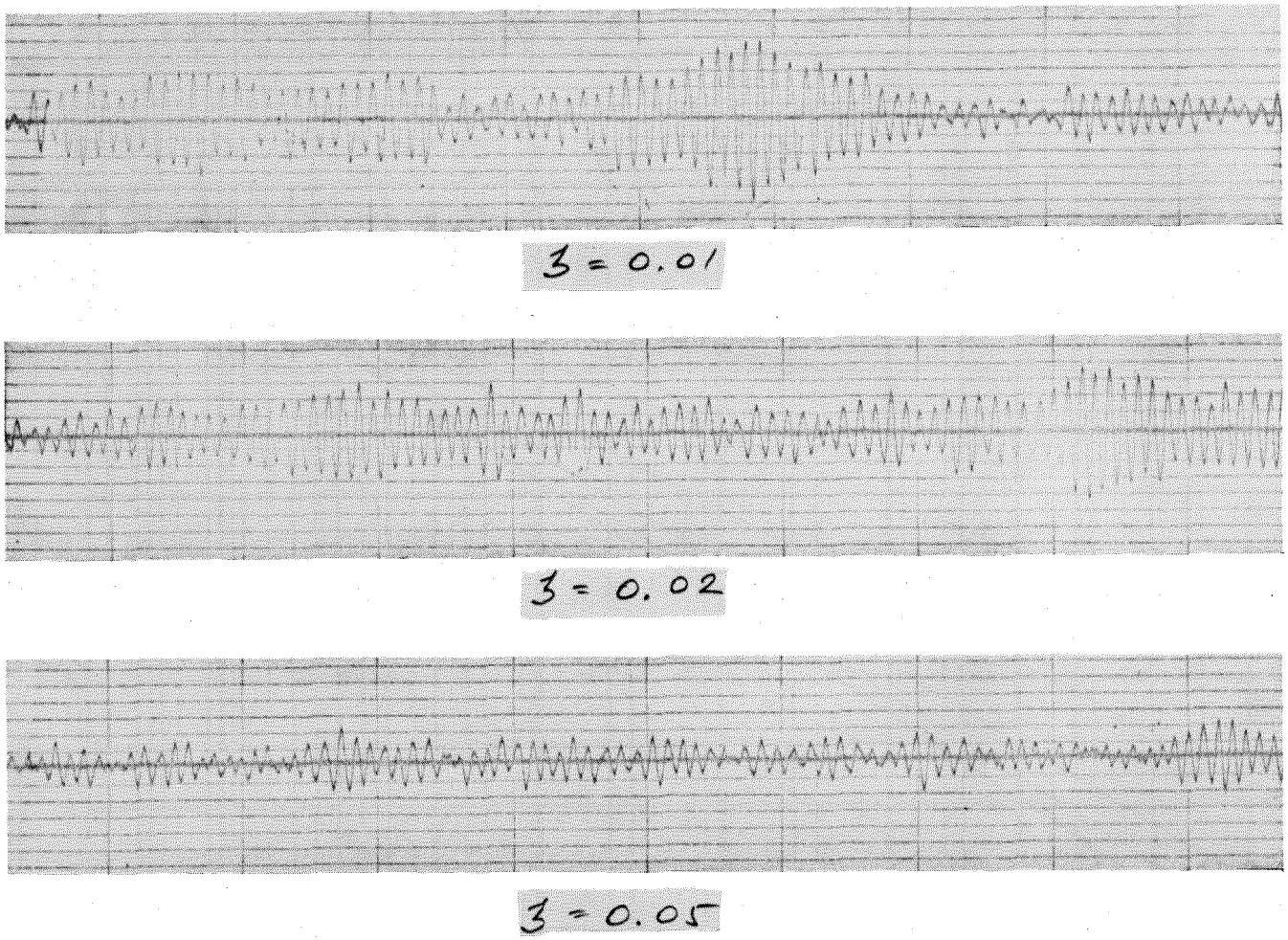

Fig. 4.24 Time-history of response of simple systems to broad band random excitation with magnitude of excitation limited at 1.0 times the rms value. Fraction of critical damping is indicated by ζ.

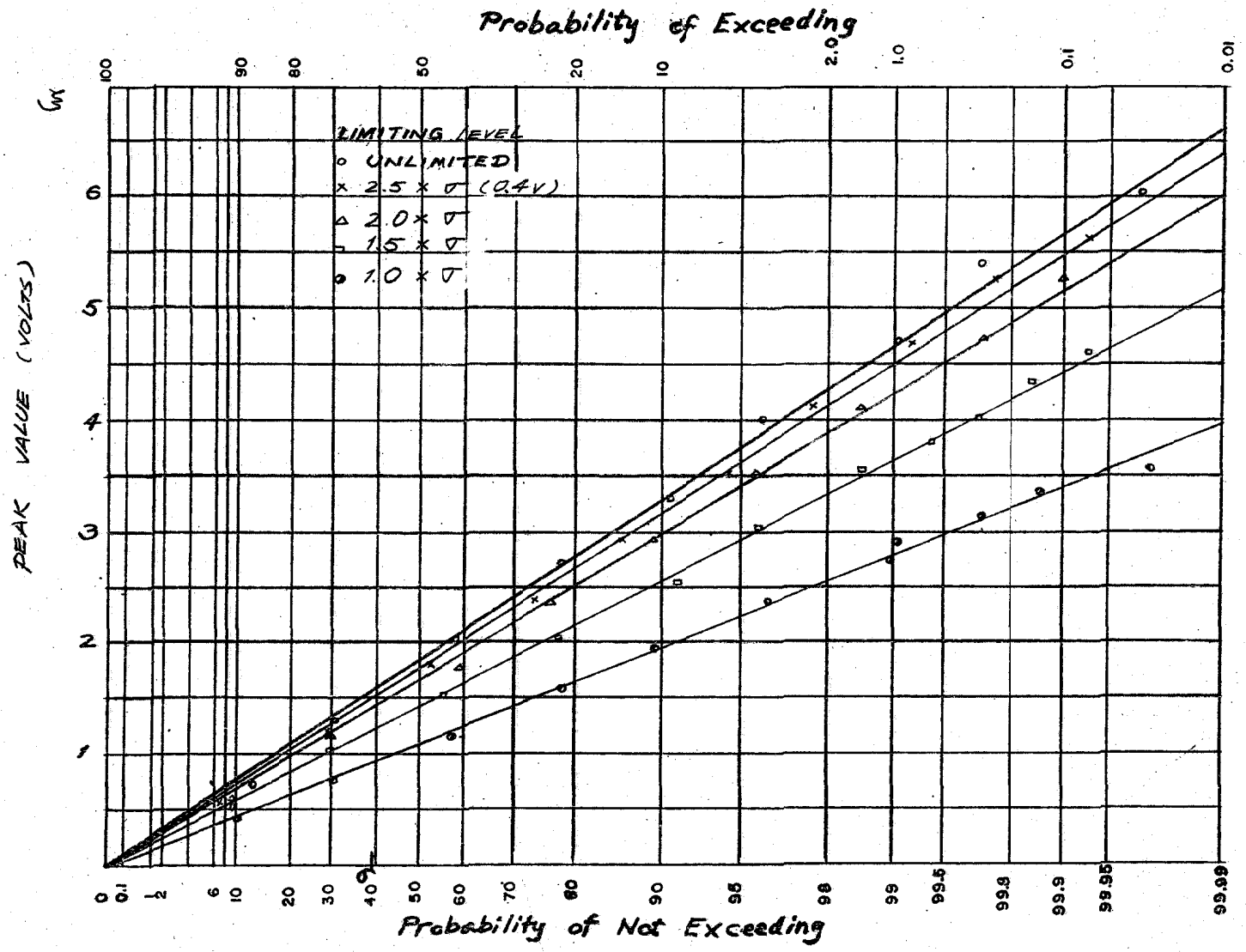

Fig. 4.25 Probability distribution of peak values in response of a system to broad band random vibration with magnitudes limited at values indicated in legend. Fraction of critical damping is $\zeta = 0.01$. Reference is 0.4 volts rms before magnitude limiting.

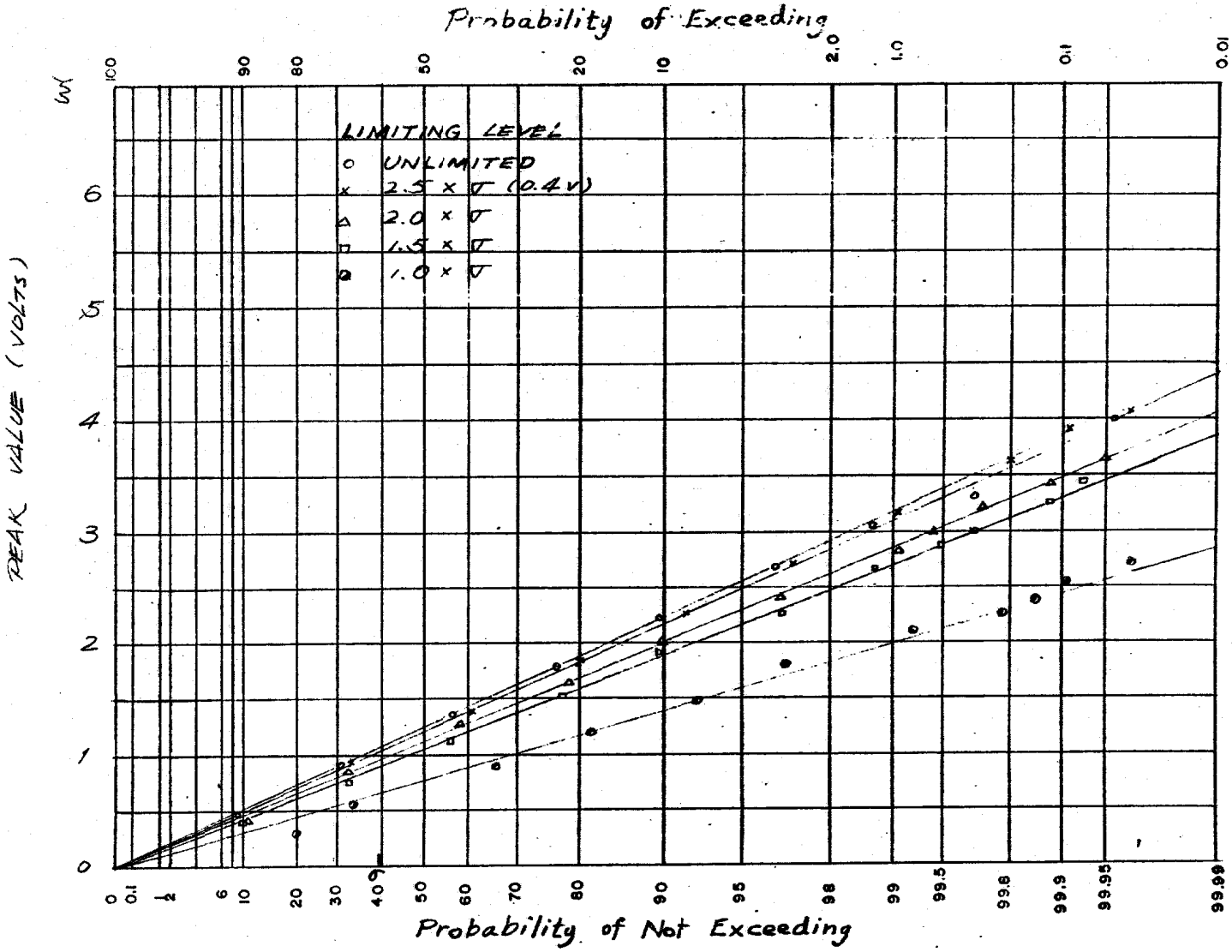

Fig. 4.26 Probability distribution of peak values in response of a system to broad band random vibration with magnitudes limited at values indicated in legend. Fraction of critical damping is $\zeta = 0.02$. Reference is 0.4 volts rms before magnitude limiting.

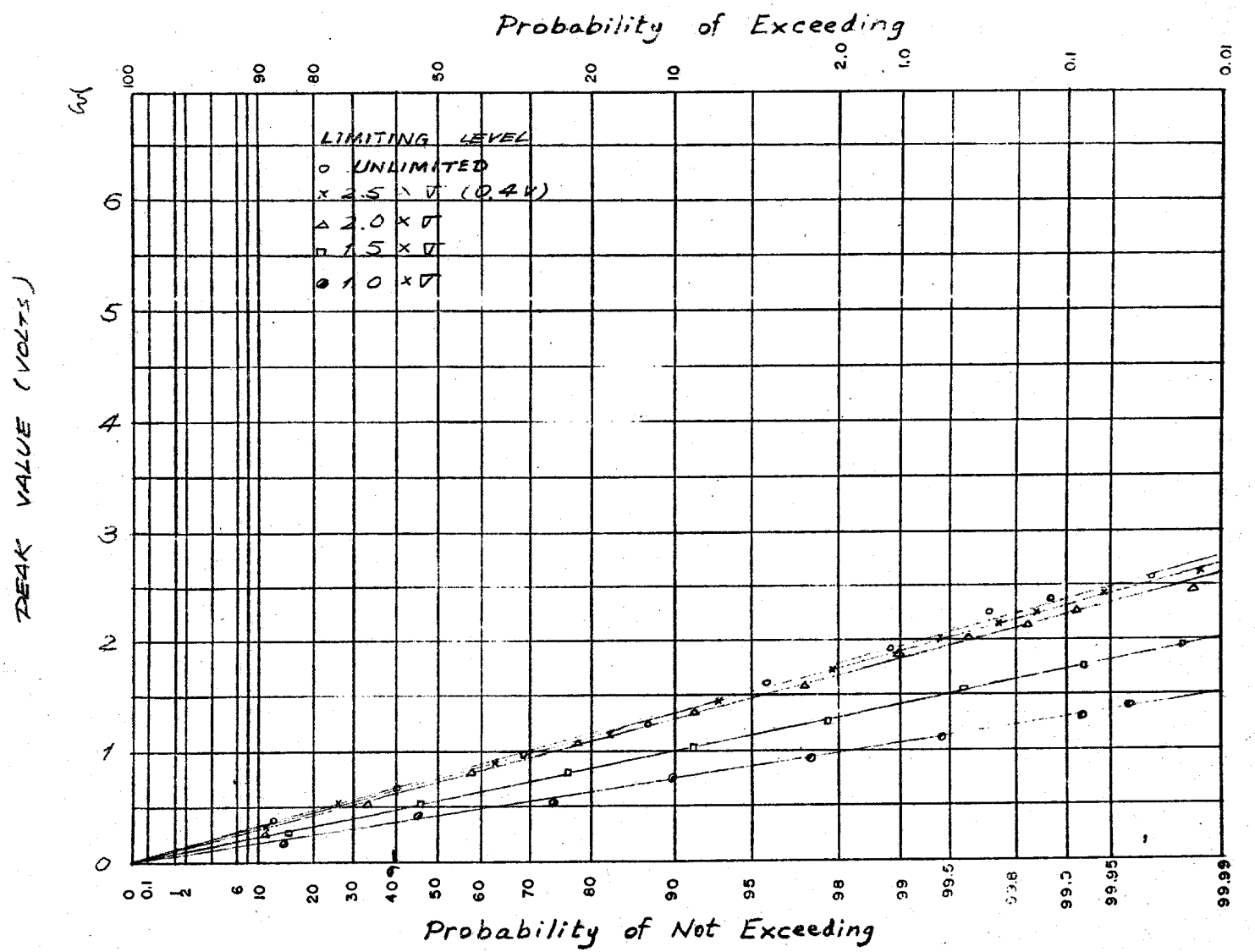

Fig. 4.27 Probability distribution of peak values in response of a system to broad band random vibration with magnitudes limited at values indicated in legend. Fraction of critical damping is $\zeta = 0.05$. Reference is 0.4 volts rms before magnitude limiting.

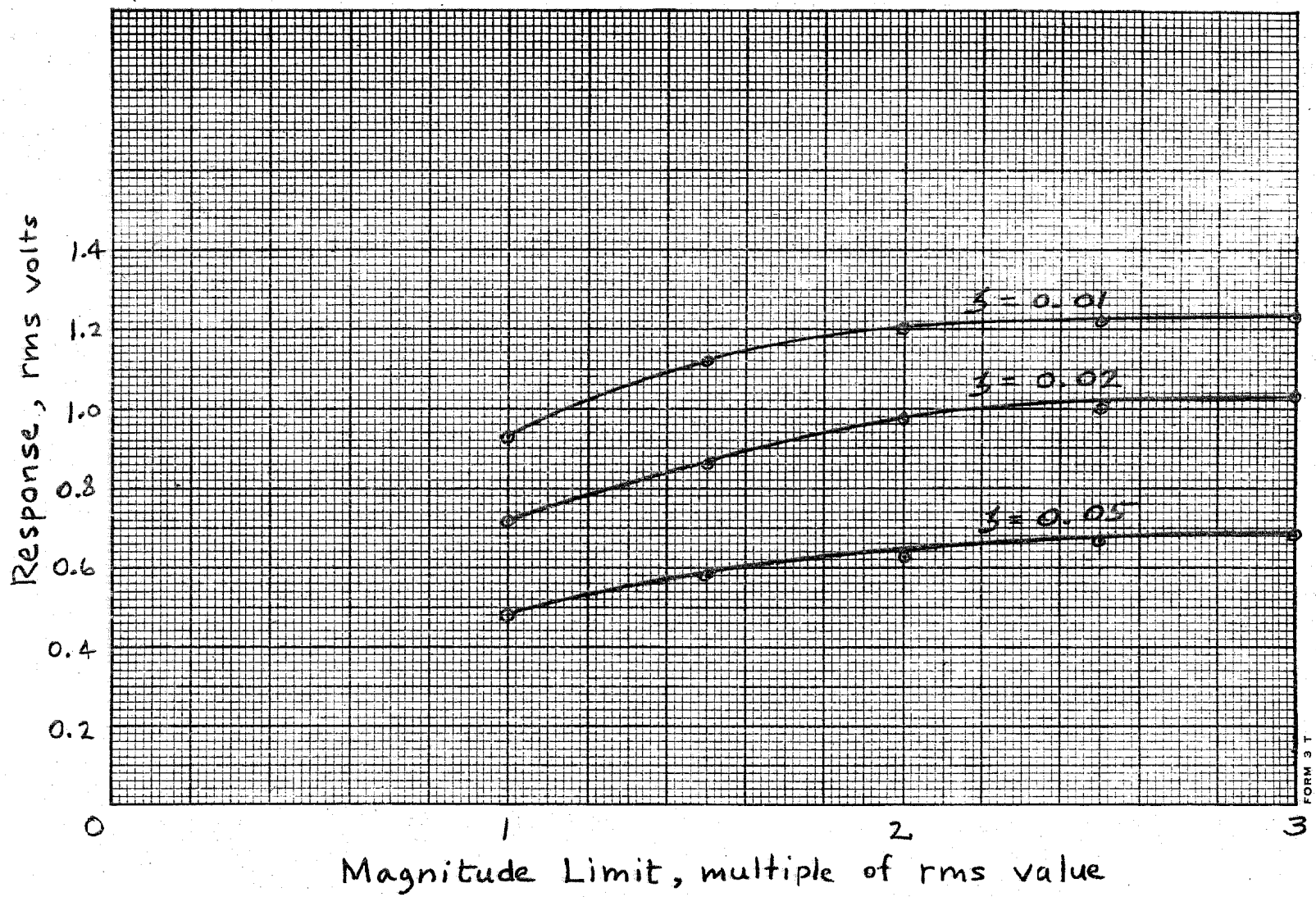

Fig. 4.28 Response in rms volts of a single degree of freedom system, with damping as noted, to broad band random excitation with magnitude limited (abscissa scale). Response is in volts; excitation is 0.4 volts for unlimited signal.

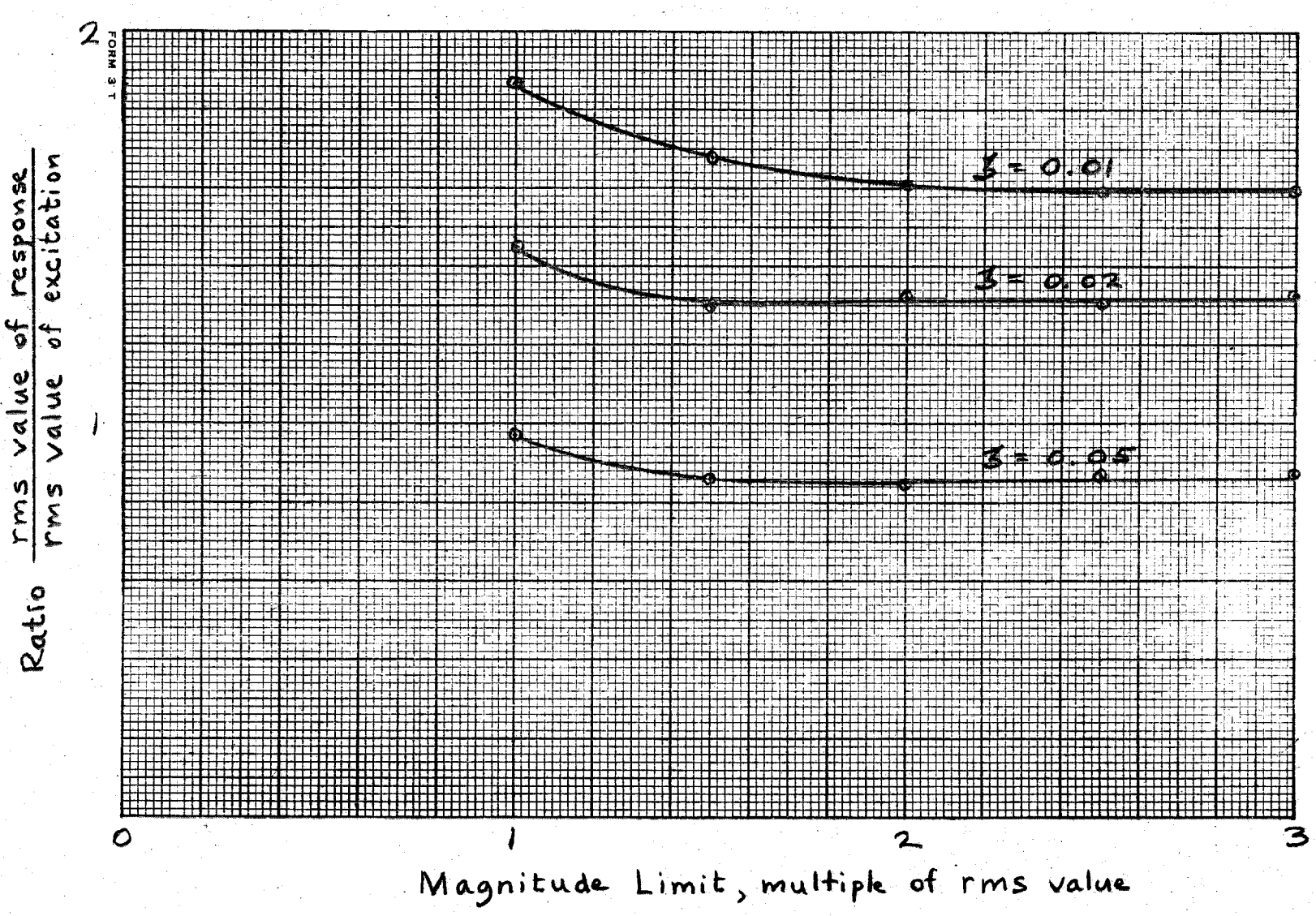

Fig. 4.29 **Transmissibility of a single degree of freedom system to broad band random excitation with magnitude limited.**

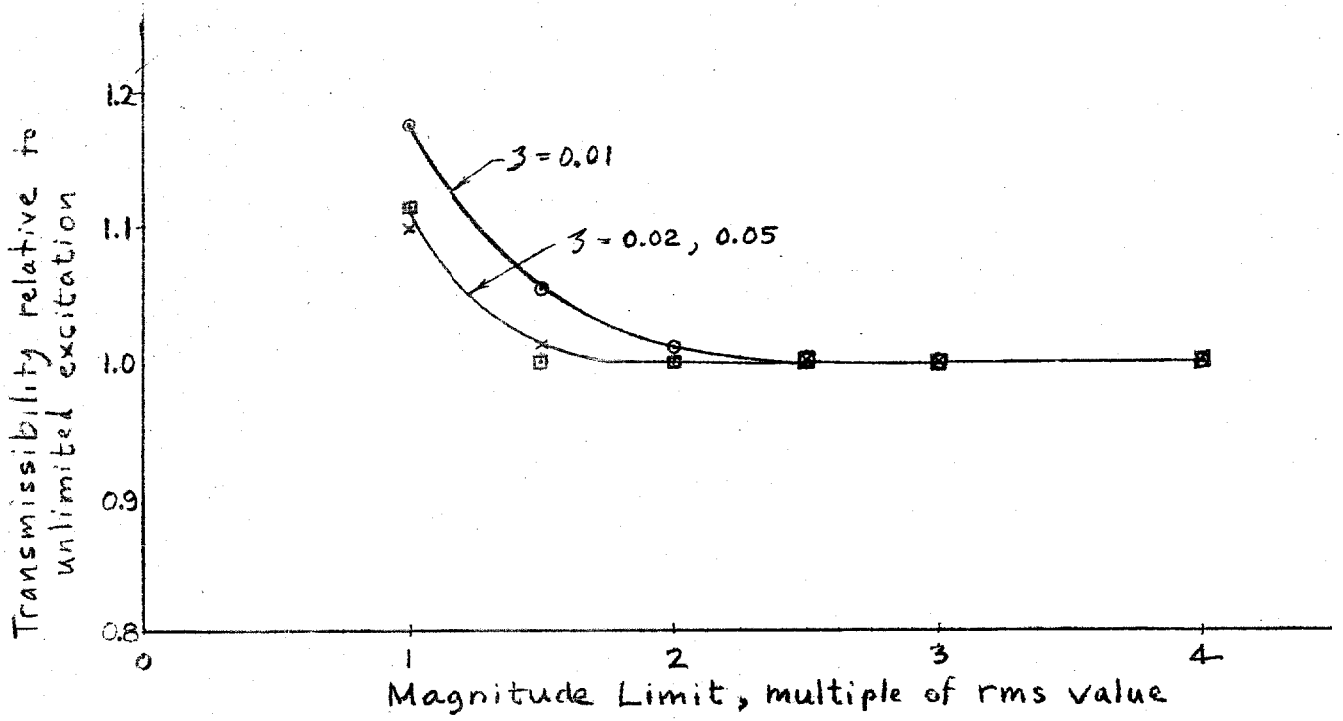

Fig. 4.30 Transmissibility with magnitude limited broad band random excitation, normalized to transmissibility with no limit on magnitude of excitation.

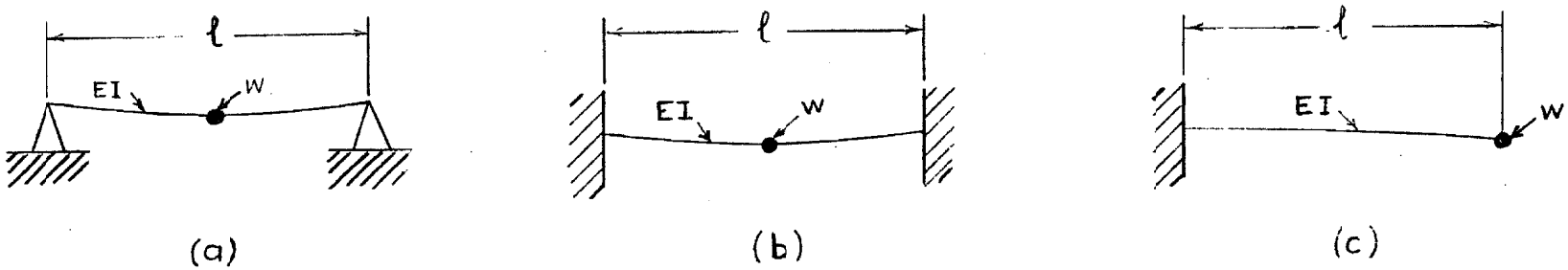

Fig. 5.1 Schematic diagrams of typical beam types

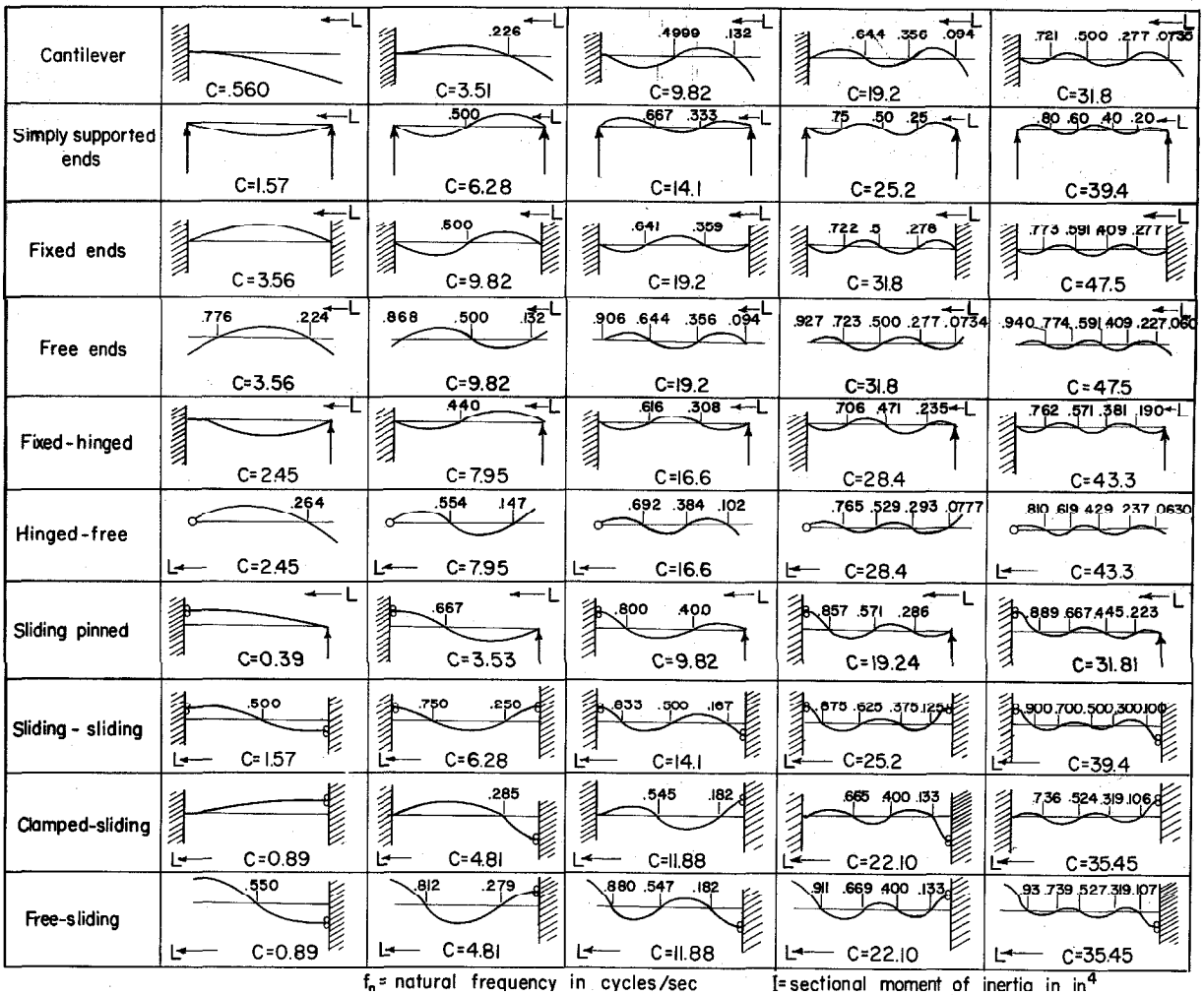

f_n = natural frequency in cycles/sec
C = constant from above table
g = 386 in./sec^2
E = modulus of elasticity in lb/in.^{2}
I = sectional moment of inertia in in^4
ω = weight of unit length beam in lb/in.
L = beam length in inches

Fig. 5.2 Natural Frequencies and Mode Shapes of Common Uniform Beams.

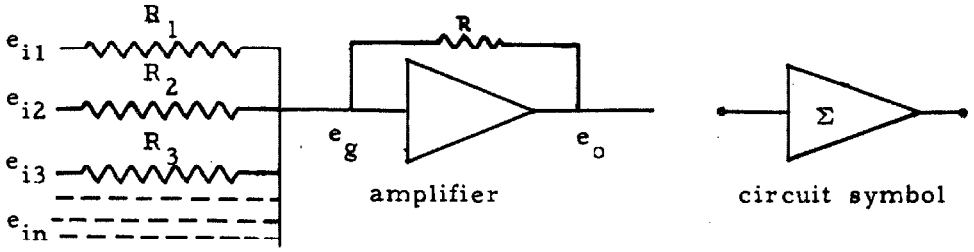

Fig. A-1 Schematic diagram of summing amplifier

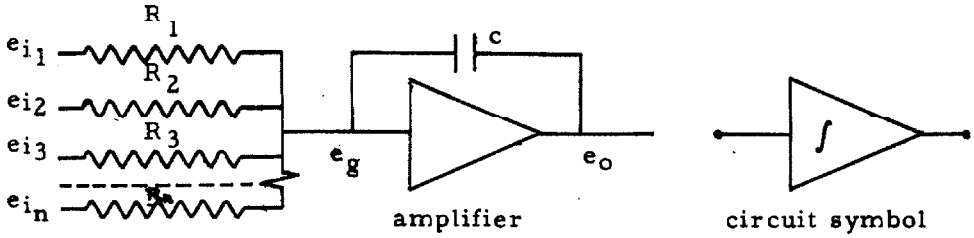

Fig. A-2 Schematic diagram of integrating amplifier

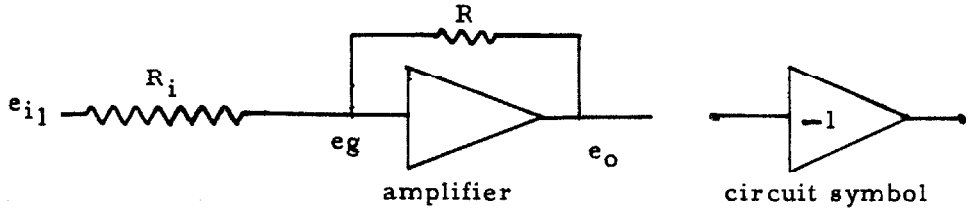

Fig. A-3 Schematic diagram of inverting amplifier

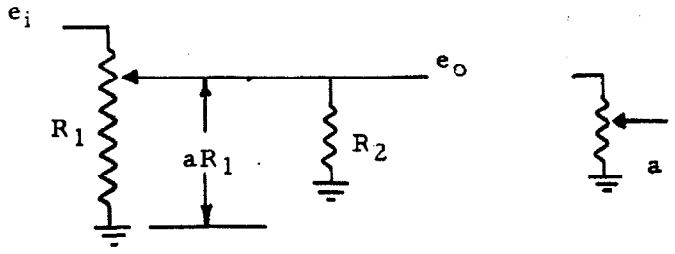

Fig. A-4 Schematic diagram of potentiometer

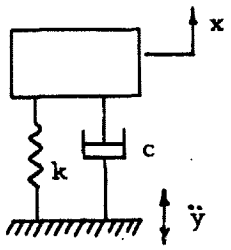

Fig. A-5 Schematic diagram of single degree of freedom system

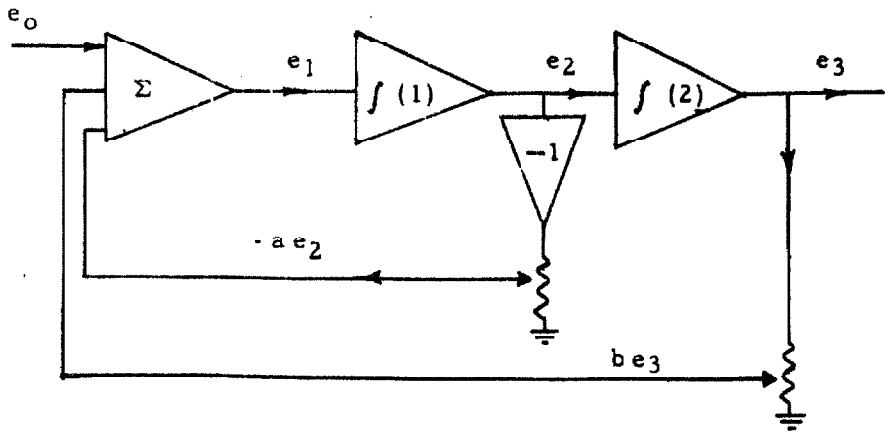

Fig. A-6 Analog circuit for mechanical system shown in Fig. A-5

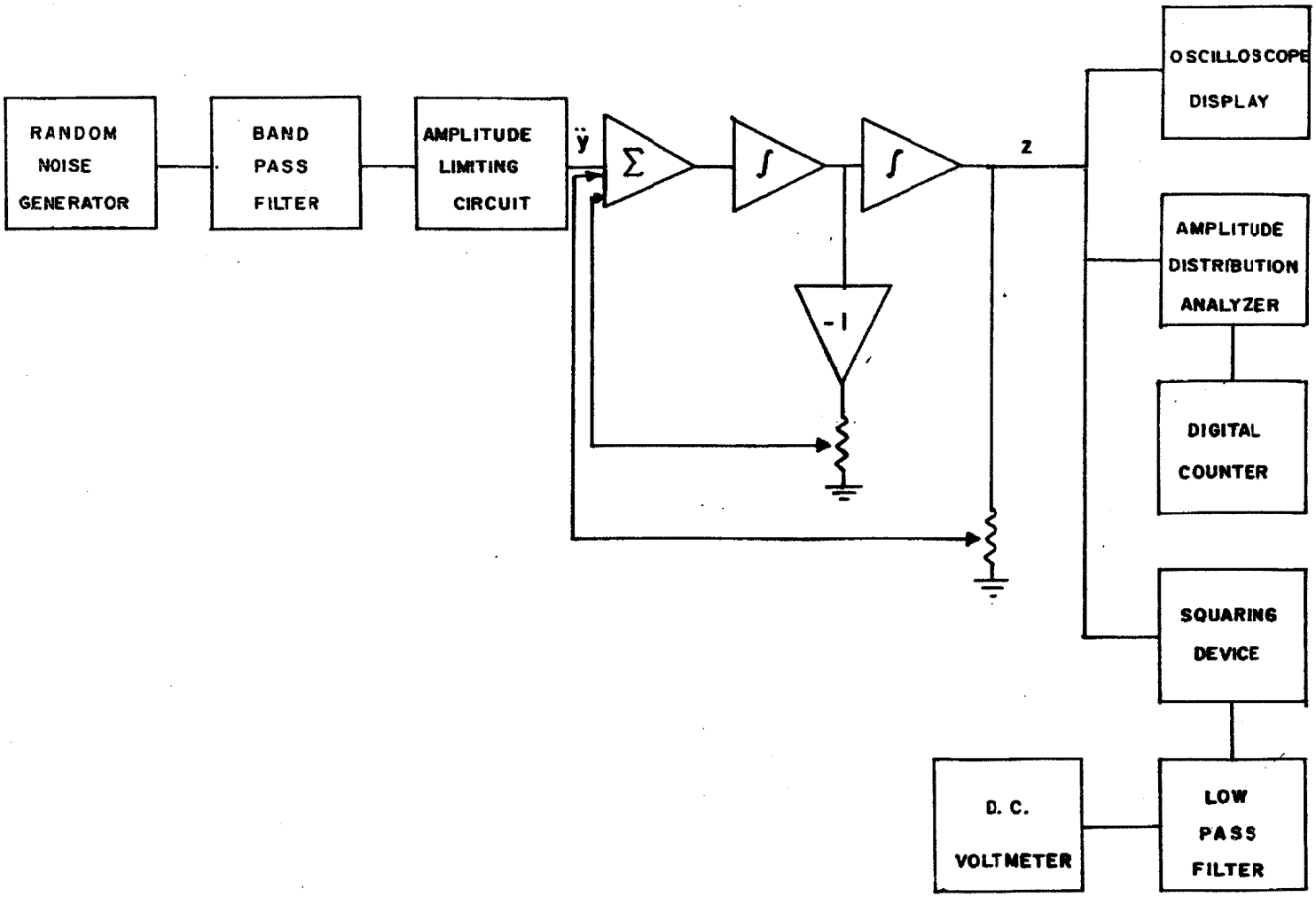

Fig. A-7 Block diagram of analog system

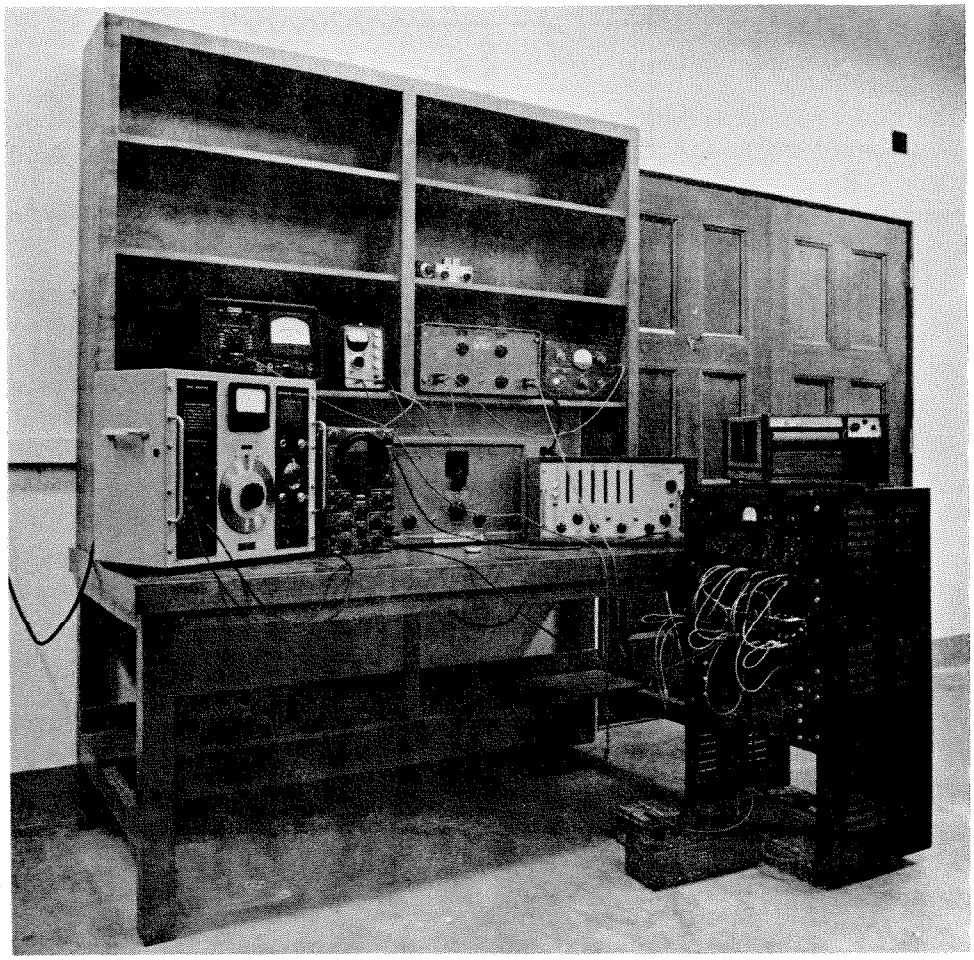

Fig. A-8 Analog computer.

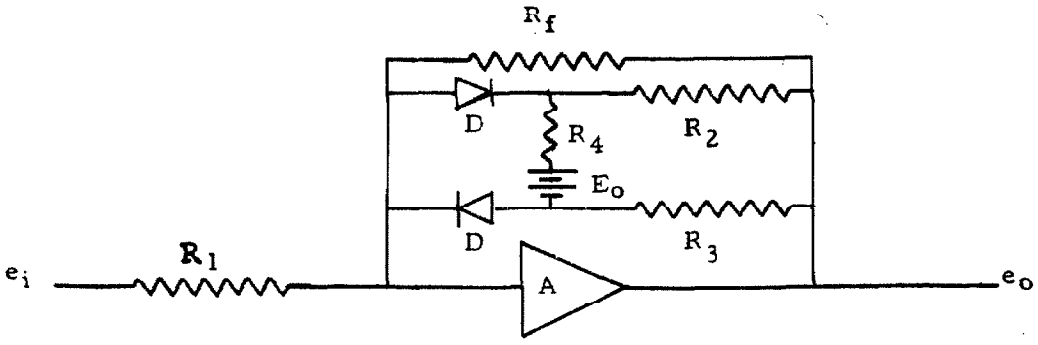

Fig. A-9 Amplitude limiting circuit

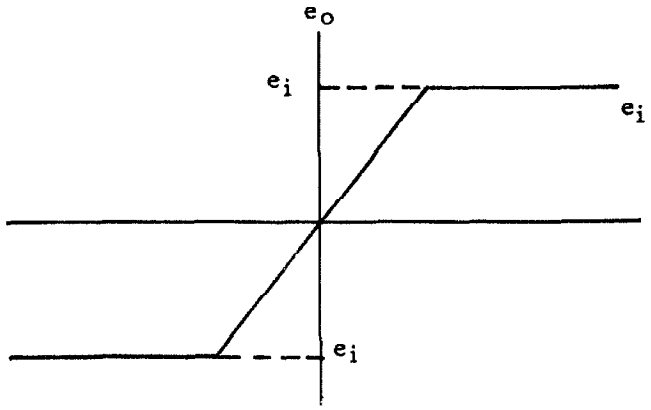

Fig. A-10 Output voltage e_o as a function of input voltage for the limiting circuit

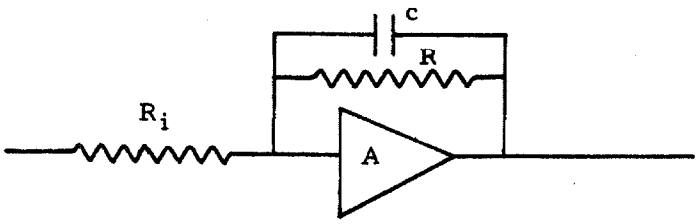

Fig. A-11 Low pass filter

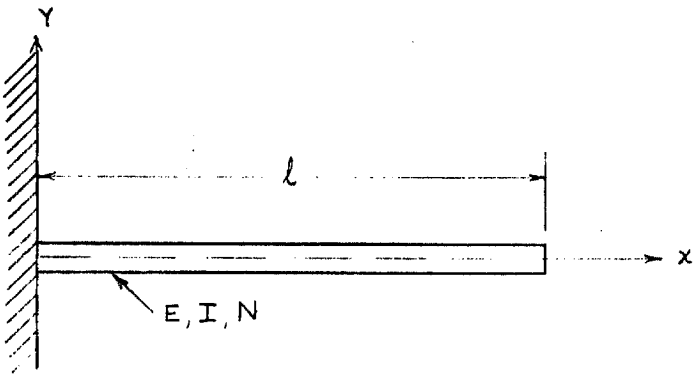

Fig. B-1 Cantilever (fixed-free) beam of uniform section

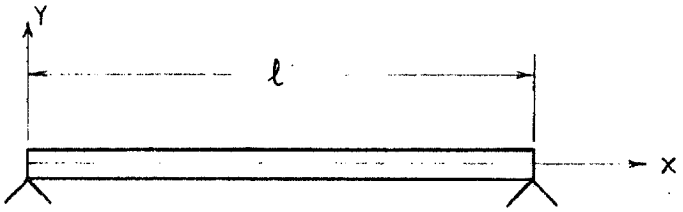

Fig. B-2 Simply supported (hinged-hinged) beam of uniform section

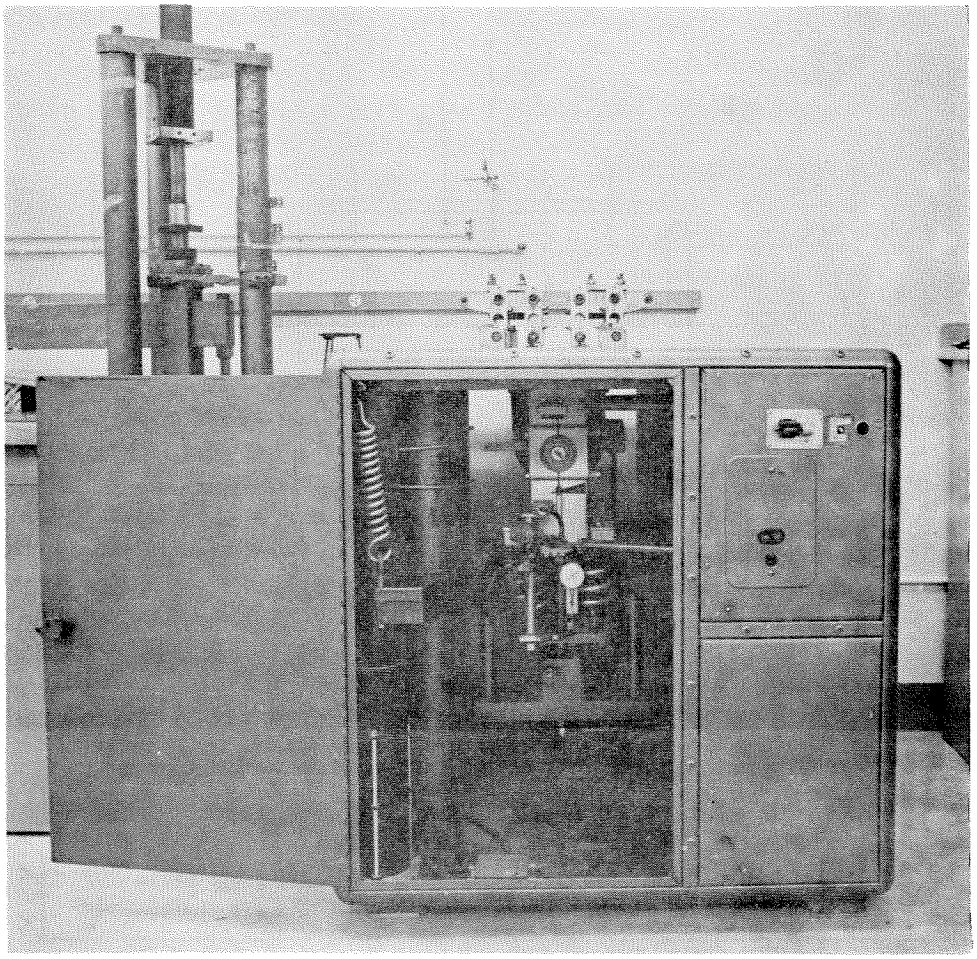

Fig. C-1 Photograph of Baldwin Universal Fatigue Testing Machine.

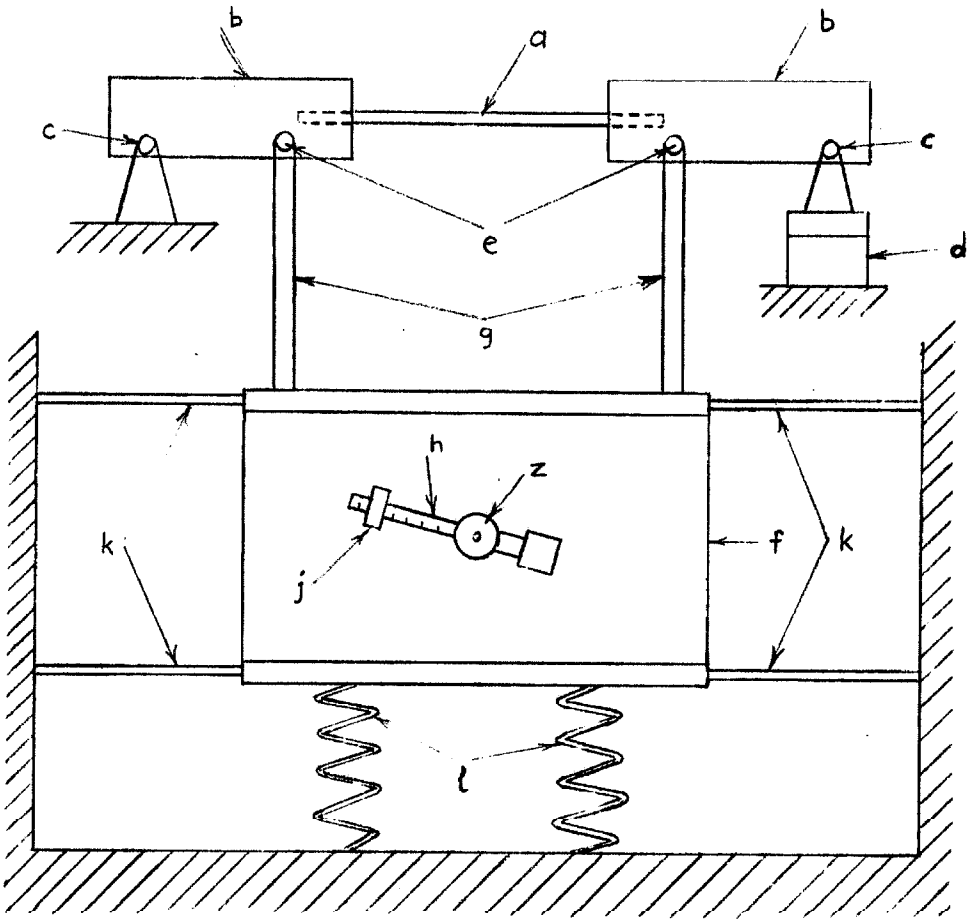

Fig. C-2 Schematic diagram of Baldwin Universal Fatigue Testing Machine

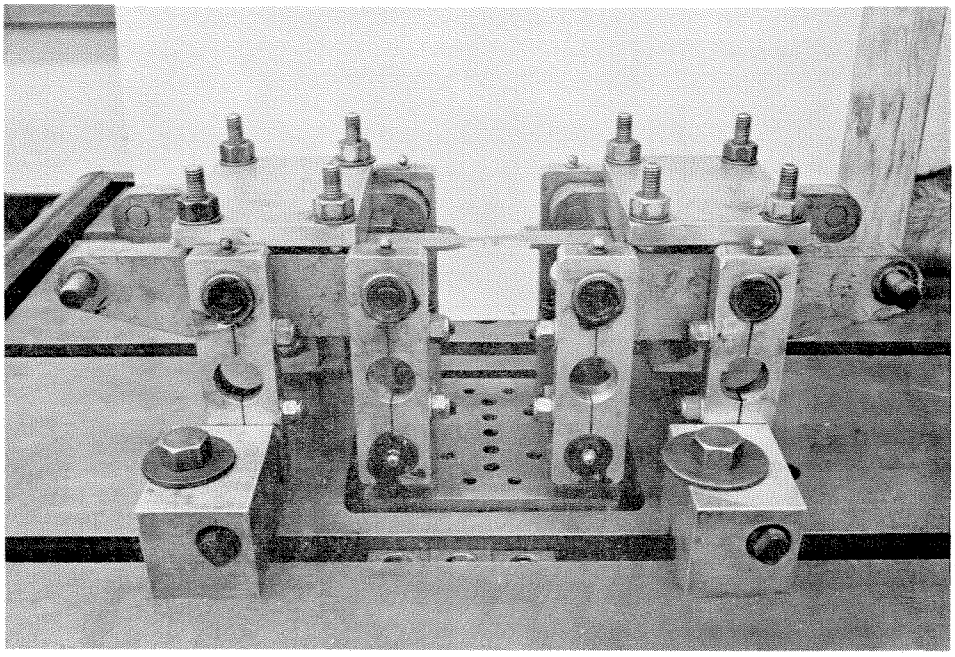

Fig. C-3 Photograph of specimen mounted in fatigue testing machine.

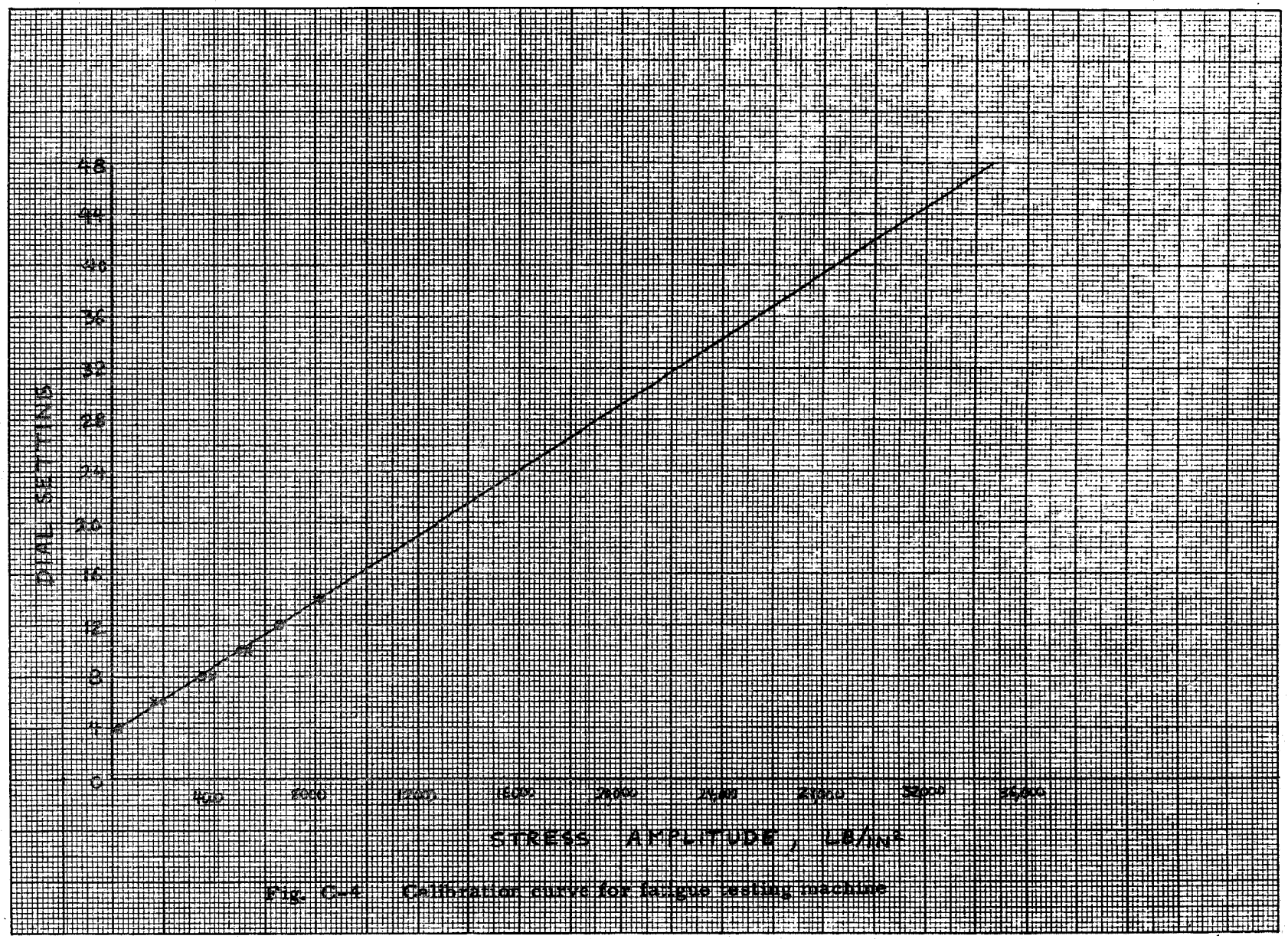

Fig. C-4 Calibration curve for fatigue testing machine

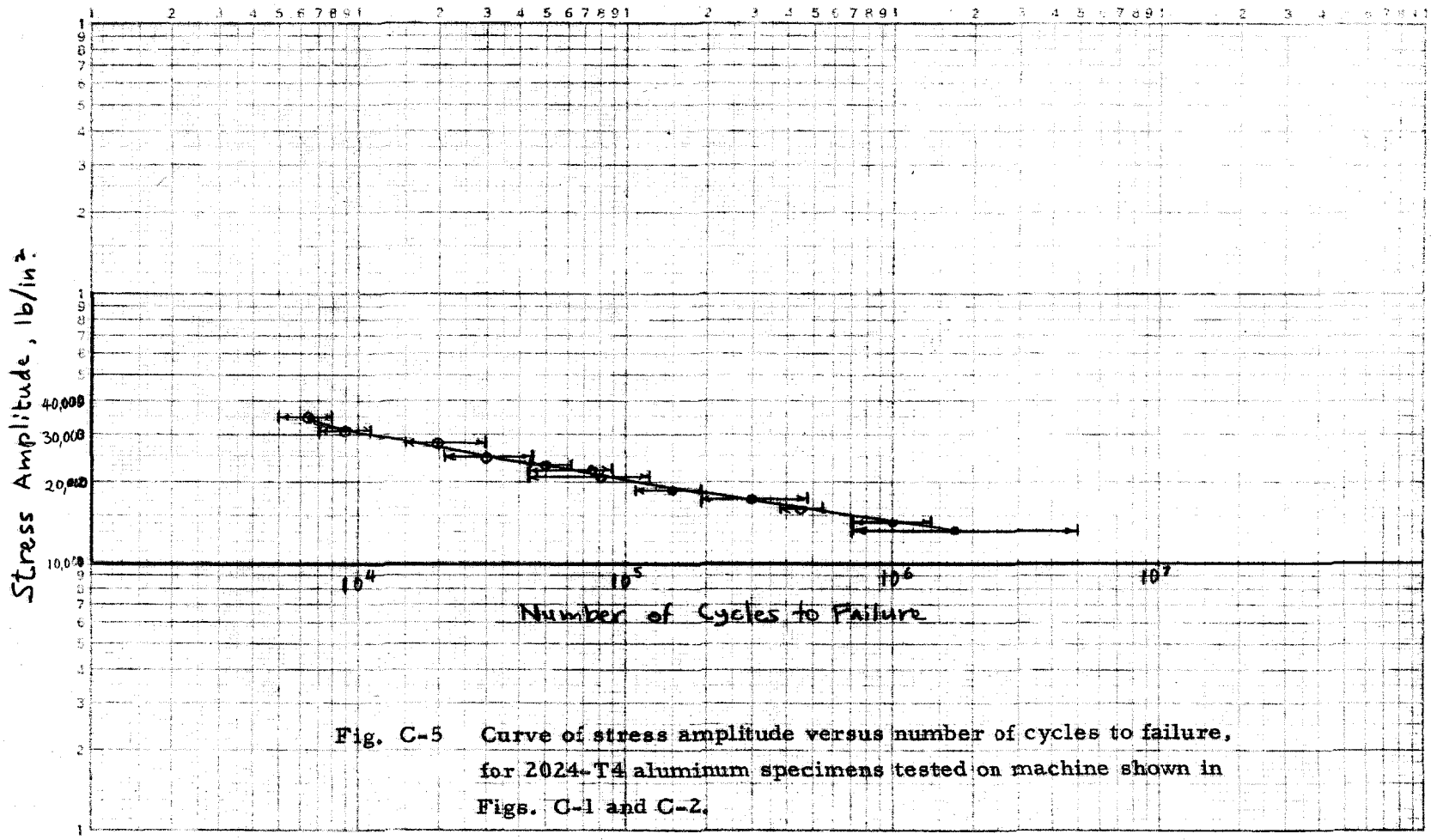

Fig. C-5 Curve of stress amplitude versus number of cycles to failure, for 2024-T4 aluminum specimens tested on machine shown in Figs. C-1 and C-2.